Università degli Studi di Ferrara

DOTTORATO DI RICERCA IN
"SCIENZE DELLA TERRA"

CICLO XXVIII

COORDINATORE Prof. Coltorti Massimo

PALAEOECOLOGICAL INVESTIGATIONS ON PLIO-PLEISTOCENE EUROPEAN RHINOCEROSES (GENUS *STEPHANORHINUS*): POWDER X-RAY DIFFRACTION, CARBON ISOTOPE GEOCHEMISTRY, TOOTH WEAR ANALYSES AND BIOMETRY

Settore Scientifico Disciplinare GEO/09

Dottorando
Dott. Ballatore Manuel

_____
(firma)

Tutore
Prof. Vaccaro Carmela

_____
(firma)

Cotutore
Dr. Breda Marzia

_____
(firma)

Anni 2013/2015

TABLE OF CONTENTS

Introduction

The PhD project focuses on four rhinoceros species of the European Plio-Pleistocene genus *Stephanorhinus*: *S. megarhinus* (Pliocene), *S. elatus* (Late Pliocene), *S. etruscus* (Early Pleistocene) and *S. hundsheimensis* (late Early-Middle Pleistocene).

S. megarhinus (de Christol 1834) is a slender and large sized rhinoceros with brachyodont teeth from the Pliocene deposits of Europe and is morphologically relatively similar to the Late Pliocene *S. elatus* (Croizet and Jobert 1828), that is slightly smaller in size. *S. etruscus* (Falconer 1868) is a small browsing rhinoceros characteristic of the Early Pleistocene deposits of Western Europe. Unfortunately, very little is known about the ecology of these ancient rhinoceros species because the previous works, in many cases quite old, reported just morphological descriptions (e.g. Azzaroli 1962, Guérin 1972, 1980, 1982, Mazza 1988, Pandolfi 2013).

From the late Early to the Middle Pleistocene the species *S. hundsheimensis* (Toula 1902) is recorded in the whole Europe, it is a generalist species and thus it deserves more attention on its diet and adaptive possibilities. Moreover *S. hundsheimensis* represents an interesting case study to test the size and proportions variations along its chronological and geographical range. Fortelius et al. (1993) and Lacombat (2006, 2009) record a noticeable dimensional variation through time with a smaller-sized form from the Upper Villafranchian and a larger one from the Galerian. Furthermore a huge geographic variability is known among coeval populations in both morphology and size, with the latter increasing from low to high latitudes (Lacombat 2009, Ballatore and Breda 2013). So *S. hundsheimensis* is very important to evaluate the adaptive meaning of these size changes against the changing climatic and environmental parameters in Quaternary rhinoceros.

In the Middle Pleistocene, other two species of the genus *Stephanorhinus* are present (but they are not included in the research project): *S. hemitoechus* (Falconer 1968), known as "the steppe rhinoceros", a robust medium-large sized rhinoceros on the most grazer side of the *Stephanorhinus* browser-grazer spectrum, and the larger *S. kirchbergensis* (Jäger 1839), known as "the forest rhinoceros", that shows the highest specialization in browsing.

In the past, the four investigated species were included in different genera (*Rhinoceros* Linnaeus 1758, *Dicerorhinus* Gloger 1841), but they have been later united in the single

Genus *Stephanorhinus* (Kretzoï 1942) by Fortelius et al. (1993). We maintain this generic attribution, because of evident morphological relations among the four species, even if some authors still prefer *Dicerorhinus* (Guérin and Tsoukala 2013) and others include the species "*megarhinus*" in the Miocene genus *Dihoplus* (Pandolfi 2013). The four analysed species are in fact close relatives by a phyletic point of view (Guérin 1980, Fortelius et al. 1993, Lacombat 2005, 2007, Van der Made 2015), but several evolutionary hypothesis have been proposed and an agreement has not been reached yet.

The ecological investigations should bring to a better understanding of the evolutionary history of the genus *Stephanorhinus* in relation to the changing environmental conditions. The four species on the focus of our research show a wide degree of adaptability to different environmental contexts from wet woodland to dry steppe and, considering the strong climatic variations occurred during the time range of their existence, the investigation of their palaeoecology (size variation, diet adaptation, niche partitioning) is of paramount interest to shed light on the evolution of natural systems in the past. This concentrates in particular on the diet through an interdisciplinary approach. Carbon isotope (that needed paired powder X-ray diffraction analysis), mesowear, 3D microwear texture analysis and morphobiometry, are among the most innovative available techniques. They lead to the acquisition of new information on the animals' life condition, on the competition with other taxa, and on the climatic variation and consequent adaptive processes, they can provide a better knowledge of the environmental condition in the past. In particular, the investigated time span, from the Late Pliocene to the Middle Pleistocene, is a period characterized by strong climatic fluctuations, that became more and more severe in the Middle Pleistocene, forcing the latest *S. hundsheimensis* populations to drastic adaptations before they become extinct.

Using rhinoceroses as working taxon is useful due to their extremely rich record in the Plio-Pleistocene deposits, since the taxon was one of the most abundant in the herbivorous communities, then macromammals lead information at a regional geographic scale, that is essential in order to reconstruct evolutionary dynamics at macroregional level (Europe). Moreover, these forms show close relation to the modern rhinoceroses so a strict comparison is possible. Finally the selected time span is useful due to the richness in the fossil record and to the fine stratigraphic resolution that allows testing evolutionary issues.

The main aims of the PhD program are:

- perform the carbon isotope analysis paired with powder X-ray diffraction to assess the preservation of the biogenic signal in fossilized biapatites;
- improving the knowledge on the palaeoecology of the more ancient species *S. megarhinus*, *S. elatus* and *S. etruscus*, by morphobiometry, mesowear and 3D dental microwear texture analyses of the teeth;
- investigating the geographical and chronological size variation of *S. hundsheimensis* and finding a possible link to the changing environmental parameters along the latitudinal gradient through Italian, French, German and British populations.

Chapter 1 constitutes an overview on the isotope geochemistry principles on which diet inferences technique is based; it explains the isotope fractionation processes in plants and the relation to animals' diet along with bone and other mineralized tissue structure and chemical alteration during diagenetic processes. In chapter 2, the rhinoceroses' evolutionary history and ecological data are given, focusing on Plio-Pleistocene *Stephanorhinus* and modern species. The following three chapters represent the main core of the project. They are intended as independent papers, and each of them deals with a specific subject: the XRD and carbon isotope analyses on all the Pliocene to Pleistocene investigated species (chapter 3), the multiple approach dietary investigation of Pliocene and Early Pleistocene species (chapter 4), and the size variability of the species *S. hundsheimensis* (chapter 5). The applied methodologies are illustrated in each chapter, then specific results are given, followed by relative discussion.

The project involves several Institutions in France, Switzerland, Austria, Germany and United Kingdom, where the investigated fossil remains are stored: Muséum National d'Histoire Naturelle Paris, Musée des Confluences Lyon, Laboratoire de Géologie de Lyon Terre Planètes Environment of the University Claude Bernard Lyon1, Naturhistorisches Museum Basel, Naturhistorisches Museum Wien, Staatliches Museum für Naturkunde Karlsruhe, Naturhistorisches Museum Mainz, Senckenberg Forschungsstation für Quartärpaläontologie Weimar, The Natural History Museum London. Moreover the Institut de Paléoprimatologie, Paléontologie Humaine: Evolution et Paléoenvironnements (iPHEP University of Poitiers and CNRS) has been involved for the 3D-DMTA analysis.

Chapter 1

ISOTOPE GEOCHEMISTRY TO INVESTIGATE THE DIET OF FOSSIL ANIMALS

1.1 Isotope geochemistry

A chemical element is not always a simple substance, composed by identical atoms, but in many cases it is a mixture of isotopes: distinct atoms of the same element differing in the number of neutrons, thus in the atomic mass. Because chemical properties depend mainly on nuclear charge and electrons distribution, isotopes of the same element usually have the same chemical behavior and chemical reactions do not lead to isotopes separation, except for lighter elements such as H, C, O and S. But in living beings biochemical reactions often operate active separation. Physical properties are more influenced by the atomic mass than chemical properties, for example heavy isotopes show lower evaporation rates, and for the above enumerated light elements, relative difference in mass is enough to lead to separation (Ehleringer and Rundel 1989, Krauskopf and Bird 1995).

The majority of natural isotopes are stable, thus persisting in the environment through time. However, stable isotopes can generate new isotopes when are affected by cosmic ray (products are called cosmogenic isotopes). Some other natural isotopes are radioactive and spontaneously decay releasing ionizing radiation; the new elements produced by radioactive decay are called radiogenic isotopes (or daughter products) (Krauskopf and Bird 1995). Radioactive decay rate is constant and is not influenced by environmental factors (temperature, pressures, pH), therefore measuring the ratio of radiogenic to radioactive isotopes can lead to events dating.

1.1.1 Stable isotopes

Stable isotopes of elements with low atomic number, due to a large relative difference in mass, undergo isotopic fractionation during common geochemical and physical processes. The different properties depend on the different vibrational frequencies of heavy and light isotopes, the latter vibrating with higher frequencies and thus having a lower bond strength

to other atoms. At high temperature the differences in vibrational frequencies became smaller and isotopic fractionation is less pronounced (Krauskopf and Bird 1995).

Fractionation is the change in the isotope ratio due to chemical, physical or biological process (White 2013). Fractionation mechanisms were described at first by Urey (1947) who also suggested its usefulness in geological studies. Mechanisms of isotopic fractionation are due to kinetic processes equilibrium exchange reaction, therefore fractionation depends on variation in chemical or physical proprieties that are proportional to differences in mass, particularly noticeable in elements with an atomic mass lower than 40 (Urey 1947, Broecker and Oversley 1976). In equilibrium reactions, fractionation depends on bond strength for isotopic species (thermodynamic properties)(Koch 1998). Considering the exchange reactions between different compounds containing isotopic variety of the same element, ideally the compounds exchange heavy and light isotopes towards an equilibrium in which isotopic ratio is the same in different compounds. But bond strength varies in different compounds (Krauskopf and Bird 1995). Kinetic processes regard rates of diffusion or reaction velocity for different isotopic species, and they are particularly important for gases diffusion and biochemical pathways. In general, light isotopes react and diffuse more rapidly and products are depleted in heavy isotopic species (Koch 1998), for example the result of an evaporation process is the concentration of the heavy isotope in the residual liquid phase and the concentration of the light one in the vapor phase, and similarly in a process of precipitation, the solid phase contains more heavy isotope than the solution. Moreover separation depends on reaction rates, that could be extremely slow at low temperature and equilibrium is not reached. But biotic factors can selectively modify reaction rate, when reactions are catalyzed by bacteria the rates can vary for different isotope, for example bacterial reduction of sulfate (SO_4^{2-}) is fast for the light sulfur isotope and operates a separation leading to a concentration of ^{32}S in the sulfide species and of ^{34}S in the residual sulfate (Krauskopf and Bird 1995).

To quantify the isotope ratio of a sample, a comparison with the ratio of standard is used (Krauskopf and Bird 1995):

$$\delta_{heavy} = \frac{R_{sample} - R_{standard}}{R_{standard}} \text{ x } 1000 \text{ ‰}$$

Fractionation in nature is reduced and isotopic amounts are reported as part per thousand (‰). A negative value of δ indicates a low ratio (R=heavy/light) in the sample, thus an impoverishment in heavy isotope relative to the standard, while positive value indicates

enrichment in heavy isotope. Four standard are admitted: SMOW (Standard Mean Ocean Water) for oxygen and hydrogen, PDB (PeeDee belemnite) for carbon and occasionally oxygen, AIR (atmospheric air) for nitrogen, CD (Canyon Diablo meteorite) for sulfur (Ehleringer and Rundel 1989). Another notation is used for isotopic fractionation between two substances: $\Delta X_{a-b} = \delta X_a - \delta X_b$ (Koch 1998).

The study of stable isotopes composition in biogenic remains leads to comprehend information on paleoenvironment and habits of fossil animals. In fact the composition of biogenic material depends on environment input (temperature influence isotopic ratio) and biological processes (diet, physiology, migration). The preferential isotopes are C, O and Sr that are well resistant to fossilization processes; N and H are useful in archaeological contests, but they are not preserved in fossils older than few million years (Kohn and Cerling 2002). These isotopes can be detected in well preserved tissue: bone, enamel and dentine (bioapatites).

The importance of isotope fractioning for palaeoclimatological reconstructions is well known: the isotope composition of shell carbonate, depends on the temperature and the isotopic composition of water (biological differences among species and post-burial effects may influence the composition but their effect is reduced for Quaternary carbonates) (White 2013). The first researcher to attempt a palaeoclimatological reconstruction on these grounds was Emiliani (1955) who analyzed $\delta^{18}O$ in foraminifera shells and recognized 15 glacial-interglacial cycles during the last 600.000 years (mainly due to orbit variations), considering that in a glacial phases the light isotope ^{16}O is stored in the ice, and the oceans are therefore enriched in the heavy isotope ^{18}O (White 2013).

1.1.2 Carbon fractionation in plants

C is a nonmetallic element of the IV group (Z=6) and three isotopes are known: ^{12}C, ^{13}C and ^{14}C. The latter is radioactive while the former two are stable isotopes. The first study on $^{13}C/^{12}C$ ratio differences in limestone carbonates, air CO_2, marine and terrestrial plants, was published by Nier and Gulbransen (1939). The variations in carbon isotopic ratio ($\delta^{13}C$ refers to standard PDB measured in carbon of belemnites from the Cretaceous Peedee formation, South Carolina) in nature are wide. Many terrestrial compounds show negative value but some carbonates have high positive values. Biochemical reactions occurring in green plant photosynthetic pathways, where the light isotopes are concentrated in the reduction of CO_2 to organic compounds, are of primary interest for palaeontological

inferences.

$\delta^{13}C$ values in ecosystems depend on plants photosynthetic pathways and environmental parameters. In particular in the atmospheric CO_2 the $^{13}C/^{12}C$ value is about -7.7‰. Its value is more negative in plants because photosynthesis favors ^{12}C and then, through the food chain it becomes gradually less negative (Koch 1998).

In land plants photosynthesis takes place in several steps, along which fractionation occurs (Park and Epstein 1960). The first step consists in CO_2 diffusion from layers around the leaf, through stomata, into the mesophyll, and in this phase a fractionation of -4.4‰ is expected (Park and Epstein 1960, White 2013), because $^{12}C^{16}O_2$ diffuses further than $^{13}C^{18}O_2$ (White 2013). The second step involves enzymatic reaction inside the cell and different pathways are possible. Three different photosynthetic mechanisms are known, and we refer to as C3, C4 and CAM.

a) C3 plants dispose the enzyme Rubisco (Ribulose bisphosphate carboxylase/oxygenase) to catalyze ribulose 1,5-bisphoshate (5C linear molecule) carboxylation to two molecules of 3-phosphoglycerid acid (3C linear molecule) by reaction with one molecule of CO_2 in the Calvin Cycle (chloroplast stroma). Because of 3-carbon product, plants are called C3 and constitute algae and the majority of land plants, all trees, most shrubs and herbs and many grasses from temperate and cold areas. The isotope fractionation associated to Rubisco carboxylation in C3 land plants is -29.4‰ (White 2013). Thus the total fractionation is expected about 33.8‰.
b) Plants C4 metabolism was discovered in the second half of the XX century (Kortschak et al. 1965, Hatch and Slack 1970) and characterizes some sedges and herbs and dry/warm climate grasses (regions regulated by monsoon system with one warm season of growth). C4 plants are more recent in the evolutionary time scale and suddenly expanded about 7 MY (Koch 1998). In these plants we find peculiar anatomical modification to reduce photorespiration by Rubisco (oxygenase activity), thus, these plants are extremely efficient in CO_2 fixation and the fractionation related to Rubisco activity is more reduced (therefore $\delta^{13}C$ values are less negative than C3). In C4 plants two photosynthetic cell types are distinguished: mesophyll cells and bundle sheath cells (those around the cribro-vascular bundle). The mesophyll cells, unlike C3, do not dispose Rubisco but a different enzyme, PEP (phosphoenol pyruvate carboxylase), that fixes CO_2 carbon in oxaloacetate (4C

molecule) than converted to malate and carried into the bundle sheath cells. Here malate is consumed in mitochondrial respiration leading to CO_2 realizing now available for Calvin Cycle in the chloroplasts where Rubisco is present (so bundle sheath cells works as C3 mesophyll cells, but here Rubisco works in isolated condition that avoid photorespiration).

c) Finally, Crassulacean Acid Metabolism (CAM) is proper of Crassulaceae and Cactaceae whose metabolic pathway comprehends both C3 and C4 types as xerophytic adaptation. Generally they use C4 pathway during the night (when stomata can be opened) but revers on C3 during day (when stomata are closed to preserve water from intense evapotranspiration). Their $\delta^{13}C$ shows intermediate values between C3 and C4.

Shortly, for our interests, isotopic studies show that C4 plants have a less negative $\delta^{13}C$ value than C3 (Bender 1971, Smith and Epstein 1971): C3 plants show a $\delta^{13}C$ value of about -27.1±2.0‰, while C4 are much less depleted than C3 with a value of -13.1±1.2‰ (O'Learly 1981).

Environmental factors influence $\delta^{13}C$ variability. Among C3 different factors cause variation in $\delta^{13}C$ values (scarcity of nutrient, light, water, CO_2 partial pressure and temperature), while more efficient C4 show little environmental variability, correlated with growing season temperature. Plants are ^{13}C-depleted with respect to CO_2, the main environmental causes are linked to dense forests because available CO_2 derive from respiration and decomposition and is ^{13}C-depleted with respect to the atmosphere (Bocherens 2003). Moreover increase in CO_2 partial pressure, depletion in nutrients and decrease of temperature contribute to low $\delta^{13}C$ values in C3 (Tieszen 1991). Water stress and saline stress on the contrary led to minor depletion and $\delta^{13}C$ values up to -20‰ (Guy et al. 1986), and similarly a decrease in CO_2 partial pressure. Variation in partial pressure have been documented during glacial/interglacial cycles (Leuenberger et al. 1992). Recent increment of CO_2 from fossil fuel combustion and deforestation with low $\delta^{13}C$ values has changed actual atmospheric isotopic value, diminishing from about -6.5‰ in 1850 to about -8‰ nowadays (Marino and McElroy 1991). Being atmospheric CO_2 the carbon source for plants, it is possible to monitor atmospheric variation in $\delta^{13}C$ trough isotopic analysis of plants tissue. Variations can be due to surface carbon cycle (on short time scale, <10 My), e.g. absorbing carbon in water from surface to deep, or the relative proportion in absorbing between land biota and oceans, and the methane release from sediments. On longer time

scale, variations depend on geological factors, as the relative rates of burial of organic carbon and inorganic carbon (carbonate), and volcanic activity. $\delta^{13}C$ of the atmosphere at the full glacial maximum was about -7.5‰, while in a pre-industrial Holocene averaged -6.5‰ (Marino et al. 1992).

1.1.3 Carbon isotope ratio and animal diet

From primary production and up to the food chain, isotopic composition becomes weakly more positive, in fact cellular respiration favours ^{12}C, with faster reaction rates due to weaker bonds, and thus heavy carbon relatively increases in the organic matter (White 2013). Carbon isotopic composition of animal tissue closely correspond to animal diet (no strong fractionation occurs in herbivores), being only 1‰ heavier then diet and it is possible to generalize that a 1‰ increase factor is correlated to each trophic level (DeNiro and Epstein 1978). Moreover some differences in $\delta^{13}C$ value in animals depend on the tissue considered. Bone collagen composition reflects the composition of the entire body and if isotopic exchange is affected during the fossilization of bone apatite, bone collagen and tooth enamel maintain their original composition (Scheoninger and DeNiro 1984, White 2013). Plants consumers reflect isotopic composition of their food, with an isotopic shift due to the particular tissue (DeNiro and Epstein 1978). $\delta^{13}C$ of herbivorous tissue is offset from diet by a specific amount, estimated for wild mammals 12/14‰ ($\Delta_{tissue\text{-}diet}{}^{13}C$) (Koch 1998). The bone $\delta^{13}C$ value is about +12‰ with respect to diet (Krueger and Sullivan 1984, Lee-Thorp et al. 1989). The bone carbonate deposits in equilibrium with blood carbonate but there are differences related to body mass: lower than +10‰ in small rodents (DeNiro and Epstein 1978, Ambrose and Norr 1993) and up to +14‰ in horses (Cerling and Harris 1999). Recent studies investigate such variation in small and large herbivorous, confirming the offset values: +11‰ and +13.5‰ (Passey at al. 2005).

In addition, Lee-Thorp (2000) underlines as the isotopic content of plants should be taken into account especially if concerning browser herbivores. In fact the carbon isotope ratio in C3 plants is assumed constant but it could be affect by many environmental parameters (aridity, osmotic stress, temperature, pCO_2, irradiance; Tieszen 1991). For example, water stress brings to isotopic enrichment due to lower photosynthetic discrimination against ^{13}C, so that aridity can led C3 plants to be enriched in heavy carbon (Lee-Thorp 2000). C4 are not affected but their geographical distribution depends on environmental parameters (Ehleringer et al. 1997).

1.2 Biological mineralized tissues

Vertebrate skeleton is composed by three biomineralized types of tissue - bone, dentine and enamel - made of inorganic (mineral) and organic (protein and lipid) components.

The ratio between organic and inorganic components is different: bone and dentine contain more than 20-30% of the dry weight of organic matrix, mainly composed of collagen, while tooth enamel is almost devoid in organic components (lesser than 2-5% of organic matrix composed by phosphoproteins and amelogenins, non-collagenous proteins) (Koch 2007, LeGeros 1981, LeGeros and LeGeros 1983, Simkiss and Wilbur 1989). Otherwise than compositional differences, physical characteristics distinguish different skeletal tissues. Bone is highly porous and poorly crystalline, with small crystals (100x20x4 nm) while enamel is non-porous and more highly crystalline, with larger crystals (1000x130x30 nm) (Koch 2007, LeGeros 1981, Simkiss and Wilbur 1989). Dentine resembles bone characteristics but shows intermediate porosity between bone and enamel (Koch 2007, Lowenstam and Weiner 1989).

The organic component is rapidly degraded as other organic soft tissues (Collins et al. 2002), in particular, the collagen, useful tool in archaeology and recent palaeontological contexts, does not survive over millennial time-scale (Lee-Thorp 2000), except for extraordinary preservation cases (100.000 years, Jones et al. 2001). The inorganic component deserves more interest for field of research considering geologically older deposits and fossils.

The mineral component is bioapatite, an impure hexagonal calcium phosphate mineral, a form of hydroxylapatite $Ca_{10}(PO_4)_6(OH)_2$ with minor and trace element substitutions and adsorptions (LeGeros 1991, Wopenka and Pasteris 2005). Bioapatite differs from apatite (syntetical or mineralogical) in several characteristics such as the small crystal size (variable among type of tissue), the high degree of isomorphic substitution and adsorpition (particularly carbonate) and lattice distortions (Lee-Thorp 2000, LeGeros 1981). Important for palaeontological and archaeological purpose are for example Sr^{2+} or Pb^{2+} substitutes for calcium and CO_3^{2-} substitutes for hydroxyl and phosphate groups (Koch 2007, Simkiss and Wilbur 1989). As a consequence of its small sized crystals, enhanced surface area and number of substitutions, bioapatite is relatively soluble (LeGeros 1981); this is a physiological specialization of the skeletal tissue, to be able to store calcium and carbonate ions to be readily released when needed (Lee-Thorp 2000, Wheeler and Lewis 1977).

During ontogenetic development, bone growth involves ossification of cartilage and

accretionary growth (Lowenstam and Weiner 1989) but after deposition bone is remodeled by dissolution and reprecipitation during the whole life (Simkiss and Wilbur 1989). On the contrary, teeth mineralization, except in mammals with ever-growing teeth, occurs early in life (Koch 2007). Enamel grows by accretion and does not undergo remodeling (Gage et al. 1989), thus its content reflects the diet of the first stages of the animal's life because formation of the dental gems occurs within few months (mineralization is complete prior eruption)(Gadbury et al. 2000, Hoppe et al. 2004). Dentine is intermediate, it grows by accretion and undergoes little post-depositional remodeling (Lowenstam and Weiner 1989); it shows incremental laminations at different time scales – from daily to annual (Carlson 1990).

1.2.1 Carbonate in bioapatite

Bioapatite includes carbonate of two different types: 1) structural carbonate and 2) labile carbonate. The structural carbonate is substituted into the crystal lattice at the OH^- position (Type A structural carbonate) and PO_4^{3-} position (Type B structural carbonate); labile carbonate is not associated with a well-defined lattice position, it is in hydration layers or in amorphous zones near crystal surface (LeGeros et al. 1969, LeGeros 1991, Elliott 2002). Carbon isotope analysis would concern structural carbonate that reflects biogenic signal and is resistant to diagenesis (McArthur et al. 1980, Land et al. 1980, McCrea 1950), except when recrystallization of bioapatite occurs. Labile carbonate is more easily dissolved and altered than the more stable structural carbonate. As a consequence, it is not a reliable biogenic signal, since it includes the exogenous contaminants deposited in the post-mortem events (Lee-Thorp 1989).

1.2.2 Diagenesis alteration

During the diagenetic process, exogenous carbonate can contaminate the fossil bioapatite. Exogenous (not biogenic) carbonate can derive from two main processes:

1) sedimentary carbonate: pore-filling cements or bicarbonate adsorbed to crystal surfaces (Krueger 1991). Since sedimentary carbonate is more soluble than bioapatite, it can be removed by acid treatment (Krueger 1991, Lee-Thorp and van der Merwe 1991)
2) post-mortem recrystallization of biogenic apatite. This is more extensive in bone and dentin due to their small-sized crystals and it is not possible to remediate, it can be detected by X-ray diffraction (Bartsiokas and Middleton 1992; Person et al.

1995). If recrystallization lead to carbonate hydroxylapatite, exogenous carbonate may be introduced (acid treatment of samples can remove diagenetic carbonate; Koch et al. 1997, Garvie-Lok et al. 2004), while if it lead to fluoroapatite the isotopic composition of structural carbonate may be unaltered (Krueger 1991). Alteration may be investigated also through analysis of carbonate yield, low carbonate yields may indicate recrystallization to fluorapatite and high values indicate contamination of sedimentary carbonates (Lee-Thorp and van der Merwe 1991). Recrystallization can be combined with enzymatically catalysed microbial effects (Blake et al. 1997; Sharp et al. 2000), leading to alteration of $\delta^{18}O$ in bone phosphate (Luz and Kolodny 1985). Enamel is not immune (Schoeninger et al. 2003), and over long time-scale, ions exchange continues in enamel and bone, and different minerals precipitate in cracks and pores (pyrite, silicates, carbonates; Hassan and Ortner 1977).

Many authors claim that carbonate in enamel is much more retentive of the original isotopic signal (Koch et al. 1997, Lee-Thorp and van der Merwe 1987, 1991; Quade et al. 1992; Wang and Cerling 1994, Bocherens et al. 1996) because it is more resistant to diagenesis (Budd et al. 2000, Hoppe et al 2003) while recrystallization of tiny bone and dentine crystals, into more stable form of apatite, is more easy (Sillen 1989). The high compact structure of enamel was shown by X-ray crystallinity investigation to change minimally also during long period (Lee-Thorp and van der Merwe 1987, Ayliffe et al. 1994) while bone undergoes rapid crystallinity increase (Trueman et al. 2004).
However bone has also been used (Lee-Thorp 2000) and it is preferable for several reasons: first of all bone material is more abundant than enamel, secondarily bones are often broken and sampling splinters are easily available while tooth are often intact and sampling of powder irreparably damage the crown surface. Moreover, while enamel formation occurs early in animal life, so that it may record a juvenile diet, bone is continuously remodelled through life span and records an average of the diet (Libby et al. 1964).

1.2.3 Powder X-Ray Diffraction (pXRD)

In order to evaluate if exogenous carbonate replaced biogenic carbonate during diagenetic processes, the crystallinity of the mineralized tissue is a good proxy. Crystallinity is the measure of size and homogeneity of the crystallites (Klug and Alexander 1974) and can be

quantified by the breadth of the picks in the diffractogram (X-ray diffraction). Apatite with high crystallinity have a low content in carbonate (LeGeros and LeGeros 1984), in fact enamel carbon content is lower than bone (Person et al. 1995), so if ancient bone apatite shows high crystallinity its structure had been remodelled and the carbon content is reduced and could not be biogenic. Person et al. (1995) estimated crystallinity by the Crystallinity Index (CI) values, that is directly correlated. The method is improved by using the crystallinity size parameter obtained by the Le Bail method that leads to more accurate data (Le Bail 2005).

It has been suggested that the increase in crystallinity in bones is not related to age but to taphonomical parameters and must occur during the early phases of diagenesis (Person at al. 1995).

Le Bail method gives cell parameters with great precision and yields indirect information of substituting ions (Michel et al. 1995). Cell parameters a and c (measured in Amstrong) undergo variations when substitutions occurs. If planar CO_3^{2-} replace tetrahedron PO_4^{3-} (Type B structural carbonate), the a parameter decrease and c parameter increase. Reverse when substitution occurs at OH^- site (Type A structural carbonate)(LeGeros 1981). So, from comparison with modern tissue, we can consider that a higher or lower (in comparison to a modern reference) a/c ratio is indicative of diagenetic substitution, therefore that the structural carbonate could not be biogenic.

1.2.4 Acid treatment

In order to remove organic and diagenetic exogenous carbon and maintaining the only structural carbonate for isotope analysis, acid treatments are commonly used (e.g. Weiner and Price 1986, Lee-Thorp and van der Merwe 1987, DeNiro and Weiner 1988, Koch et al. 1997, Cerling et al. 1999, Boisserie et al. 2005, Kingston and Harrison 2007, Clementz et al. 2009). The several authors use a double soaking, at first with NaOCl or H_2O_2 (different concentration and soaking duration) for the removal of organic matter, and then acetic acid or acetic acid/calcium acetate (different concentration and soaking duration) for the removal of exogenous carbonate. The method proposed by Koch et al. (1997) is the most suitable for our investigation on Plio-Pleistocene bone and teeth.

As a matter of fact, acid treatment can heavily compromise the samples, the main related problems are the following:

- sample recrystallization (Lee-Thorp 1989, Lee-Thorp and van der Merwe 1991, Koch et al. 1997, Nielsen-Marsh and Hedges 1997). Even if no new mineral phases

are detected after treatment, the increase of crystallinity is warning of recrystallization (Nielsen-Marsh and Hedges 1997). The risk is associated with acid concentration, time treatment and fossilisation degree (age of samples);

- loss of sample by dissolution (Nielsen-Marsh and Hedges 1997, Balasse 2002). It depends on acid concentration and soaking duration (Koch et al. 1997, Lee-Thorp et al. 1997) but also on particle size of powder, since extremely finely grounded samples are more vulnerable to dissolution (Lee-Thorp et al. 1997);
- isotopic offset with increased $\delta^{18}O$ values and dropped $\delta^{13}C$ values in enamel and bone (Lee-Thorp and van der Merwe 1991, Quade et al. 1992, Koch et al. 1997). To explain the decrease of carbon isotope ratio, Koch et al. (1997) proposed that Type A and Type B structural carbonate are involved in different chemical bonds and therefore isotopic fractionation, depending on bond energy differences, change from each site, and the weakly bonded site is more exposed to removal. Treatment with 1 M acetic acid-calcium acetate buffer or 0.1 M acetic acid induces the smallest isotopic offsets in both bone and enamel (Koch et al. 1997).

Chapter 2

FOSSIL AND EXTANT RHINOCEROSES: EVOLUTION, ECOLOGY AND GENERAL OVERVIEW

2.1 Introduction

Rhinoceroses belong to the order Perissodactyla, which includes odd-toed ungulate herbivorous, along with horses (suborder Hippomorpha, family Equidae) and tapirs (suborder Ceratomorpha, family Tapiroidea) (Froehlic 1999, Prothero et al. 1989).

The family Rhinocerotidae originated in Asia in the Middle Eocene and grow up with several forms which widespread into Eurasia, North America and Africa. The subfamily Rhinocerotinae originated in Europe in the Oligocene and reached Africa during the Miocene in different migration waves. It comprehends the Euroasiatic tribe Rhinocerotini and the African tribe Dicerotini (Prothero et al. 1989, Cerdeño 1995, 1998).

The first European Rhinocerotini appeared in the late Early Miocene with *Lartetotherium sansaniense* who shows long and massive limbs, brachiodont cheek teeth and functional incisors; the species become extinct in the Late Miocene without leaving descendants (Heissig 1999).

African Dicerotini reached South-Eastern Europe in the Middle Miocene, but did not give descendants. In the Late Miocene, the Asian genus *Dihoplus* entered Europe with the species *D. pikermiensis* (restricted to South-Eastern Europe; Giaourtsakis et al. 2006, Hessig 1999) and *D. schleiermacheri*. The latter was the largest form of the Miocene, with brachiodont teeth and well developed incisors, and is probably the first representative of the Plio-Pleistocene European lineage since it is supposed ancestor to *Stephanorhinus megarhinus* (Hessig 1999). The Pliocene rhinoceroses belong to the sole genus *Stephanorhinus*, supposed descendant from the Miocene *Dihoplus* (Hessig 1999, Lacombat and Mörs 2008, Pandolfi 2013) who survived until the Late Pleistocene.

Other genera of Asian origin, *Coelodonta* and *Elasmotherium*, immigrated into Europe in the Middle Pleistocene:

- the massive *Coelodonta antiquitatis*, the well known “wooly rhino” found in cold

environmental condition, with hypsodont and plagiolofonont teeth and completely ossified nasal septum;

- the giant *Elasmotherium sibiricum*, actually poorly recorded in Europe, with a characteristic single huge frontal horn (Guérin 1980).

2.2 Plio-Pleistocene European *Stephanorhinus*

During the Pliocene and the Pleistocene, several rhinoceroses species of the genus *Stephanorhinus* inhabited Europe and are described below.

Class Mammalia (Linnaeus, 1758)
Order Perissodactyla (Owen, 1848)
Suborder Ceratomorpha (Wood, 1937)
Superfamily Rhinocerotoidea (Owen, 1845)
Family Rhinocerotidae (Owen, 1845)
Subfamily Rhinocerotinae (Dollo, 1885)
Tribe Rhinocerotini (Gray, 1821)
Subtribe Rhinocerotina (Dollo, 1885)
Genus *Stephanorhinus* (Kretzoï, 1942)

Species:	*S. megarhinus* (de Christol, 1834)	Pliocene
	S. miguelcrusafonti (Guérin and Santafé, 1978)	Pliocene
	S. elatus (Croizet and Jobert, 1828)	Late Pliocene
	S. etruscus (Falconer, 1868)	Early Pleistocene
	S. hundsheimensis (Toula, 1902)	Early-Mid Pleistocene
	S. hemitoechus (Falconer, 1868)	Mid-Late Pleistocene
	S. kirchbergensis (Jäger, 1839)	Mid-Late Pleistocene

2.2.1 Stephanorhinus megarhinus *(de Christol 1834)*

The species *Rhinoceros megarhinus* has been introduced by de Christol (1834) on the rhinoceros remains from the type locality of Montpellier (Hérault, France). Actually, the species had been earlier described as *Rhinoceros leptorhinus* by Cuvier (1822), on Italian remains from Monte Zago near Piacenza (Cortesi 1806, 1819), later destroyed (Azzaroli 1962). A complete overview of the synonymies is given by Guérin et al. (1969). The

generic allocation of the species "*megarhinus*" is debated. Thenius (1955) placed the species into the genus *Dicerorhinus*. This approach is still followed by Guérin (Guérin 1980, Guérin and Tsoukala 2013) even if Groves (1983) maintains that this genus should be restricted to the living *D. sumatrensis* and fossils ex-*Dicerorhinus* have to be included into either *Lartetotherium* or *Stephanorhinus*. Fortelius et al. (1993) ascribe the species to the genus *Stephanorhinus* while Heissig (1999) proposes the genus *Dihoplus*. Fortelius et al.'s (1993) choice is here preferred so we use the name *S. megarhinus*.

The species is typical of the Mammal Neogene chronozone (hereafter MN) 14-15 (Guérin 1980) and did not survive into the Pleistocene. Guérin (1975) individuated two evolutionary stages with a reduction of the size from the early population from Montpellier (sub-zone d'Hautimagne, MN14) to the more recent populations from Perpignan (sub-zone de Perpignan, MN15). In the following MN zone of Etouaires (MN 16) the species is replaced by *S. elatus* (but no phyletic relationship between the two are suggested by Guérin 1975). Nevertheless some remains from the Late Pleistocene of Gross-Rohrheim (Hesse, Germany) and of Meyrargues (Bouches-du-Rhône, France) have been considered *S. megarhinus* by Koenigswald (1988) and Fortelius et al. (1993), respectively. Also from the Middle Pleistocene locality of Boxgrove (West Sussex, Britain) some rhinoceros specimens have been supposed to match *S. megarhinus* morphology by Breda et al. (2010), but the attribution has been partially revised (Ballatore and Breda 2013). We believe that also a revision of the specimens from Gross-Rohrheim and Meyrargues is needed.

S. megarhinus is a large sized and relatively robust rhinoceros but little is known on its ecology since no specific studies have been devoted to this topic, apart from some general hypothesis based on the structure of the teeth: "Les dents brachyodontes ne suggèrent pas une nourriture à base de graminées" (Guérin 1975).

2.2.2 Stephanorhinus miguelcrusafonti *(Guérin and Santafé 1978)*

Stephanorhinus miguelcrusafonti is a very poorly known species, described on scanty postcranials remains from Perpignan (Pyrénées-Orientales, France) and Layna (Soria, Spain) (Guérin and Santafè 1978). The French material was at first described as *D. megarhinus* (Depéret 1885), while the Spanish bones were ascribed to *D. etruscus* (Crusafont et al. 1969), as a prove for the great similarity of these species. We include the species into the genus *Stephanorhinus* according to Fortelius et al. (1993).

2.2.3 **Stephanorhinus elatus** ***(Croizet and Jobert 1828)***

The species *Rhinoceros elatus* has been described by Croizet and Jobert (1828) on fossil remains from different localities in the Perrier Mountain (Auvergne, France) but it was not recognized as a distinct species for a long time. More than a century later, remains form the locality of Vialette (Haute-Loire, France) were identified with this species but given a different name, *Dicerorhinus jeanvireti* (Guérin 1972), which must thus be considered a junior synonym. In recent years, the old (rightful) synonym has been employed again by several authors (e.g. Munteanu et al. 2008, Masini and Sala 2007, Palombo 2004, Radulescu et al. 2003), thus both the names are in use. The confused nomenclatural situation has been investigated through a detailed analysis of the literature and re-analysis of the type material of both *S. elatus* and *S. jeanvireti*. As a result, the two names are truly synonyms and the older name retains the right of priority according to the International Code of Zoological Nomenclature. The details of this review are going to be published soon (Ballatore and Breda, in press). From the generical point of view, the species has been placed into the genus *Stephanorhinus* by Fortelius et al. (1993). The almost general agreement on this solution is not shared by Guérin (e.g. Guérin and Tsoukala 2013) who still prefer the genus *Dicerorhinus*.

In Europe the species is characteristic of the Late Pliocene (MN16, Guérin 1972, 1980), Early Villafranchian (Rook and Martinez-Navarro 2010), but it is very poorly recorded. The main localities are those of Vialette (Guérin 1972), Etouaires (Ballatore and Breda, in progress) and Villafranca d'Asti Area (Campanino et al. 1994). Few remains have been collected from other minor localities: Hambach (Lacombat and Mörs 2008), several Italian sites (Pandolfi 2013), Hajnáčka (Fejfar 1964, Guérin 1972) and some Romanian localities (Radulescu et al. 2003).

S. elatus is a quite large sized rhinoceros of slender proportion. Pandolfi (2013) suggests it is not so different from *S. megarhinus* in the postrcranials as it clearly is in the skull. No palaeoecological work has been published on this species either, but it is supposed to be related to a humid climate with forest environment (Guerin 1972, Lacombat and Mörs 2008).

2.2.4 **Stephanorhinus etruscus** ***(Falconer 1868)***

The species *Rhinoceros etruscus* has been described by Falconer (1868) on a single skull (IGF 756, Museum of Geology and Palaeontology of the University of Florence) from the Upper Valdarno (Tuscany, Italy). Since the description of the species was limited to the

skull, no postcranial data were available as comparison for the identification of other remains and several erroneous attributions occurred. In particular, the species is very similar in morphology and partially in size to the later species *S. hundsheimensis*, so much that Guérin (1980) suggested they were the same species, being differentiated only at a subspecific level, with respectively the nominal subspecies *D. etruscus etruscus* and the later subspecies *D. etruscus brachycephalus*. The revision of the Tuscan remains, along with the re-identification of important European remains previously attributed to *R. etruscus*, have been performed by Mazza (1988) who well defined the morphological and dimensional reference for the specie, re-named *Dicerorhinus etruscus*. Later, Fortelius et al. (1993) include the species into the genus *Stephanorhinus*.

The species is recorded in the European Early Pleistocene, from the Middle Villafranchian of Saint Vallier (Guérin 1980, Mazza 1988) and Huelago (Van der Made 2010, 2015), to the Late Villafranchian of Tasso (Van der Made 2010, 2015).

Mazza (1988) suggests the species lived in a humid, woody landscape, with open grasslands spaces, but no proper ecological studies have been published yet.

2.2.5 Stephanorhinus hundsheimensis *(Toula 1902)*

The species has been described on the almost complete skeleton from the Middle Pleistocene of Hundsheim (Austria) by Toula (1902), but it is recorded already in the late Early Pleistocene of Pietrafitta (Mazza et al. 1993). Fortelius et al. (1993) report a dimensional variation through time with a small-sized form from the Late Villafranchian and a larger one from the Galerian. Mazza et al. (1993) prudently use *S.* cf. *hundsheimensis* for the small-sized form. Then Lacombat (2005) identifies two forms: the first evolutionary form (or small-sized form) from Pietrafitta and Pirro (namely the *S.* cf. *hundsheimensis* of Mazza et al. 1993) together with the rhinoceroses from the coeval French localities of Le Vallonet and Tour de Grimaldi and the German site of Untermassfeld, the second evolutionary form from the beginning of the Middle Pleistocene of Soleilhac and Isernia (Lacombat 2005).

S. hundsheimensis was a generalist specie (Kahlke and Kaiser 2011) and its varied diet provided it with huge adaptive possibilities, allowing the species to spread in the whole of Europe, from Southern Italy to Britain and from Spain to Germany.

For these reasons *S. hundsheimensis* deserves particular attention as an interesting case study to understand the evolutionary pathways in the Quaternary period and our project will investigate both diet and size variation of the species.

2.2.6 Stephanorhinus hemitoechus *(Falconer 1868) and* S. kirchbergensis *(Jäger 1839)*

In the Middle Pleistocene two Asiatic species invaded Europe and probably led to extinction the local *S. hundsheimensis*: *S. kirchbergensis*, which is a large-sized rhinoceros with large brachiodont teeth (therefore often considered as "forest rhino" but actually a generalist species like *S. hundsheimensis*; Kahlke and Van Asperen 2015), and *S. hemitoechus*, which is a medium-sized species characterized by more hypsodont teeth and robust limb structure. They both survived until the beginning of the Last Glaciation, together with the woolly rhino.

2.3 Extant rhinoceroses

Five species of rhinoceroses survive into present day, although in a reduced number of individuals and geographical restricted areas of distribution, being among the most endangered large mammal species (**Figure 1**).

The African species, *Diceros bicornis* and *Ceratotherium simum*, represent a single clade (Loose 1975, Groves 1983, Prothero et al. 1989) originated in the Late Miocene from the common ancestor *Ceratotherium neumayri*, a generalist rhinoceros from which two distinct ecological morphotypes arose at the Miocene-Pliocene boundary (Geraads 2005): one line with progressive grazer dental specialization led to *C. simum* and the other lineage to the browser *D. bicornis*. Both the modern species appeared in the Early Pleistocene.

The Asian species represent instead the last survivors of a larger Euro-Asiatic clade (Rhinocerotina), whose strict phylogenetic reconstruction is made difficult by the frequent wrong attributions and by the complex nomenclatural situation (Groves 1983) (e.g. the use of *Rhinoceros* and *Dicerorhinus* in palaeontological works from the XIX century until today). The genus *Dicerorhinus* is considered the most ancestral and therefore isolated into the Dicerorhinina subtribe. The lineage diverged in Europe in the Middle-Late Miocene from the Asian Rhinocerotina, but later several species spread into Asia, were the species *D. sumatrensis* survives now (Gerdaas 2005). The Asian group comprehends the fossil and modern *Rhinoceros*, recorded from the Pliocene, with the close fossil relatives *Punjabitherium* and *Gaindatherium* (the three genera coexisted in the Asian Pliocene) plus *Stephanorhinus* and *Coelodonta* (Groves 1983).

Class Mammalia (Linnaeus, 1758)
Order Perissodactyla (Owen, 1848)
Suborder Ceratomorpha (Wood, 1937)
Superfamily Rhinocerotoidea (Gray, 1821)
Family Rhinocerotidae (Gray, 1821)
Subfamily Rhinocerotinae (Dollo, 1885)
Tribe Dicerotini
Genus *Diceros* (Gray, 1821)
Species: *D. bicornis* (Linnaeus, 1758) Early Pleistocene → present
Genus *Ceratotherium* (Gray, 1867)
Species: *C. simum* (Burchell, 1817) Early Pleistocene → present
Tribe Rhinocerotini (Gray, 1821)
Subtribe Dicerorhinina
Genus *Dicerorhinus* (Gloger, 1841)
Species: *D. sumatrensis* (Fischer, 1814) Early Pleistocene → present
Subtribe Rhinocerotina (Dollo 1885)
Genus *Rhinoceros* (Linnaeus, 1758)
Species: *R. sondaicus* (Desmarest, 1822) Early Pleistocene → present
R. unicornis (Linnaeus, 1758) Middle Pleistocene → present

2.3.1 Black rhino - **Diceros bicornis** *(Linnaeus 1758)*

The so called "black rhino" is a medium-large sized rhinoceros of about 1.6 m height at the shoulder and 3.3-3.6 m in length (Dollinger and Geser 2007). An adult weights from 800 to 1400 kg, with females generally smaller than males (Hillman-Smith and Groves 1994). It is a double horned species with the larger nasal horn typically around 70 cm long (Hillman-Smith and Groves 1994).

The common name "black rhino" was to distinguish the species from the other African rhino (the so called "white rhino"), but it originated from a misunderstanding and the two species cannot be identified by the color of the skin. The "black rhino" can be distinguished by the "white rhino" thanks to clear morphological differences: the shorter head, the pointed and prehensile upper lip, and the absence of the dorsal hump (Hillman and Groves 1994).

Figure 1: Extant rhinoceros species: A, *Diceros bicornis*; B, *Ceratotherium simum*; C, *Dicerorhinus sumatrensis*; D, *Rhinoceros unicornis*; E, *R. sondaicus*.


A


B


C


D


E

It is a Critically Endangered species in the IUCN Red List (International Union for Conservation of Nature), led to the brink of extinction by illegal poaching for its horn (particularly in the second half of the XX century) and by loss of habitat. Three subspecies are found in the south and eastern central Africa (**Figure 2**). A fourth subspecies, the west African black rhino (*D. b. longipes*), once living in Cameroon, has been declared extinct (World Conservation Union, 2006).

This species is a browser herbivorous feeding on leafy plants, branches, shoots, thorny wood bushes and fruit, in savannahs, acacia scrub and tropical bush-land habitats. Its teeth are brachiodont and reduced to the only jugals. In the hottest time of the day the rhinos are

resting, sleeping or wallowing in the mud. Wallowing is functional in all the species in cooling down the body temperature and protecting against parasites. They are solitary animals with bad eyesight, and scent marking is often used to identify other individuals (Emslie and Brooks 1999, Rookmaaker 2005). *Diceros bicornis*'s life lasts around 30-35 years in the wild and more than 45 years in captivity (Dollinger and Geser 2007).

2.3.2 White rhino - Ceratotherium simum *(Burchell 1817)*

The so called "white rhino" is among the largest land animals of the world, with the Indian rhinoceros, just second after the elephants. It is tall about 1.5-1.8 m at the shoulder and long about 3.3-4.2 m, with an average weight of 1400-1700 kg for females and 2000-3600 kg for males; the nasal hors is larger than the frontal one and long 60-100 cm (Nowak 1991).

It shows a characteristic dorsal hump on the neck and flat wide lips. The common name "white" rhinoceros derives from the wrong translation of the African word "wyd" that means "wide" and refers to the width of the lips. The alternative name "square-lipped rhino" is therefore more precise, but very rarely used.

It is a Near Threatened species in the IUCN Red List. This is the only rhino well recovered from the brink of extinction (poaching and loss of habitat), even if the northern subspecies *C. s. cottoni* is very reduced. The southern white rhino, *C. s. simum* has a numerosity estimated in around 14.500 individuals, up from about 50 only one century ago (Markey 2006) (**Figure 2**).

The species is a pure grazer of grasslands and savannah habitats, with hypsodont and plagiolophodont teeth and tick cementum. The species is the most tame and gregarine among rhinoceroses (Groves 1982) and in the wild the length of life is about 40-50 years (Emslie and Brooks 1999).

2.3.3 Sumatran rhino - Dicerorhinus sumatrensis *(Fischer 1814)*

The Sumatran rhino is the smallest among extant rhinoceroses, tall about 1.10-1.40 m at the shoulder, long around 2.40-3.00 m and with a weights of 650-1000 kg (Groves and Kurt 1972). The species is double horned, the nasal horn is larger and long around 25-80 cm, the frontal horn is smaller, particularly in females where it can be absent (Groves and Kurt 1972). An important character shared by all the Asian species is the presence of incisor teeth.

Figure 2: African species distribution from Emslie and Brooks (1999): A) *Diceros bicornis* and B) *Ceratotherium simum*.

A

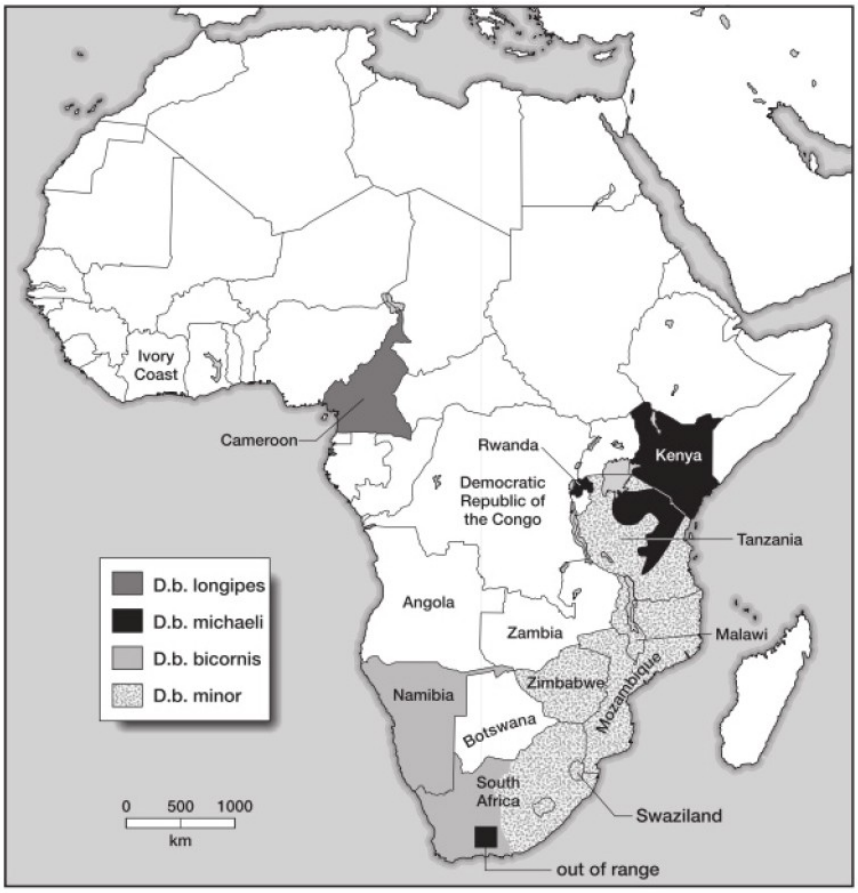

B

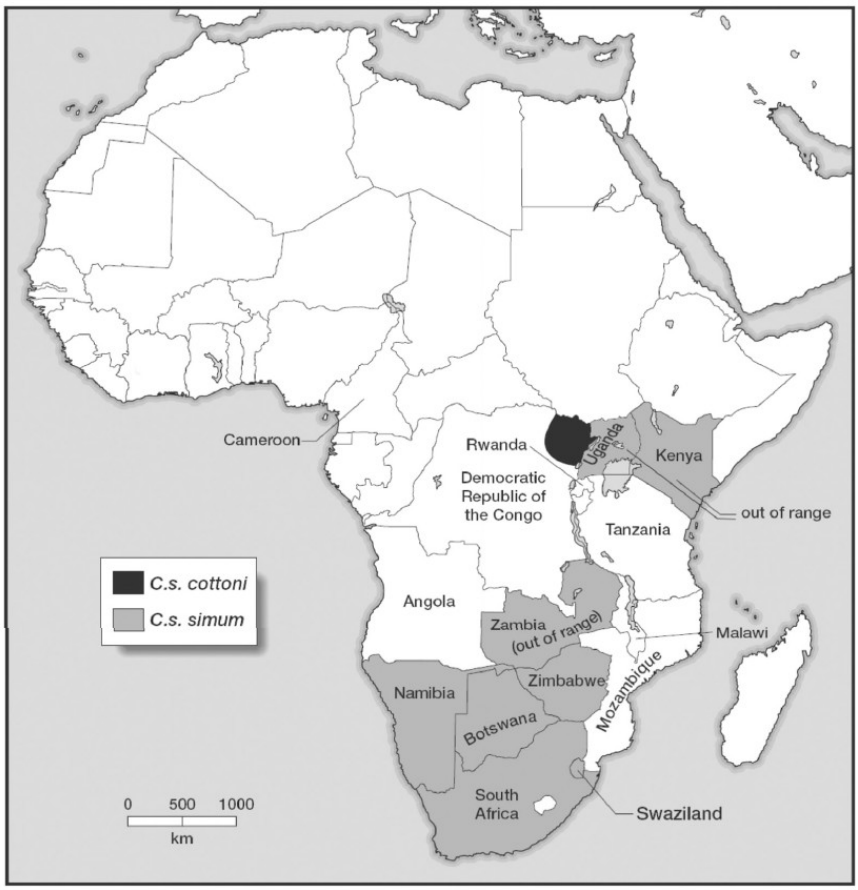

This is the most hairy rhinoceros, particularly calves and young adults have long and dense red-brown hairs, the color turns to black in old individuals (Groves and Kurt 1972).

It is a Critically Endangered species in the IUCN Red List, in fact was once widespread in the Southeast Asia but now not more than 300 individuals are estimated to survive, divided in several small and isolated populations (**Figure 3**) as a result of poaching and destruction of habitat (Rabinowitz 1995, Van Strien 2001). Two subspecies are recognized: the western Sumatran rhino, *D. s. sumatrensis* is the nominal subspecies, and the smallest form, *D. s. harrisoni*, living in Borneo (eastern Sumatran rhino). A the third subspecies, now extinct, was the northern *D. s. lasiotis*, once found in India and Bangladesh, which was the biggest among *D. sumatrensis* subspecies (Rookmaaker 1984).

The habitat of the Sumatran rhinoceros are lowland and highland rainforest, swamps and cloud forests, in areas close to water, in fact it spends a large amount of time in wallowing, feeding before nightfall and in the morning (Foose and Van Strien 1997). *D. sumatrensis* is a pure browser and its diet is based on young saplings, leaves, fruits, twigs and shoots (Van Strien 1974).

Adults individuals are solitary and the life time is estimated in around 30-45 years in the wild (Groves and Kurt 1972). This species is the most vocal among the rhinoceros; vocalizations is thought to convey danger, sexual readiness, and location and can be heard at a great distance (Von Muggenthaler et al. 2003).

2.3.4 Indian rhino - Rhinoceros unicornis *(Linnaeus 1758)*

Similar in size to the African white rhino, *R. unicornis* has a body length of 3.1-3.8 m and height at the shoulder of 1.5-1.86 m, with a weight of about 1600-3000 kg (Nowak 1991, Owen-Smith 1984). Males are larger than females. *Rhinoceros* are single horned rhinos, with the nasal horn present in both males and females in *R. unicornis* (while in *R. sondaicus* females can lack it). The length of the horn is just about 25 cm (Dinerstein 2003). The typical characteristic of the species is the presence of evident skin folds that confer the strange aspect of armoured animal, so evident in the first representations (e.g. Dürer 1515).

It is classified as Endangered species in the IUCN Red List, although once diffused from Pakistan to Bangladesh, and may have even be found in China, the human impact has reduced its range and now it survives in small populations in northeastern India and Nepal (Foose and Van Strien 1997) (**Figure 4**).

Figure 3: Asian species distribution from www.rhino-irf.org: A) *Dicerorhinus sumatrensis*, B) *Rhinoceros sondaicus.*

A

B

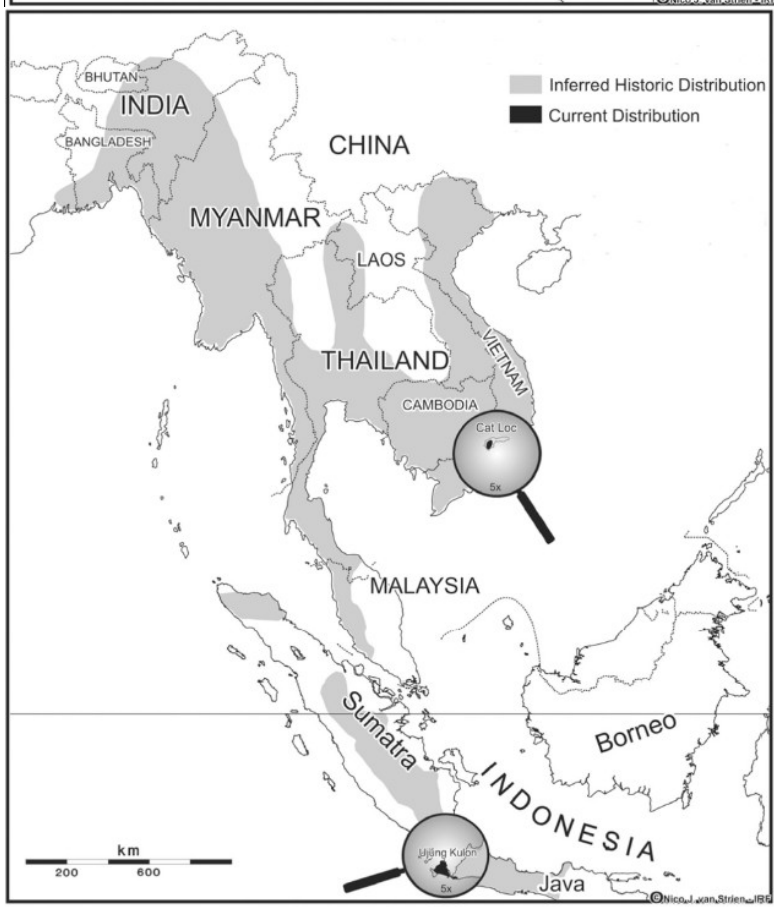

Its diet is mainly based on grasses, but includes also leaves, branches of shrubs and trees, fruits and submerged and floating aquatic plants. Therefore it is considered a mixed feeder. The species inhabits tall grasslands and forests in the foothills of the Himalaya, in Nepal and in Assam (Northeast India). It is a solitary species but some individuals can aggregate occasionally at bathing areas.

2.3.5 Javan rhino - **Rhinoceros sondaicus** *(Desmarest 1822)*

Very similar to the congeneric Indian rhinoceros, *R. sondaicus* is smaller in size, about 3.1-3.2 m long and 1.6-1.7 m high at the shoulder with an average weight of about 1500-2000 kg (Nowak 1991). The single horn is short, about 15 cm long, and it can be absent in females (Nowak 1991) who are larger than males (Groves 1982).

The species' areal ranged from Assam and Bengal, thus overlapping with both the Sumatran and Indian Rhino (Rookmaaker 2002), to Myanmar, Thailand, Cambodia, Laos, Vietnam, and to the Malay Peninsula and the islands of Sumatra, Java and possibly Borneo (Piper 2007). But now the species is listed as Critically Endangered in the IUCN Red List since it survives in two nationally-protected areas: the Ujung Kulon National Park in western Java, where the nominal subspecies *R. s. sondaicus* is find, and the Cat Tien National Park in Vietnam, subspecies *R. s. annamiticus* (Prithiviraj et al. 2006) (**Figure 3**). A third subspecies, *R. s. inermis* was known in Bengal and Myanmar but it has gone extinct at the beginning of 1900 (Foose and Van Strien 1997, Rookmaaker 1997, 2002).

The Javan rhino is a browser herbivorous and eats shoots, twigs, young foliage and fallen fruit; its primary habitat is dense lowland rain forest, wet grasslands and large floodplains, or wet areas with many mud wallows. It is a solitary species but some individuals can aggregate occasionally at bathing areas.

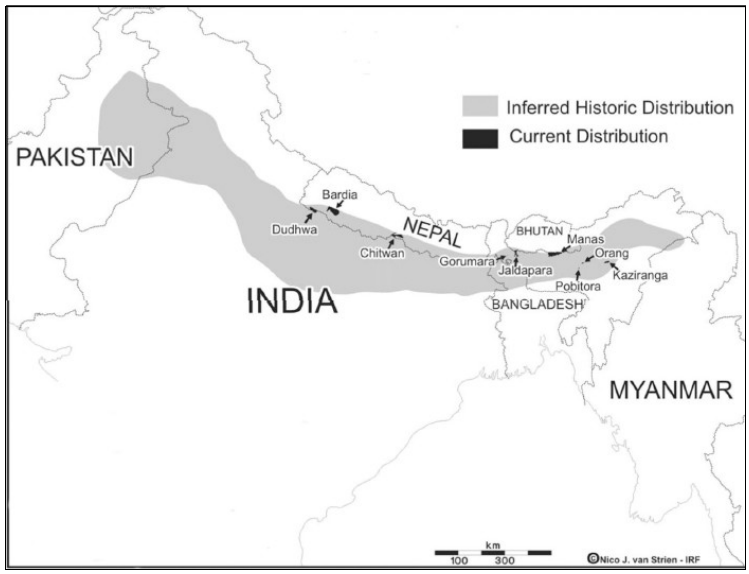

Figure 4: *Rhinoceros unicornis*' distribution, from www.rhino-irf.org.

Chapter 3

DIET INVESTIGATION THROUGH POWDER X-RAY DIFFRACTION AND CARBON ISOTOPE ANALYSES IN THE EUROPEN PLIO-PLEISTOCENE GENUS *STEPHANORHINUS* (MAMMALIA, RHINOCEROTIDAE)

3.1 Introduction

The use of carbon isotope biogeochemistry in past ecology reconstruction is now common practise in archaeology and palaeontoloyg. In fact, due to different carbon fixation processes, C_4 plants have a lesser negative $\delta^{13}C$ value than C_3 plants (Bender 1971, Smith and Epstein 1971). According to O'Learly (1981) C3 plants show a $\delta^{13}C$ of about -27.1±2.0‰ while C4 have a value of about -13.1±1.2‰.

The biogenic signal retained in enamel bioapatite is preserved in very ancient remains and it is largely used in palaeontology (e.g. Widga et al. 2010, Garcia et al. 2009, Kingston and Harrison 2007, Boisserie et al. 2005, Gaboardi et al. 2005, Palombo et al. 2005, Grimes et al. 2004, Cerling et al. 1999, MacFadden 1998, Bocherens et al. 1996, Bocherens et al. 1993, MacFadden et al. 1999). Along with enamel, bone is used in archaeology (e.g. Clementz et al. 2009, Metcalfe et al. 2009, Garvie-Lok et al. 2004, Bocherens et al. 2000, Koch et al. 1997) but the use of bone for isotopic studies of palaeontological material is not diffused because the carbon signal retention is weak in remains older than the Middle Pleistocene (Lee-Thorp 2000, Lee-Thorp and Sponheimer 2003, Palombo et al. 2010, Iacumin et al. 1997). The present research aims to investigate the diet of European rhinoceroses species (Genus *Stephanorhinus*) through the carbon isotope ratio in bone and dentine bioapatite. However, since the biogenic signal could have been lost during fossilization processes, due to bioapatite recrystallization and exogenous carbonate contamination, we pair powder X-ray diffraction analysis and carbon isotope analysis. Powder X-ray diffraction is a powerful tool to evaluate the good preservation of the biogenic information (Trueman et al. 2004, Person at al. 1995, Michel et al. 1995, LeGeros

1981) and to avoid misleading interpretation of the isotopic data; this is particularly important when dealing with poorly crystalline tissue such as bone and dentine.

In the European Pliocene the large rhinoceros *Stephanorhinus megarhinus* (de Christol 1835) is present. It is a largely browser species proper of wooded environment (Guérin 1980). In the Late Pliocene it is replaced by *S. elatus* (Croizet and Jobert 1828), a form very similar in the ecology and feeding habits but slightly smaller in size (Guérin 1972). In the Early Pleistocene a new species, *S. etruscus* (Falconer 1868) is found. This is a small forest rhinoceros, still similar to the previous species and evidently adapted to wooded and humid environment (Mazza 1988, 1993). These three species show therefore a very interesting resemblance in the ecology and diet adaptation, in spite of their different size. In the Middle Pleistocene the species *S. hundsheimensis* (Toula 1902) is recorded in Europe, it shows an extreme variability in size and diet adaptation to very different environment (Lacombat 2009, Kahlke and Kaiser 2011). In some localities it seems sympatric with other rhinoceroses species, such as the very large Middle Pleistocene *S. kirchbergensis* which has often been regarded as a pure browser and forestry species (Mazza 1993). The coexistence of different rhinoceroses species is not surprising, since ecological example are given by modern African species, so niche partitioning among browser *S. kirchbergensis* and more flexible and generalist *S. hundsheimensis* can be supposed (Fortelius et al. 1993, Kahlke and Kaiser 2011), even if recently it has been shown a more flexible diet in *S. kirchbergensis* too (Van Asperen and Kahlke 2015).

We investigated representative populations for each species: *S. megarhinus* from Montpellier (Hérault, France – Ruscinian, Pliocene), *S. elatus* from Vialette (Haute-Loire, France – Early Villafranchian, Late Pliocene), *S. etruscus* from Senèze (Haute-Loire, France – early Late Villafranchian, Lower Pleistocene), *S. hundsheimensis* from Mauer (Baden-Wurttemberg, Germany – Galerian, early Middle Pleistocene) and both *S. hundsheimensis* and *S. kirchbergensis* from Mosbach2 (Hessen, Germany – Galerian, early Middle Pleistocene).

3.2 Materials

A set of 26 samples including bone and dentine from fossil and modern rhinoceroses is analysed (**Table 1**). Fossil samples have been collected from French and German localities, ranging from the Pliocene to the Middle Pleistocene (**Figure 5**). Samples were provided by

the Laboratoire de Géologie de Lyon Terre Planètes Environment of the University Claude Bernard Lyon1 (UCBL), the Naturhistorisches Museum Basel (NMB), the Naturhistorisches Museum Mainz (MNHM) and the Staatliches Museum für Naturkunde Karlsruhe (SMNK).

The whole samples, consisting of small splinters and fragments (from few millimetres to centimetre average size), have been shoot with a Leica stereomicroscope (Archaeozoology Lab, Department of Human Studies, University of Ferrara), in order to collect a reference data base prior to destroy the samples.

The powder X-Ray diffraction analysis has been done under the supervision of G. Cruciani (Department of Physics and Earth Sciences, University of Ferrara) and the isotope analysis has been performed by C. Natali (Department of Physics and Earth Sciences, University of Ferrara).

Table 1: Specimens of fossils and modern rhinoceroses analyzed by pXRD and carbon biogeochemistry.

N°	Tissue	Element	Catalogue	Museum	Locality	Species	Author
B15	bone	vertebra	FSL 210959	UCBL	Senèze	*S. etruscus*	Guérin 1980
B16	bone	indet.	FSL 210959	UCBL	Senèze	*S. etruscus*	Guérin 1980
B17	bone	mandible	FSL 40079	UCBL	Montpellier	*S. megarhinus*	Guérin 1980
B18	bone	nasal	FSL 440	UCBL	Montpellier	*S. megarhinus*	Guérin 1980
B19	bone	femur	FSL 40896	UCBL	Montpellier	*S. megarhinus*	Guérin 1980
B20	bone	femur	FSL 40424	UCBL	Montpellier	*S. megarhinus*	Guérin 1980
B21	bone	indet.	no number	NMB	Vialette	*S. elatus*	Guérin 1972
B22	bone	scapula	M.P. 644	NMB	Montpellier	*S. megarhinus*	Guérin 1980
B23	bone	indet.	Se. 1711	NMB	Senèze	*S. etruscus*	Guérin 1980
B24	bone	radius	Se. 1703	NMB	Senèze	*S. etruscus*	Guérin 1980
B26	bone	humerus	MS 0622	SMNK	Mauer	*S. hundsheimensis*	Schreiber 1999
B27	bone	humerus	PW 1973/305	MNHM	Mosbach2	*S. hundsheimensis*	Ballatore, unpublished
B28	bone	humerus	PW 1940/207	MNHM	Mosbach2	*S. hundsheimensis*	Ballatore, unpublished
B29	bone	humerus	PW 1968/358	MNHM	Mosbach2	*S. kirchbergensis*	Ballatore, unpublished
D01	dentin	mandible	FSL 211112	UCBL	Senèze	*S. etruscus*	Guérin 1980
D02	dentin	lower tooth	FSL 210928	UCBL	Senèze	*S. etruscus*	Guérin 1980
D04	dentin	upper tooth	M.P. 448	NMB	Montpellier	*S. megarhinus*	Guérin 1980
D05	dentin	lower tooth	PW 1988/302	MNHM	Mosbach2	*S. kirchbergensis*	Ballatore, unpublished
D06	dentin	lower tooth	MS 0849	SMNK	Mauer	*S. hundsheimensis*	Schreiber 1999
M01	bone	vertebra	7351	NMB	Bhutan	*Rhinoceros unicornis*	
M02	bone	indet.	n.N. 009	NMB	(unknown)	*Rhinoceros unicornis*	
M03	bone	vertebra	10885	NMB	Java	*Rhinoceros sondaicus*	
M04	bone	rib	10529	NMB	Basel Zoo	*Dicerorhinus sumatrensis*	
M05	bone	rib	10594	NMB	SwissCircus	*Diceros bicornis*	
M06	bone	rib	n.N. 082	NMB	(unknown)	*Diceros bicornis*	
M07	bone	rib	8029	NMB	Uganda	*Ceratotherium simum*	

Figure 5: Location of the European Plio-Pleistocene localities included in the XRD and carbon biogeochemistry analyses.

Mosbach2	Middle Pleistocene	Late Galerian	0.6-0.4 MY (Schreiber et al. 2007)
Mauer	Middle Pleistocene	Late Galerian	0.6-0.4 MY (Schreiber et al. 2007)
Senèze	Lower Pleistocene	early Late Villafranchian	2.2 MY (Nomade et al. 2014)
Vialette	Late Pliocene	Early Villafranchian	3.1 MY (Thouveny and Bonify 1984)
Montpellier	Pliocene	Ruscinian	6.5-4.5 MY (Guérin 1982)

3.3 Methods

3.3.1 Powder X-Ray Diffraction (pXRD) analysis

Porous spongy bone have been manually removed and compact bone carefully selected. Then each sample has been pulverized into fine powder in agate mortar (modern samples have been heated to 100°C for 2 h before powdering). XRD has been performed at the University of Ferrara (Diffraction Lab, Department of Physics and Earth Sciences). Row data have been refined with Le Bail method in order to obtain cell parameters, cell volume and crystallite size.

3.3.2 Carbon Isotope analysis

The experimental procedure for carbon isotope analysis encompassed the following steps:

1. Thermal treatment. In order to remove any organic matter, the samples have been heated in muffle-furnace to 400°C for 12 h, as suggested by Grimes et al. (2004). We used an average of 60 mg of powder for fossil specimens and about 120 mg for modern specimens. The treatment removes organic carbon without alteration of the carbonate carbon (Lindars et al. 2001). It does not affect the crystalline structure since apatite recrystallization occurs at 600°C (Holden et al. 1995).
2. Acid treatment. An acid treatment for the removal of diagenetic carbonates has been performed following Koch et al. (1997): samples have been soaked for 3 days in 0.1 M acetic acid solution (pH≈2.9) using 0.04 ml solution/mg sample, then rinsed five times with excess deionized water. Finally the samples have been dried at 60°C for 12 h.
3. Isotopic analysis. The carbon isotope ratio has been detected through EA-IRMS (Elemental Analysis – Isotope Ratio Mass Spectrometry, at the Department of Physics and Earth Sciences, University of Ferrara).

3.4 Results

3.4.1 pXRD

The crystallite size obtained by the full profile fitting (Le Bail) is reported in **Table 2**. It shows evident trends related to carbonate substitution. The crystallite size decreases as the cell volume increases. As a matter of fact, modern bone has a high cell volume and very

low crystallite size and there is no differences between bone and dentine (**Figure 6**-A). The volume reduction in recrystallization, from the comparison with the modern bone, involves Type B structural carbonate inclusion, replacing for bone phosphate, that is evident from the high c/a ratio (c increasing and a decreasing is related to Type B substitution, Michel et al. 1995).

This proves crystallite size as a good predictor in estimating the biogenic signal retention. Most of the fossil samples here analysed turned to have a crystallite size too high to preserve the biogenic isotopic ratio.

Looking at the variation of the crystallite size during time (**Figure 7**), there is no strong correlation with age, even if the crystallite size is higher in fossil samples with respect to modern ones and it seems to increase slightly in earlier specimens (especially in bone). But the two distinct localities of Mosbach2 and Mauer show how the crystallinity value can vary noticeably in coeval samples, suggesting that it depends mainly on taphonomy and not on age (as reported by Person et al. 1995). The influence of different taphonomical conditions is evident also within a single locality, as it is shown by the samples from Senèze.

Locality	**n.**	**Tissue**	**Crystallinity size (nm)**	**$\delta^{13}C$ (‰)**
Montpellier	B17	Bone	14,950	-14,3±0,1
Montpellier	B18	Bone	14,810	-13,8±0,1
Montpellier	B19	Bone	15,520	-13,9±0,1
Montpellier	B20	Bone	16,480	/
Montpellier	B22	Bone	15,170	-13,0±0,1
Montpellier	D04	Dentine	12,343	-15,1±0,1
Vialette	B21	Bone	14,230	-8,4±0,1
Senèze	B15	Bone	13,690	/
Senèze	B16	Bone	13,320	-15,0±0,1
Senèze	B23	Bone	17,180	/
Senèze	B24	Bone	11,496	/
Senèze	D01	Dentine	12,490	-15,1±0,1
Senèze	D02	Dentine	10,277	-14,5±0,1
Mauer	D06	Dentine	/	-18,0±0,1
Mauer	B26	Bone	14,340	/
Mosbach2	B27	Bone	8,533	/
Mosbach2	B28	Bone	10,649	-16,3±0,1
Mosbach2	B29	Bone	8,528	-16,7±0,1
Mosbach2	D05	Dentine	8,980	-16,1±0,1
R. unicornis	M01	Bone	5,997	/
R. unicornis	M02	Bone	/	-15,8±0,1
R. sondaicus	M03	Bone	/	-18,5±0,1
D. sumatrensis	M04	Bone	/	-18,1±0,1
D. bicornis	M05	Bone	/	-16,7±0,1
D. bicornis	M06	Bone	/	-17,8±0,1
C. simum	M07	Bone	/	-6,6±0,1

Table 2: Crystallinity size and $\delta^{13}C$ values for the fossil and modern rhinoceroses specimens analysed.

Figure 6: Fossil bone and dentine powder diffraction data (Le Bail refinement) compared to modern bone. A) Crystallite size vs cell volume, B) crystallite size vs cell parameter ratio.

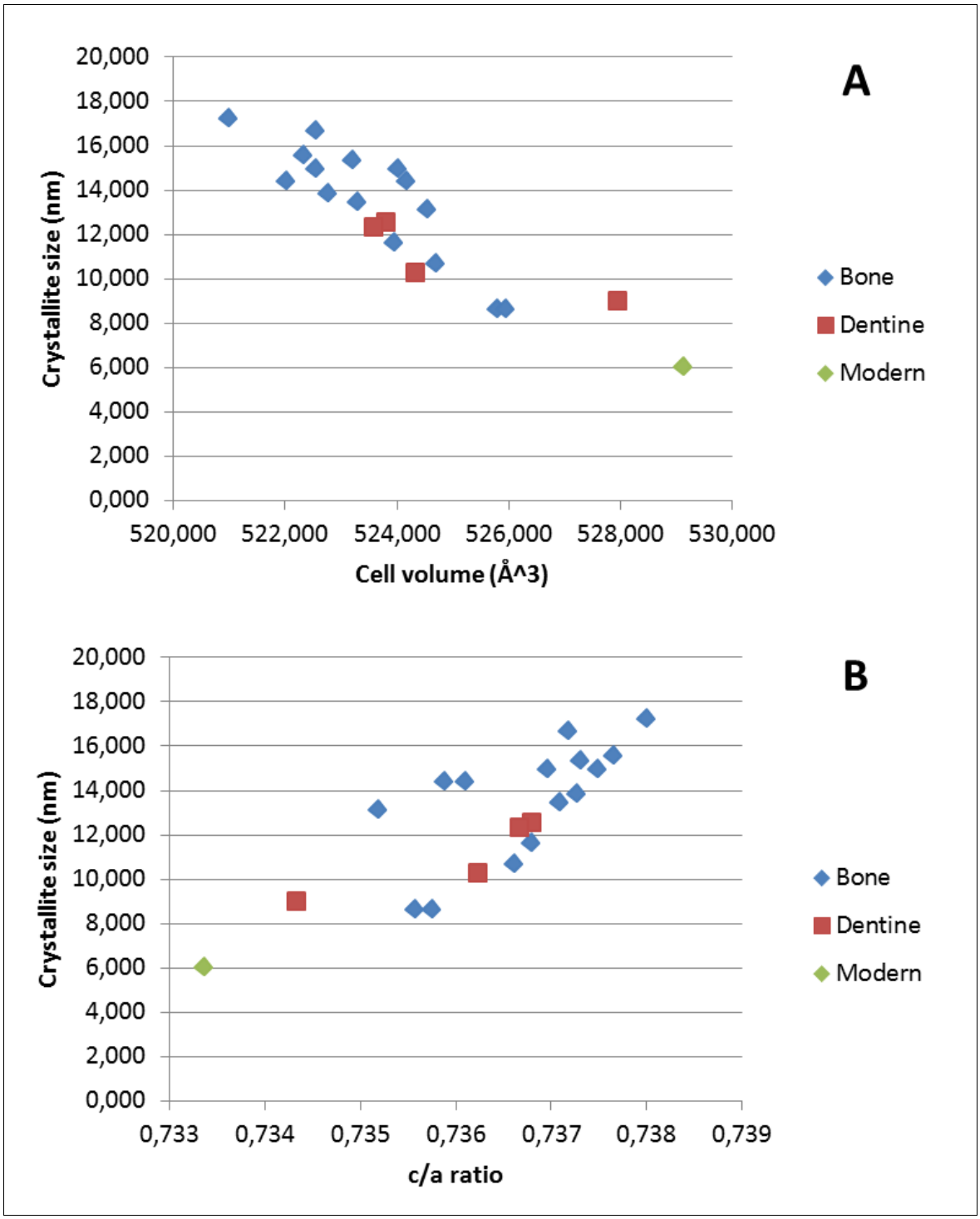

3.4.2 Thermal and acid treatments

Fossil bone and dentine show a similar pattern of weight loss during thermic and acid treatments. As expected, the percentage of weight loss is considerably lower than in modern bone's samples. Table of weight data are provided in attachment (**Attachment I**).

Figure 7: Crystallinity size variations in relation to age. 0-Montpellier (6.5-4.5 MY), 1-Vialette (3.1 MY), 2-Senèze (2.2 MY), 3-Mauer (lower line) and Mosbach2 (0.6-0.4 MY), 4-modern sample.

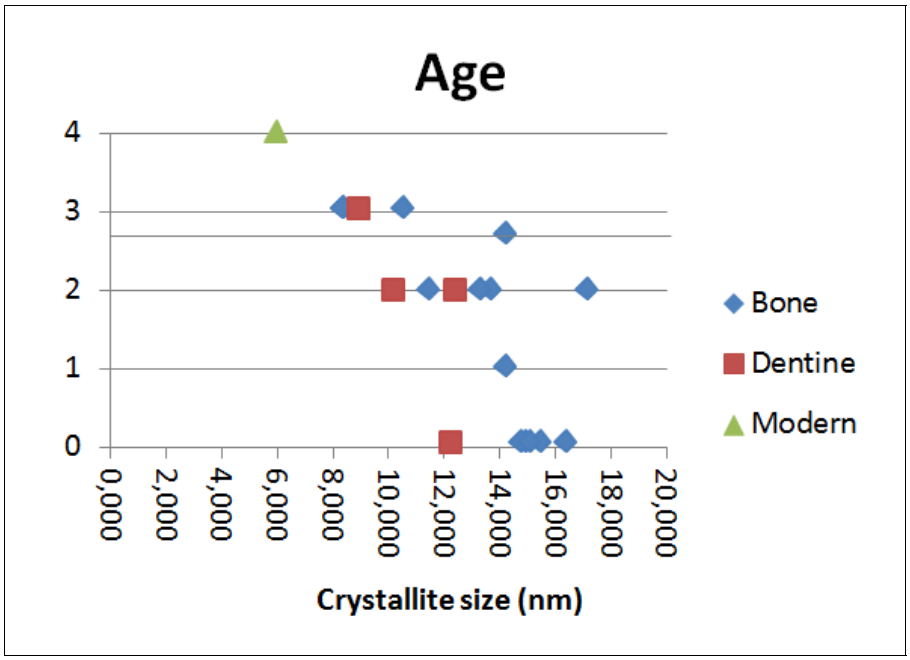

3.4.3 Isotope geochemistry

The $\delta^{13}C$ values are reported in **Table 2** and plotted in **Figure 8**, no differences are evident between bone and dentine samples. Among the modern samples, one specimen of *D. bicornis* (M05) shows a lesser negative value, close to the mixed feeder *R. unicornis,* but this specimen comes from a circus so the animal grew in captivity.

The rhinoceroses *S. hundsheimensis* and *S. kirchbergensis* from Mosbach2 show the same $\delta^{13}C$ value and are intermediate between the modern browsers (*Rhinoceros sondaicus, Dicerorhinus sumatrensis* and *Diceros bicornis*) and mixed feeder (*R. unicornis*), in particular they are closer to the latter. The palaeopopulations from Montpellier and Senèze show similar values, less negative than modern browsers, fossil rhinoceroses from Mosbach2 and modern mixed-feeders (but still far from the modern grazers). Therefore they are significantly different from the palaeopopulation from Mosbach2. The extent of the differences among these populations is investigated through coupled Student's *t*-test whose associated *p*-values are reported in **Table 3**.

As concerning the palaepopulation from Vialette, the single sample available, releases a high $\delta^{13}C$ value, very close to the value of the grazer *Ceratotherium simum*. Since the morphological structure of the teeth from Vialette is not compatible with such an abrasive diet, the data must be affected by some bias. As a matter of fact, a single specimen is not

enough for reliable interpretations.

Also from the locality of Mauer a single sample releases carbon isotope values (unfortunately this is not the same sample which gave cristallinity size). This results more negative than the specimens from the coeval locality of Mosbach2, thus indicating a pure browsing diet comparable with the modern *D. sumatrensis* and *R. sondaicus*.

Since there is no correlation between the $\delta^{13}C$ value and the carbon percentage (wt%), the variation in the isotope ratio must be related to diet or diagenesis (**Figure 9**).

Figure 8: $\delta^{13}C$ values form fossil bone and dentine and modern bone. 0-Montpellier (*Stephanorhinus megarhinus*), 1-Vialette (*S. elatus*), 2-Senèze (*S. etruscus*), 3-Mauer (lower line, *S. hundsheimensis*) and Mosbach2 (h, *S. hundsheimensis*; k, *S. kirchbergensis*), 4-Modern species (A, *Rhinoceros sondaicus*; B, *Dicerorhinus sumatrensis*; C, *Diceros bicornis*; D, *Rhinoceros unicornis*; E, *Ceratotherium simum*).

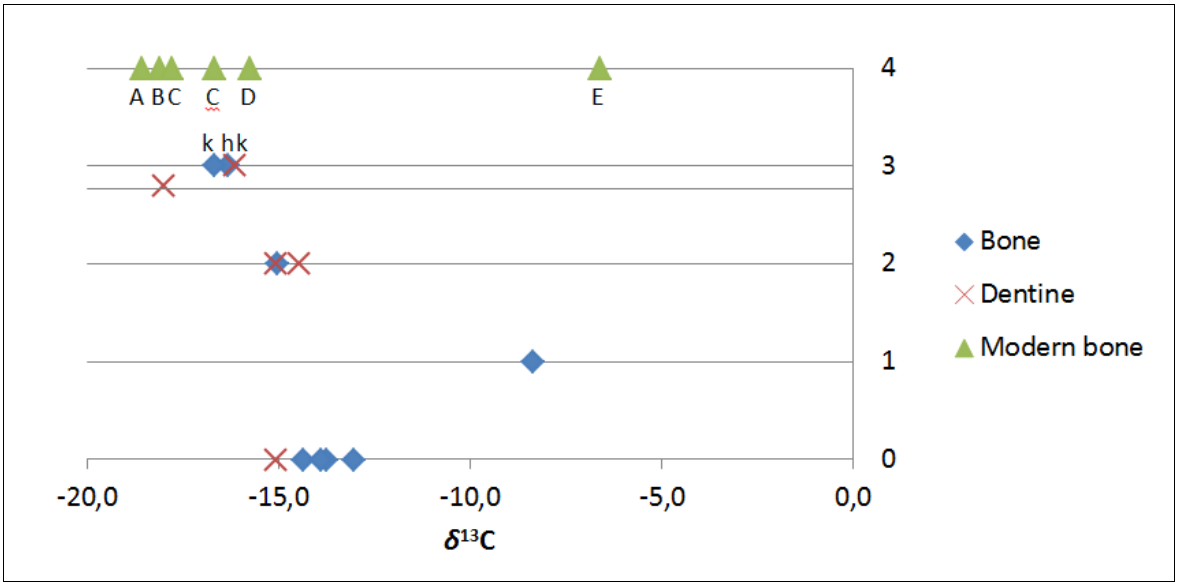

	Montpellier	Senèze	Mosbach2
Senèze	**0.2291**		
Mosbach2	0.0011	0.0076	
Modern browsers	0.0000	0.0006	0.0029

Table 3: Student's *t*-test associated *p*-value (significance level α=0.05) for $\delta^{13}C$ value of selected populations (Vialette and Mauer are not included because only one sample is available for each). Not significant values (p>0.05) are given in bold type. Modern browsers species are: *R. sondaicus, D. sumatrensis* and *D. bicornis* (captivity specimen excluded).

Figure 9: Plot of carbon content and $\delta^{13}C$ values for the modern and fossil samples included in the analyses.

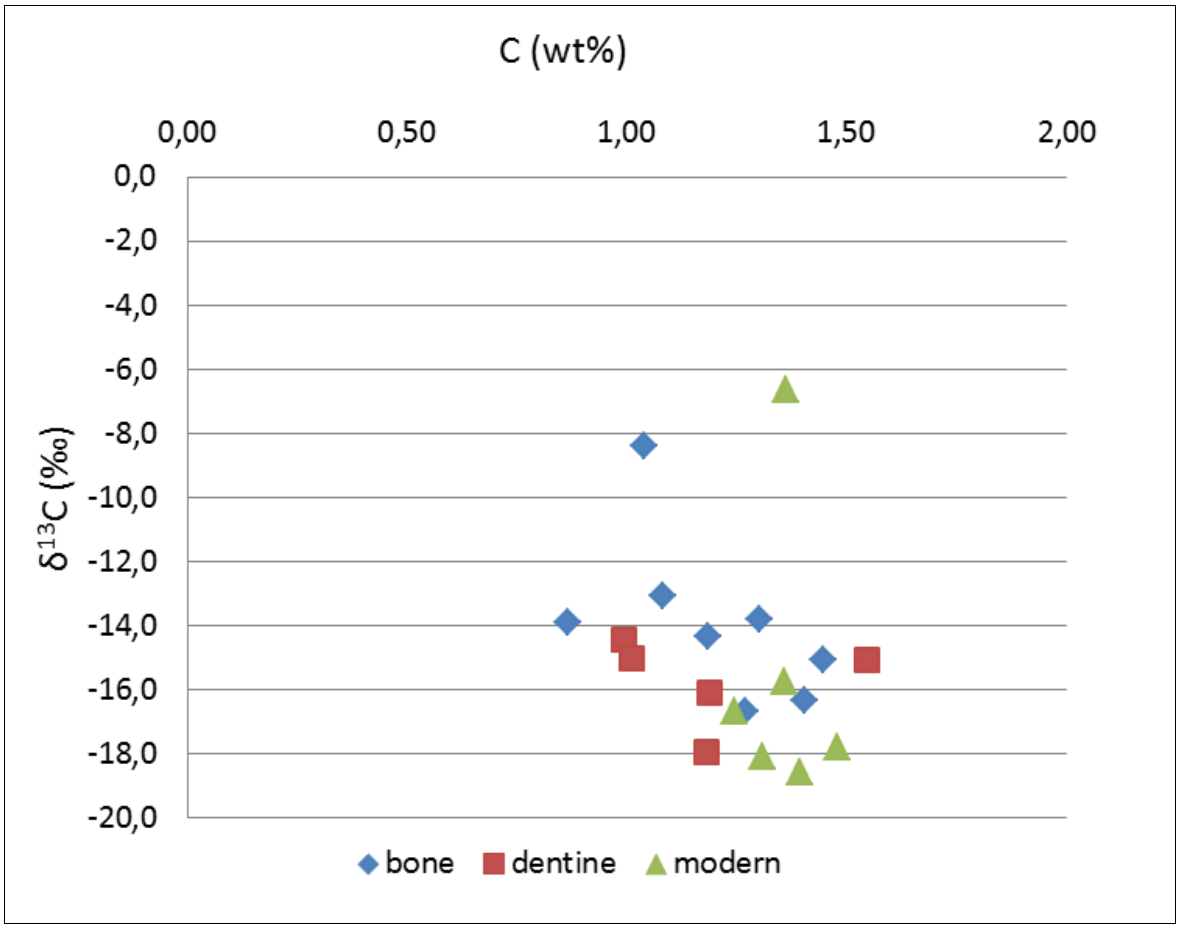

3.5 Discussion

The samples from the Middle Pleistocene locality of Mosbach2 show the lowest crystallite size and reliable carbon isotope ratio comparable with modern not grazer species, and particularly close to the mixed feeder *R. unicornis*. However, no difference in the carbon ratio appears between the two sympatric species *S. hundsheimensis* and *S. kirchbergensis*, so the hypothesis of niche partitioning cannot be supported and further investigations are needed to assess whether the two species were not sympatric but simply alternated in the same area.

From the Middle Pleistocene of Mauer, a single specimen of *S. hundsheimensis* (D06) gives isotopic result, but we have no diffraction data to predict the isotopic biogenic signal alteration. Moreover it shows a more negative $\delta^{13}C$ values (-18,0 ‰) than the specimens from Mosbach2 and thus suggests a pure browser diet. This is not in agreement with enamel data (Pushkina et al. 2015) reporting lesser negative values (-14,92/-13,31‰) for

the rhinoceros of Mauer.

The other samples have a high crystallite size that suggests an alteration of the isotopic ratio. This is confirmed by the isotope analysis of the sample from Vialette which gives an anomalous value. Even if the value has no absolute significance, we could consider the relative difference between the populations from Montpellier and Senèze. They result similar, both in the crystal size range and in the $\delta^{13}C$ values, further analysis including mesowear and microwear can solve the problem relative to these different sized species with an apparently similar diet (cfr. Chapter 3).

As concerning the modern species, the classical mesowear classification by Fortelius and Solounias (2000) is confirmed by carbon isotope analysis, with *R. unicornis* as "mixed feeder" and *D. bicornis, D. sumatrensis* and *R. unicornis* as "browsers".

3.6 Conclusion

The powder X-ray diffraction as a test on the structural carbon retention and the successive isotope ratio analysis led to the general methodological conclusion that crystallite size predicts the good preservation of the isotopic biogenic signal or its alteration; high crystallinity indicates heavy bone recrystallization and exogenous carbonate inclusion. Bone tissue gives reliable isotopic information in specimens younger than the Middle Pleistocene with a low crystallinity index, specimens with high crystallinity are not suitable for carbon isotope data (as it is confirmed by the geochemical analysis).

As concerning the diet inferences through carbon isotope in the investigated species, the two rhinoceros species recorded at Mosbach2, *S. hundsheimensis* and *S. kirchbergensis*, have the same diet. They are close to the extant *R. unicornis* so they should be considered as generalists mixed feeders. Thus isotope results are in good agreement with the recent mesowear analyses that indicate as generalist feeders other palaeopopulations of the two species (*S. hundsheimensis*, Kahlke and Kaiser 2011; *S. kirchbergensis*, Van Asperen and Kahlke 2015). Moreover the hypothesis of sympatry of the two species at Mosbach2 (Fortelius et al. 1993 – they suggest a third rhinoceros species were present, *S. hemitoechus*) should be reviewed with more attention since niche partitioning is not supported by the isotopic data.

For the most ancient species, *S. megarhinus*, *S. elatus* and *S. etruscus*, no diet inferences are possible due to the occurred recrystallization of bioapatite and to the loss of biogenic

isotopic signal (further investigations are proposed in Chapter 4).

Among the modern rhinoceroses species three groups can be distinct by the carbon isotope ratio of the bone: 1) *C. simum* (grazer), 2) *R. unicornis* (mixed feeders), 3) *D. bicornis*, *R. sondaicus*, *D. sumatrensis* (browsers).

Chapter 4

PALAEOECOLOGICAL INFERENCES FROM THE DENTAL MATERIAL OF PLIOCENE TO EARLY PLEISTOCENE EUROPEAN RHINOCEROSES: MORPHOBIOMETRY, MESOWEAR AND 3D-DMTA ANALYSES

4.1 Introduction

European Plio-Pleistocene rhinoceroses have been studied by a morphological and biometrical point of view by Guérin (1980) and then only partially reviewed because most of the following authors take into consideration only the Pleistocene species (Mazza 1993, Fortelius et al. 1993, Lacombat 2005). In particular, the ecology of the Middle Pleistocene species, namely *S. hundsheimensis*, *S. hemitoechus* and *S. kirchbergensis*, has been investigated in detail (Kaiser and Kahlke 2005, 2011, Van Asperen and Kahlke 2015, Pushkina et al. 2015) while nothing has been done concerning the earlier species. However during the Pliocene and Early Pleistocene significant climatic fluctuation and related vegetational changes occurred. In the Pliocene the forest cover was dominant in central-northern Europe, while grasses were progressively expanding in the south (Mediterranean coastal region) and two cooling phases occurred around 4.5 and 3.5 My (Suc et al. 1995). From the latter episode, a modern thermic and hydric seasonality characterized Europe with a warm and dry episode in the Upper Pliocene at 3.1-3.0 My with important diffusion of herbs grassland (Suc et al. 1992, Suc and Cravatte 1982). From the beginning of the Pleistocene the climatic fluctuations became more rapid, with vegetational alternation of Mediterranean steppe and deciduous forests (Suc and Zagwijn 1983), or coniferous and deciduous forests, at higher altitudes or latitudes (Ravazzi 1993), in correspondence of glacial and interglacial periods.

So the rhinoceros species from the European Pliocene and Early Pleistocene deserve particular interest by an ecological point of view, and our purpose is to fill such gap in their

study. We consider the Pliocene species *S. megarhinus* and *S. elatus* and the Early Pleistocene *S. etruscus*. From a phylogenetic point of view, these three species are closely related with evident differences in their size. A third described Pliocene species, *S. miguelcrusafonti*, is represented by very few teeth from a single locality and it is not included in the analysis.

4.1.1 Differences in size

According to Guérin (1972, 1980), there is an evident size difference among the three species, plus some morphological characters. To test this assumption, we compare the length ranges of the limbs' bones (humerus, radius, McIII, femur, tibia and MtIII) provided by Guérin (1980) for the three species among each other and to the same measures in the three palaeopopulations analysed in this research, respectively from Montpellier, Vialette and Senèze. Thus we cancheck the position of each population within the ranges of the relative species (**Figure 10**). *S. etruscus* has a distinctly small size range, with proportions similar to *S. elatus*. *S. elatus* and *S. megarhinus* have a bigger size with wide overlapping, but they differ in the proportions: *S. megarhinus* has longer proximal bones and shortened metapodials (in particular in the posterior limb), as expected from its heavier body mass (*S. megarhinus* reaches the biggest size). The palaeopopulation from Senèze fits in the range of the species *S. etruscus* given by Guérin (1980), sometimes plotting in its lower part (radius and metapodials). The population from Vialette also matches the range of *S. elatus* given by Guérin (1980), with the only exception of the femur which exceeds the range of the species (probably due to a different orientation of the bone in the measuring technique, such amount of difference is not surprising in very long and big bones). The palaeopopulation from Montpellier also fits in the range given by Guérin (1980) for *S. megarhinus* but the zeugopodium (radius and tibia) plots on the upper side of this range.

Figure 10: Ranges of the length of the long bones (humerus, radius, McIII, femur, tibia and MtIII - measurements in mm) for the species *S. megarhinus*, *S. elatus* and *S. etruscus* (data from Guérin 1980). The black superposed lines are the ranges of the palaeopopulations measured in this research, respectively: *S. megarhinus* from Montpellier, *S. elatus* from Vialette and *S. etruscus* from Senèze.

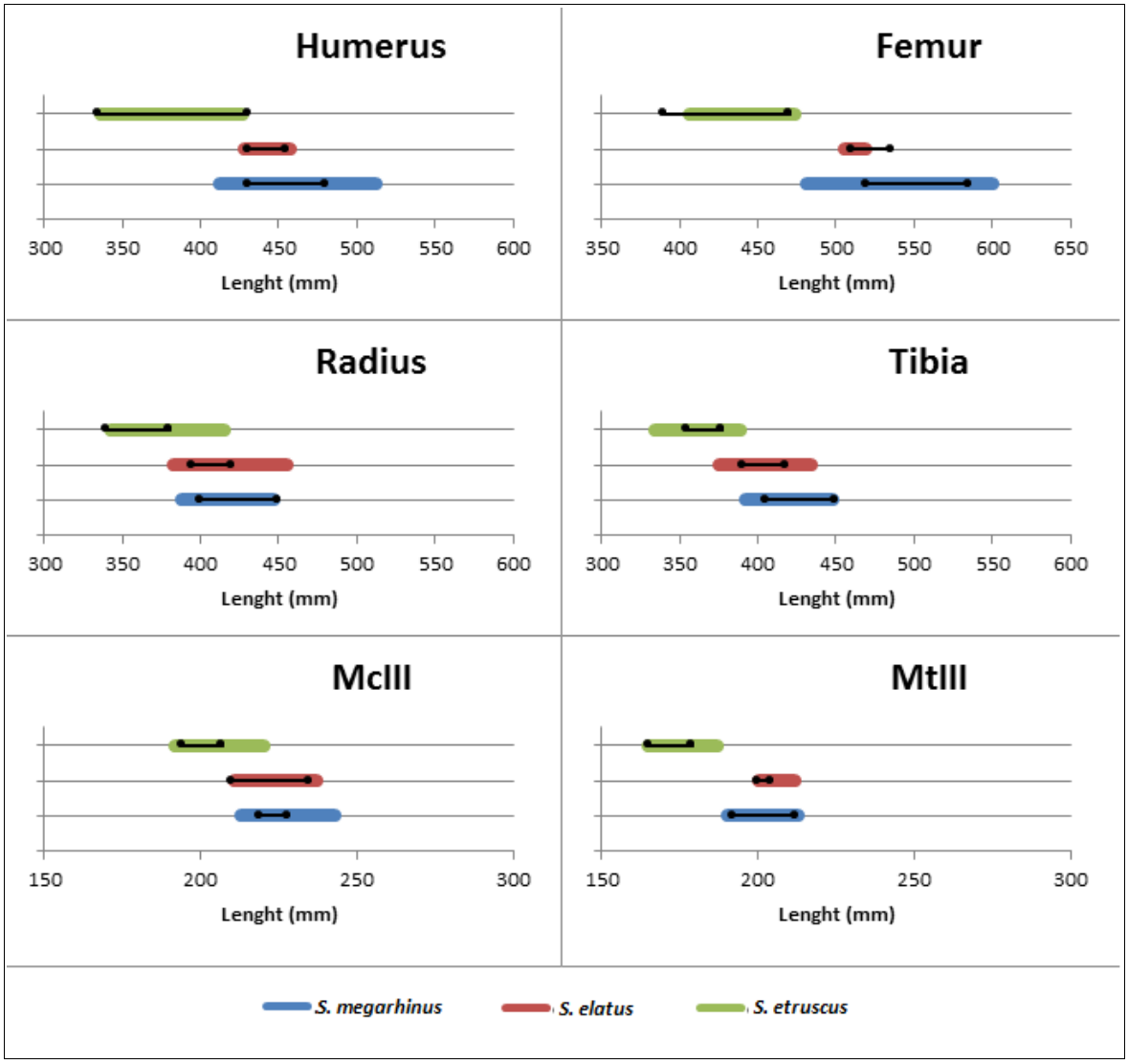

4.2 Localities

One palaeopopulation has been chosen for each species: Montpellier for *S. megarhinus*, Vialette for *S. elatus* and Senèze for *S. etruscus* (**Figure 11**). The palaeopopulations from Montpellier and Vialette are the most representative for the relative species, while as *S. etruscus* is concerned, the Tuscan type population from the Upper Valdarno should be considered as a better comparative set. However, during the PhD it was not allowed to study the collection of Florence (because of ongoing reorganization works at the exhibition

hall, where the material is mostly stored), thus we choose the palaeopopulation from Senèze as it is quite rich and is stored in the same French and Swiss museums as the remains from Montpellier and Vialette.

4.2.1 Montpellier (Hérault, France) – Ruscinian, Pliocene

Fossils from the locality of Montpellier have been known since the beginning of the XIX century (de Serre 1819, Cuvier 1822, Bravard 1828). The fauna of Montpellier was collected from several different outcrops opened in marine and continental deposits: marine sands, fluviatile gravels, marls and lacustrine formation (although no rhinoceros remains have been found in the upper lacustrine deposits, Michaux 1969).

The locality is referred to the MN 14, sub-zone of Hautimagne (Guérin 1975), and no absolute dating are available. Guérin reports an estimated age of 5-4.5 My (Guérin 1980) and 6.5-4.5 My (Guérin 1982).

Figure 11: Investigated localities.

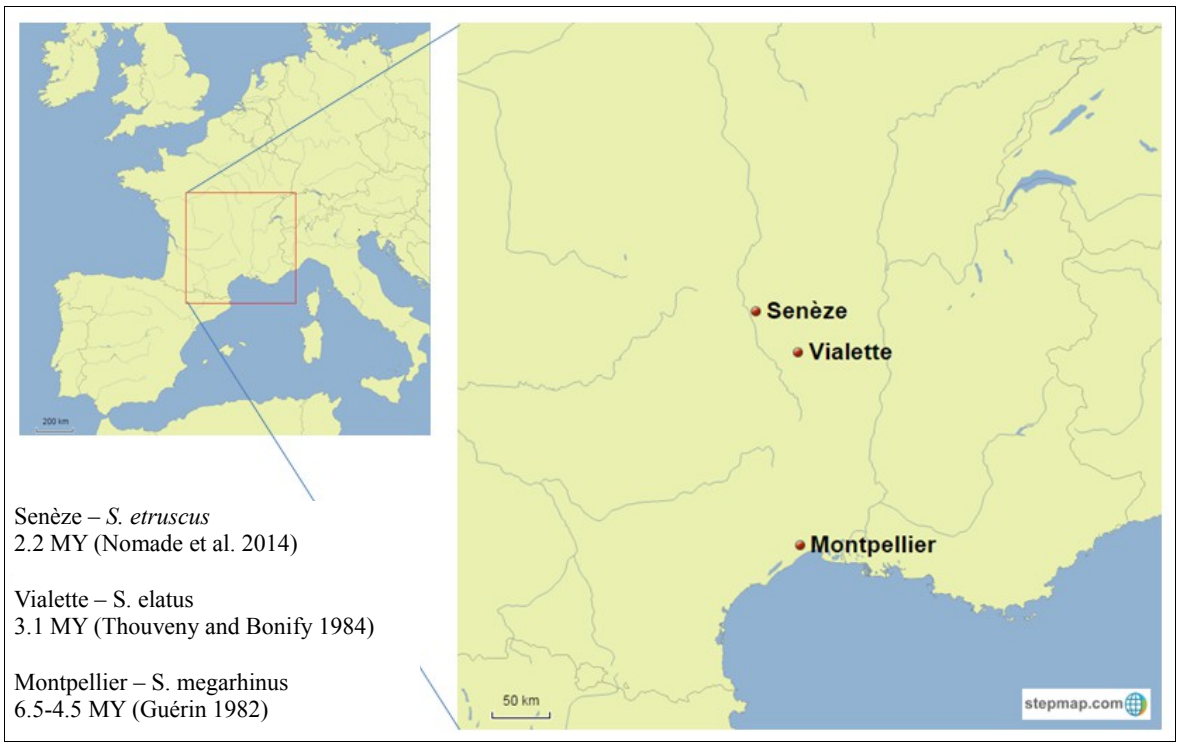

The faunal assemblage includes the following species (according to Michaux 1969): *Promimomys insuliferus, Apodemus* cf. *dominans, A. jeanteti, Parapodemus* sp., *Rhagapodemus frequens, Hylopetes* sp., *Muscardinus* cf. *pliocaenicus, Chalicomys sigmodus, Castor fiber, Prolagus corsicanus, Lepus* sp., *Pliohyrax occidentalis, Palaeoryx cordieri, Hipparion crassum, Tapirus arvernensis, Sus arvernensis, Antilope* sp., *Cervus cauvieri, Cervus australis, Paracervulus* sp., *Mastodon arvernensis, Semnopithecus monspessulanus, Macacus priscus, Pithecus maritimus, Hyaenarctos insignis, Ursus arvernensis, Viverra* aff. *pepraxti, Hyena* sp., *Felis christoli, Machairoidus* sp., *Plesiogulo monspessulanus, Lutra affinis, Meles gennvauxi, Pristiphoca occitana, Rorqualus priscus, Physalus antiquus, Balenoptera priscus, Delphinus pliocaenicus, Felsinotherium serresii*.

The rhinoceros remains consist in a great amount of isolated specimens and are the type-series of the species *S. megarhinus* (de Christol 1834, Gervais 1852). Guérin et al. (1969) chose as a neotype the partial skeleton from Millas (Eastern Pyrenees) described by Maurette (1910).

No palaeoenvironmental data are available concerning this locality (Guérin 1980 – no later works have been published), however, we can consider as a comparison the coeval locality of Saint Laurant des Arbres (Gard, France), which includes remains of *S. megarhinus* as well (Guérin et al. 1969), characterized by quite warm and humid climate with woods and forests interspersed with grasslands (Guérin 1975).

4.2.2 Vialette (Haute-Loire, France) – Early Villafranchian, Late Pliocene

The palaeontological remains from Vialette originate from a lacustrine deposit of a dammed lake (Couthures 1979). The site was discovered and excavated by Aymard (second half of the XIX century) and the first reliable faunal list was published by Depéret et al. (1923), but after them several authors dealt with the fossil remains from Vialette (e.g. Bout 1960, Kurten 1963, Heintz 1970, Guérin 1972, Heintz et al. 1974). Guérin (1980) refers the locality to the MN 16 and reports many absolute dating (3.8-3.3 My, Bout 1975; 3.3-2.6 My, Bandet et al. 1978). The fossil bearing layer is allocated in the normal magnetized subchrone Gauss, prior to the Mammuth event, and dated at 3.1 My (Biquand et al. 1981, Thouveny and Bonify 1984). Lacombat et al. (2008) assign the site to the Early Villafranchian (Triversa FU).

The most recent faunal list is provided by Lacombat et al. (2008) and includes: *Lynx issiodorensis*, *Canis* sp., the bears *Agriotherium* and *Ursus* gr. *minimus-thibetanus*, a small bovid (*Gallogoral meneghinii* or *Pliotragus ardei*), *Gazzella* cf. *Gazzella borbonica*,

Equus sp., the cervids "*Cervus*" *pardinensis*, *Croizetoceros ramosus*, cf. *Eucladoceros* sp. and *Procapreolus cusanus*, the hyenidae *Pliocrocuta perrieri*, the mastodonts *Mammut borsoni* and *Anancus arvernensis*, *Tapirus arvernensis*, primates indet. ("*Dolichopithecus*" *arvernensis* in Heintz et al. 1974).

Two almost complete rhinoceroses skeletons were retrieved with few isolated remains. Their specific attribution was very controversial (Pictet 1853, Pomel 1854, Falconer 1868, Sacco 1895, Depéret et al. 1923, Viret 1954, Thenius 1955, Bout 1960, Kurtèn 1963, Azzaroli 1962, Hurzeler 1967). At present, the rhinoceroses from Vialette are attributed to *S. elatus* (Guérin 1972, Ballatore and Breda, in press). The locality is renown due to the first occurrence in western Europe of the genus *Canis*, *Equus* and *Eucladoceros* (Lacombat et al. 2008). Humid forest taxa like *Mammut borsoni* and *Tapirus arversensis* are still present from the Ruscinian, but a climatic deterioration is suggested by the presence of species indicating open landscapes and dryer climatic condition (*Equus* and *Gazzella*) (Lacombat et al. 2008). This climatic deterioration correlates with the aridity peak recorded at 3.2-3.0 My (e.g. Shackleton 1995, Suc et al. 1992). However other new mammals, *S. elatus* and *Pliocrocuta perrieri*, are related to wooded environment (Rook and Martinez-Navarro 2010). The palaeoflora reconstruction includes many forest species: pine, juniper, linden, birch, alder, elm, beech and hornbeam (Méon-Vilain 1972).

4.2.3 Senèze (Haute-Loire, France) – early Late Villafranchian, Early Pleistocene

The locality of Senèze (Haute-Loire, France) is an ancient volcanic lake discovered in 1892. The mammal fauna was first described by Depéret and Mayet (1911). Azzaroli (1962) ascribes the locality to the Late Villafranchian and Guérin (1980) agrees correlating it to MN 18, but the real age of the site is more ancient. Indeed, Azzaroli et al. (1988) individuate two distinct mammal faunas: the ancient mammal fauna of Senèze I, from maar lacustrine deposit, referred to the Middle Villafranchian, and the more recent fauna of Senèze II, in slope deposit at the base of the crater wall, referred to the Late Villafranchian. The authors agree with Thouveny and Bonify (1984) who correlate a short normal magnetized episode (Prevot and Dalrymple 1970), recorded in the reverse maar beds below the fossiliferous layer, to the Réunion event, giving an age of 2.12-2.14 My (Azzaroli et al. 1988). This finds confirmation in the $^{40}Ar/^{39}Ar$ dating of a tephra level discovered within the normal magnetized event and dated to 2.1 My (Roger et al. 2000). Lacombat (2005) follows Bonifay (2002) in setting the fossil bearing sediments as late as 1.8-1.6 My, however the site seems to be more ancient. Breda and Marchetti (2005) considered the

fauna a homogeneous Middle Villafranchian assemblage and refer it to MIS 78 or 76. This is coherent with the latest work by Nomade et al. (2014) who place the palaeontological level between 2.21 and 2.13 My, in good agreement with Roger et al. (2000). We assess the locality to the early Late Villafranchian (Olivola FU) following Rook and Martinez-Navarro (2010).

The mammal fauna from Senèze includes (according to Lacombat 2005, Breda and Marchetti 2005): giant cheetah *Acinonyx pardinensis*, scimitar-toothed cat *Homotherium sainzelli*, saber-toothed cat *Megantereon megantereon*, raccoon *Nyctereutes megamastoides*, hyena *Crocuta perrieri*, bear *Ursus etruscus*, *Canis arnensis*, suid *Sus strozzii*, cervides *Croizetoceros ramosus, Cervus philisi* and *Eucladoceros senezensis*, small bovid *Gazellospira torticornis, Gallogoral meneghinii* and *Megalovis latifrons*, equids *Equus stehlinis* and *E. bressanus*, *Arkidiskodon meridionalis*, singe *Dolichopithecus arvernensis*. As concerning the investigated taxon, Senèze gave numerous remains of rhinoceroses, including some complete individuals, attributed to *S. etruscus* (Guérin 1980, Mazza 1988, Lacombat 2005).

Pollen analysis from the maar lacustrine sediments (core 1965) have been carried out by Elhaï (1969) who identifies five pollen units (V-I) and Roger et al. (2000) point out the correlation between the pollen units and the marine isotopic stages (MIS 85-76). The normal magnetized event occurs at the base of unit I, so the palaeontological remains (Azzaroli et al. 1988's Senéze I) can be ascribed to MIS 78 or 76 (Breda and Marchetti 2005).

4.3 Materials and methods

The material analysed includes the teeth of the three palaeopopulations from Montpellier, Vialette and Senéze. The specimens are stored in the Laboratoire de Géologie de Lyon - Terre Planètes Environnement (Université Claude Bernard Lyon 1, UCBL), at the Naturhistorisches Museum Basel (NMB), at the Muséum National d'Histoire Naturelle in Paris (MNHN) and at the Musée des Confluences in Lyon (MHNL). **Table 4** summarizes the sample size for each analysis, while the complete specimens' list is given in **Attachment II**.

The 3D-DMTA has been performed with Dr. G. Merceron (iPHEP - University of Poitiers and CNRS).

Table 4: Sample size for each performed analysis.

	Montpellier	Vialette	Senèze
Morphobiometry			
Upper teeth	13	4	6
	20	4	4
	22	3	4
	19	4	4
	17	6	6
	18	4	6
Mesowear			
Upper teeth	6	-	-
	6	4	3
Tot.	12	4	3
3D-DMTA			
Upper teeth	7	2	2
Lower teeth	7	3	7
	-	1	-
	-	1	-
Tot.	14	7	9

4.3.1 Morphobiometry

Only the upper teeth have been studied since the morphological distinction of isolated teeth is easier than on lower teeth. The identification of P2 and M3 is extremely easy. The distinction between P3 and P4 is problematic thus we included only associated P3 and P4, so that their identity is certain. In order to distinguish M1 and M2 we consider that M2 has a more distally elongated metaloph with respect to M1, resulting in a wider lingual valley and in a more trapezoidal occlusal outline of the tooth (see **Figure 12** for dental nomenclature). In this way a size-based distinction is avoided and results are free from data circularity.

Morphological characters used in previous studies on this taxon by Guérin (1980), Lacombat (2005), Ballatore and Breda (2013), seem not strongly diagnostic in the distinction of the different *Stephanorhinus* species (due to a wide interspecific variability). However they facilitate the comparison of the complex tooth morphology. The following characters are used here (**Figure 13**):

- the presence/absence of crochet, crista and antecrochet;
- the median fossettes and medisinuses closure;
- the protocone constriction development;
- the paracone fold development;
- the presence/absence of cingula.

These selected characters have been scored on the upper teeth in order to detect any differences.

Dental size has been assessed by the measurement of the two main dimensions taken at the basis of the tooth, maximum length (ML) and maximum breadth (MB) (**Figure 14**). These two measurements have been chosen because of the high precision in repeated measurements. The method is described in Ballatore and Breda (2013) and summarizes previous works (Guérin 1980, Lacombat 2005). The biometrical comparison among the three palaeopopulation is summarized by descriptive statistics (mean, standard deviation and coefficient of variation) and the extent of size differentiation is investigated through coupled Student's *t*-test (two tails, significance level α=0.05) that verifies the null hypothesis of identity of two groups, by their mean and standard deviation comparison. Scatter plot diagrams show the comparison including two measurements at once.

Figure 12: Nomenclature of rhinoceros upper teeth: A, upper M1 or M2; B, upper M3; occlusal view (drawings by M. Ballatore).

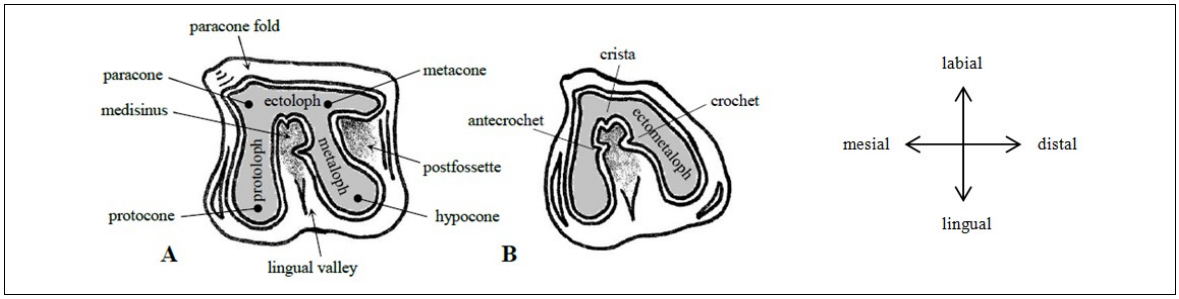

Figure 13: Morphological characters on upper tooth in occlusal view (drawings by M. Ballatore):
d) Median fossettes: 0, medisinus open; 1, mediofossette close; 2, secondary mediofossette close; 3, medisinus close.
e) Protocone constriction: 0, absent; 1, light; 2, medium; 3, strong.
f) Paracone fold: 0, absent; 1, light; 2, medium; 3, strong.

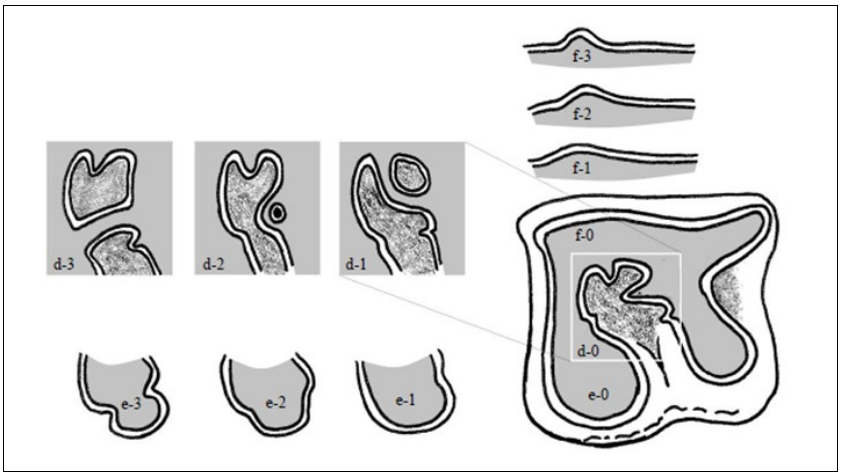

Figure 14: Dental measurements taken in this work: ML (maximum length), MB (maximum breadth). A, upper M1 or M2; B, upper M3; occlusal view (drawings by M. Ballatore).

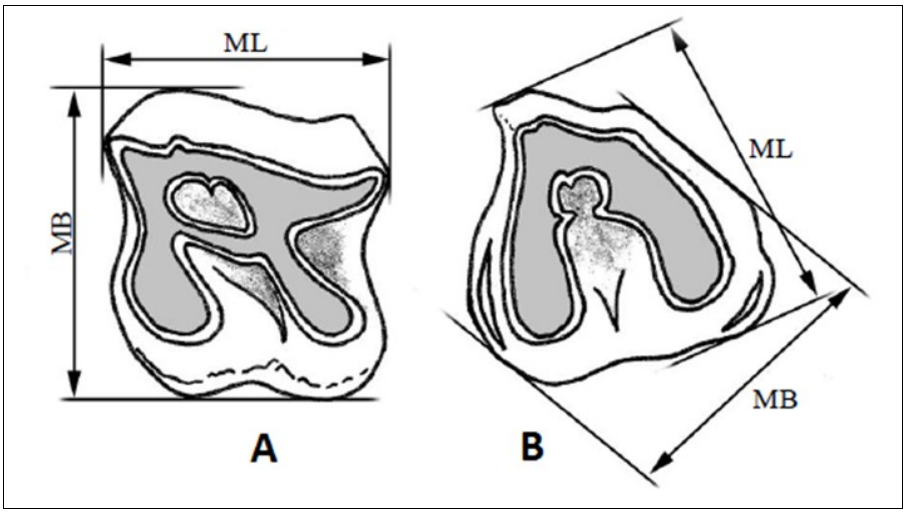

4.3.2 Mesowear analysis

Mesowear is a method envisaged by Fortelius and Solounias (2000) to quantify the modification of the labial occlusal outline of the teeth produced by the procession of food. The masticatory stroke, in the rhinoceroses, consists of two phases: during phase I the lower teeth move upward and match with the uppers, this phase is characterized by prevalent attrition (sharing component – tooth/tooth); in phase II the lower teeth move inward and the phase is dominated by abrasion (crushing-grinding components – tooth/food) (Fortelius 1982). Attrition generates high and sharp cusps while abrasion deletes them (low and blunt cusps). The mesowear technique quantifies the development of these morphologies due to attrition/abrasion prevalence considering that different kinds of food have different abrasive effects. The labial occlusal morphology has a "W" shape since two cusps are present on the labial wall of the rhinoceros upper teeth (corresponding to the paracone and the metacone)

The mesowear technique analyses two variables:

- the cusp relief (difference in height between cusps tip and inter-cusp valley: high/low);
- the cusp shape (shape of the tip of the cusp: sharp/rounded/blunt).

Then the overall mesowear score is given combining the two variables as commonly used (after Mihlbachler and Solounias 2006): 0= high/sharp, 1= high/round, 2= low/sharp, 3= low/round, 4= low/blunt (teeth with blunt cusp always show low relief so the combination high/blunt is never observed). Among these scores, 0 is the most attrition dominated part of the spectrum while 4 is the most abrasion dominated signature.

We take into account upper M1 and M2 (following Van Asperen and Kahlke 2015) and exclude unworn/very little worn teeth and teeth in late wear stages (following Fortelius and Solunias 2000). The selection of homogenous wear conditions is important, indeed Rivals et al. (2007) point out how age affects the mesowear signal that is not stable during the life of an individual, particularly in brachyodont species. Kaiser and Kalhke (2011) use the wear stages 2 and 3 proposed by Kaiser et al. (2003) for hippariones teeth. We redefine these stages for rhinoceroses as shown in **Figure 15**.

We avoid a qualitative scoring of the cusp relief and prefer a quantitative distinction between high and low relief (as suggested by Fortelius and Solounias 2000), in particular we measure the perpendicular distance between the line connecting two cusps' tips and the bottom of the in-between valley, then we calculate the ratio of the two values (distance/length, see **Figure 16**) and use the mean (0.16) as limit value distinguishing among low and high relief ("high">0.16). To take measurements on digitalized photos we use "ImageJ" software and "ObjectJ" plug-in (Scott et al. 2013).

The scoring of the cusp shape (sharp/round/blunt) is necessarily qualitative but, to reduce the subjectivity as much as possible, we adopted a direct visual comparison to three chosen standard shapes (**Figure 17**). As suggested by Fortelius and Solounias's (2000), we score this character on the metacone cusp, because the paracone cusp in rhinoceroses is modified by the development of structural elements (e.g. the paracone fold). This approach is known as the one cusp model, recently adopted for rhinoceroses by Van Asperen and Kahlke (2015), while other authors believe that both cusps can be scored (two cusp model, Kaiser and Kalhke 2011). In our opinion the indifferent (or mixed) use of the two different cusps could be imprecise.

We analyse by mesowear the three fossil species and the five extant species. The means of the mesowear score for each population/species are compared, then each mesowear variable (cusp relief and shape), given as percentage of teeth with high relief, sharp cusps and round cusps (indeed teeth with blunt cusp show low relief), are compared through hierarchical cluster analysis (UPGMA method, with Euclidean distance). The five extant species are classified according to the "conservative" dietary classification by Fortelius and Solounias (2000) based on mesowear: browsers (*Dicerorhinus sumatrensis, Rhinoceros sondaicus, Diceros bicornis*), mixed feeder (*R. unicornis*) and grazer (*Ceratotherium simum*).

Figure 15: Wear stage 2 (tooth with entire occlusal face beginning to wear, but with narrow protoloph, metaloph and distal ectoloph) and wear stage 3 (wear level reaches the mesial cingulum, but postfosset is not closed jet) exemplified by A (*S. etruscus* from Senèze - NMB Se.548) and B (*S. megarhinus* from Montpellier - NMB M.P.851) respectively. Upper molars in occlusal view not in scale.

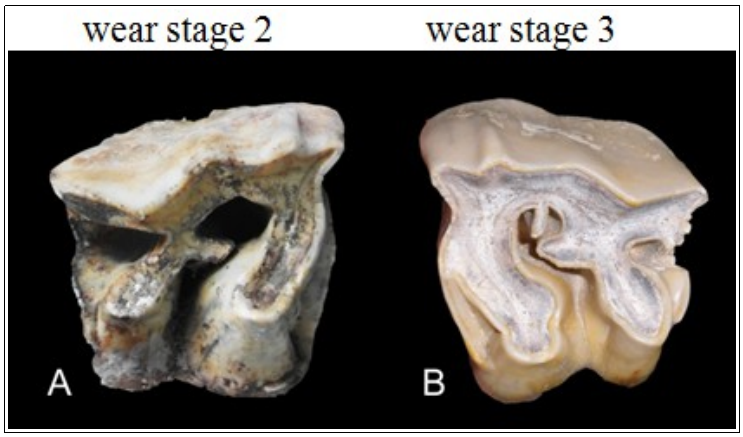

Figure 16: Cusp relief has been quantified by measuring the length (L) of the line connecting two cusps' tips and its perpendicular distance (d) from the bottom of the in-between valley. The mean value of the ratio d/L is chosen as limit. A, *S. megarhinus* from Montpellier - NMB M.P.851; B, *S. etruscus* from Senèze - NMB Se.548; upper molars in labial view not in scale.

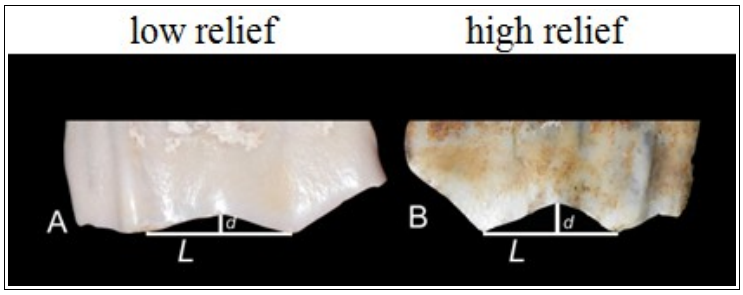

Figure 17: Cusp shape selected standards: A) sharp (*S: etruscus* from Senèze - UCBL FSL 211118), B) round (*S. megarhinus* from Montpellier - UCBL FSL 40441), C) blunt (*C. simum* - MNHN 1928-310). Upper teeth in labial view not in scale.

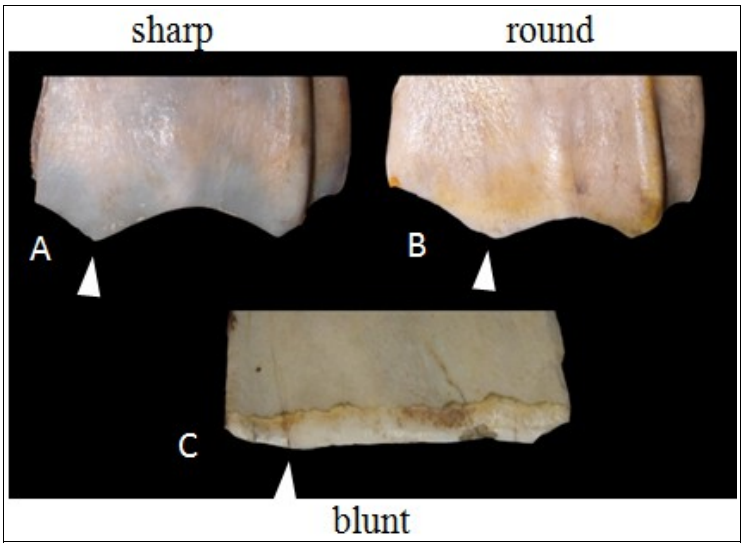

4.3.3 Dental Microwear Texture Analysis (3D-DMTA)

Dental microwear analysis, introduced by Solounias and Semprebon (2002) is based on the counting and measuring of wear micro characters (scratches, pits and gouges) on SEM acquired images. The method is heavily limited by subjectivity and observer error rate (Grine et al. 2002). Moreover 2D images are not good representations of the dental surface and the specimen's orientation affects the resulting image (Gordon 1988). Recently, a new observer error-free method has been developed (Ungar et al. 2003, Scott et al. 2005). The 3D-DMTA is based on the automated quantification of 3D enamel surfaces by using a scale-sensitive fractal analysis (Scott et al. 2006).

Moulds of the enamel facets have been taken with dentistry silicone (Regular Body President, Coltène-Whaledent) after cleaning three times each surface with acetone-soaked cotton swabs. Surfaces of 280x200 μm were scanned using high-definition confocal light microscope (Leica DCM8, iPHEP at the University of Poitiers and CNRS) using a 100x objective. Acquired scans have been leveled and dirt and defects have been removed processing with Laicamap software and four adjoining subareas (a-d) are obtained from the whole surface (**Figure 18**). Scale-sensitive fractal analysis (SSFA) has been performed through the Toothfrax software on each subarea and then median values have been calculated for each parameter for each surface. SSFA is based on fractal geometry, according to which the apparent area and related included volume of a rough surface (and the length of the section profile) change at different observation scales. Scott et al. (2005, 2006) describe four parameters to characterize the microwear surface texture:

- Complexity (*Asfc*, Area-scale fractal complexity): it is the slope of the steepest portion of the curve fitted to the plot of relative area over scale (Scott et al. 2006; **Figure 19**). If the relative area, that is the measure of a surface at a given scale, increases at a lower scale, also the complexity increases. A more complex surface has relief of different sizes overlying, therefore increasing the relative area at the finest scale.
- Heterogeneity (*HAsfc*, Heterogeneity of Area-scale fractal complexity): it is the relative variation in complexity of set of different-sized subareas, the scanned area is subdivided into equal subareas (9 cells and 81 cells) and differences in complexity at different places is calculated. Therefore heterogeneity indicates surface that shows different texture at different places (at different scale).
- Anisotropy (*epLsar*, exact proportion Length-scale anisotropy of relief): it is the length of the mean vector among the normalized vectors that define the relative

length at different orientations (5° intervals) of a depth profile. If the roughness of a surface is anisotropic, relative lengths of profiles change at different orientations, therefore *epLsar* indicates that surfaces reliefs show similar orientation (Scott et al. 2006).

- Textural fill volume (*Tfv*): it is the difference between the total fill volume and the structural fill volume (**Figure 20**). The total fill volume is obtained by filling the surface with cuboids of square face 10 μm^2, the structural fill volume is generated at a finer scale by cuboids of square face 2 μm^2.

The 3D Dental Microwear Texture Analysis provides information for a timescale ranging from a few days to a few weeks, so the method is an appropriate proxy to detect seasonal variations in diet and to pinpoint the exploitation of fallback foods (Merceron et al. 2010).

Figure 18: Example of scanned surface (Laicamap software, Trident Project): 1) 2D image of the scanned surface (280x200 µm), 2) the same surface seen on photosimulation, a-d) the four extracted subareas.

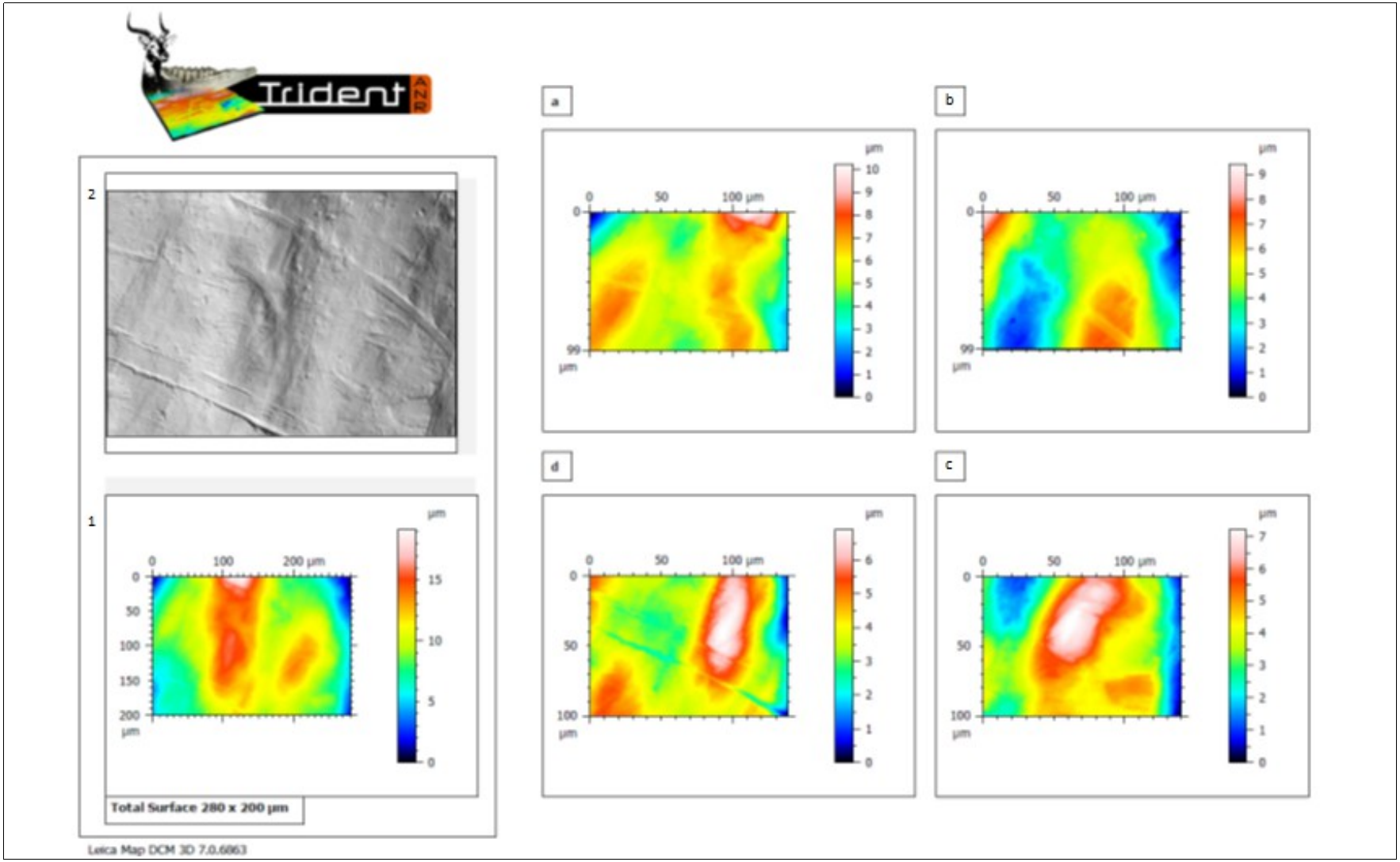

Figure 19: Scott et al. (2006), Fig. 3: "Area-scale analysis. A virtual algorithm using triangles of different size can be used to measure surface roughness (compare a, b and c). Complexity is represented by the steepest part of a curve fitted to the plot of relative area over scale (d)."

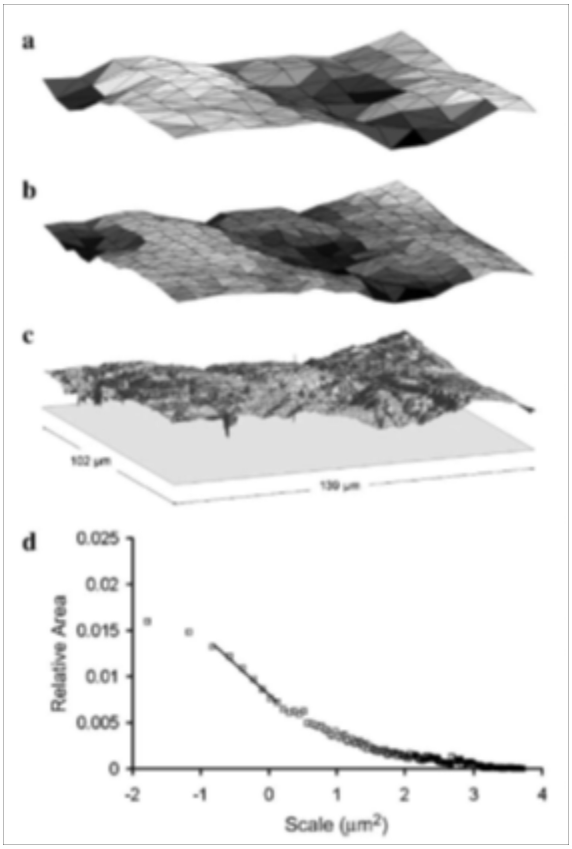

Figure 20: Scott et al. (2006), Fig. 6: "Schematic comparing surfaces with (a) lower and (b) higher structural fill volumes. Finer scale prisms (c) yield structural and textural fill volumes. Textural volume is calculated by subtracting b from c."

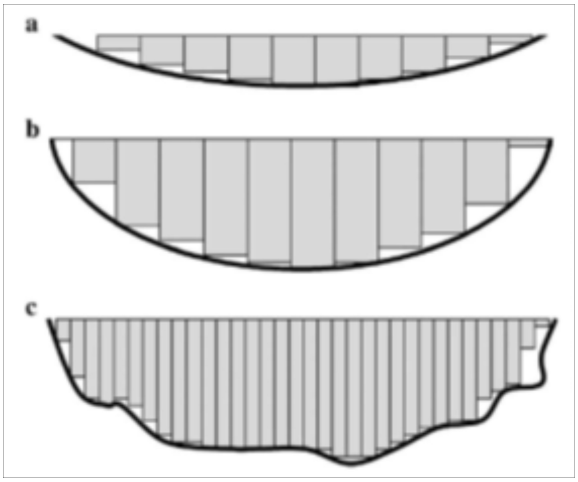

We select two different types of facets: A) the facet in the very enamel thickness and B) the buccal (on lowers teeth) or lingual (on uppers teeth) side enamel edge facet (that is commonly developed in browser rhinoceroses) (**Figure 21**-B). On the upper molars, labial facet A is selected on the ectoloph, in the valley between the paracone style and metastyle, in its mesial part; lingual facet A in the very lingual part of the protocone (sometimes a lingual facet B can be present in the disto-lingual part of the protocone, but it is not always a distinct facet and we do not include it in the analysis). On the lower molars, only labial facets have been used: labial facet A and B are both selected in the very lingual (or linguo-distal) part of the hypolophid (this correspond to facets 6 and 7 in Hernesniemi et al. 2011). The exact location of the facets is shown in **Figure 21-**C.

Figure 21: A) General structure and nomenclature of rhinoceroses upper and lower teeth. B) Section of lower molar showing the orientation of A and B facets. C) Location of sampled A and B facets on upper and lower molars.

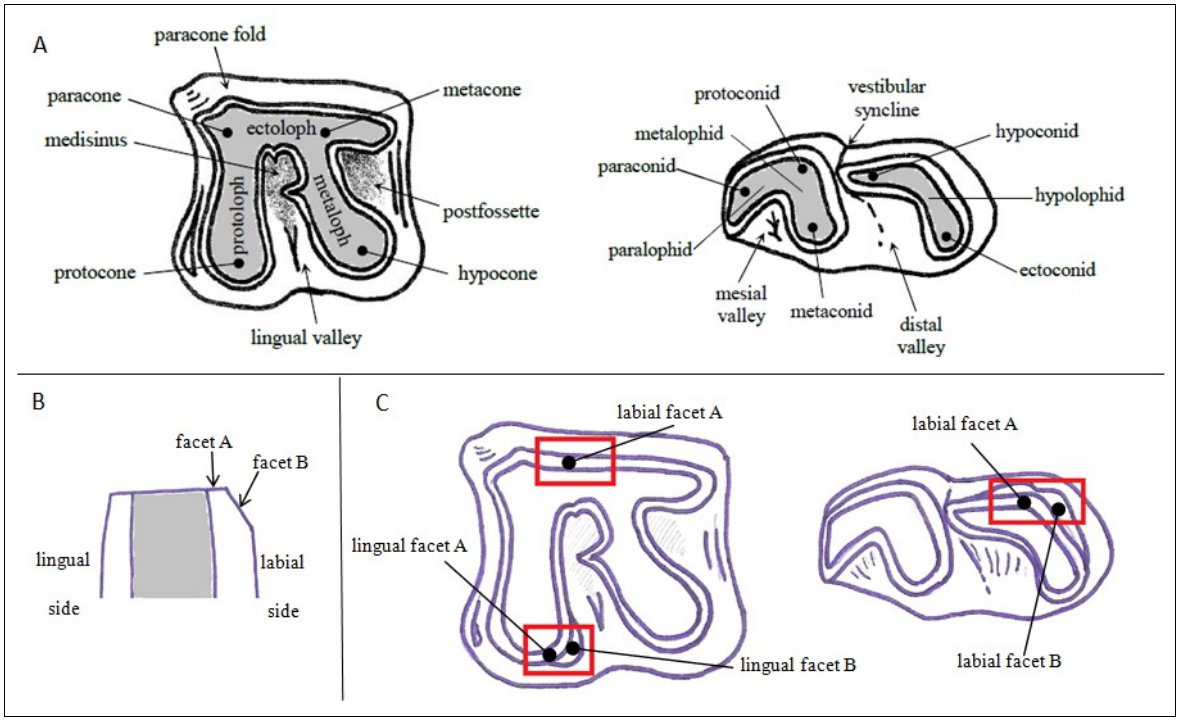

Facets A and B originate during the two phases that can be identified in the masticatory stroke: phase I is characterized by attrition (sharing component – tooth/tooth contact) and phase II by abrasion (crushing-grinding components – tooth/food contact), and in hypsodont dentitions phase I is generally reduced (Fortelius 1982). According to Rensberger and Koenigswald (1980), facets A (corresponding to their facets II) originate in phase II, they are convex, smoothly polished and poorly defined, because food abrasion is dominant and teeth surface often do not make direct contact. Facets B (Rensberger and Koenigswald's facets I) originate in phase I, they are flat and sharply bounded because of direct contact attrition, moreover the occlusal pressure is high because the area of contact is smaller than when the teeth are more fully occluded. Actually during phase I labial facet B on lower tooth makes direct contact with labial facet A on upper tooth (Ballatore, pers. obs.). Therefore we do not use Rensberger and Koenigswald's (1980) nomenclature of facets I and II but propose the labels A and B as pictured and described above.

On facets A a regular pattern of ridges, perpendicularly aligned to the outer surface, can be observed by the unaided eye (as already described by Rensberger and Koenigswald 1980). These ridges are present both on upper and lower labial A facets (even if they are involved

in different masticatory phases) and are developed in the inner half of the enamel, close to the enamel-dentine junction, and fade before reaching the outer surface (**Figure 22**-C). The ridges derive by two components: food abrasion and micro-structure of the enamel (Rensberger and Koenigswald 1980). On the contrary B facets are smooth and other regularly spaced striae are visible, they are produced by the contact with the ridges of the occluding A facet on the opposite tooth and do not depend on the underlying enamel structure (Rensberger and Koenigswald 1980).

Enamel structure is formed by prisms (bundles of hydroxyapatite crystallites) that originate at the enamel-dentine junction and grow in the direction of the outer surface, so that individual prisms extend through the thickness of the enamel (Rensberger and Koenigswald 1980). Prisms are arranged in 3D layers of alternating directions, that is evident from the optical phenomenon of the Hunter-Schreger bands. These are light and dark bands visible on the occlusal surface of rhino's teeth under light microscopy, as a consequence of the variation in the reflective property of sets of prisms (Rensberger and Koenigswald 1980). Observing under the SEM the surface etched with acid, parallel to the wear plane, it shows the alternate structure of prisms' layers (**Figure 22-**A, B): prisms of type B descend obliquely from the occlusal surface and enamel-dentine junction, then a thin transitional zone (T) with prisms in horizontal position (parallel to the occlusal surface) and the opposite oriented prisms of type A which rise obliquely toward the occlusal surface and outer enamel surface (Rensberger and Koenigswald 1980).

The ridges arose as a consequence of the position of the angle between the prisms and the wear surface, and of the direction of the abrasion vector. Indeed, prisms with axes orientation almost parallel to the abrasion vector show maximum resistance to wear and form prominent ridges (**Figure 22**-C). In the protocone and hypocone of the upper teeth and in the protoconid and hypoconid of the lower teeth, a set of double ridges occurs; each set derives from prisms of type A and type B (**Figure 22**-D).

Figure 22: In each part of the figure, prisms of type B are labelled with letter B, transitional zone with letter T and prisms of type A with letter A. A) Etched surface on hypoconid of *Subhyracodon* (middle Oligocene, North America)(Rensberger and Koenigswald 1980, Fig.3); B) magnification of the dotted square in A (Rensberger and Koenigswald 1980, Fig.4); C) "ridges formed by opposite prism types on opposing enamel layers of single cusp. Prism with axes almost nearly parallel to the abrasion vector offer maximum resistance to wear" (Rensberger and Koenigswald 1980, Fig.15); D) Occlusal (naturally worn) surface on hypoconid of *Subhyracodon* (middle Oligocene, North America) with ridge formed by prisms of type A and B; I = facet B with striae (adapted from Rensberger and Koenigswald 1980, Fig.2).

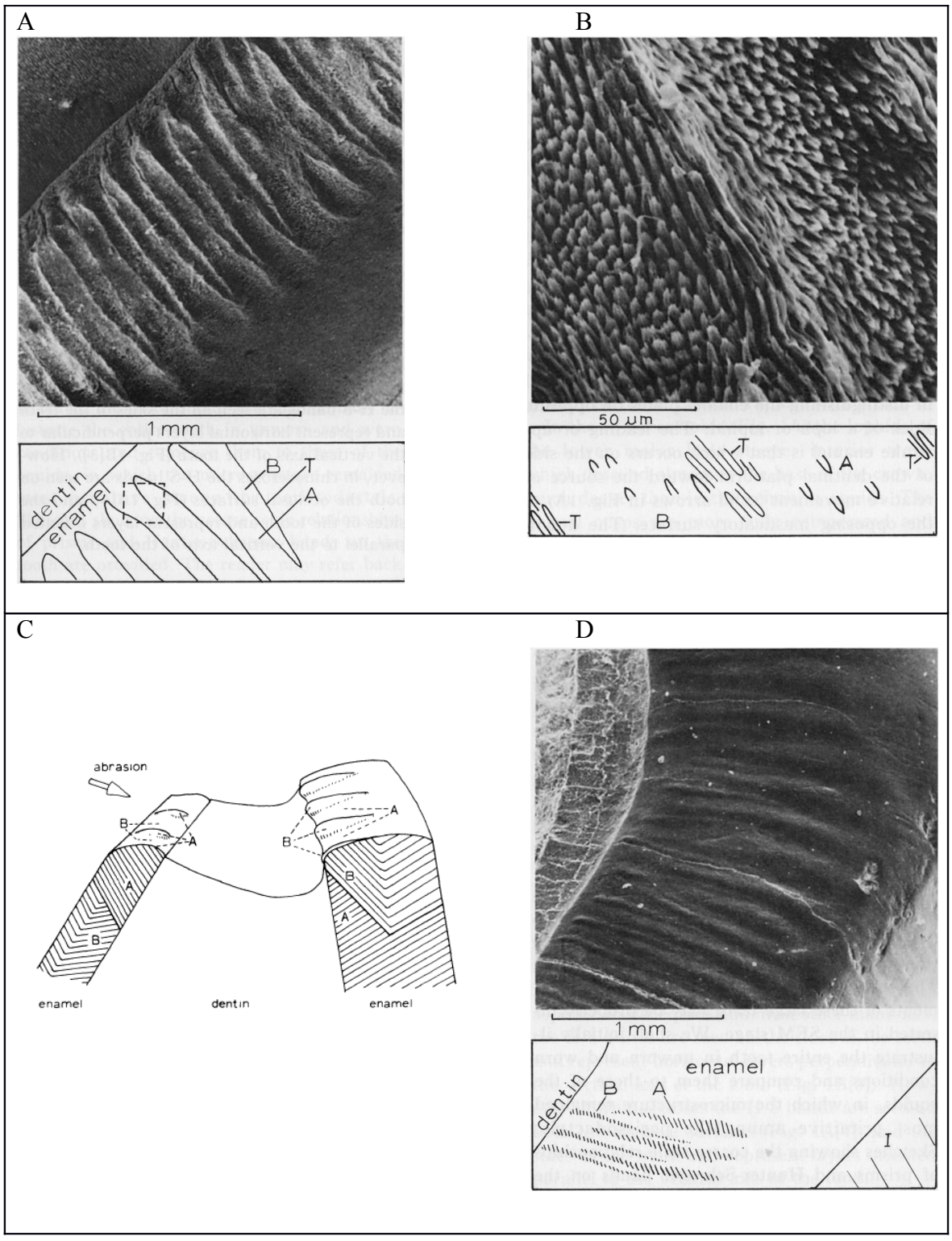

We compare the labial facets of the three species (for the labial facets A of upper molars, labial facets A and B in lower molars), to evaluate which facet is the best diet proxy and which microwear texture parameter distinguishes the species. In order to test the extent of the differences in the microwear texture parameters, the paired Mann-Whitney *U*-test has been calculated on www.socscistatistics.com/tests/mannwhitney (significance level α=0.05). Since this is the first 3D DMTA performed on rhinoceros teeth, no data on modern samples of known diet are available, so we cannot ascribe the scanned surface to a specific diet type (browser, mixed-feeder, grazer) but just observe relative differences among the populations.

Moreover we aim to assess the textural differences among the different surfaces (lower molars' labial facets A and B, and uppers' labial facet A).

4.4 Results

4.4.1 Morphobiometry

From a morphological point of view, the following features can be observed in the analysed palaeopopulations:

- *Premolars*

a) The crochet is always present (single or multiple) in the three palaeopopulations; the antecrochet is always absent (except a single specimen from Senèze, P4 NMB Se. 1785); the crista is always present in the specimens from Montpellier and Senèze but it is absent in the teeth from Vialette (except P4 UCBL FSL 211182).
b) Lingual cingula are mostly present in the three palaeopopulations, as a distinct rib descending from the metacone (it originates from the distal cingulum) and reaching the hypocone (it continues in the mesial cingulum). However, in two specimens from Montpellier (4/18 P3 and 3/15 P4) and one from Senéze (UCBL FSL 211118) the lingual cingulum is missing.
c) Vestibular cingula are always absent.

- *Molars*

d) The crochet is always present (usually single, rarely double); the antecrochet and crista are absent on the molars from Vialette while they are both absent or present (single) in the species from Montpellier and Senèze.
e) The lingual cingulum is absent in the palaeopopulations from Montpellier and

Vialette (a single specimens from Viallette, M2 MNHN VIA 472, has a weak discontinuous cingulum made up of several isolated bulges), more frequent in the rhinoceros from Senèze (2/5 M1, 1/4 M2 and 2/5 M3).

f) Vestibular cingula are absent in the palaeopopulation from Senèze and Vialette. It is mostly absent also in Montpellier but in some M1 a very low (just at the base of the crown) series of small bulges form a weak vestibular cingulum (precisely in 6/15 specimens, being very marked on 3 of them – **Figure 23**).

Other characters are common in the three populations:

- the medisinus is open in all the teeth (only one individual of *S. etruscus* from Senèze, NMB Se. 1785, shows close medisinus in the molars);
- the protocone constriction is present, but not strong, in M1 and M2;
- the paracone fold is weak on the premolars (increasing gradually from P2 to P4) and strong on the molars (particularly on M1 and M2, less on M3);
- mesial and distal cingula are always present on all the teeth.

Figure 23: Labial cingula on the M1 upper molars of *S. megarhinus* from Montpellier. A: specimen NMB M.B. 851; B: specimen NMB M.P. 446; C: specimen UCBL FSL 40125b.

Biometric results for the upper teeth are given in **Table 5**, **Table 6** and **Figure 24**:

- The upper P2 from Montpellier are clearly larger than those of the more recent species, but distinguishing the teeth from Vialette from those from Senèze is not so easy: they differ in their length but fall in the same breadth range.
- The upper P3 and P4 show a gradual decrease in size from the older population of Montpellier to the younger of Senèze, with little superposition between each range.
- The upper M1 from Senèze and Vialette fall in the same length range but the latter is more large. Montpellier's M1 shows a bigger size.
- In the M2 the size range of the rhinoceros from Vialette superposes with the other two

populations, no superposition occurs among those from Montpellier and Senèze.

- The upper M3 is clearly larger at Montpellier while it is not distinguishable between Vialette and Senèze.

The null hypothesis of species identity cannot be rejected when the palaeopopulations of Vialette and Senèze are metrically compared, the two populations are slightly different only in the length of the teeth (see **Table 6**).

Table 5: Upper teeth metric data. Sample size *N* is given in brackets. ML= max. length; MB= max. breadth. Measurements in mm.

ML		***S. megarhinus*** **Montpellier**	***S. elatus*** **Vialette**	***S. etruscus*** **Senèze**
P2	*mean*	39.3 (13)	36.2 (4)	32.2 (6)
	st.dev.	14.8900	0.9574	2.4014
	CV	0.3788	0.0264	0.0747
P3	*mean*	43.4 (20)	41.7 (4)	39.5 (4)
	st.dev.	3.4853	1.2583	2.6457
	CV	0.0803	0.0301	0.0669
P4	*mean*	46.7 (22)	44.3 (3)	42.0 (4)
	st.dev.	3.8164	0.5773	1.8257
	CV	0.0815	0.0130	0.0434
M1	*mean*	55.9 (19)	49.7 (4)	48.5 (4)
	st.dev.	16.5532	0.5000	1.2909
	CV	0.2958	0.0100	0.0266
M2	*mean*	60.1 (17)	53.6 (6)	49.8 (6)
	st.dev.	3.6722	1.7511	2.4832
	CV	0.0610	0.0326	0.0498
M3	*mean*	60.7 (18)	54.0 (4)	51.7 (6)
	st.dev.	2.8862	5.9442	4.1312
	CV	0.0475	0.1101	0.0800
MB				
P2	*mean*	43.1 (13)	38.5 (4)	34.0 (5)
	st.dev.	15.5460	1.7321	9.0554
	CV	0.3603	0.0450	0.2663
P3	*mean*	54.9 (20)	49.2 (4)	46.0 (4)
	st.dev.	3.5078	2.2173	3.4641
	CV	0.0638	0.0450	0.0753
P4	*mean*	60.3 (22)	54.3 (3)	53.0 (4)
	st.dev.	3.5373	3.7859	2.1602
	CV	0.0586	0.0696	0.0407
M1	*mean*	63.3 (19)	53.7 (4)	51.7 (4)
	st.dev.	18.7912	3.8622	2.6299
	CV	0.2967	0.0718	0.0508
M2	*mean*	67.1 (17)	58.1 (6)	54.1 (6)
	st.dev.	3.6380	4.3550	3.4880
	CV	0.0542	0.0748	0.0643
M3	*mean*	58.3 (18)	48.5 (4)	43.3 (6)
	st.dev.	3.0098	3.6968	8.8694
	CV	0.0516	0.0762	0.2047

Table 6: Student's *t*-test associated *p*-value (significance level α=0.05) for upper teeth measurements. Not significant values (p>0.05) are given in bold. ML= max. length; MB= max. breadth. *Stephanorhinus megarhinus* from Montpellier (Mo.), *S. elatus* from Viallette (Vi.), *S. etruscus* from Senèze (Se.).

	ML			**MB**		
	Mo.-Vi.	Vi.-Se.	Mo.-Se.	Mo.-Vi.	Vi.-Se.	Mo.-Se.
P2	0.0056	0.0072	0.0001	0.0046	**0.3336**	0.0013
P3	**0.1216**	0.0316	0.0488	0.0049	0.0380	0.0077
P4	0.0110	**0.0785**	0.0037	**0.0976**	**0.6227**	0.0011
M1	0.0000	**0.1474**	0.0000	0.0098	**0.4290**	0.0004
M2	0.0000	0.0129	0.0096	0.0022	**0.1110**	0.0000
M3	**0.1060**	**0.5255**	0.0080	0.0080	**0.2436**	0.0001

4.4.2 Mesowear analysis

The mesowear score gives the following results (**Figure 25**, **Table 7**):

- The range of the sample from Montpellier shows large variability, clearly indicating a not pure browsing diet. In fact this palaeopopulation is intermediate among the modern mixed feeder *Rhinoceros unicornis* and the browsers (*R. sondaicus* and *Dicerorhinus sumatrensis*), statistically closer to the former. From the comparison with the other fossil species, the population from Montpellier is clearly different from that from Senèze, while it is similar to that from Vialette. However, the small sample size available for the populations from Vialette (N=4) and Senèze (N=3) should be considered, and the apparent distinct diet of the rhinoceros from Montpellier and Senèze is not certain.

- The populations from Vialette and Senèze, although considering the sample size, are similar to the modern browsers (*Rhinoceros sondaicus* and *Dicerorhinus sumatrensis*) and the difference between them is not significant. The same result appears looking at the single mesowear variables (**Table 8**). Compared in the framework of the five extant species, the fossil species are close to the browser *D. sumatrensis* and *R. sondaicus* (the "browser" *D. bicornis* results indeed most mixed feeder as *R. unicornis*).

Figure 24: Scatter plot diagrams of the upper teeth of *Stephanorhinus megarhinus* from Montpellier (Mo.), *S. elatus* from Vialette (Vi.) and *S. etruscus* from Senèze (Se.). ML= max. length; MB= max. breadth. Measurements in mm.

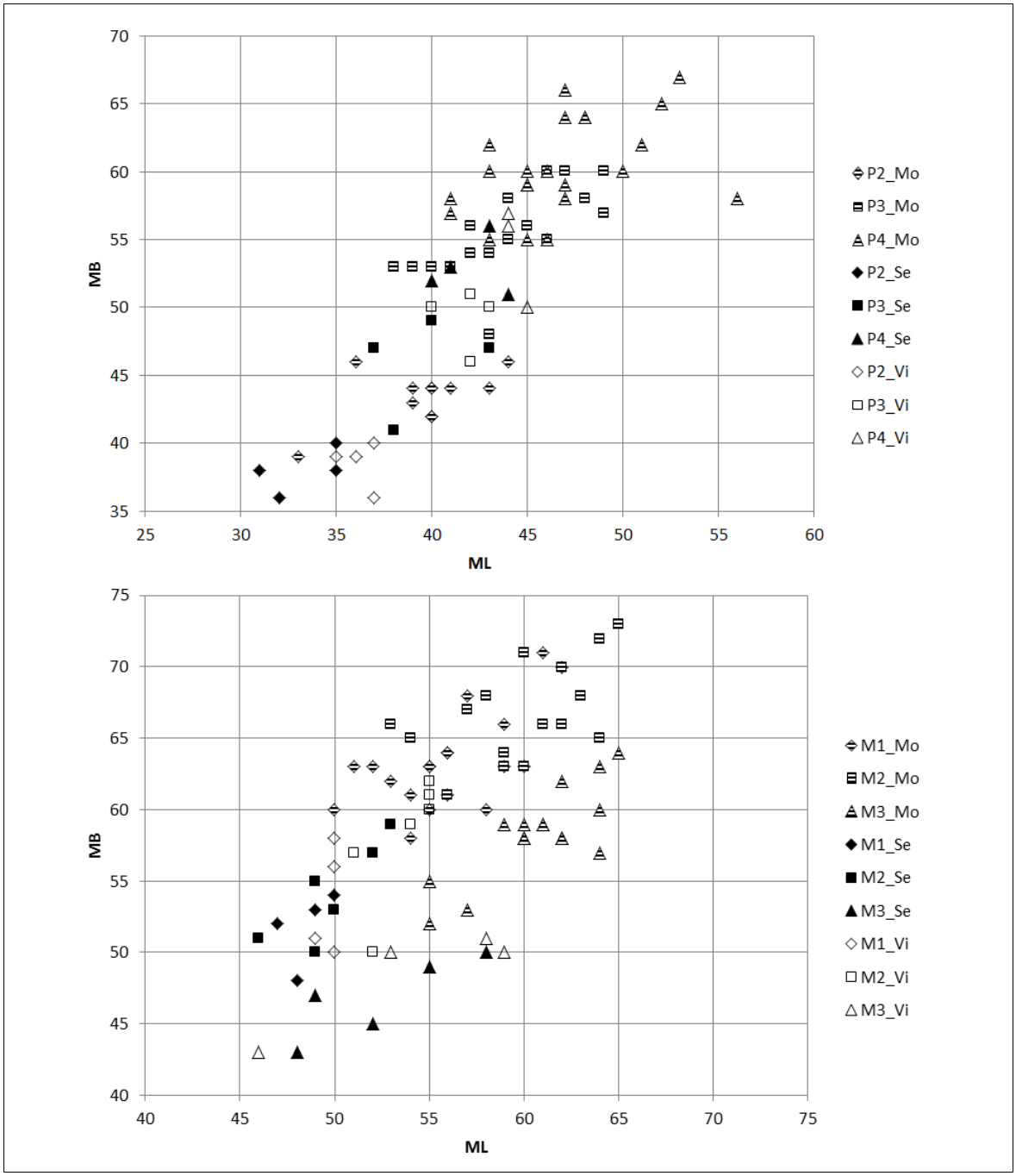

Figure 25: Mesowear score (mean and standard deviation) of the three investigated palaeopopulations (*S. megarhinus* from Montpellier, *S. elatus* from Vialette, *S. etruscus* from Senèze) in comparison with the five extant species. 0 is the most attrition dominated part of the spectrum while 4 the most abrasion dominated signature.

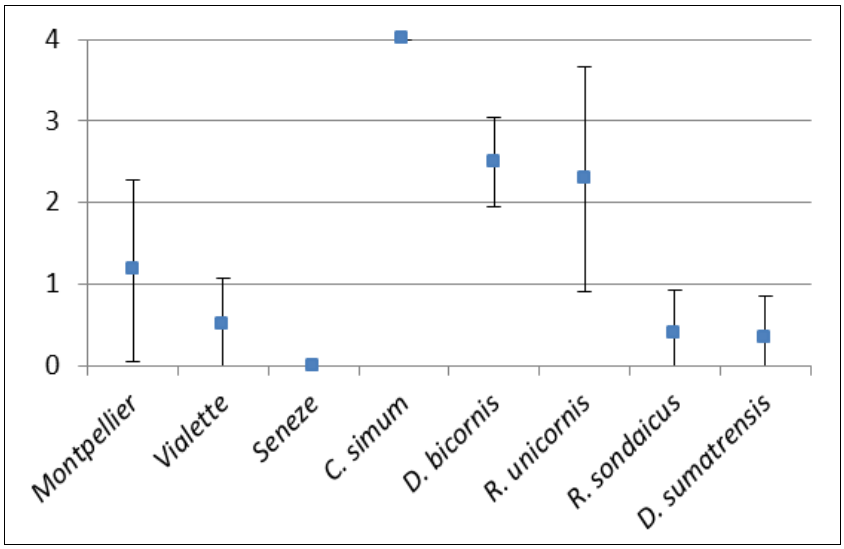

Table 7: Student's *t*-test associated *p*-value (significance level α=0.05) for the mesowear score of the three investigated palaeopopulations (*S. megarhinus* from Montpellier, *S. elatus* from Vialette, *S. etruscus* from Senèze) in comparison with the five extant species. Not significant values (p>0.05) are given in bold.

	S. megarhinus **Montpellier**	***S. elatus*** **Vialette**	***S. etruscus*** **Senèze**
Montpellier		**0.1523**	
Vialette			**0.1817**
Senèze	0.0040		
C. simum	0.0000	0.0012	0.0000
D. bicornis	0.0036	0.0013	0.0001
D. sumatrensis	0.0457	**0.6574**	**0.1747**
R. sondaicus	0.0494	**0.7750**	0.0368
R. unicornis	**0.0962**	0.0158	0.0047

Table 8: Mesowear variables for the three investigated palaeopopulations (*S. megarhinus* from Montpellier, *S. elatus* from Vialette, *S. etruscus* from Senèze) and the five extant species).

	N	**% high**	**% sharp**	**% round**
Montpellier	12	50.00	50.00	50.00
Vialette	4	100.00	50.00	50.00
Senèze	3	100.00	100.00	0.00
C. simum G	6	0.00	0.00	0.00
D. bicornis B	6	0.00	50.00	50.00
D. sumatrensis B	6	100.00	66.67	33.33
R. sondaicus B	10	100.00	60.00	40.00
R. unicornis M	7	28.57	28.57	57.14

4.4.3 Dental Microwear Texture Analysis (3D-DMTA)

The comparison of the three populations and the paired Mann-Whitney *U*-test clearly shows that there is no difference among them in the microwear texture parameters (**Table 9**, **Figure 26**).

However, looking at the textural parameter in the different facets (examples of the three different surfaces in **Figure 27**), we can observe that the facets have the same degree of heterogeneity (*HAsfc*), at different scales, and anisotropy (*epLsar*) (**Figure 28**). The textural volume (*Tfv*) is reduced in the lower molars' labial facet B in respect to lower molars' labial facets A. It is intermediate in the upper molars' labial facet A (**Figure 29**). Moreover it appears that complexity (*Asfc*) varies in a large range in the A facets of both upper and lower molars, while its variation range is abruptly reduced in the B facets of the lower molars (**Figure 29**).

Table 9: Mann-Whitney *U*-test associated p-value (significance level α=0.05) for the textural parameters, the null hypothesis of identity between paired species cannot be rejected.

Paired populations	**Asfc**	**epLsar**	**Smc**	**HAsfc** (81 cells)	**Tfv**
	Lower teeth – A labial facet				
Montpellier - Vialette	68	68	61	63	56
Vialette - Senèze	65	62	55	62	64
Montpellier - Senèze	95	87,5	86,5	95,5	90
	Lower teeth – B labial facet				
Montpellier - Vialette	68,5	69,5	65	64,5	48
Vialette - Senèze	65	67,5	66,5	65,5	65
Montpellier - Senèze	96	96,5	86	97,5	55
	Upper teeth – A labial facet				
Montpellier - Vialette	36,5	34,5	41,5	37	38

Figure 26: Plots of complexity (*Asfc*) vs textural volume (*Tfv*) and anisotropy (*epLsar*) for each scanned facet in the three compared palaeopopulations (*S. megarhinus* from Montpellier, *S. elatus* from Vialette and *S. etruscus* from Senèze).

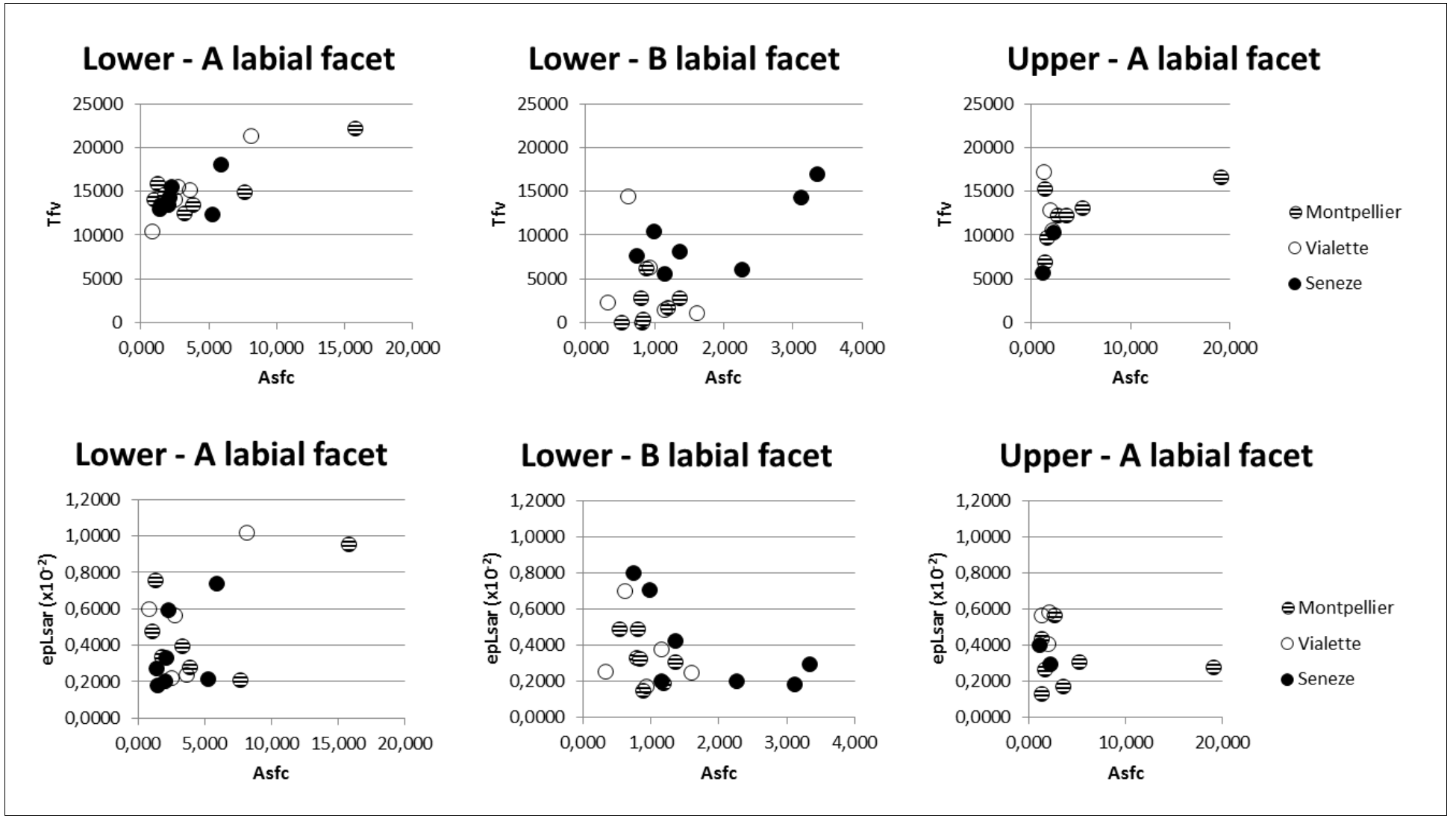

Figure 27: Examples of surfaces: 3D view, 2D view and photosimulation. A) Surface on labial A facet of lower molar VIA475 (*S. elatus* from Vialette, MNHN); B) surface on labial B facet of lower molar M9 (*S. megarhinus* from Montpellier, UCBL); C) surface on labial A facet on upper molar VIA 435 (*S. elatus* from Vialette, MNHN).

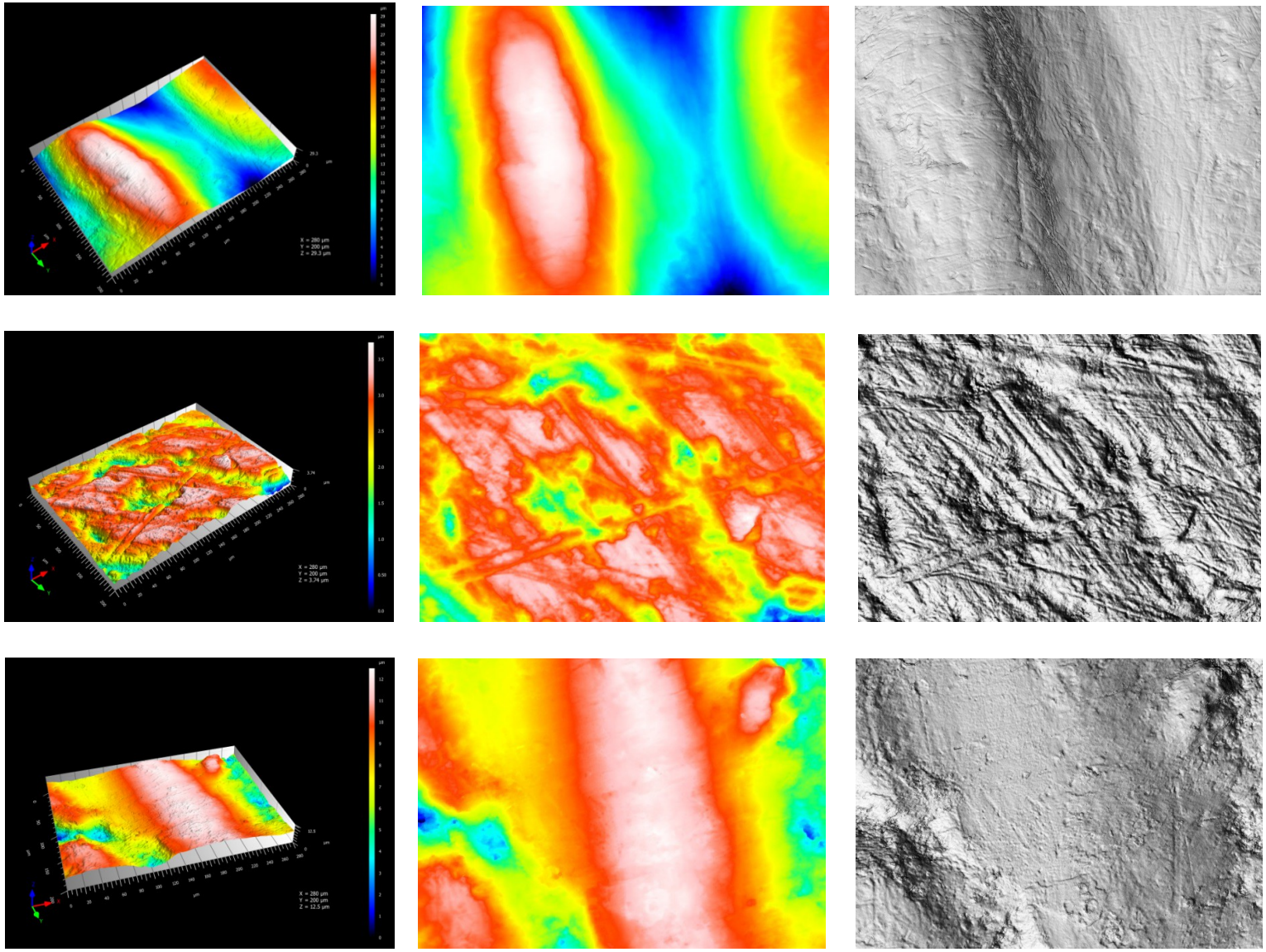

Figure 28: Heterogeneity (*HAsfc*) vs anisotropy (*epLsar*), the two parameters do not show any differences among the three different facets (labial facets A and B on lower molars and A on upper molars).

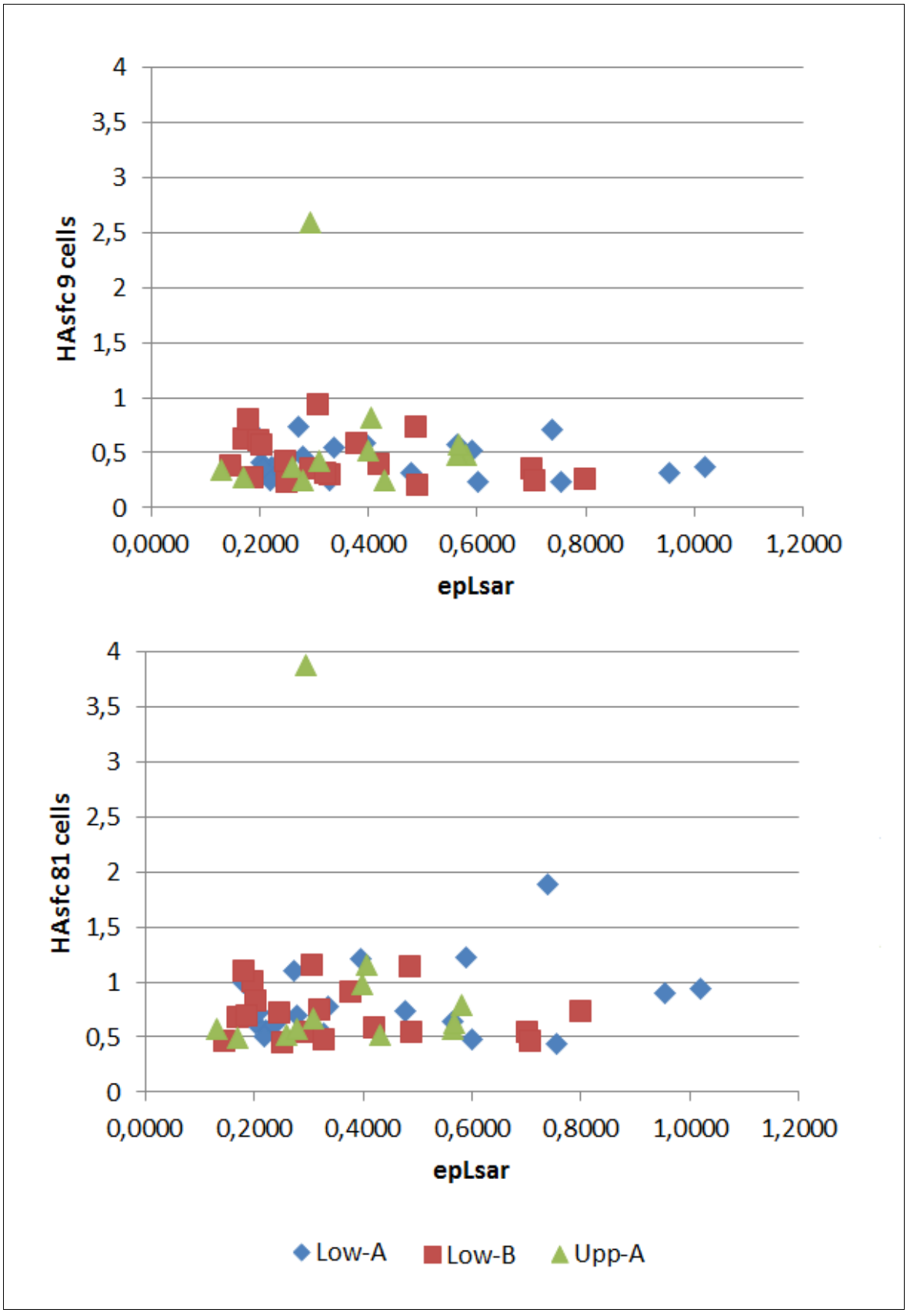

Figure 29: Textural volume (*Tfv*) vs complexity (*Asfc*).

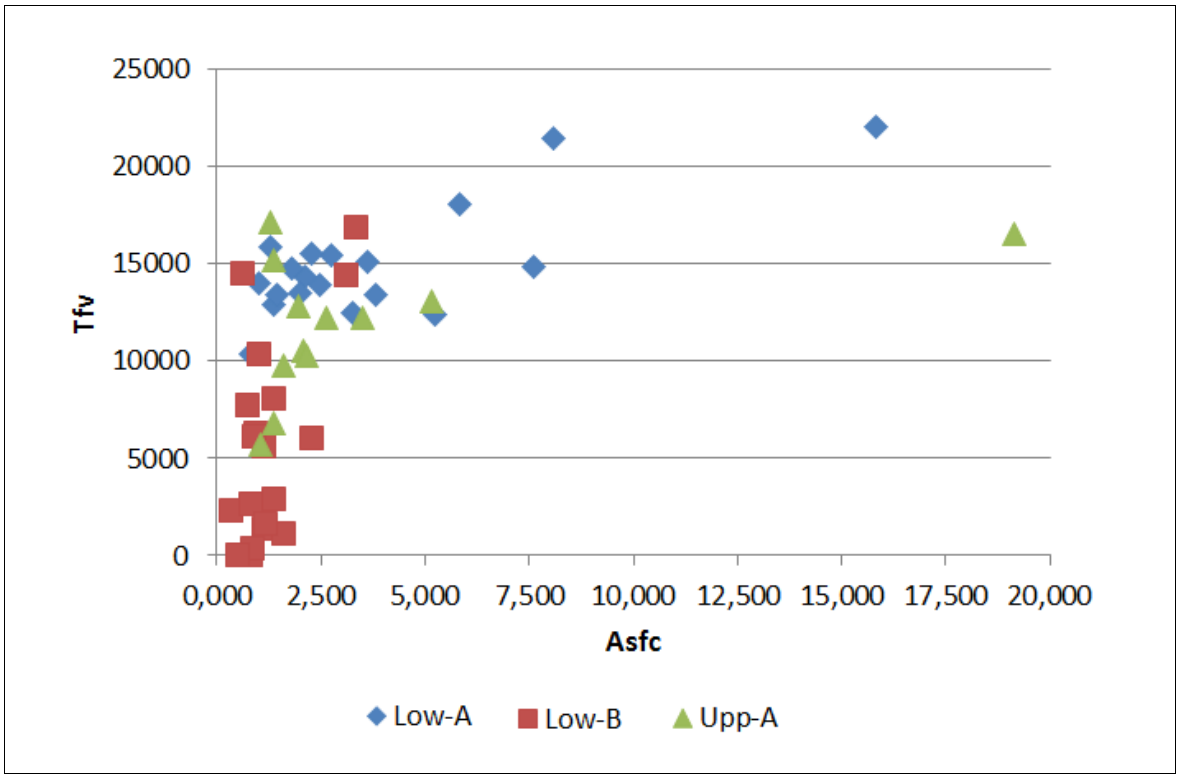

4.5 Discussion

The teeth of the three species have a similar morphology and the small differences on single characters that can sometimes be detected among the species are not correlated among each other, so that characters associations are not identifiable. For example the presence of the vestibular cingulum in the teeth from Montpellier is not associated to other characters distinguishing *S. megarhinus* from the other populations (e.g. the occasional presence of the lingual cingulum is found in Senèze and not in Montpellier). On the other side, the size of the teeth clearly separates the bigger rhinoceros from Montpellier from those from Vialette and Senèze, the teeth of the two more recent populations are not distinguishable by size. This must be discussed in relation to the general body size difference: *S. megarhinus* from Montpellier is the biggest both in the postcranial elements than in the teeth, on the contrary *S. etruscus* from Senèze is the smallest. Interestingly, the intermediate *S. elatus* from Vialette has a body size closer to *S. megarhinus* (with overlapping ranges) but its teeth are as small as those of *S. etruscus* from Senèze, therefore it has disproportionately small teeth in comparison to the body size.

We tried to evaluate if such consideration can be valid for the whole species and not only for our three palaeopopulations. By comparing the teeth dimensions of the specie (data

from literature, **Figure 30**), *S. etruscus* from Senèze results in the middle-lower part of the range of the species as reported by Guèrin (1980) and the type remains from Tuscany seem to be smaller (a part from a possible bias due to measuring technique). *S. elatus* from Vialette is in the lower dimensional range of the species, since the remains from Milia (Greece) are larger. As the *S. megarhinus* from Montpellier is concerned, it falls in the middle-upper part of the range of the species. Taken into account such information, it is clear that the differences we have noticed among the three palaeopopulations cannot be extended at the species level. We have compared a "medium" *S. etruscus* with a "small" *S. elatus*, but the similarity among our palaeopopulations would probably reduce if the smaller *S. etruscus* from Tuscany were compared to the larger *S. elatus* from Greece. Also the difference highlighted among the rhinoceroses from Vialette and Montpellier should be correlated with the particular populations: we have compared a "large" *S. megarhinus* from Montpellier with a "small" *S. elatus* from Vialette, including some smaller *S. megarhinus* and the larger *S. elatus* from Milia would lead to a smaller difference. This confirms how the influence of local environmental conditions affects the size variation and, as a consequence, the high interspecific size variability (phenotypical plasticity) observed in these species.

Figure 30: Size comparison of the upper teeth from Senèze, Vialette and Montpellier with the relative species: *S. etruscus* (Guérin 1980 – Localities: Senèze, Valdarno, Puebla, Blassac, Villaroya, Lumena, Chilhac, Red Crag, Incisa Balbo (Asti), Muzzano and Lodesana (Parma), Chagny, Cheilly, Chointré, Lachar; Mazza 1988 – Upper Valdarno, Olivola, Mugello), *S. elatus* (Guérin 1972 – Vialette; Guérin and Tsoukala 2013 – Milia), *S. megarhinus* (Guérin et al. 1969 – St. Laurent-des-Arbres; Guérin 1980 – Montpellier, St. Laurent-des-Arbres, Monte Giogo, Perpignan, Villafranca, Autrey, Wolfesheim). The differences shown in the M3 can be due to a different orientation of the calliper in the measuring technique.

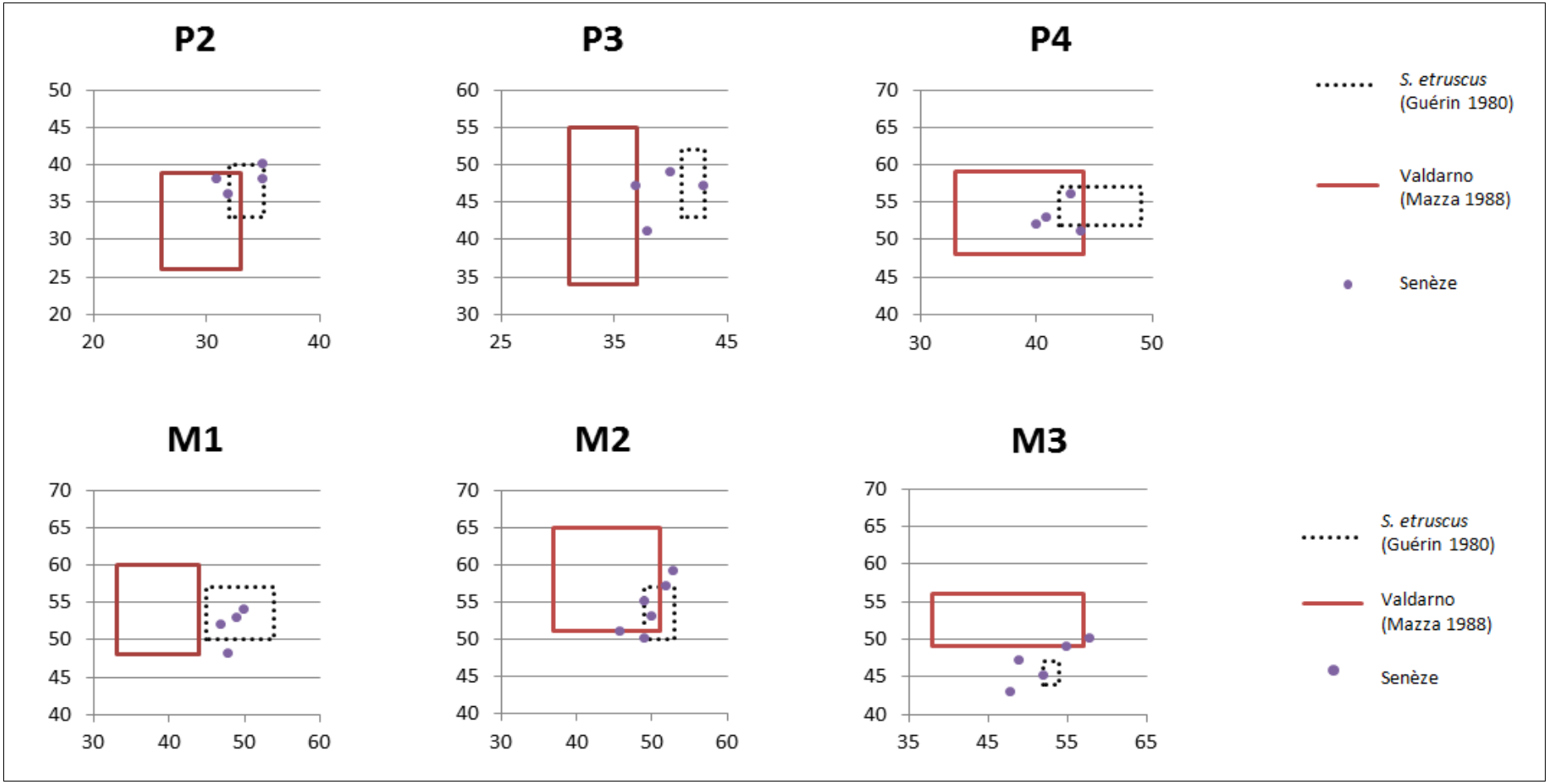

Figure 30: (continues)

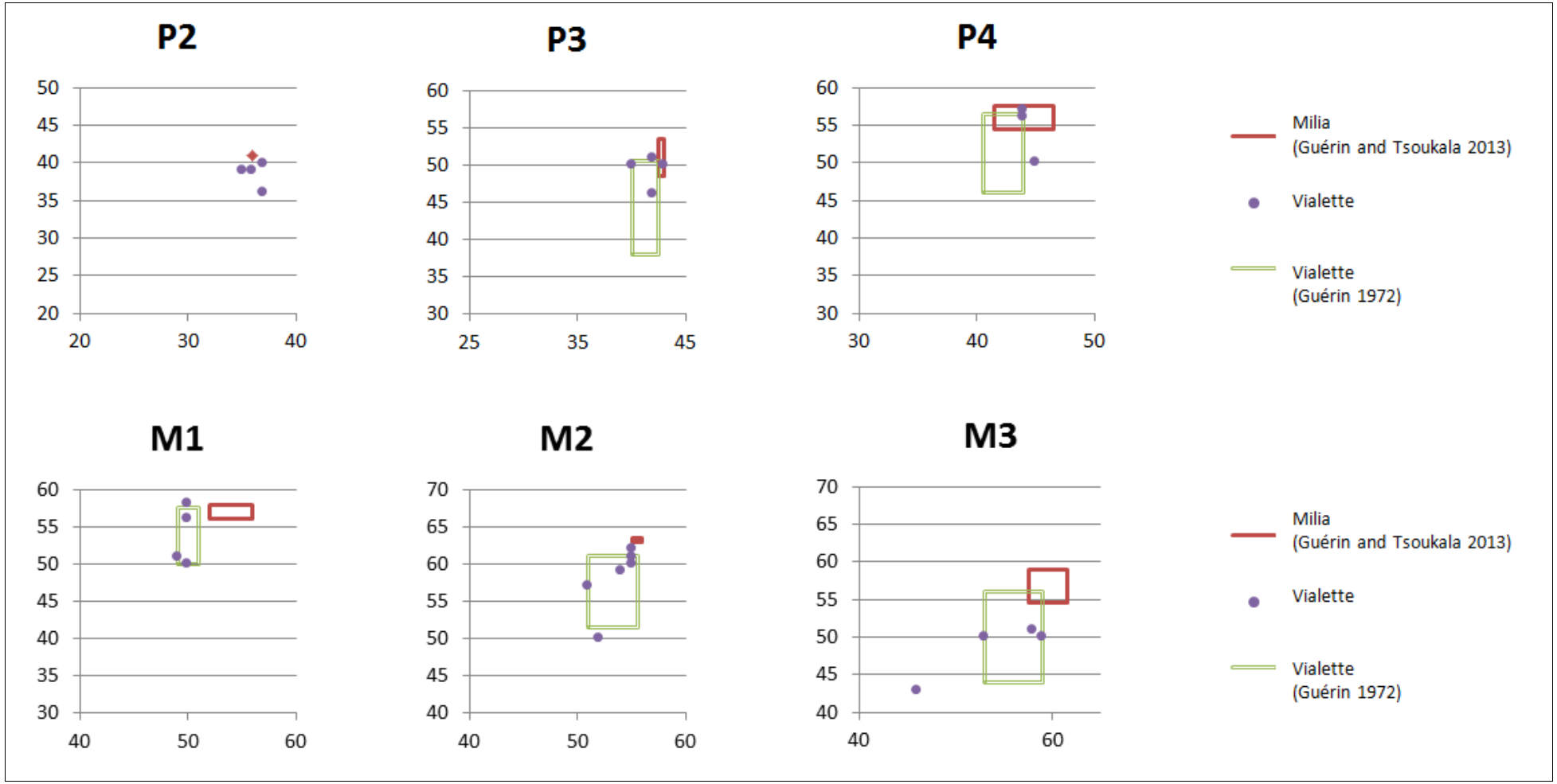

Figure 30: (continues)

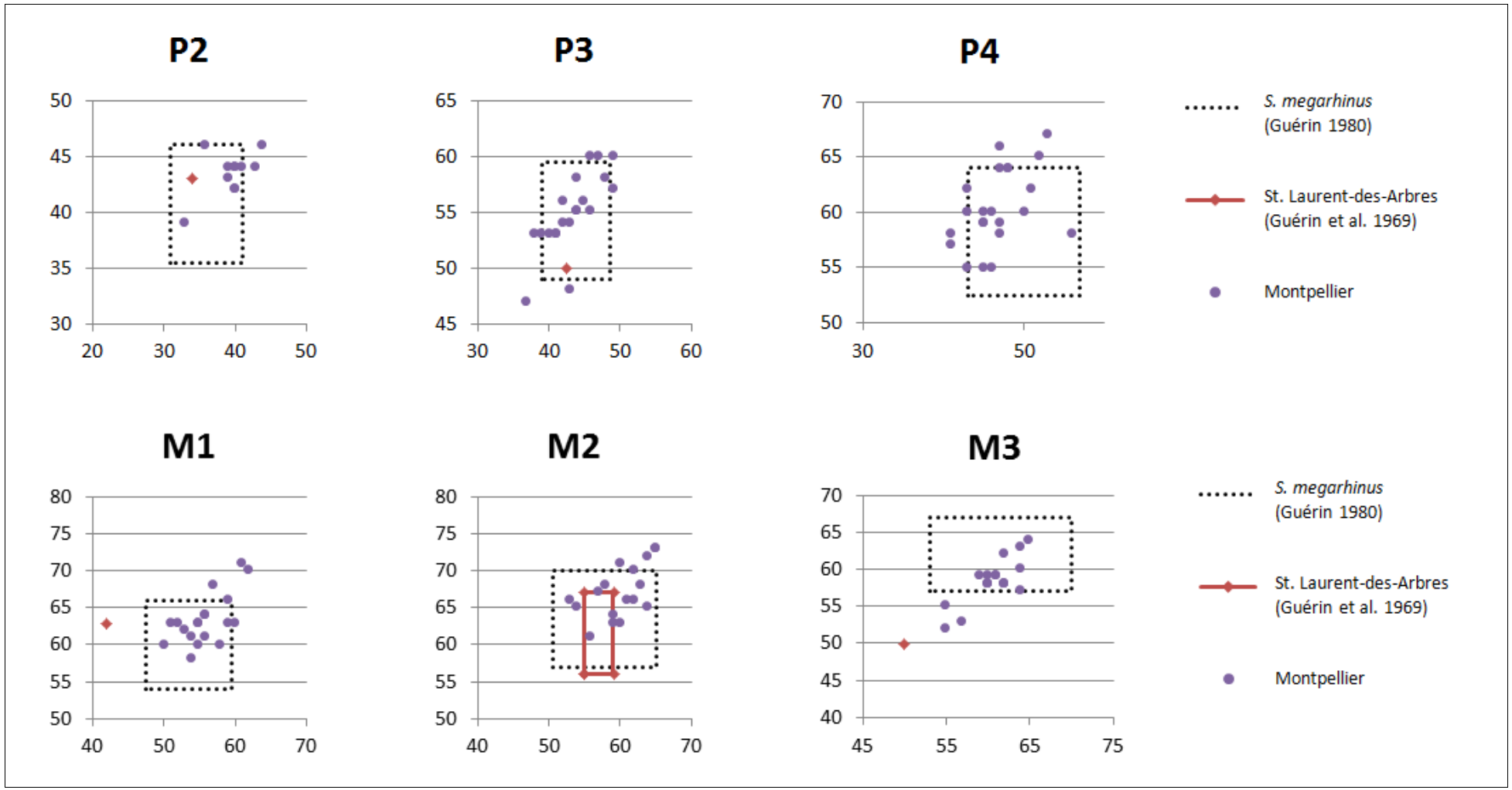

The mesowear analysis, leading information regarding the average diet during a long period (years), and 3D-DMTA, bringing information for a much shorter timescale (weeks), give congruent results, demonstrating that the different species had similar diet habits and no occasional exploitation of fallback food distinguishes them. So, nevertheless the presence of grass in their environment of life (possibly more extended in the Late Pliocene and Early Pleistocene) the rhinoceroses prefer browsing on soft vegetables, even if with a more flexible subsistence strategy than the modern browsers, as the wide mesowear range of *S. megarhinus* shows (the narrower range of *S. elatus* and *S. etruscus* is possibly due to the small sample size).

As concerning the textural parameters variation on the different facets, the unvaried anisotropy shows that the masticatory direction and the micro-structure of the enamel are not affecting this textural parameter. In fact we could expect that labial A facet on upper molars and labial B facet on lower molars, making contact with each other during phase I, would have a similar anisotropy if it should depend on food abrasion and masticatory direction. Otherwise we could imagine a similar anisotropy on labial A facets of both upper and lower molars, related to the micro-structure of the enamel (ridges). Evidently both these factors do not affect the micro-texture anisotropy.

The textural volume increases from labial B facet on lower molars to labial A facet on upper molars and to labial A facet on lower molars. So it is lower in attrition dominated facets (B on lower molars) and higher in abrasion dominated facets (A on lower molars); in fact the abrasion emphasizes the micro-structure of the enamel leading to the visible ridges on A facets, these structure amplify the textural volume at fine scale. The A facets on upper molars show a reduced volume in comparison with lower molars' A facets, due to the influence of attrition against lower molars' B facet during phase I.

The complexity, largely variable in A facets both on lower and upper molars, should be mainly related to the underlying enamel structure while attrition leads to complexity reduction (facet B).

4.6 Conclusion

From the analysis of the three palaeopopulations from Montpellier, Vialette and Senèze, we observe that, despite the climatic fluctuations from the Pliocene to the Early Pleistocene,

the European rhinoceroses do not change their dietary habit (mesowear and 3D-DMTA). The ecology of the different species is therefore the same, so that doubts arise about the supposed coexistence of two species (as suggested for the locality of Etouaires; Guèrin 1972, Heintz et al. 1974).

The differences observed in the size are not correlated to any difference in the dietary habit, so other evolutionary factors and more complex processes of adaptation should explain size and body mass diversity of the species.

Moreover 3D-DMTA brings information on the main components affecting enamel texture: 1) enamel micro-structure (leading to the visible ridge on A facets) does not affect anisotropy but textural volume; 2) attrition influences the micro texture leading to a reduction of both textural volume and complexity.

Chapter 5

SIZE VARIABILITY IN THE LONG-LIVED EUROPEAN PLEISTOCENE RHINOCEROS *STEPHANORHINUS HUNDSHEIMENSIS* (TOULA 1902)

5.1 Introduction

The species *Stephanorhinus hundsheimensis* (Toula 1902) is recorded in Europe from the late Early Pleistocene to the Middle Pleistocene, and during such extended period, of about 1 million years, the specie shows wide size variability. *S. hundsheimensis* is a generalist species (Kahlke and Kaiser 2011) and its varied diet provided it with huge adaptive possibilities, allowing the species to spread into the whole Europe, from Southern Italy to Britain and from Spain to Germany. For these reasons *S. hundsheimensis* deserves particular attention as an interesting case study to test the size and proportions variations along the chronological and geographical range. So *S. hundsheimensis* is very important to evaluate the adaptive meaning of these size changes against the changing climatic and environmental parameters in the Quaternary large mammals.

At first, Fortelius et al. (1993) report a dimensional variation through time with a small-sized form, from the Late Villafranchian, and a larger one from the Galerian (Mazza et al. (1993) prudently use *S*. cf. *hundsheimensis* for the small-sized form). After Fortelius et al. (1993), Lacombat proposes again the distinction in two forms in his thesis (2005), including the German site of Untermassfeld in the small-sized *S. hundsheimensis*. Later, Lacombat (2006b) sums up the populations from Southern and Western Europe (Italy, France, Spain) as follows:

- small form: Pirro Nord, Pietrafitta (Mazza et al. 1993's *S*. cf. *hundsheimensis*), Fuente Nueva 3, Barranco Léon 5 (Martinez-Navarro et al. 2003), Ceyssaguet, Sainzelles, Le Vallonet and Tour de Grimaldi (Lacombat 2005);
- large form: Durfort, Soleilhac, Isernia (Lacombat 2005).

As a confirmation of such chronological increase of size, Kahlke (2006) reports that a

continuous size increase is evident from the Upper Villafranchian remains from Southern Europe up to the more recent remains from the Central-European "pre-Elsterian" early Middle Pleistocene (Kahlke 2006).

Finally Lacombat (2009) performs a wide comparative study, including German populations along with Italian and French remains. From the comparison he confirms the existence of two forms, but he suggests that the rhinoceros from Untermassfeld is larger than the coeval population from Le Vallonet and claims a latitudinal gradient as an explanation. Precisely, Lacombat (2009) groups the localities yielding *S. hundsheimensis* in two geographical realms: the southern populations (Le Vallonet, Soleilhac and Isernia) and the northern populations (Untermassfeld, Süssenborn, Voigtstedt, Mosbach2 and Mauer) and describes two trends: the size increase during time from Le Vallonet to Isernia, in southern regions, and from Untermassfeld to Mauer-Mosbach2, in the northern ones (Lacombat 2009). So a geographic gradient of size increase with latitude among coeval populations, superposes to a chronological gradient of size increase with time (Lacombat 2009).

To test such hypothesis, we analyzed the size variability of dental material of *S. hundsheimensis* from the early Middle Pleistocene comparing the population from Isernia with several coeval localities of the British Cromer Forest Bed Formation in Norfolk and Suffolk (Ballatore and Breda 2013). The comparison has been made on the teeth only because postcranial remains are poorly preserved from these localities. The biometrical comparison shows a slightly larger size of the British specimens, in agreement with the latitudinal gradient of Lacombat (2009). This observation is interesting in that it conforms to the ecogeographic principle known as Bergman's rule. Although the postcranials are scarcely represented, the British localities will be included in morphometrical analysis to investigate the size variation over a wider geographical range.

5.2 Localities

The selected localities give a well representative framework of the geographic (**Figure 31**) and chronological (**Table 10**) span of the species *S. hundsheimensis*:

- the earliest populations from the late Early Pleistocene: Pietrafitta, Saint-Prest and Untermassfeld;
- the in-between populations from the early Middle Pleistocene: Soleilhac, Cromer Forest-

bed Formation, Voigtstedt and Süssenborn;
- the latest populations from the Middle Pleistocene: Isernia, Mauer, Mosbach, Boxgrove and Hundsheim.

Some of these localities give particularly rich information due to the good preservation and abundance of the remains (e.g. Untermassfeld, Voigtstedt, Hundsheim), others are represented by scantier remains (e.g. Saint-Prest, Boxgrove).
Lacombat (2009) approaches the topic by comparing the size index of some of these palaeopopulations (Untermassfeld, Soleilhac, Süssenborn, Voigtstedt, Isernia, Mauer and Mosbach2, plus that from Le Vallonet not included here). He does not take into account the earlier populations from Pietrafitta and Saint-Prest and the later population from the type locality of Hundsheim, neither the northern most populations from Britain.

Table 10: Chronology of the investigated localities.

Locality	Geochronology	Biochronology	MY	MIS
Hundsheim	Middle Pleistocene	-	-	13 (Made and Grube 2010)
Boxgrove	Middle Pleistocene	-	-	13 (Roberts and Parfitt 1999)
Mosbach2	Middle Pleistocene	-	0.6-0.4 (Schreiber et al. 2007)	15-13 (Lacombat 2009)
Mauer	Middle Pleistocene	-	0.6-0.4 (Schreiber et al. 2007)	15-13 (Lacombat 2009)
Isernia	Middle Pleistocene	Galerian Isernia FU (Gliozzi et al. 1997)	0.61 (Coltorti et al. 2005)	15 (Lacombat 2009)
Süssenborn	early Middle Pleistocene	-	0.71-0.62 (Kahlke 2002)	17-16 (Maul 2002)
Voigtstedt	early Middle Pleistocene	-	0.7 (Bassinot et al. 1994)	17 (Maul et al. 2007)
Cromer Forest-bed	early Middle Pleistocene	-	-	17-15 (Preece and Parfitt 2008)
Soleilhac	early Middle Pleistocene	Early Galerian MNQ20 (Palombo and Valli 2004)	0.71-0.62 (Lacombat 2009)	17-16 (Lacombat 2009)
Saint-Prest	late Early Pleistocene	Early Galerian MNQ20 (Guérin et al. 2003)	ca. 1 (Guérin et al. 2003)	-
Untermassfeld	late Early Pleistocene	Epivillafranchian MNQ20 (Kahlke 2006)	1.05 (Kahlke 2006)	31 (Kahlke 2006)
Pietrafitta	Early Pleistocene	Late Villafranchian Farneta FU (Masini e Sala 2007)	-	-

Figure 31: Map of Europe with the location of the investigated localities. Green: Early Pleistocene; yellow: early Middle Pleistocene; red: Middle Pleistocene.

5.2.1 Pietrafitta (Umbria, Italy – Early Pleistocene)

A considerable collection of fossil vertebrates was collected from the lignite mine at Pietrafitta (Perugia), excavated from 1958 by the ENEL thermoelectric plant (Mazza et al. 1993).

The first note is due to Pantanelli (1886) and a preliminary description to Ambrosetti et al. (1987). Extensional tectonic movements led to the formation of the Pietrafitta lacustrine basin in the Late Pliocene and Early Pleistocene time span (Ambrosetti et al. 1987). A marshy environment originated and vegetable remains turned to peat and lignite. Then the basin was filled by sands and clay during later tectonic activity (Mazza et al. 1993).

No absolute dating is available, but the site is placed in the Lower Pleistocene, Farneta FU

(Ferretti 1999, Masini and Sala 2007).

The rhinoceroses have been attributed to *S.* cf. *hundsheimensis* by Mazza et al. (1993) then considered *S. hundsheimensis* by Lacombat (2005). The remains are well preserved and quite abundant, but they were only partly accessible for the present research.

5.2.2 Untermassfeld (Thüringen, Germany – late Early Pleistocene)

The site was discovered in 1978, between the town of Meiningen and Untermassfeld on the right slope of the valley of the river Werra in southern Thuringia. The excavation has been conducted by the Institute for Quaternary Palaeontology, Weimar, since 1983 and is still progressing (Kahlke 2006).

The bone bearing level is a sand fluviatile deposit formed by the infill of an erosional channel (Upper Fluviatile Sands, Channel Infill) cutting into the underlying levels: a floodplains deposit (Lower Fluviatile Sands), a clayey to silty floodplain deposit and, in the N-NW excavation area, in the more deep weathered coarse gravels deposit (Younger Weathered Coarse Gravels). In the N-NW area fossil remains have been collected in the Lower Fluviatile Sands too, but the concentration of the find is lower than in the main sector of the Channel Infill (see Kahlke 2006 and reference therein). Carnivores activity is proved by tooth marks on several herbivorous taxa (Kahlke 2006 and reference therein), with particular evidence for *Pachycrocuta brevirostris* (R.-D. Kahlke 1997).

Palaeomagnetic studies report a normally magnetized polarity for the upper level of the Lower Fluviatile Sand and the overlying Upper fluviatile Sands, against the reversed magnetization of the underlying strata (R.-D. Kahlke 1999). That normal magnetization is interpreted as the beginning of the Jaramillo Subchron (R.-D. Kahlke 2000), therefore correlated with the MIS 31 (Shackleton 1995, Kahlke 2006). The Jaramillo event starts at 1.07 My (Berggren et al. 1995, Shackleton 1995) so the fauna of Untermassfeld has to be referred to 1.05 My "slightly over one million years" (Kahlke 2006). It correlates with the beginning of Guérin's (1990) MNQ 20 (Kahlke 2006) and with the Protogalerian (*sensu* Caloi and Palombo 1995). Breda and Marchetti (2005) refer the locality to the Colle Curti FU. However, since the fauna is intermediate between the Villafranchian and Galerian funas, the Epivillafranchian unit (Bourdier 1961) has been resumed and extensively applied to Untermassfeld (Kahlke 2006).

The rhinoceros remains consist of a great amount of specimens, included several partial individuals and articulated limbs enumerated by H.-D. Kahlke (2001 - we make use of this numbering in the description of the material). Few cranial portion are present, mainly

young mandibles, so no permanent dental material is available for morphometric analysis. The rhinoceros remains have been described at first by H.-D. Kahlke (2001) who attributes them to the specie *S. etruscus*. Lacombat (2005, p.144) prefers the name *S. hundsheimensis* explaining that a different interpretation of the taxonomy lead R.-D. Kahlke (2001) to use "*etruscus*", but he would refuse the subspecific rank of Guérin (who divided the earlier *Dicerorhinus etruscus etruscus* from the later *D. etruscus brachycephalus*) thus using "*hundsheimensis*". The question is confirmed in R.-D. Kalhke (2006, p.25) where reference to the two subspecies "*S. etruscus etruscus* and *S. etruscus hundsheimensis*" is explicit but the fact this population is intermediate between these two alleged subspecies leads to the conclusion that "it was not subsumed under one of the known subspecies, but a new subspecies name was not given either".

5.2.3 Saint-Prest (Eure-et-Loir, France – late Early Pleistocene)

The mammal fossil assemblage from Saint-Prest has been discovered by de Boisvillette (1848, 1850) in a karstic depression in the Eure Valley. The material is housed at the Muséum National d'Histoire Naturelle in Paris and at the Musée des Sciences Naturelles et de Préhistoire de Chartres (Guérin et al. 2003).

No absolute dating is available, and the site is referred to the MNQ 20 at the end of the Lower Pleistocene, about 1 million years ago (Guérin et al. 2003).

The rhinoceros remains studied here are few isolated bones stored in Paris. The specific attribution made by Guérin et al. (2003) is *Dicerorhinus etruscus brachycephalus*, synonymous to *S. hundsheimensis*.

5.2.4 Soleilhac (Haute-Loire, France – early Middle Pleistocene)

The fauna from Soleilhac, a lacustrine deposits near Le Puy-en-Velay, has been discovered in the XIX century (Guérin et al. 2003, Lacombat 2005). Most of the fossil remains are stored at the Museum National d'Histoire Naturelle in Paris and at the Musée Crozatier du Puy-en-Velay (Lacombat 2005). The presence of archaic hominids is documented at the site (Bonifay 2002) as far as the exploitation of elephants and deer (Fosse 1994).

No absolute dating is available, and the site is referred to MNQ 20 and early Galerian (Palombo and Valli 2004).

We analyze the metacarpal bones and few carpals of a single individual, plus other isolated bones (basipodials and metapodials) preserved at the Museum National d'Histoire Naturelle in Paris. The specie attribution agrees with that of Lacombat (2005).

5.2.5 British Cromer Forest-bed Formation (Norfolk and Suffolk, Britain – early Middle Pleistocene)

Five localities of the British south-eastern coast are included in our study: Pakefield (Suffolk), West Runton (Norfolk), Trimmigham (Norfolk), Sidestrand and Overstrand (Norfolk). The Cromer Forest-bed Formation is a complex stratigraphic series ranging from the Upper Villafranchian to the Middle Pleistocene (Azzaroli 1953, West 1980). The fossil mammal remains, have been collected since the beginning of the XIX century, found on the beach and foreshore after the winter storms. Most of them lacks any stratigraphic information (Stuart and Lister 2010). Two main faunas have been identified based on deer species (Azzaroli 1953, Lister 1993): the older correlates with the Upper Villafranchian of Senèze, therefore its rhinoceros should belong to *S. etruscus*, the younger brings remains of *S. hundsheimensis* (Breda et al. 2010) and correlates with the fauna of Süssenborn-Mauer-Mosbach (Azzaroli 1953, Lister 1993). According to Lister (1993) we consider the remains from the localities of West Runton, Pakefield and Trimingham belonging to the early Middle Pleistocene. The rhinoceroses from West Runton and Pakefield have been reviewed by Breda et al. (2010) and attributed to *S. hundsheimensis*. (No revision is available for the rhinoceroses from Trimingham and since some older remains have been collected there, the presence of *S. etruscus* can be supposed, in particular we found a single individual possibly belonging to this species). The remains from the localities of Overstrand and Sidestrand are instead more problematic since these faunas consist in a mixture of Early Pleistocene and early Middle Pleistocene (Lister 1993) and the rhinoceros have not been reviewed in a modern key. We include the scanty remains from these localities as *S. hundsheimensis* since the size is congruent with the range of the specie, however a more detailed revision (including dental material and morphological comparison) should be carried out.

5.2.6 Süssenborn (Thüringen, Germany – early Middle Pleistocene)

The fauna from the Süssenborn's gravel deposit by the Ilm river was known from the XIX century (Kahler 1969). The river deposit sequence represents a long time span within the early Brunhes magnetochrone, is covered by ground moraine of the Elster glaciation, and consists of two successions separated by an interglacial weathering. The sequence records several climatic oscillations but the faunal assemblage does not indicate periglacial condition (nor a steppe-tundra environment) (R.-D. Kahlke 1999), and the single occurrences of *Ranifer tarandus stadelmanni* and *Ovibos moschatus suessenbornensis* are

considered sporadic appearances from sub-Arctic regions (R.-D. Kahlke 1999).
The rhinoceros remains have been first described by H.-D. Kahlke (1969) as *Dicerorhinus etruscus* (then including the nominal species *D. etruscus etruscus* and the derived form *D. etruscus brachycephalus*, Guèrin 1980), later reviewed by R.-D. Kahlke (2002) and finally assigned to *S. hundsheimensis* as part of a nomenclatural update rather than of a different morphological interpretation (Kahlke and Kaiser 2011). The rhinoceros remains consist of isolated teeth and postcranial bones.

5.2.7 Voigtstedt (Thüringen, Germany – early Middle Pleistocene)

The locality of Voigtstedt has been excavated in 1954-1966 (H.-D. Kahlke 1965). The faunal remains come mostly from the middle level, coarse sands at the base of the "Lehmschichten" ("Lehmzone" clays and organic silts) that contains forest type pollen and represents the Voigtstedtian warm phase (pre-Elsterian). It lies between the "Oberen Kiesen" (upper gravel sands) and the "Unteren Kiesen" (lower gravel sands) palaeomagnetically dated to the Matuyama/Brunhes boundary (Wiegank 1990), probably to MIS17 (Maul et al. 2007) and therefore about to 0.7 My (Bassinot et al. 1994).
The Lehmzone has been divided in two parts: the lower part contains the "main fossil stratum" (Hauptfundschicht), deposited in a small lake with calm waters and the sediments suggest a mild climatic condition; the upper part originated during a period of cold climatic conditions in running water (Ruske 1965).
The rhinoceros remains consist in the almost complete skeletons of two individuals plus several isolated bones and have been first described by H.-D. Kahlke (1965) as *Dicerorhinus etruscus* (then comprehensive of the nominal species *D. etruscus etruscus* and derived form *D. etruscus brachycephalus*, Guérin 1980). As the rhinoceros from Süssenborn, the material from Voigtstedt has been later reviewed by R.-D. Kahlke (2002) and finally assigned to *S. hundsheimensis* as a nomenclatural update (Kahlke and Kaiser 2011).

5.2.8 Isernia (Molise, Italy – Middle Pleistocene)

The Palaeolithic site of Isernia La Pineta has been discovered in 1978 and is still being excavated at present. The extremely rich palaeontological assemblage and lithic artefacts are evidence of human settlement along the river side (Peretto 1994). The fossil bearing layer is dated to 610.000 years (Coltorti et al. 2005). The faunal remains are abundant but made up of isolated and often fragmented specimens, among which the most represented

species is the bison (*Bison schoetensacki*), followed by the rhino (*S. hundsheimensis*) and the elephant (*Palaeoloxodon antiquus*) (Thun Hohenstein et al. 2009). Due to the rich fauna, Isernia is the type locality of the homonymous Faunal Unit (Gliozzi et al. 1997).
The rhinoceroses have been described by Sala and Fortelius (1993) and attributed to *S. hundsheimensis*. They are represented by a huge amount of dental remains (Ballatore and Breda 2013) and fragmented cranial remains, while the postcranial are scanty and badly fractured.

5.2.9 Mauer (Baden-Württemberg, Germany – Middle Pleistocene)

The locality of Mauer, famous for the oldest human remain found in Germany, known as "the Mauer jaw", of *Homo heidelbergensis*, is a fluviatile sandy deposit, formed during the Cromerian interglacial (Schreiber 1999) and dated to 600.000-400.000 years (Schreiber et al. 2007).
The rhinoceros is represented by isolated but quite abundant remains at first attributed to *R. mercki* (Meyer 1864) and *D. etruscus* (Schroeder 1898, Wüst 1901, Adam 1961, Kahlke 1973, Loose 1975, Kraatz 1985, Koenigswald and Tobien 1987), and finally to *S. hundsheimensis* (Fortelius et al. 1993, Koenigswald 1997). Schreiber's (1999, 2005) latest review confirms the coexistence at the site of this latter species with the species *S. kirchbergensis*.

5.2.10 Mosbach (Baden-Württemberg, Germany – Middle Pleistocene)

The fossiliferous finds from the sands of Mosbach (now Biebrich) were known from the XIX century (Meyer 1842): a limestone cave was active in Mosbach to supply the cement industry (Brüning 1970). The sand quarry is still excavated at present and, recently, rhinoceros remains have been found in situ (Koenigswald et al. 2007). The sand deposited in the confluence of the river Rhine and Main, forms a sequence of several levels of different sedimentology (Brüning 1978) among which three faunal levels have been individuated (Kahlke 1961, Tobien 1980, Koenigswald and Tobien 1987): Mosbach1, Mosbach2 and Mosbach3 (the latter does not yield rhinoceros rests, Fortelius et al. 1993).
The rhinoceros included in the present study comes from Mosbach2, the richest fossiliferous level, correlated with the late stage of the Cromerian complex (Koenigswald et al. 2007), where the species *S. hundsheimensis* coexists with *S. kirchbergensis* (Fortelius et al. 1993).

5.2.11 Boxgrove (West Sussex, Britain – Middle Pleistocene)

The hominid locality of Boxgrove has been investigated since the 1970s. The fossil bearing level (Unit 4c, palaeosol horizon) is the top of an interglacial sequence, covered by slope deposits and periglacial sediments of the Anglian stage. It brings hominin remains and artefacts, along with a rich vertebrate fauna (Roberts and Parfitt 1999, Preece and Parfitt 2000). Despite the interglacial period of formation of the terrestrial deposit (Unit 4c), the fauna indicates a cool and continental climate (Parfitt 1998).

The rhinoceros rests consist of few autopodial bones (plus teeth and skulls portions not included here) they have been reviewed by Breda et al. (2010) and attributed to *S. hundsheimensis*.

5.2.12 Hundsheim (Niederösterreich, Austria – Middle Pleistocene)

The karstic crevice of Hundsheim is the type locality of the species *S. hundsheimensis* (Toula 1902) and the fossil assemblage is referred to the Middle Pleistocene (Döppes e Rabeder 1996).

The rhinoceros remains consist in the complete skeleton of the holotype individual plus several isolated bones, all described by Toula (1902, 1906) and never reviewed later.

5.3 Materials and methods

S. hundsheimensis postcranial elements from the 12 investigated localities are housed in different European Institutions as detailed below (complete list of the specimens is given in **Attachment III**):

- Institute for Quaternary Palaeontology Weimar – IQW (Untermassfeld, Süssenborn, Voigtstedt);
- Staatliches Museum für Naturkunde Karlsruhe – SMNK (Mauer);
- Naturhistorisches Museum Mainz – MNHM (Mosbach);
- Natural History Museum London – NHM (Pakefield, West Runton, Trimigham, Sidestrand, Overstrand, Boxgrove)
- Naturhistorisches Museum Wien – NHMW (Hundsheim)
- Institute for Palaeontology University of Wien – IPW (Hundsheim)
- Muséum National d'Histoire Naturelle de Paris – MNHN (Saint-Prest, Soleilhac);

- Museo Paleontologico Luigi Boldrini, Pietrafitta – MPLB (Pietrafitta);
- Museo Paleontologico Piero Leonardi, Ferrara – MPPL (Isernia);
- Museo del Paleolitico, Isernia – MPI (Isernia).

S. etruscus specimens from the locality of Senèze (Haute Loire, France) are included as a comparison, since the Tuscan type was not available to the study. The specimens are stored in the Laboratoire de Géologie de Lyon - Terre Planètes Environnement (Université Claude Bernard Lyon 1, UCBL), at the Naturhistorisches Museum Basel (NMB) and at the Muséum National d'Histoire Naturelle Paris (MNHN).

The anatomical nomenclature of rhinoceroses is shown in **Figure 32**. Not all the postcranial elements have been studied, vertebrae (atlas and axis) and scapulae are not enough represented in the compared palaeopopulations, or their preservation is poor, so they have been omitted. Extremely variable and small carpals (pisiform, trapezoid and trapezium), tarsals (first and second cuneiforms), and McV have been omitted as well, together with fibula and patella.

Figure 32: Anatomical nomenclature of rhinoceroses. Anatomical elements included in the study are filled in grey. A) Complete rhinoceros skeleton, lateral view (adapted by Kahlke and Kaiser 2011), B) right carpus, dorsal view (drawing by M. Ballatore), C) left tarsus, dorsal view (drawing by M. Ballatore).

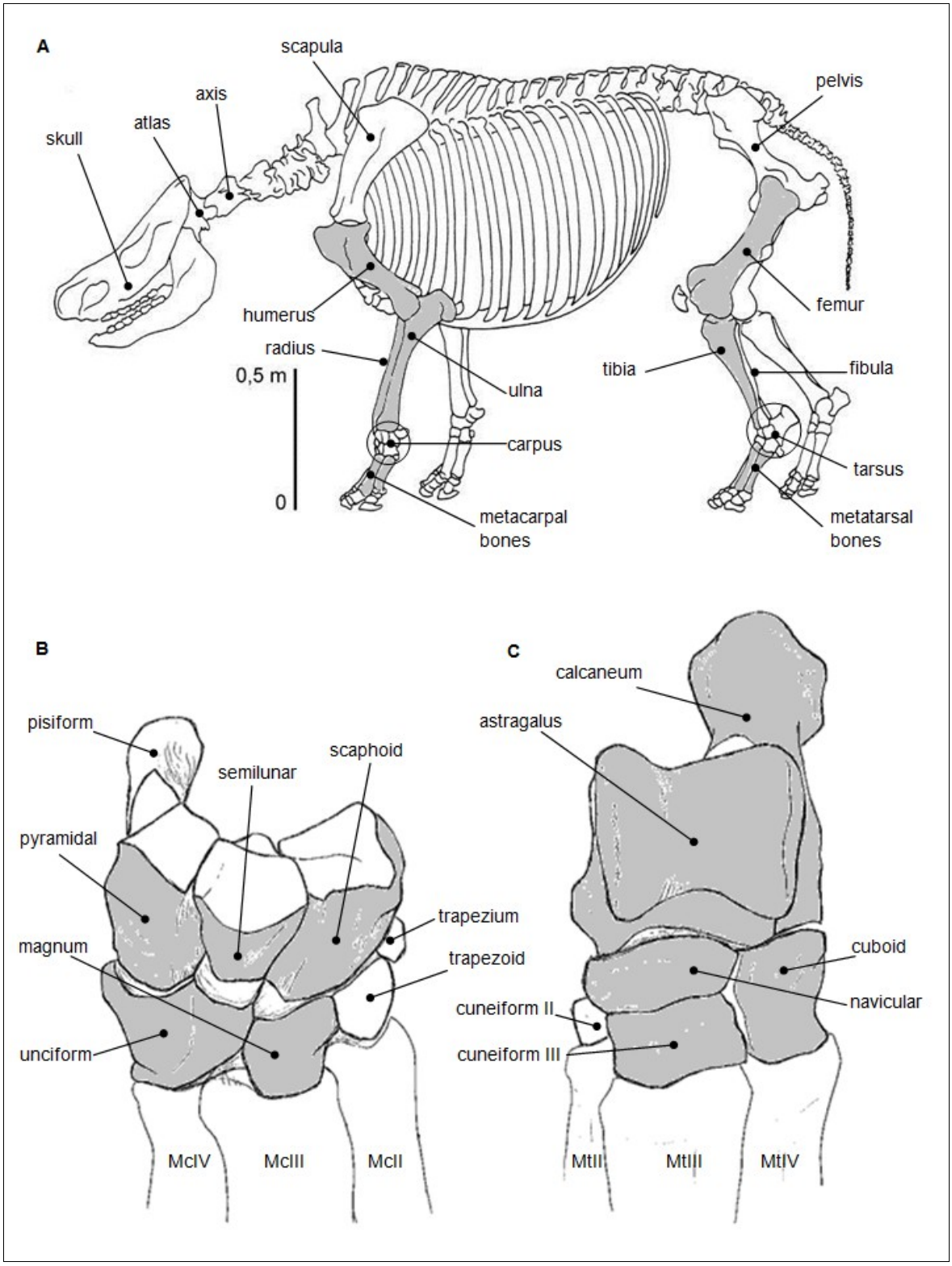

5.3.1 Biometry

Measurements are taken following the biometric method set up by Ballatore (**Attachment IV**), which sums up those used in previous works (Guérin 1980, Fortelius et al. 1993, Mazza 1988, Lacombat 2005, Van der Made 2010), selecting and modifying some measurements in order to reduce the inter-observer error and thus enhancing the precision of the results. For the same reason, no measurement from literature is included in the analysis, to avoid the error due to inconsistencies in the researchers' measuring techniques.

Some indexes and ratios have been defined for some anatomical elements, with particular reference to the strength of the long bones:

- for the radius we consider the ratio between the breadth and depth of the proximal articular surface (2P/3P – illustrating the flattening of the proximal articular surface), and an index of the strength of the bone given by the ratio between the breadth of the diaphysis and the breadth of the proximal epiphysis (2d/2P – as the value approximates 1 the strength increases);
- for the metapodial bones we consider the ratio between the length and the proximal breadth (1/2P), which is an index of the proportional size variability (a high value indicates a tall individual not proportionally robust, a low value a more stocky individual).

5.3.2 Size index

Following Lacombat (2009) we consider 12 measurements and use the population from Untermassfeld as a reference (**Table 11**). We use the size index described in archaeozoology (Uerpmann 1986, Meadow 1986, 1999) and applied to palaeontology (Eisenman and David 2002, Lacombat 2009):

$$I_s=50(m_r-x)/2sd_r$$

where m_r is the mean of the chosen measure in the reference population and sd_r is the standard deviation. We calculate the size index I_s for each specimen of the compared population (x is the measure of each individual).

Then we calculated the frequencies of individuals whose size index falls in classes of measures separated from the reference mean by 1, 2, 3… etc standard deviation. If one measure (x) is greater than the reference mean (m_r) by 1 standard deviation, it falls in the class -25, if the measure is smaller by the same quantity it falls in the class +25. So we represent the indexes on histograms with the frequency on the ordinate axis and the classes of size variation on the abscissa axes (0 is the reference, negative classes are bigger while positive classes are smaller; the distance from 0 is the amount of the size variation).

Table 11: Measures selected by Lacombat (2009) and statistics of the reference population (*S. hundsheimensis* from Untermassfeld, measurements in mm). *) Lacombat (2009) uses the diameter of the diaphysis while we use the diameter of the proximal epiphysis whose measurement is more precise; °) Lacombat (2009) does not specify the measurement of the astragalus, we choose the distal breadth which is more precise than the maximum breadth.

Element	Measurement	*N*	mean	st. dev.
Humerus	2D	8	132	4,87
Radius	2AD	8	78	26,68
Scaphoid	2	8	80	5,03
McII*	2P	9	48	5,57
McIII	2P	15	59	4,54
Femur	2d1	6	68	26,00
Tibia	2AD	10	79	2,00
Astragalus°	2D	13	77	4,00
Calcaneus	2	12	40	1,73
MtII	2P	6	30	2,42
MtIII	2P	10	53	2,71
MtIV	2P	8	43	14,58

5.4 Results

5.4.1 Biometrical analysis

Complete table of metric raw data is reported in **Attachment V**.

Anterior limb

- Humerus (**Figure 33**)

Few complete humeri are present, and several localities are just represented by a single individual. The variability in the general size of the bone shows a good correlation between the physiological length and the distal breadth, with longer bones more robust. The population from Mauer and Voigtstedt are the biggest while those from Pietrafitta and Saint-Prest the smallest (being even smaller than *S. etruscus* from Senèze), in between the (non coeval) rhinoceros from Untermassfeld and Hundsheim.

As far as the epiphyses are concerned, the number of proximal articular heads preserved is too low to allow a size comparison so only the distal trochlea is considered. It shows a isometric scaling between length and breadth, with longer bones more robust. A part from the small individuals from Saint-Prest and Pietrafitta, the whole Middle Pleistocene populations and the large sample from the Early Pleistocene of Untermassfeld fit in a narrow range of size variability.

Figure 33: Humerus dispersion graph: Hu = Hundsheim, Mo = Mosbach, Ma = Mauer, Vo = Voigtstedt, Pa = Pakefield, SP = Saint-Prest, Un = Untermassfeld, Pi = Pietrafitta, Se = Senèze. Measurements in mm.

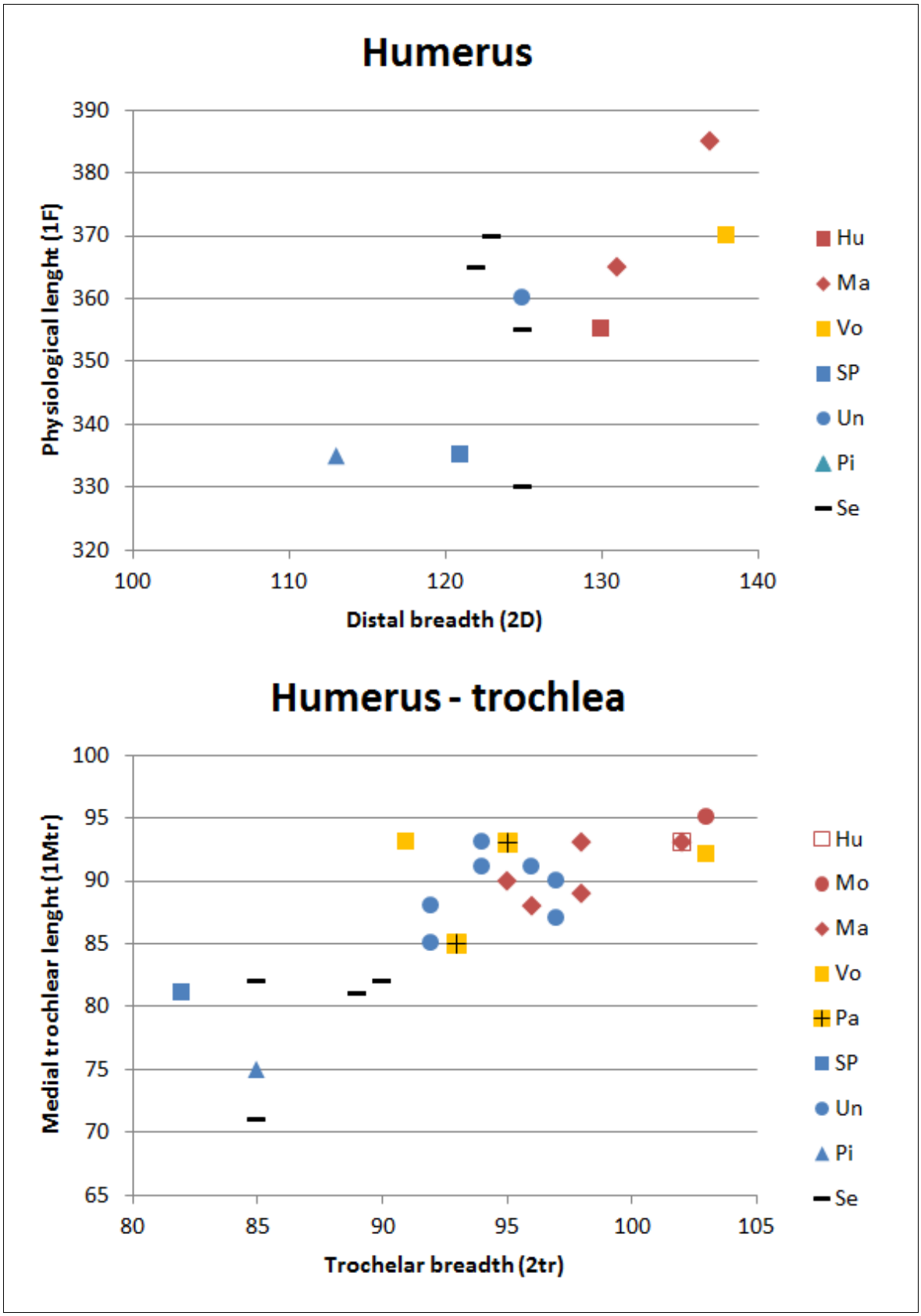

- Radius (**Figure 34**)

The radius is the most represented postcranial element. It shows a clear linear correlation between length and proximal breadth (isometric scaling). The smaller individuals are those from Pietrafitta and Saint-Prest; the Middle Pleistocene populations plus Untermassfeld fall in the same range of variation (with *S. etruscus* from Senèze in its lower part). The largest individuals are recorded from Voigtstedt and Süssenborn plus a single large individual from Untermassfeld which plots well beyond the range of its locality.

Despite the size variability, we find the same geometrical similarity of the bone by comparison of the following indexes: ratio between the proximal articular surface breadth and depth (2P/3P); breadth of the diaphysis and the proximal epiphysis (2d/2P). The smallest specimens have the same robustness of the biggest (see **Attachment V**).

Figure 34: Radius dispersion graph: Hu = Hundsheim, Mo = Mosbach, Ma = Mauer, Vo = Voigtstedt, Su = Süssenborn, Tr = Trimingham, SP = Saint-Prest, Un = Untermassfeld, Pi = Pietrafitta, Se = Senèze. Measurements in mm.

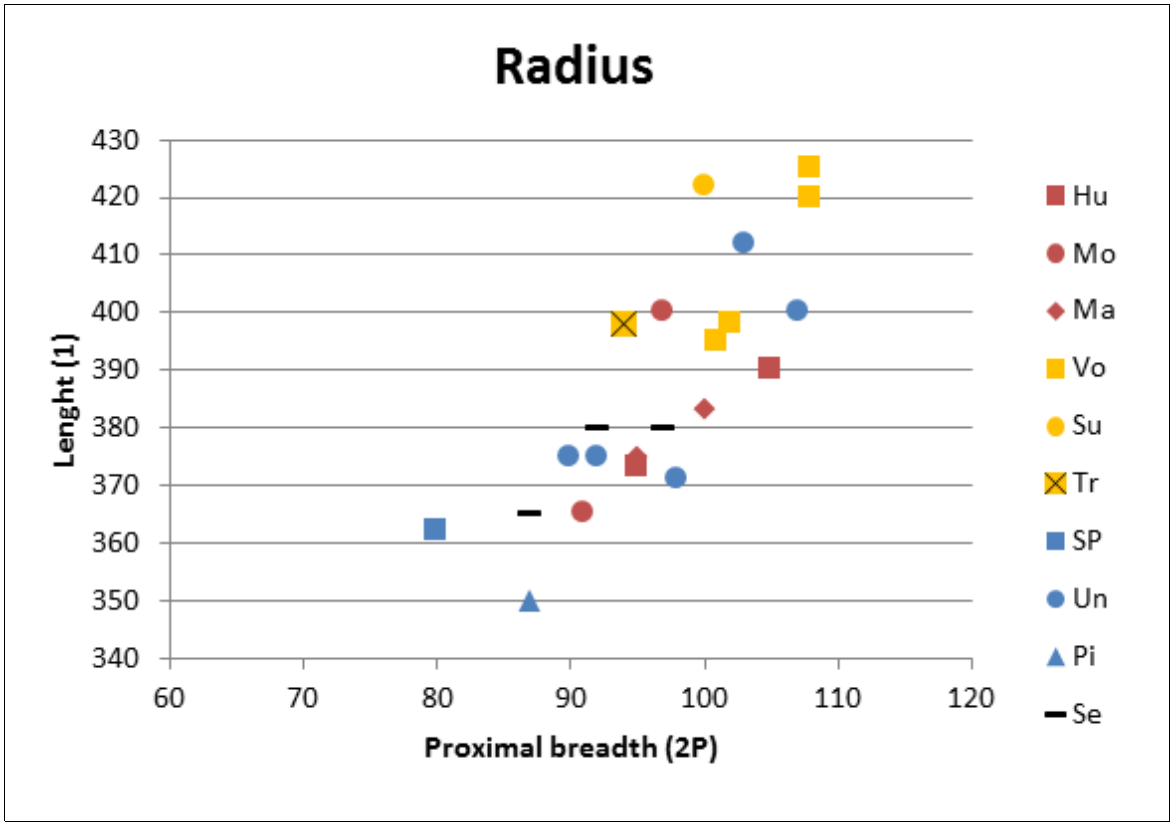

- Ulna (**Figure 35**)

A scanty number of complete ulnae is available. The size range of the population from Untermassfeld comprehends the other populations (apart from the specimens from Pietrafitta which are slightly smaller). This is evident in the size of the whole bone and also in the size comparison of the proximal articular surface.

Figure 35: Ulna dispersion graph: Hu = Hundsheim, Bo = Boxgrove, Ma = Mauer, Vo = Voigtstedt, Su = Süssenborn, Un = Untermassfeld, Pi = Pietrafitta, Se = Senèze. Measurements in mm.

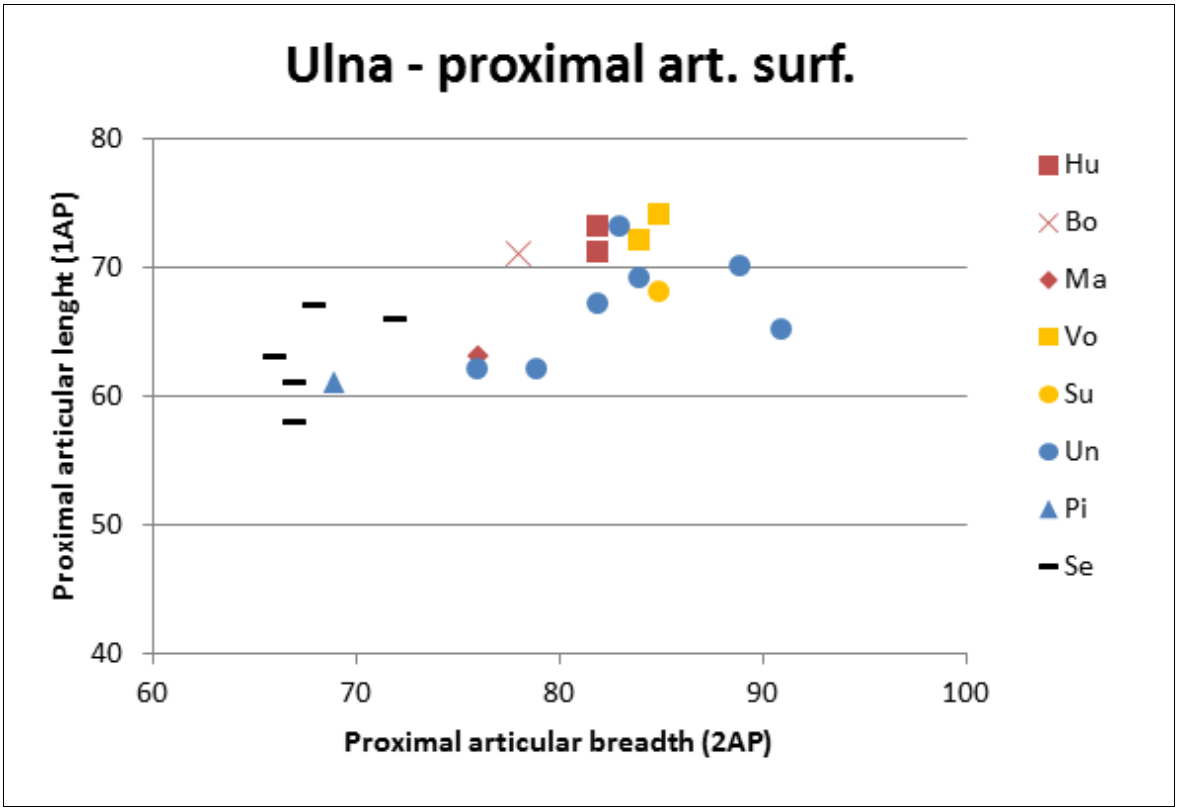

- Carpus (**Figure 36**)

Five carpals are included in the study. Scaphoid, semilunar and pyramidal are proximal elements of the carpus; the former two articulate to the radius while the pyramidal articulates to the ulna. A fourth bone, the pisiform, lies in contact with the pyramidal (and the ulna) in the lateral part of the carpus but its morphology is extremely variable also within the right and left side of the same individual; moreover it is not recorded with high frequency so we exclude this bone from the analysis. The other two bones included are the unciform and magnum. The former articulates proximally to the pyramidal and semilunar and distally to the IV metacarpal bone, the latter to the scaphoid and to the III metacarpal bone. Trapezoid and trapezium are not included since they are very small, almost isodiametrical and poorly recorded.

Scaphoid – Bone dimensions scale isometrically. The populations from Süssenborn, Voigtstedt and Mauer are bigger than those from Mosbach2 and Hundsheim. The smallest are those from West Runton and Soleilhac. The rhinoceros from Untermassfeld are mostly large, but a single bone (belonging to an adult individual – ind.V in H.-D. Kahlke 2001, hereafter) is the smallest, so that the range of Untermassfeld includes all the other populations.

Semilunar – The bone is variable in its depth, independently from the length. In general each population has a narrow range of variability in length but different individuals show considerable variation in depth. The only exception is Untermassfeld, whose specimens cover the whole variation range of the other populations. In the higher side of the range we find the specimens from Mauer and some individuals from Untermassfeld. In the middle the populations from Hundsheim, Mosbach2, Isernia, Voigtstedt and Untermassfeld. In the lower part Untermassfeld (ind. V and VII) and the smallest Soleilhac.

Pyramidal – All the populations have a very narrow range of depth variability, while the length of the bone varies considerably. The populations from Soleilhac, Mosbach2, Boxgrove and some individuals from Untermassfeld fall in the lower side of the length range, those from Hundsheim, Mauer, Isernia, Voigstedt and some from Untermassfeld in the upper side.

Unciform – With the exception of Soleilhac and Mosbach2 (that are proportionally smaller than the others), the remaining populations fit in a single cluster with e very reduced variability in the depth of the bone.

Magnum – Apart from the populations of Voigtstedt and Süssenborn, the others (those represented by more than one individual) have a large variability range. The smallest individuals are from Soleilhac and Untermassfeld (ind. IX).

Figure 36: Carpus dispersion graph: Hu = Hundsheim, Bo = Boxgrove, Mo = Mosbach, Ma = Mauer, Is = Isernia, Vo = Voigtstedt, Su = Süssenborn, WR = West Runton, Si = Sidestrand, Ov = Overstrand, Pa = Pakefield, So = Soleilhac, Un = Untermassfeld, Se = Senèze. Measurements in mm.

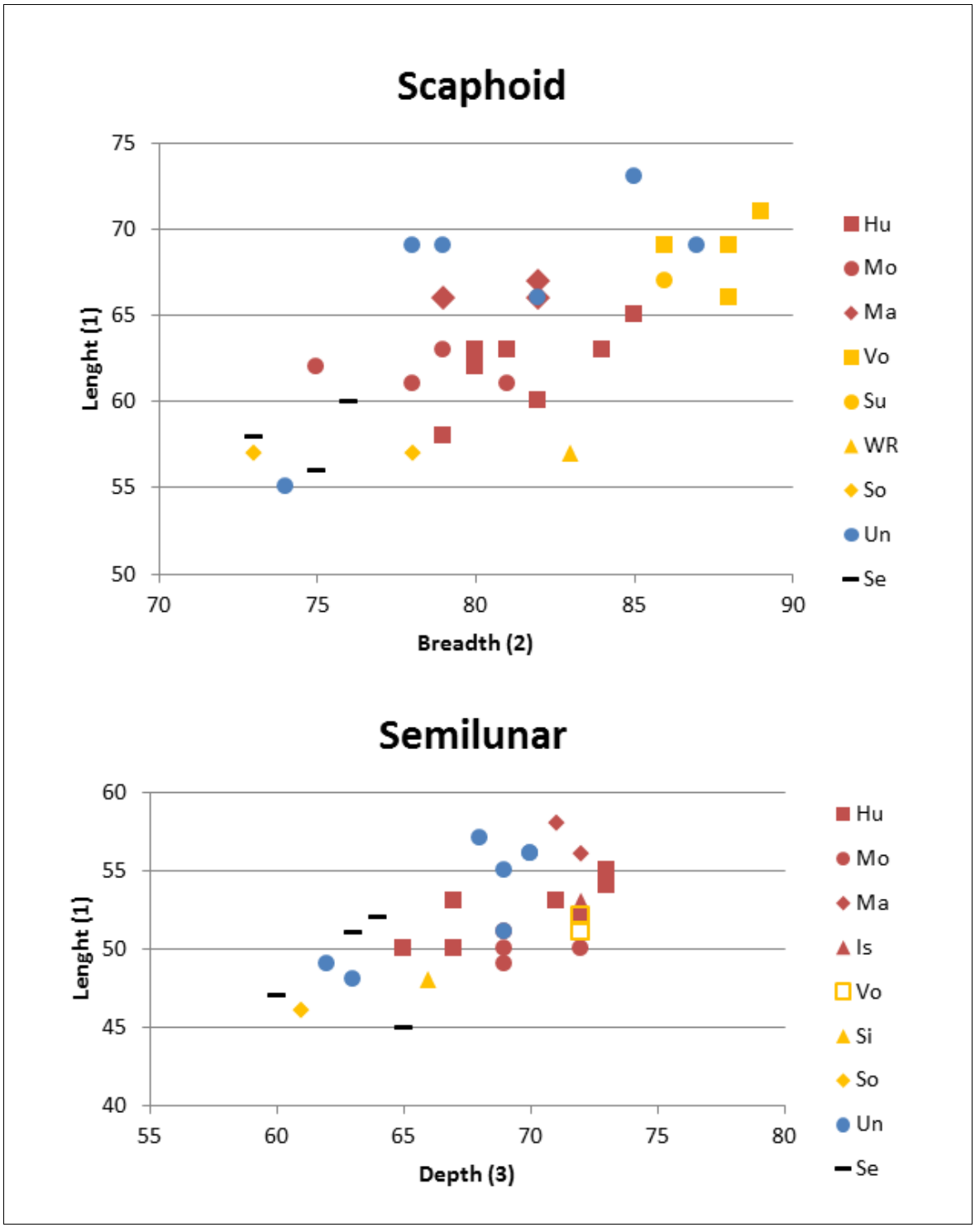

Figure 36: (continues)

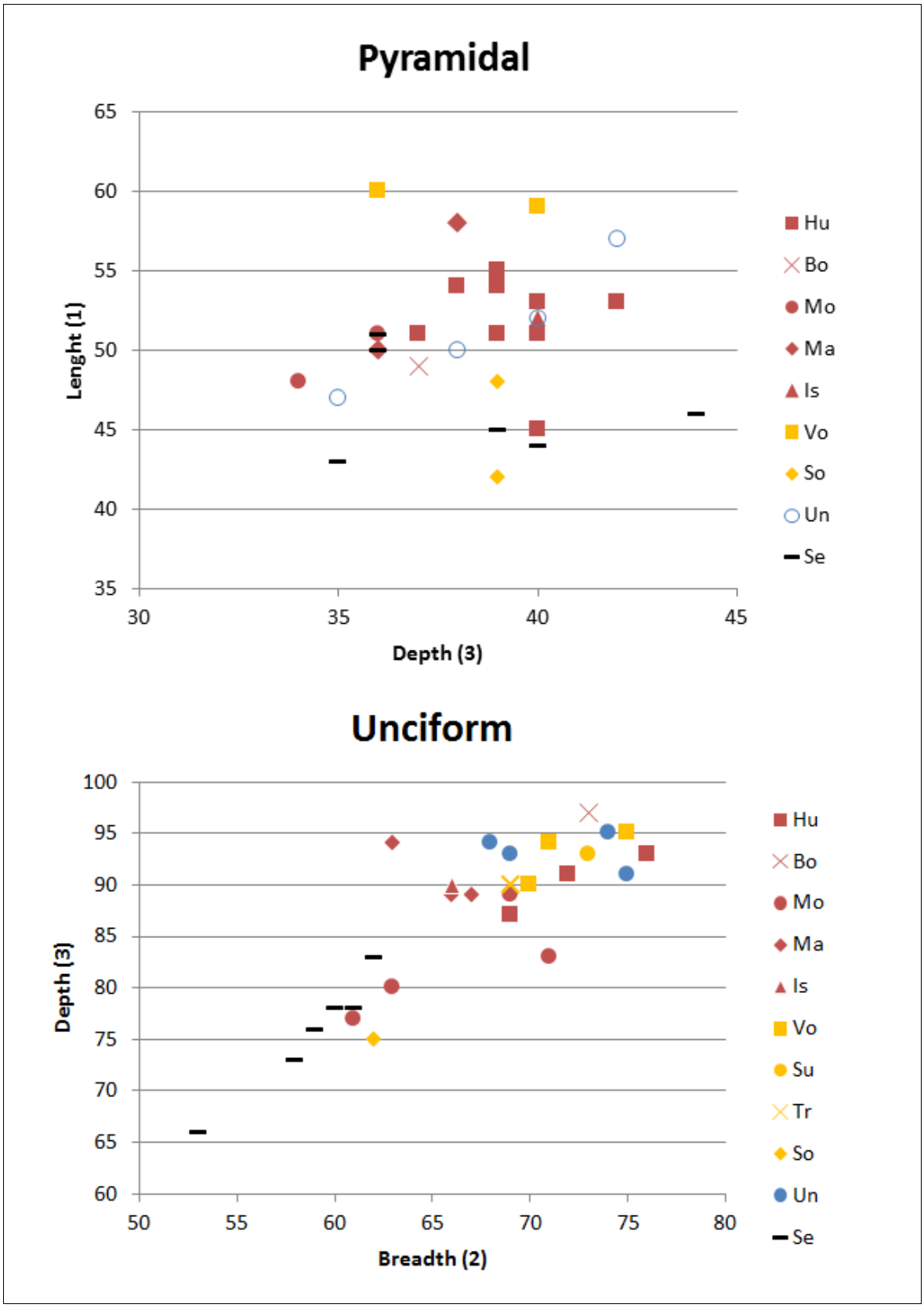

Figure 36: (continues)

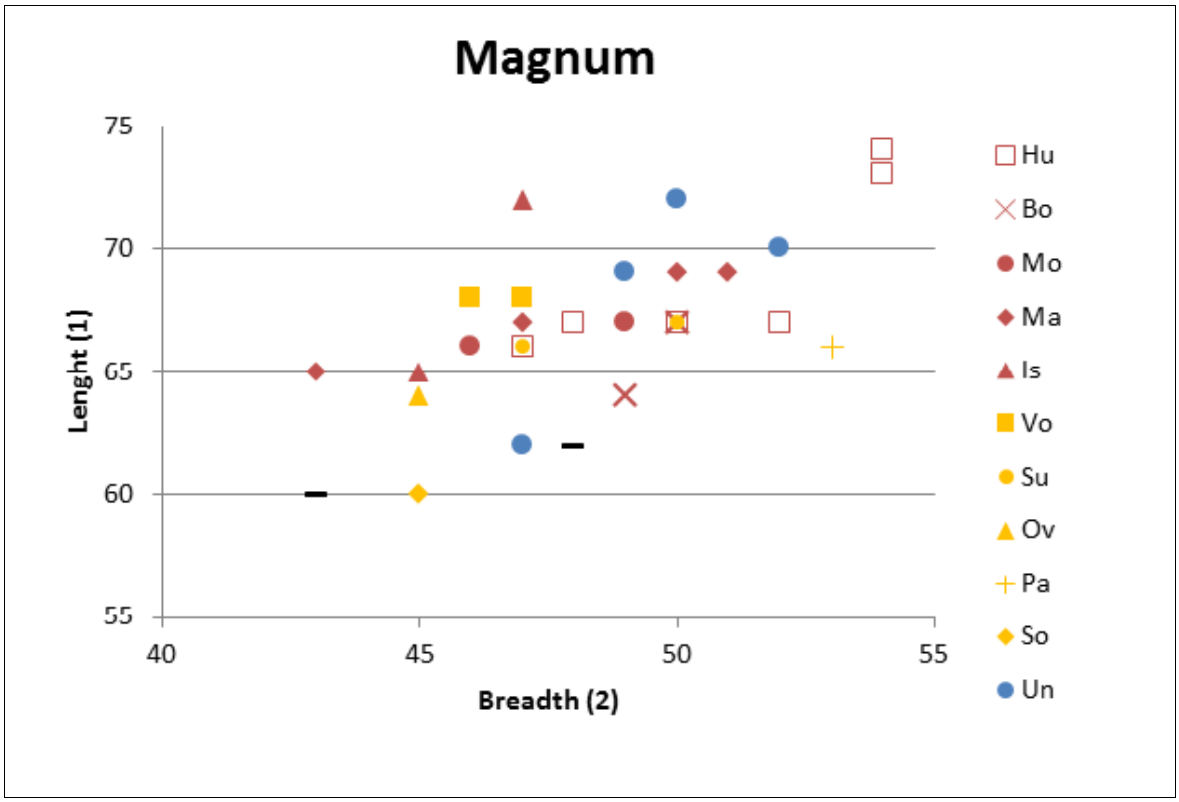

- Metacarpal bones (**Figure 37**)

McII – The bone shows a high degree of intra-population variability in the length, but the size increase is allometric with the longer bones very slender (this is confirmed by the ratio between the length and the proximal breadth 1/2P, see **Attachment V**). With few exception, each population has bones of comparable size. The smallest are the specimens from Mosbach and Soleilhac. While the biggest are those from Voigtstedt.

McIII – A part from the individuals from Pietrafitta and Soleilhac that are particularly small (as much as some small individuals from Senèze), the other populations are similar among them (and to most *S. etruscus* from Senèze). Differently from the McII the increase in size is isometric, with longer bones being more robust. Each population is highly variable.

McIV – The bone scales more allometrically than McIII but the variability range of the length is less extended than in McII. The rhinoceros from Pietrafitta is the smallest (also smaller than the *S. etruscus* specimen from Senèze); among the other populations Soleilhac, Trimingham and some individuals from Untermassfeld (limb II and individual V) are in the lower part of the range, the remaining populations, including some individuals from Untermassfeld, are in the higher part.

Figure 37: Metacarpal dispersion graph: Hu = Hundsheim, Mo = Mosbach, Ma = Mauer, Vo = Voigtstedt, Su = Süssenborn, Tr = Trimingham, So = Soleilhac, Un = Untermassfeld, Pi = Pietrafitta, Se = Senèze. Measurements in mm.

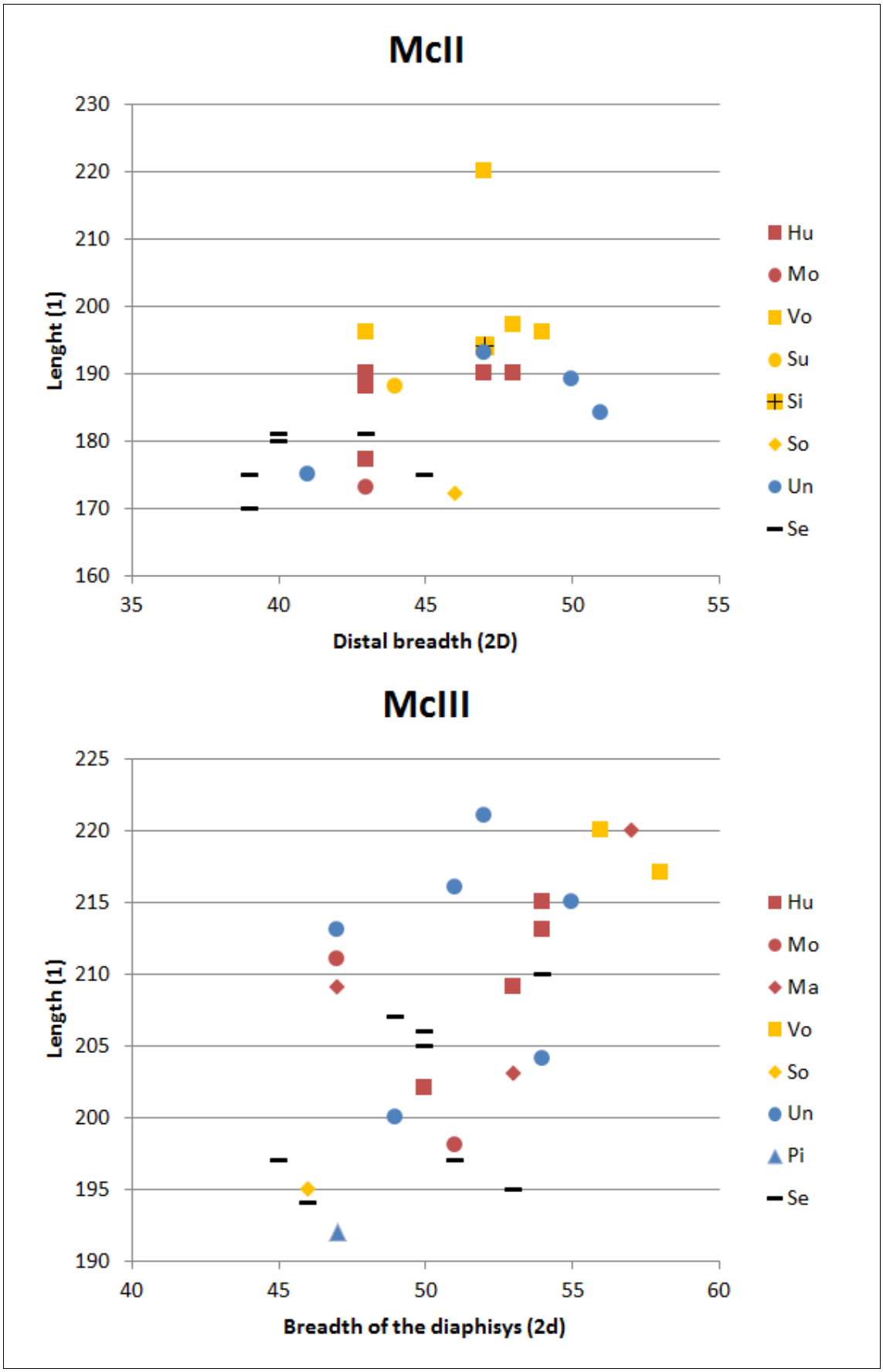

Figure 37: (continues)

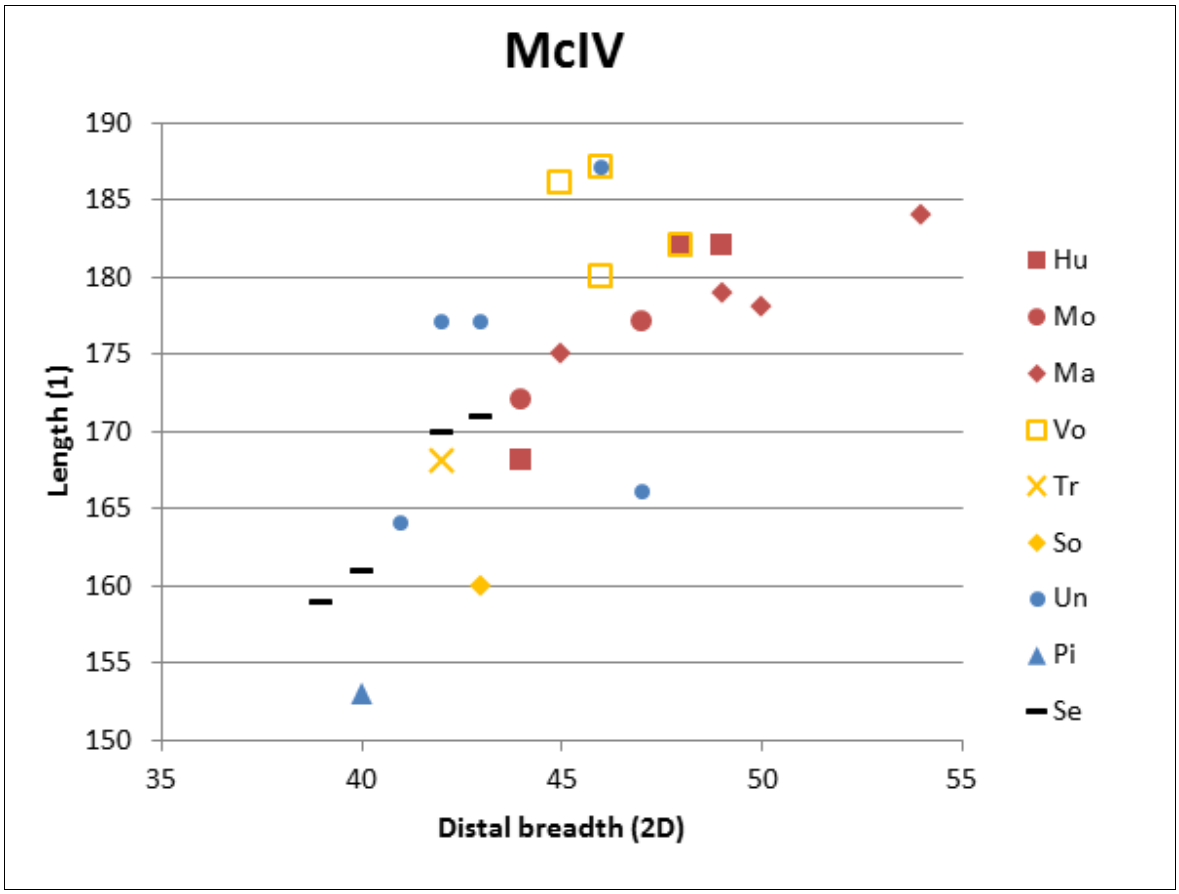

Posterior limb

- Femur (**Figure 38**)

Few complete femurs are available, but a linear correlation between the length and the distal breadth of the bone is evident. The population from Untermassfeld is the largest while the coeval remain from Pietrafitta is considerably smaller.

The size of the proximal articular head scales isometrically to the bone. Its size confirms Untermassfeld as the largest population and Pietrafitta as the smallest; the other populations are close to Untermassfeld.

- Tibia (**Figure 39**)

The tibia can be more or less robust (on the proximal breadth) in each population independently from the length. The specimen from Trimingham has the same length of the other populations but is very slender. A single individual from Untermassfeld (isolated specimen) is particularly long and relatively slender. The population from Mosbach2 shows a general size more similar to that of *S. etruscus* from Senèze, with short and stocky tibias.

Figure 38: Femur dispersion graph: Hu = Hundsheim, Ma = Mauer, Vo = Voigtstedt, Su = Süssenborn, Un = Untermassfeld, Pi = Pietrafitta, Se = Senèze. Measurements in mm.

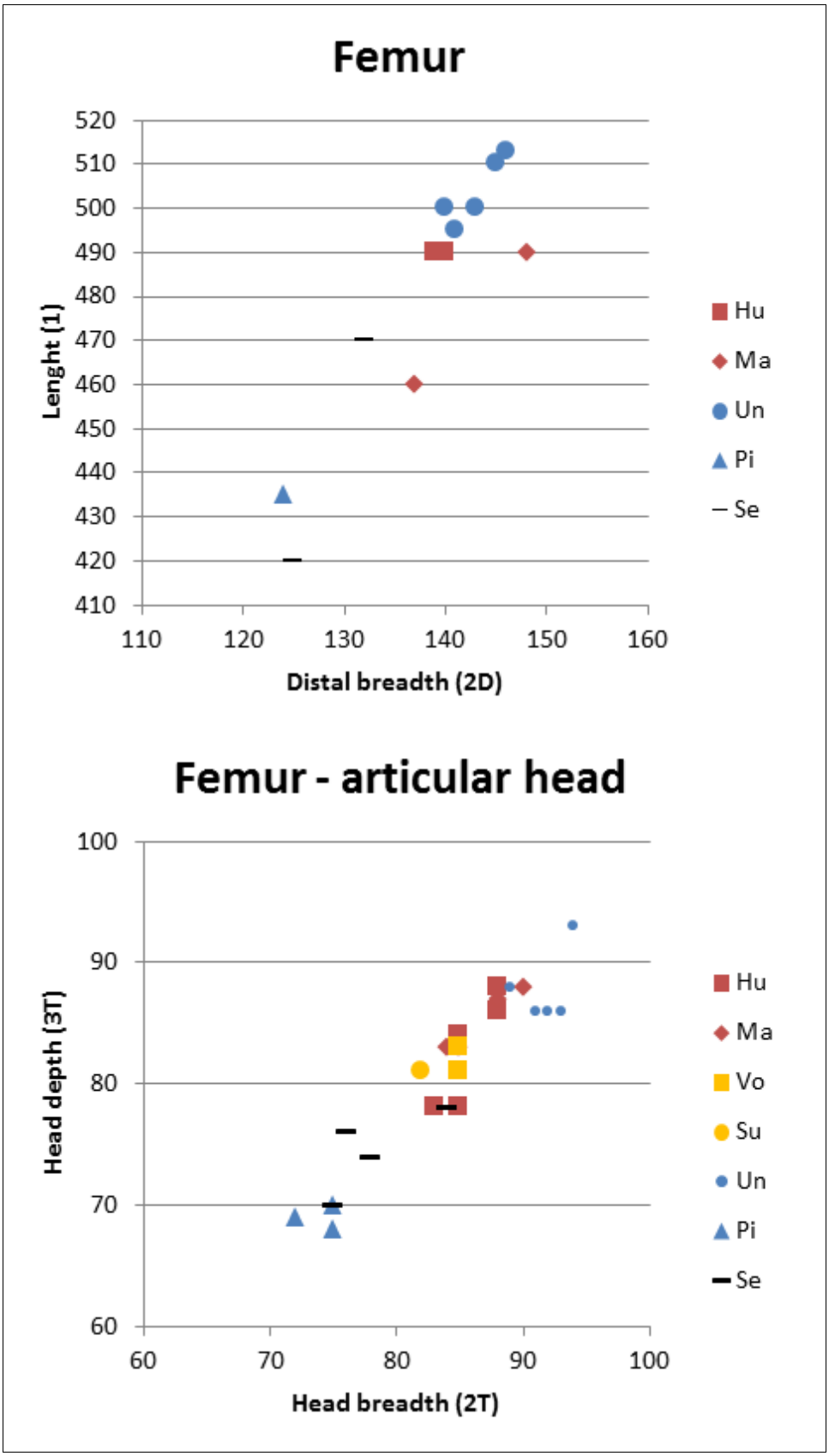

Figure 39: Tibia dispersion graph: Hu = Hundsheim, Mo = Mosbach, Ma = Mauer, Vo = Voigtstedt, Tr = Trimingham, Un = Untermassfeld, Se = Senèze. Measurements in mm.

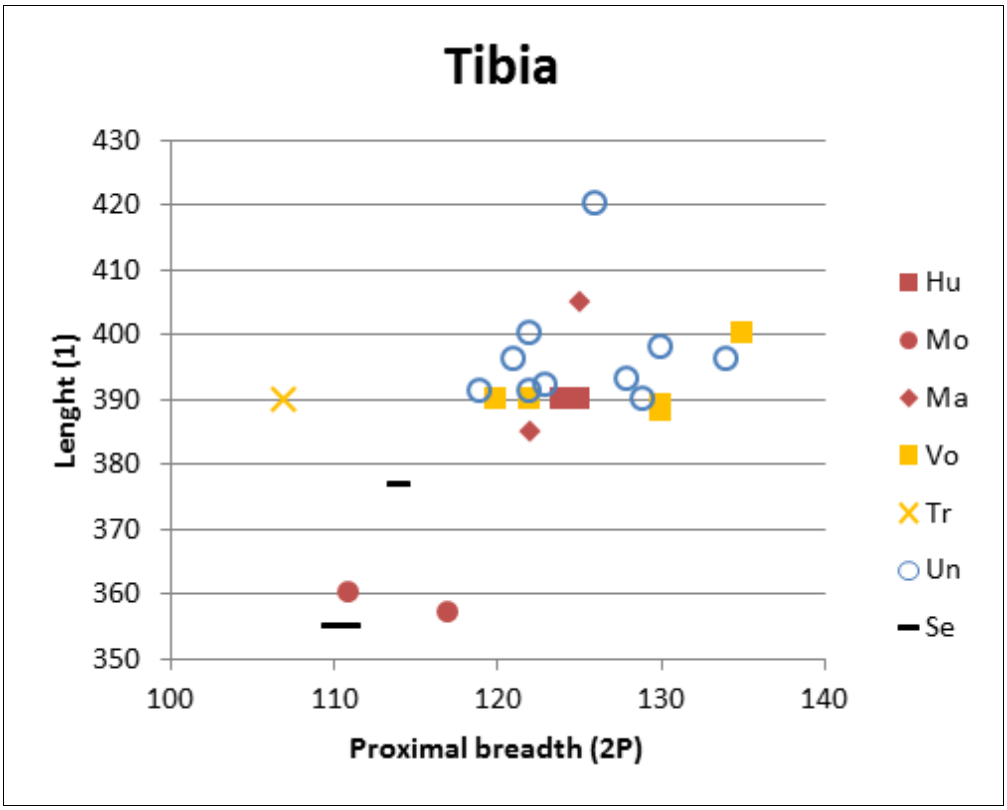

- Tarsus (**Figure 40**)

Astragalus – The size of the bone increases proportionally in each population and the range is similar among Hundsheim, Mauer and Untermassfeld (the lower part of the range overlaps with that of *S. etrucus* from Senèze). The population from Voigtstedt and the individuals from Süssenborn and Isernia are in the higher part of the range. In Pietrafitta and in specimen XI from Untermassfeld, an allometry is evident with longer and relatively thinner bones. The opposite applies to the population from Mosbach2 with short and stocky bones.

Calcaneus – In each population, with the exception of Untermassfeld, the bone scales isometrically through its size range. The population from Untermassfeld shows the largest range of length variability with some allometric individuals (individual VII is extremely short but not proportionally narrow). The smallest individuals are those from Pietrafitta and Soleilhac. Also from the locality of Trimingham a single individual shows very reduced size, considering that some older remains have been collected there, we can suppose the specimens belongs to *S. etruscus*. The largest specimens are those from Voigtstedt and Untermassfeld.

Figure 40: Tarsus dispersion graph: Hu = Hundsheim, Bo = Boxgrove, Mo = Mosbach, Ma = Mauer, Is = Isernia, Vo = Voigtstedt, Su = Süssenborn, WR = West Runton, Si = Sidestrand, Tr = Trimingham, So = Soleilhac, Un = Untermassfeld, Pi = Pietrafitta, Se = Senèze. Measurements in mm.

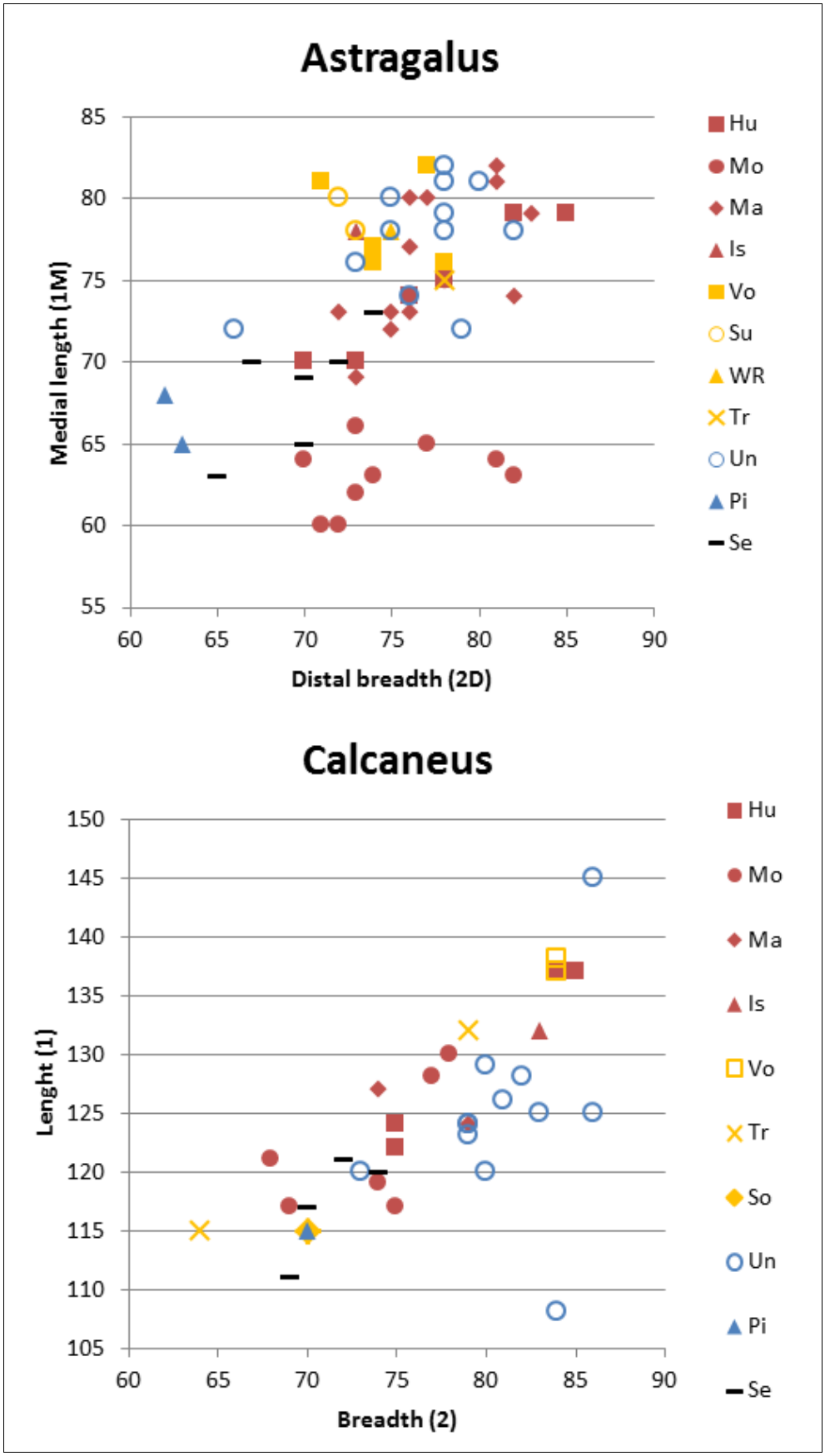

Figure 40: (continues)

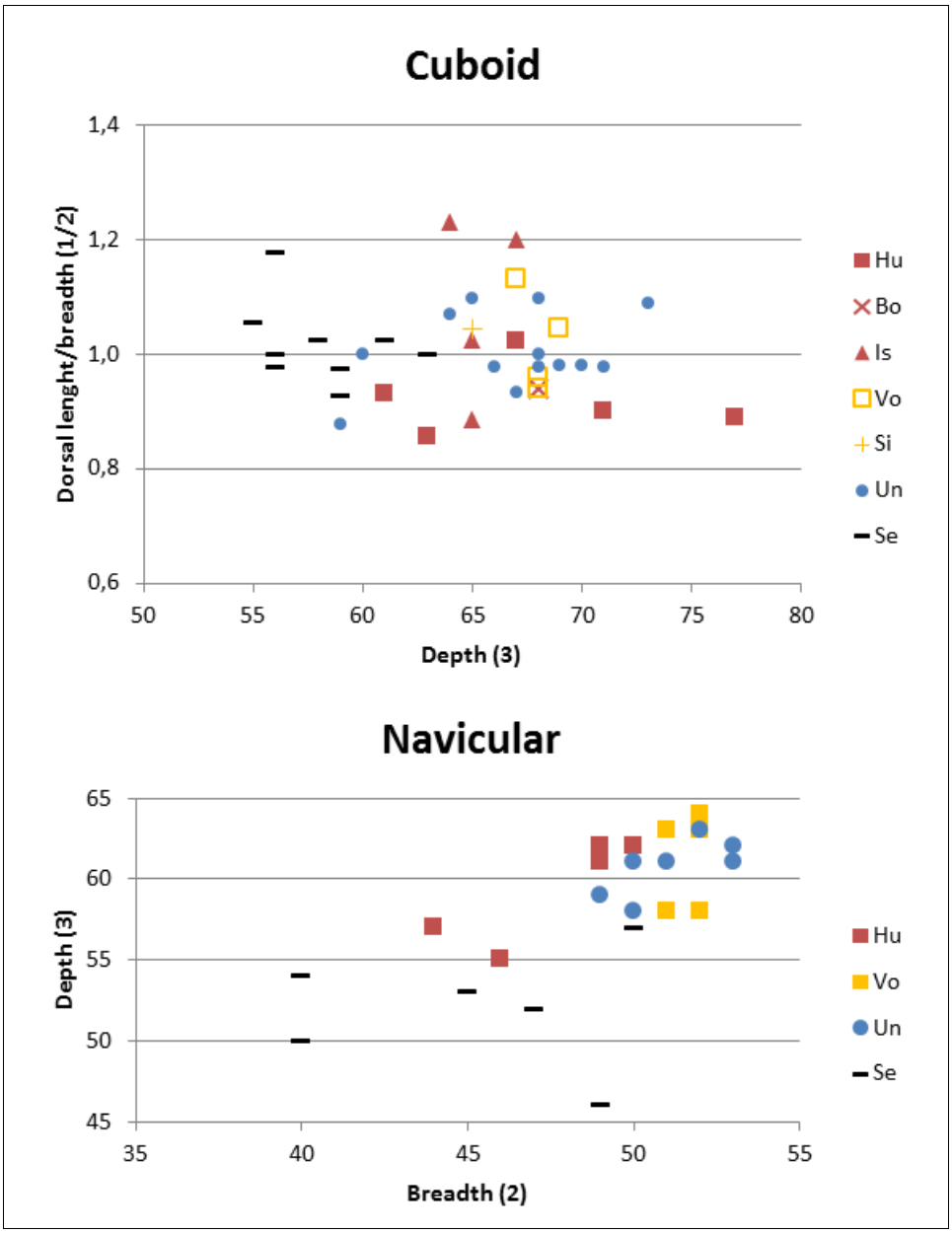

Cuboid – The ratio between the dorsal length and breadth (1/2) is the index quantifying the shape of the squared dorsal surface. The surface is high and narrow for values higher than 1, short and enlarged (proximo-distally compressed) for lower values. The shape is variable in each population in a similar way, the rhino from Hundsheim only has a distinct compressed bone, those from Untermassfeld are instead isodiametric. The depth of the bone varies allometrically without correlation to the size of the dorsal surface; the populations from Untermassfeld and Hundsheim show the largest size range.

Navicular – Only three populations are compared and they fall in the same range even if

some individuals from Hundsheim are smaller. The size variability of the bone is reduced (on the contrary the species *S. etruscus* from Senèze shows a wider variability).

- Metatarsal bones (**Figure 41**)

MtII – The populations from Voigtstedt, Hundsheim, Isernia and Untermassfeld fall in the same range of variability, while the rhinoceros from Mauer shows a broader range, with allometric size variation. The specimen from Pietrafitta is smaller than the other co-specifics, and than *S. etruscus* from Senèze.

MtIII – All the individuals fall in the same narrow breadth range , while the variability in the length is wider (as it can be expected). Noticeably, the most elongated bones are those from Untermassfeld, the shortest, from Isernia, Untermassfeld, Mauer and Hundsheim. The specimen from Pietrafitta is smaller than S. *etruscus* from Senèze too.

MtIV – The bones of the different populations have a very reduced variability range, the only exception is the specimen form Pietrafitta, which is even smaller than *S. etruscus* from Senèze. Also the specimen from Mosbach is proportionally slightly smaller.

Figure 41: Metatarsal bones dispersion graph: Hu = Hundsheim, Mo = Mosbach, Ma = Mauer, Is = Isernia, Vo = Voigtstedt, Tr = Trimingham, Un = Untermassfeld, Pi = Pietrafitta, Se = Senèze. Measurements in mm.

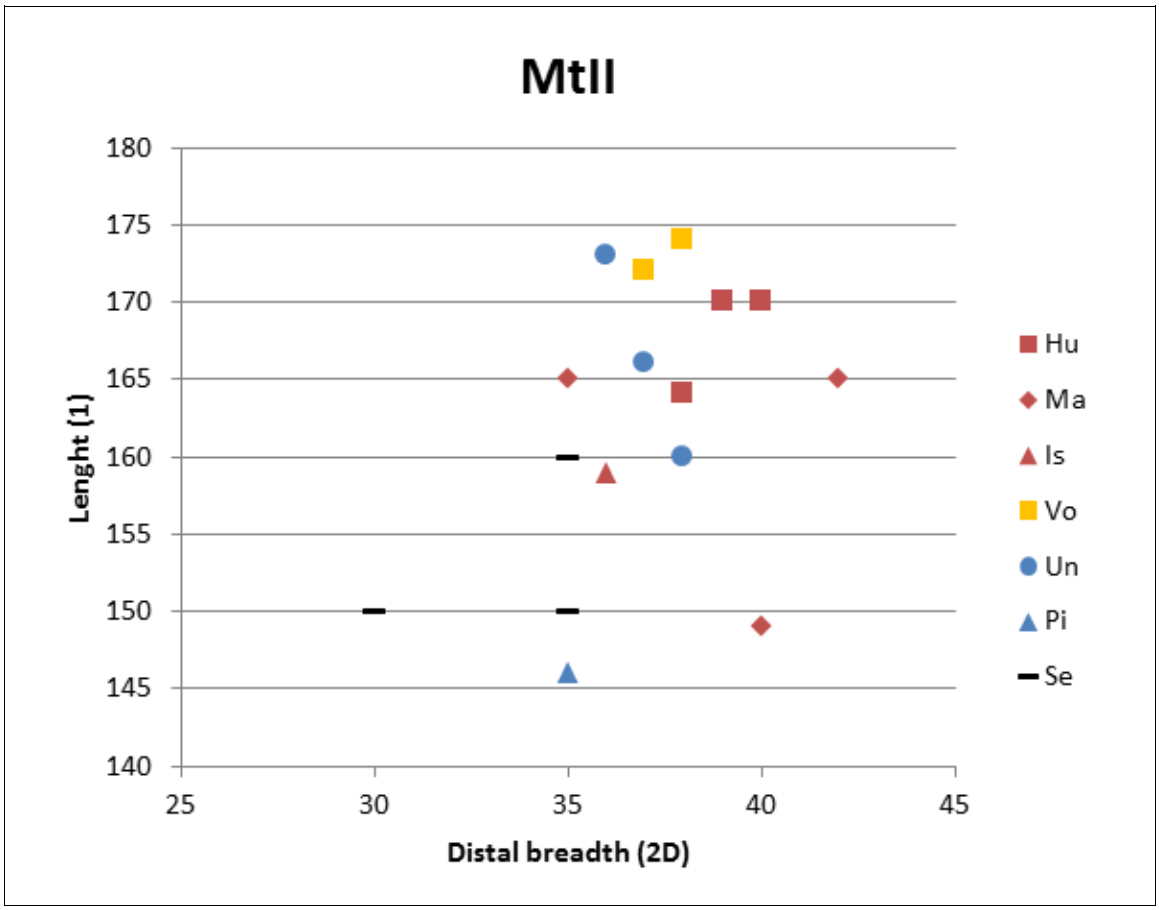

Figure 41: (continues)

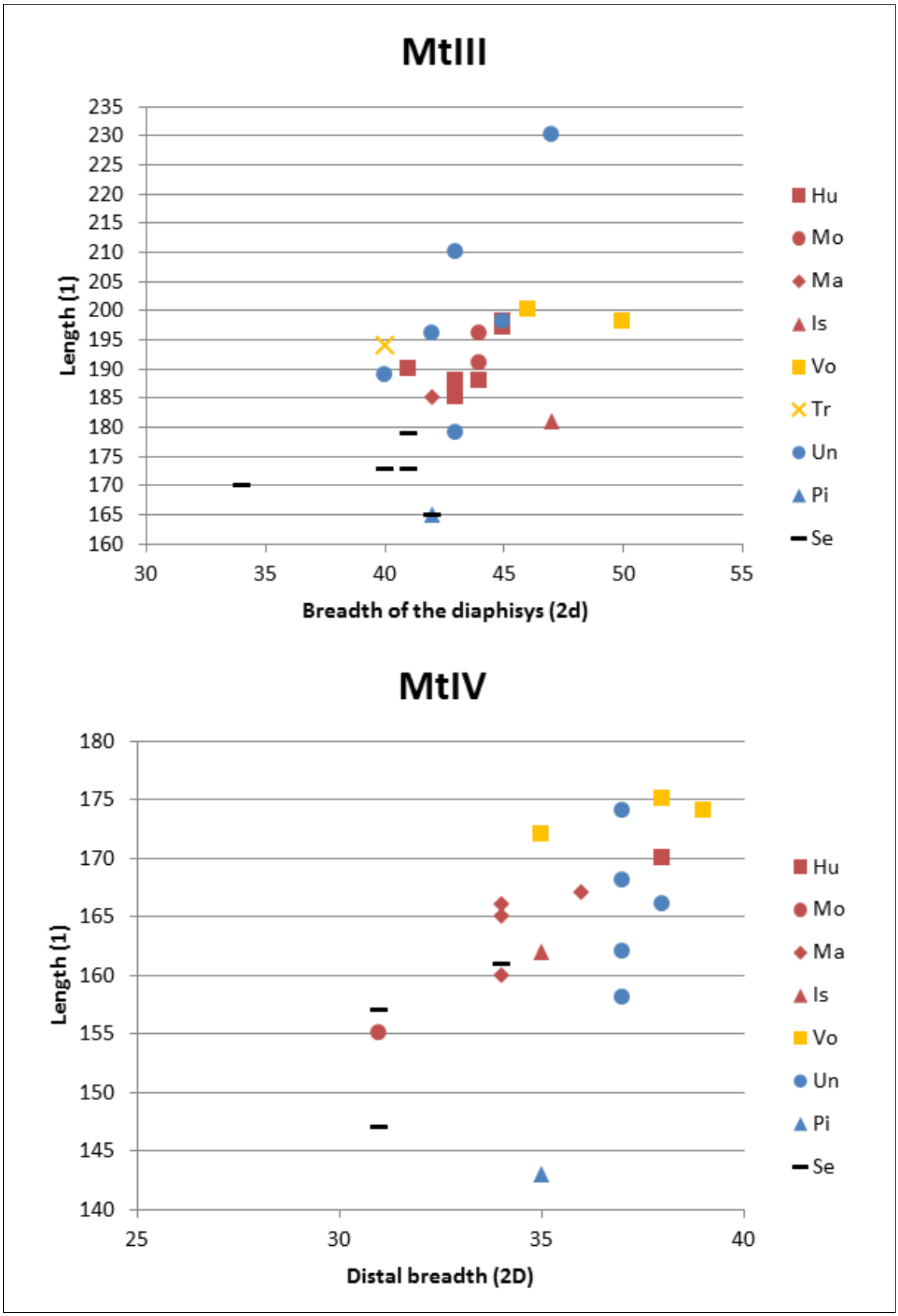

5.4.2 Size index

The size index comparison of the investigated populations is illustrated through histograms in **Figure 42**.

In the Middle Pleistocene, the size of the *S. hundsheimensis* populations from Hundsheim and Mosbach2 is comparable to the size of the earlier population from Untermassfeld. Also the population from Mauer has roughly the same size but a certain amount of bones falls in the lower side of the dimensional range. Other species from Mauer show a similar reduction in size, e.g. the roe deer *Capreolus priscus* (Soergel 1914, Pfeiffer 1998, Van der Made et al. 2014) and the moose *Cervalces latifrons* (H.-D. Kahlke 1990, Breda and Marchetti 2005) . The population from Boxgrove is underrepresented and does not allow any general comparison, but the few bones are similar to the other coeval populations from central Germany, so that the expected increase in size along the latitudinal gradient is not evident.

The early Middle Pleistocene populations from Voigtsted and Süssenborn are comparable in size and slightly larger than the reference population from Untermassfeld, while the population from Isernia has the same size as Untermassfeld. The British populations from the Cromer Forest-bed Formation are slightly smaller than the reference, and this is particularly evident in specimens from Sidestrand and Trimingham. However, we should underline that from these two localities older levels outcrop with the main early Middle Pleistocene layers (Lister 1993), and therefore we cannot completely exclude that these "small" bones belong to a "large" *S. etruscus*

The earliest populations from the Early Pleistocene have an evident smaller size than Untermassfeld and the size increase at higher latitude (evident between Pietrafitta and Untermassfeld), is not confirmed at Saint-Prest which is quite small sized.

Figure 42: Size index comparison. The size index of each individual can fall in classes of measures separated from the reference mean (Untermassfeld) by 1, 2, 3… etc standard deviations. If one measure (x) is greater than the reference mean (m_r) by 1 standard deviation, the relative size index falls in the class -25, if the measure is smaller by the same quantity it falls in the class +25. So we represent the indexes on histograms with the classes of size variation on the abscissa axes (0 is the reference, negative classes are bigger while positive classes are smaller; the distance from 0 is the amount of the size variation) and the frequency of each class on the ordinate axis.

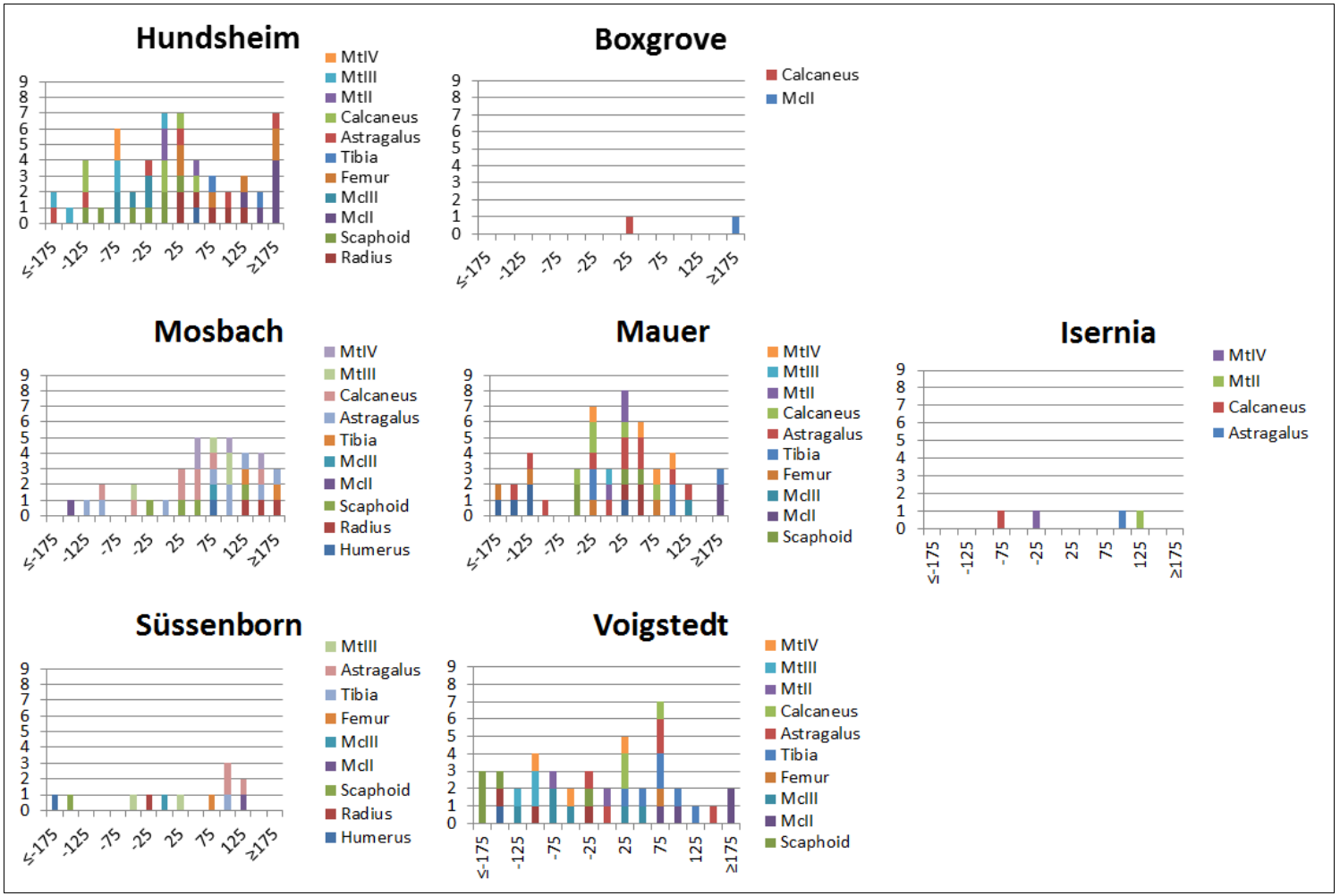

Figure 42: (continues)

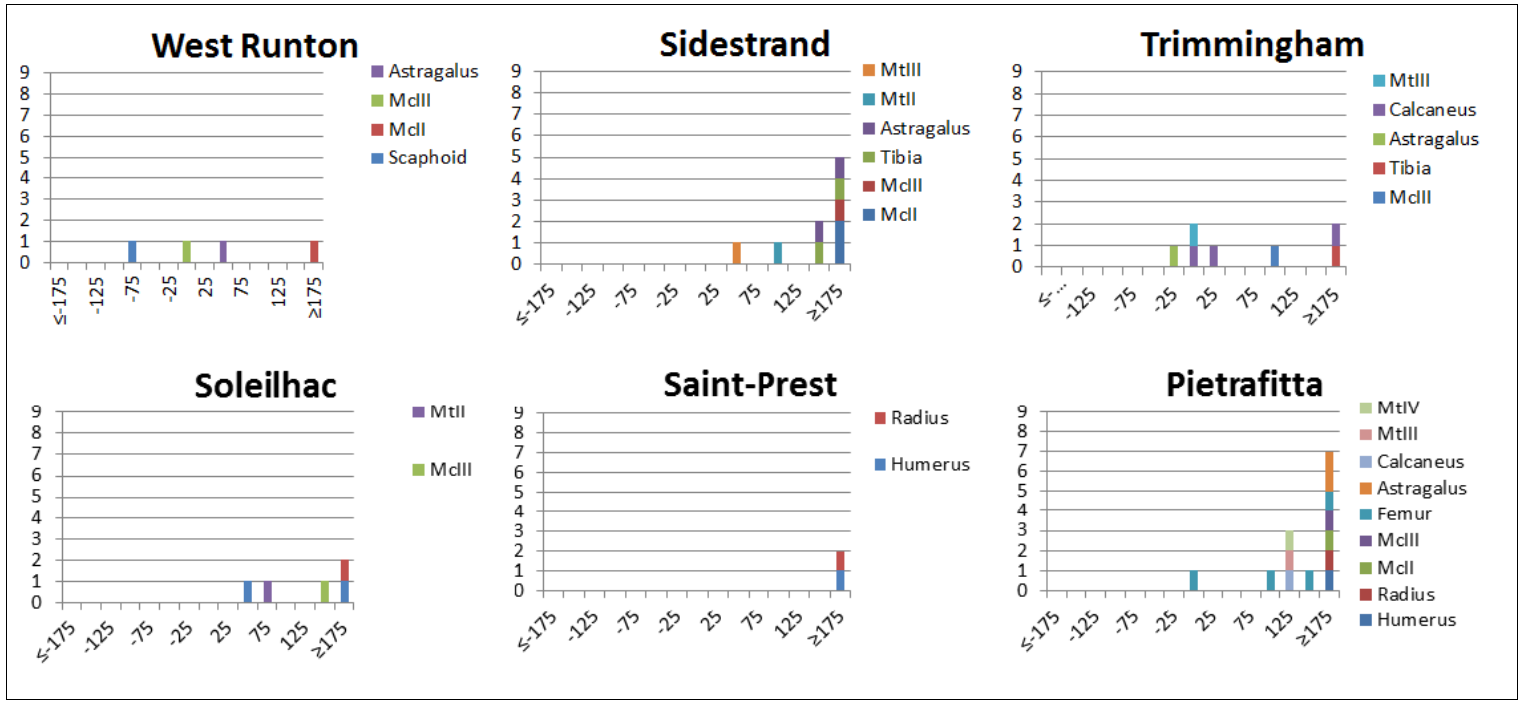

5.6 Discussion

The hypothesis of two size-classes for the species *S. hundsheimensis* cannot be supported because the population from the late Early Pleistocene of Untermassfeld clearly shows a wide variability range encompassing a "small-form" and a "large-form" (**Figure 43**). Only the populations from the early Middle Pleistocene of Voigtstedt and Süssenborn sometimes exceed this range in the radius, scaphoid and metacarpal bones II. Among the smallest bones from Untermassfeld we find some associated elements (individuals V, VII, IX, XI and anterior limb II) but the small size is not always evident in all the elements of the same individual, so that the size variability seems to depend on each anatomical element.

In the Early Pleistocene a particularly small form is found at Pietrafitta and slightly bigger at Saint-Prest whose rhinoceros sometimes reaches the dimensional range of Untermassfeld and partial overlap occurs (in the radius). The geographic distribution of these three populations suggests that there is not a latitudinal size gradient among coeval populations. (At this regard other "small" *S. hundsheimensis* population, comparable in size to that from Pietrafitta, is reported at Westerhoven, The Netherlands, which is even northern than Untermassfeld and Saint-Prest; Mazza et al. 1993).
In the early Middle Pleistocene, the southern population from Soleilhac is smaller than the coeval northern population from Süssenborn and Voigtstedt, as suggested by the hypothesis of latitudinal size increase gradient. If the northernmost British coeval populations are included in the comparison, they are comparable with the size of the Soleilhac population, thus in contrast with the supposed increasing size with the latitudinal gradient, but, in this case, an insularism process affecting the body mass could be claimed. Interestingly, this is not in agreement with our previous results given by dental size comparison (Ballatore and Breda 2013), showing a slightly larger size for the British teeth when compared with Isernia. A different scaling of teeth and postcranials could thus be suggested for the Cromer Forest-bed, in which the postcranials are smaller than the coeval continental sample but the teeth are, on the contrary, larger. This would suggest that insular conditions might affect the body mass more than the teeth.
In the Middle Pleistocene the populations from Isernia and Hundsheim have the same size (comparable to the older population from Untermassfeld) while the population from Mauer and particularly Mosbach are relatively smaller and finally the smallest population is that from Boxgrove. It could appear an inverse latitudinal gradient (size decrease), but each

geographical context needs distinct discussion.

A size increase-decrease trend through time is evident at least among the Central Germany populations. The rhinoceroses from Süssenborn and Voigtstedt are, in fact, slightly larger than those from Untermassfeld, as already suggested by R.-D. Kahlke (2006). Moreover H.-D. Kalhke (2001) reports that "when compared with older or more southern populations, the rhinoceroses from Untermassfeld bear evidence of a lengthening of the extremities. This feature marks the beginning of an adaptational process that later allowed the animals to endure increasing continentality, at least in Central Europe (e.g. Süssenborn)". From our results, it is evident that the metapodial bones from Untermassfeld are elongated: metacarpals are similar in the general size to those from Voigtstedt and Süssenborn, while in the metatarsals some differences arise. Some MtIIIs are extremely elongated at Untermassfeld and shortened at Voigtstedt, while the paired 2nd and 4th metatarsals attain the same length at Untermassfeld and Voigtstedt. As a result, these Untermassfeld foot has a proportionally longer 3rd toe. The Middle Pleistocene populations from Mauer and particularly Mosbach, that are the latest known records of the species ante extinction, show a reduction of size. This is not confirmed by the southern population from Hundsheim. This trend of size reduction can be interpreted as related to changing environmental conditions and species demise: climatic degradation seems to have been more emphasized in Central Germany with respect to Austria. The coeval population from Isernia is comparable in size to that from Hundsheim, in this case the influence of the Mediterranean can explain the absence of this trend of size reduction.

As concerning the British Isles, the specimens from Boxgrove are well comparable with the older Cromerian populations, so no change in size occurred during time and the whole British populations are smaller than coeval continental populations. Insularism processes can explain such results and persisting size through time indicates that more constant climatic conditions could have been present in Britain thanks to the mitigating effect of the sea.

Figure 43: Size comparison of the length of the radius to show the inconsistence of the hypothesis of two size-forms for the species *S. hundsheimensis*. The largest (Voigtstedt and Süssenborn) and smallest (Saint-Prest and Pietrafitta) specimens are plotted with the larger and smaller specimens from Untermassfeld. Pictured specimens: 1) Pietrafitta MPLB #22, 2) Untermassfeld IQW 1990/23580 (Mei. 23109), 3) Untermassfeld IQW 1980/17397 (Mei. 16919), 4) Voigtstedt IQW 1966/5692 (Voi. 64); scale bar 10 cm.

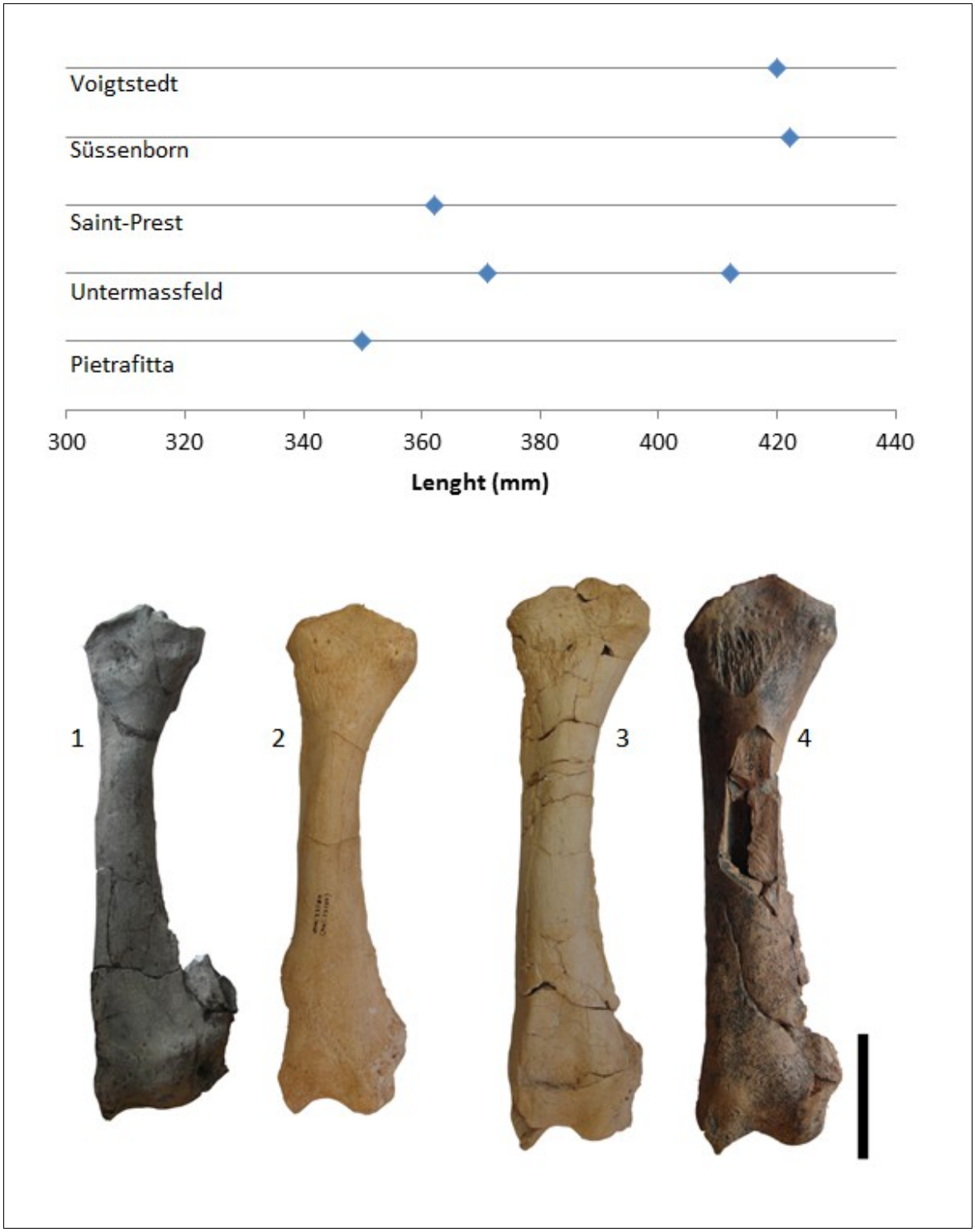

5.7 Conclusion

The biometric analysis of 677 postcranial elements of *S. hundsheimensis* from several European localities from the Early Pleistocene to the Middle Pleistocene clarify the status of the species and its evolutionary history:

- The distinction of two different size groups as claimed by Lacombat (2005, 2009) and Fortelius et al. (1993) is not supported. Although a very small form of the species is present in some localities of the Early Pleistocene (Pietrafitta, Soleilhac and Saint-Prest), since these fall in the range of *S. etruscus*, a detailed morphological comparison among the two species and these small forms is desirable prior to conclude something about the origin of *S. hundsheimensis* and its relation to *S. etruscus*. The remains from Pietrafitta, need an extended revision since just a small amount was available for this research.
- The populations of *S. hundsheimensis* from continental Europe undergo a general trend of size increase through time from the Early Pleistocene locality of Untermassfeld to those of the early Middle Pleistocene of Voigtstedt and Süssenborn, then, in the Middle Pleistocene, the size decreases in Central Germany (Mauer and Mosbach2), while it remains unvaried in the southern region of Hundsheim.
- In Britain the *S. hundsheimensis* populations seem not to vary with time but their size is evidently reduced in comparison to coeval continental populations.
- The great size variability of the species is in good agreement with the ecological plasticity proved at Süssenborn and Voigtstedt (Kahlke and Kaiser 2011) and further ecological research, regarding mesowear analysis of Mosbach2, Mauer and British samples, will give interesting information.

Conclusions

The ecology of extinct animals can be inferred through several kinds of analysis (palaeoenvironment data, pollen analyses, faunal lists, cranial morphology, dental morphology, hypsodonty index…). Quite reliable results come from two modern tools: carbon isotope analysis and dental wear. These analyses were applied to the species *S. megarhinus* (Pliocene), *S. elatus* (Late Pliocene), *S. etruscus* (Early Pleistocene) and *S. hundsheimensis* (Middle Pleistocene). Only the last one has already been palaeoecologically investigated, therefore our work aims to provide the first palaecological analysis of the earlier species and add some information on the variability of *S. hundsheimensis*.

Palaeoecological inferences from carbon isotope analysis (Chapter 3)

For the carbon isotope analysis, we collected rhinoceroses' samples from the Pliocene to the Middle Pleistocene. Since bone and dentine are poorly crystalline tissues, recrystallization could have occurred during fossilization processes, so we used powder X-ray diffraction to assess the validity of the isotopic signal. As a result:

- the crystal size increases in relation to the increasing c/a ratio, therefore it is correlated with the carbonate substitution: Type B structural carbonate inclusion, replacing for bone phosphate, leads to the increase of c cell parameter and a decreasing (Michel et al. 1995). Since crystal size is a good predictor in estimating the biogenic signal retention, we can exclude the samples with high crystallinity;
- the crystal size is not correlated with the geological age. In the Middle Pleistocene collections we have both well preserved samples (from Mosbach2) and samples with high crystallinity (from Mauer).

So we can conclude that pXRD should be paired with carbon isotope analysis since crystallinity is a good predictor for the retention of biogenic isotopic signal.

Concerning the dietary information derived from the carbon isotope analysis, we gained the following results:

- the rhinoceroses *S. hundsheimensis* and *S. kirchbergensis* from Mosbach2 show the same $\delta^{13}C$ value, comparable with the modern *Rhinoceros unicornis*. These isotopic results are in good agreement with the mesowear data that indicate flexible diet

including hard food with soft leaves, as a generalist subsistence strategy (for the species *S. hundsheimensis*, Kahlke and Kaiser 2011; for the species *S. kirchbergensis*, Van Asperen and Kahlke 2015). Therefore, it is difficult to believe that the two species recorded from Mosbach2 might have been sympatric, as suggested in the past (Fortelius et al. 1993), since niche partitioning is not possible because of their similar generalist diet;

- from the Middle Pleistocene of Mauer, a single specimen of *S. hundsheimensis* gives isotopic results, but we have no diffraction data to predict the isotopic biogenic signal alteration so we cannot assume its validity.
- the samples from the earlier localities of Senèze, Vialette and Montpellier have a high crystallinity so the isotopic signal is not valid.

Since the ecology of the species *S. megarhinus* (Pliocene), *S. elatus* (Late Pliocene) and *S. etruscus* (Early Pleistocene), has not been previously investigated in the literature (only the Middle Pleistocene species have been object of previous studies), and since the isotopic signal is not valid in these earlier species, we approached the study of their ecology through the analysis of their teeth at different levels: morphobiometry, mesowear and 3D dental texture microwear analyses.

Palaeoecological inferences from dental analyses (Chapter 4)

The mesowear and 3D-DMTA results are consistent with each other:

- the three species show a similar diet; despite the climatic fluctuations from the Pliocene to the Early Pleistocene, the European rhinoceroses do not change their dietary habit (mesowear and 3D-DMTA). Since the ecology of these different species is the same, doubts arise about the supposed coexistence of two species (Guèrin 1972, Heintz et al. 1974);
- the mesowear score places these fossil species between the browsers modern species, *D. sumatrensis* and *R. sondaicus*, and the mixed feeder, *R. unicornis*, so they were not pure browsers but neither as generalists as the Pleistocene *S. hundsheimensis* (which is closer to *R. unicornis* by the previous geochemical results);
- (3D-DMTA does not give information of a specific diet since no data are available on modern rhinoceroses of known ecology, however the comparison of the textural parameters among different types of facets, involved in different masticatory phases, brings information on the main components affecting enamel texture. The enamel

micro-structure influences the textural volume and attrition leads to a reduction of both textural volume and complexity.)

This correspondence in the diet habit gains particular interest when the differences in size are considered. The three species are indeed quite distinct:

- *S. etruscus* has a clearly smaller size range, with proportions similar to *S. elatus*;
- *S. elatus* and *S. megarhinus* have a bigger size with wide overlapping, but they differ in the proportions: *S. megarhinus* has longer proximal bones and shortened metapodials (in particular in the posterior limb), as expected from its heavier body mass (*S. megarhinus* reaches the biggest size).

The teeth biometry clearly separates the bigger rhinoceros from Montpellier from those from Vialette and Senèze (the teeth of the two more recent populations are not distinguishable by size) but such a difference is simply related to the single palaeopopulations investigated and cannot be extended to the three species since there is an high inter-specific size range for each tooth. This confirms how the influence of local environmental conditions affects the size variation and, as a consequence, the high phenotypical plasticity observed in these species. The differences observed in the body size are not correlated to any difference in the dietary habit, so other evolutionary factors and more complex processes of adaptation should explain size and body mass diversity.

This is not surprising for rhinoceroses, among which *S. hundsheimensis* had been recognized by several author (Fortelius et al. 1993; Mazza et al. 1993; Mazza 1993; Lacombat 2005, 2006; Kahlke and Kaiser 2011; Ballatore and Breda 2013) as an extremely flexible species, characterized by high adaptability and plasticity. Given its wide recorded size range, we studied in detail its biometry in order to gain a better clarification of its evolutionary pathways.

Evolutionary remarks on *S. hundsheimensis* through size variability analysis (Chapter5)

The size of *S. hundsheimensis* is extremely variable and size variability is not simply related either to a general chronological trend of size increase (with two different forms) or to a latitudinal gradient:

- the distinction of two different size groups as claimed by Lacombat (2005, 2009) and Fortelius et al. (1993) is not supported. Although a very small form of the species is present in some localities of the Early Pleistocene (Pietrafitta, Soleilhac and Saint-

Prest), the coeval rhinoceros from Untermassfeld clearly shows a wide size range encompassing the "small-form" and the "large-form". Since these small *S. hundsheimensis* fall in the range of *S. etruscus*, a detailed morphological comparison among these two species is desirable prior to conclude something about the origin of *S. hundsheimensis* and its relation to *S. etruscus*. The chronologically important remains from Pietrafitta, need an extended revision since just few of them were available for this research;

- the populations of *S. hundsheimensis* from continental Europe underwent a general trend of size increase through time from the Early Pleistocene locality of Untermassfeld to those of the early Middle Pleistocene of Voigtstedt and Süssenborn, then, in the Middle Pleistocene, the size decreased in Central Germany (Mauer and Mosbach2), while it remained unvaried in the southern region of Hundsheim (Austria). This highlights the main influence of local environmental factors driving the evolution of this flexible species;
- in Britain the *S. hundsheimensis* populations seem not to vary with time but their body size is reduced in comparison to coeval continental populations. The persisting size through time might indicate more constant climatic conditions thanks to the mitigating effect of the sea while the size reduction could tentatively be explained by a mild insularism process. Interestingly, our previous results, given by dental size comparison (Ballatore and Breda 2013), show a slightly larger size for the British teeth when compared with the coeval teeth from Isernia, so a different scaling of teeth and postcranials could be suggested, with British postcranials smaller but teeth larger than the coeval continental sample.

The great size variability of the species is in good agreement with the ecological plasticity proved at Süssenborn and Voigtstedt (Kahlke and Kaiser 2011) and further ecological research, regarding mesowear analysis of Mosbach2, Mauer and British localities, would give interesting information. Therefore the size variability, the ubiquity and longevity of the species are well congruent with the ecological plasticity that characterizes it.

Acknowledgments

The work carried out during the PhD is based on the fossil and modern collections of several European Institutions I got the opportunity to visit thanks to different grants I won in 2014, so this research received support from:

- IUSS Ferrara (University of Ferrara)
- Giovani Ricercatori (University of Ferrara)
- DAAD (Deutscher Akademischer Austausch Dienst)
- FR-TAF-3273 SYNTHESYS Project
- GB-TAF-5189 SYNTHESYS Project
- AT-TAF-5188 SYNTHESYS Project

Moreover some visits have been supported for a courtesy of Dr. Marzia Breda who set available her personal research resources (FAR), to whom I am very grateful.

I wish to remark my gratitude to the curators and technicians of the visited Institutions who allowed me to access the material, supported the applications and provided every help and comfort:

- Prof. Adrian Lister, Dr. Pip Brewer and Dr. Roberto Portela-Miguez (The Natural History Museum London)
- Prof. Dr. Eberhard Frey and Dr. Dieter Schreiber (Staatliches Museum für Naturkunde Karlsruhe)
- Prof. Dr. R.-D. Kahlke, Dennis Roessler, Baerbel Fidler (Senckenberg Forschungsstation für Quartärpaläontologie Weimar)
- Dr. Christine Argot, Dr. Joséphine Lesur and Dr. Virginie Boutel (Muséum National d'Histoire Naturelle Paris)
- Dr. Didier Berthet (Musée des Confluences Lyon)
- Dr. Emmanuel Robert (Laboratoire de Géologie de Lyon Terre Planètes Environment of the University Claude Bernard Lyon1)
- Dr. Gildas Merceron and Ramdarshan Anusha (iPHEP University of Poitiers and CNRS)
- Dr. Herbert Lutz and Thomas Engel (Naturhistorisches Museum Mainz)

- Dr. Loïc Costeur and Martin Schneider (Naturhistorisches Museum Basel)
- Dr. Ursula Göhlic, Dr. Frank Zachos and Dr. Alexander Bibl (Naturhistorisches Museum Wien)
- Nila Orlandi (Associazione Pro Museo Boldrini, Pietrafitta)

Finally I want to thank Prof. Giuseppe Cruciani (University of Ferrara) who collaborated in the PhD project (pXRD analysis) for his competence and willingness during the whole period of the work, and Dr. Claudio Natali (University of Ferrara) for the carbon isotope analysis (EA-IRMS).
Of course I should thank, for courtesy and help in my work in the laboratories of the University of Ferrara, Marina Cangemi and Marco Bertolini (Department of Human Studies), Lisa Volpe, Carmelisa d'Antone, Beatrice Pelorosso, Sabrina Russo, Salvatore Pepi and Mirella (Department of Physics and Earth Sciences).

Grazie ad Anna e Nico per l'ospitalità in quel di Ferrara
Grazie a tutti gli amici vicini e lontani
Grazie agli amici musici dell'IMensemble
Grazie al Vox Viva e alla sua magia ;-)
Grazie alle corde dei QuartATTACK!
Grazie agli amici e colleghi di "ventura" del MAcA
Grazie agli amici e scienziati di Xké?
Grazie alle ragazze del Tavolo di merende
Grazie a tutta la mia famiglia

Bibliography

Adam K.D. (1961) – Die Bedeutung der pleistozänen Säugetier-Faunen Mitteleuropas für die Geschichte des Eiszeitalters. Stuttgarter Beiträge zur Naturkunde, 78, 1-34.

Ambrose S.H., Norr L. (1993) – Experimental evidence for the relationship of the carbon isotope ratios of whole diet and dietary protein to those of bone collagen and carbonate. Prehistoric human bone. Springer Berlin Heidelberg, 1-37.

Ambrosetti P., Faraone A., Gregori L. (1987) – Pietrafitta: un museo di paleontologia in Umbria. Museol. Sci., IV, 1-2.

Asperen E.N. van, Kahlke R.-D. (2015) – Dietary variation and overlap in Central and Northwest European *Stephanorhinus kirchbergensis* and *S. hemitoechus* (Rhinocerotidae, Mammalia) influenced by habitat diversity: "You'll have to take pot luck!"(proverb). Quaternary Science Reviews, 107, 47-61.

Ayliffe L.K., Chivas A.R., Leakey M.G. (1994) – The retention of primary oxygen isotope compositions of fossil elephant skeletal phosphate. Geochimica et Cosmochimica Acta, 58(23), 5291-5298.

Azzaroli A. (1953) – The deer of the Weybourn crag and Forest Bed of Norfolk. British Museum (Natural History).

Azzaroli A. (1962) – Rinoceronti pliocenici del Valdarno inferiore. Palaeontographia Italica, 57, 11-20.

Azzaroli A., De Giuli C., Ficcarelli C., Torre D. (1988) – Late Pliocene to early mid-Pleistocene mammals in Eurasia: faunal succession and dispersal events. Palaeogeogr., Palaeoclimat., Palaeoecol., 66, 77-100.

Balasse M. (2002) – Reconstructing dietary and environmental history from enamel isotopic analysis: time resolution of intra tooth sequential sampling. International Journal of Osteoarchaeology, 12(3), 155-165.

Ballatore M., Breda M. (2013) – *Stephanorhinus hundsheimensis* (Rhinocerontidae, Mammalia) teeth from the early Middle Pleistocene of Isernia La Pineta (Molise, Italy) and comparison with coeval British material. Quaternary International, 302, 169-183.

Bandet Y., Donville B., Michaux J. (1978) – Etude géologique et géochronologique du site villafranchien de Vialette (Puy-de-Dôme). Bull. Soc. Géol. Fr., Paris, 7, t, XX, n. 3, p. 245-251.

Bartsiokas A., Middleton A.P. (1992) – Characterization and dating of recent and fossil bone by X-ray diffraction. Journal of Archaeological Science, 19(1), 63-72.

Bassinot F.C., Labeyrie L.D., Vincent E., Quidelleur X., Shackleton N.J., Lancelot Y. (1994) – The astronomical theory of climate and the age of the Brunhes-Matuyama magnetic reversal. Earth and Planetary Science Letters, 126, 91–108.

Bender M.M. (1971) – Variations in the $^{13}C/^{12}C$ ratios of plants in relation to the pathway of photosynthetic carbon dioxide fixation. Phytochemistry, 10(6), 1239-1244.

Berggren W.A., Hilgen F.J., Langereis C.G., Kent D.V., Obradovich J.D., Raffi I., Raymo M.E., Shackleton N.J. (1995) – Late Neogene chronology: new perspectives in high-resolution stratigraphy. Geological Society of America Bulletin, 107(11), 1272-1287.

Biquand D., Cassignol C., Chambaudet A., Couthures, J. (1981) – Nouvelles données chronostratigraphiques concernant les dépôts lacustres de Vialette (Haute-Loire). Bulletin de l'Association française pour l'étude du Quaternaire, 18(2), 83–87.

Blake R.E., O'Neil J.R., Garcia G.A. (1997) – Oxygen isotope systematics of biologically mediated reactions of phosphates: I. Microbial degradation of organophosphorus compounds. Geochimica et Cosmochimica Acta, 61(20), 4411-22.

Bocherens H. (2003) – Isotopic biogeochemistry and the paleoecology of the mammoth steppe fauna. Deinsea, 9, 57-76.

Bocherens H., Friis E., Mariotti A., Pedersen K.R. (1993) – Carbon isotopic abundances in Mesozoic and Cenozoic fossil plants: Palaeoecological implications. Lethaia, 26(4), 347-358.

Bocherens H., Koch P.L., Mariotti A., Geraads D., Jeager J.J. (1996) – Isotopic biogeochemistry (^{13}C, ^{18}O) of mammalian enamel from African Pleistocene hominid sites. Palaios, 306-318.

Bocherens H., Mashkour M., Billiou D. (2000) – Palaeoenvironmental and archaeological implications of isotopic analyses (13C, 15N) from Neolithic to Present in Qazvin Plain (Iran). Environmental Archaeology, 5(1), 1-19.

Boisserie J.R., Zazzo A., Merceron G., Blondel C., Vignaud P., Likius A., Mackaye H.T., Brunet M. (2005) – Diets of modern and late Miocene hippopotamids: evidence from carbon isotope composition and micro-wear of tooth enamel. Palaeogeography, Palaeoclimatology, Palaeoecology, 221(1), 153-174.

Bonifay E. (2002) – Les premiers peuplements de l'Europe. Ed. La maison des Roches, 117 p.

Bourdier F. (1961) – Le bassin du Rhône au Quaternaire. Géologie et préhistoire, 1.

Bout P. (1960) – Le Villafranchien du Velay et du Bassin hidrgraphique moyen et superieur de l'Allier. Jeanne d'Arc, Le Puy, 334 p.

Bout P. (1975) – The contribution of the volcanic Massif Central of France to European quaternary chronology. Moutonédit, La Hague, Paris, 73-98.

Bravard A. (1828) – Monographie de la Montagne de Perrier, près d'Issoire (Puy-de-Dome) et de deux espèces fossiles du genre Felis, découvertes dans l'une de ses couches d'alluvion: avec une carte et deux planches. Dufour.

Breda M., Collinge S.E., Parfitt S.A., Lister A.M. (2010) – Metric analysis of ungulate mammals in the early Middle Pleistocene of Britain, in relation to taxonomy and biostratigraphy: I: Rhinocerotidae and Bovidae. Quaternary International, 228(1), 136-156.

Breda M., Marchetti M. (2005) – Systematical and biochronological review of Plio-Pleistocene Alceini (Cervidae; Mammalia) from Eurasia. Quaternary Science Reviews, 24(5), 775-805.

Broecker W.S., Oversley V.M. (1976) – Chemical Equilibria in the Earth. McGraw-Hill, New York.

Brüning H. (1970) – Zur Klima-Stratigraphie der pleistozänen Mosbacher Sande bei Wiesbaden (Hessen). Mainzer Naturwissenschaftliches Archive, 204-256.

Budd P., Montgomery J., Barreiro B., Thomas R.G. (2000) – Differential diagenesis of strontium in archaeological human dental tissues. Applied Geochemistry, 15(5), 687-694.

Caloi L., Palombo M.R. (1995) – Late Early Pleistocene mammal faunas of Italy: biochronological problems. Il Quaternario, Ital. Journ. Quatern. Sci., 8(2), 391-402.

Campanino F., Forno M.G., Mottura A., Ormezzano D., Sala B. (1994) – *Stephanorhinus jeanvireti* (Guérin) 1972 (Rhinocerotidae, Mammalia) from Roatto near Villafranca d'Asti, NW Italy. Revision of the specimen from Dusino. *Bollettino del Museo Regionale di Scienze Naturali* 12(2): 439-499.

Carlson S.J. (1990) – Vertebrate dental structure. In: Carter J.G. (ed.), Skeletal Biomineralization: Patterns, Processes and Evolutionary Trends, Vol. 1, Van Nostrand Reinhold, New York, 531-556.

Cerdeño E. (1995) – Cladistic Analysis of the Family Rhinocerotidae (Perissodactyla). American Museum Novitates, 3143, 1-25.

Cerdeño E. (1998) – Diversity and evolutionary trends of the Family Rhinocerotidae (Perissodactyla). Palaeogeography, Palaeoclimatology, Palaeoecology, 141, 13-34.

Cerling T.E., Harris J.M. (1999) – Carbon isotope fractionation between diet and bioapatite in ungulate mammals and implications for ecological and paleoecological studies. Oecologia, 120(3), 347-363.

Cerling T.E., Harris J.M., Leakey M.G. (1999) – Browsing and grazing in elephants: the isotope record of modern and fossil proboscideans. Oecologia, 120(3), 364-374.

Christol J. de (1834) – Recherches sur les grandes especes de rhinoceros fossiles. Montpellier, J. Martel, 1-70.

Clementz M.T., Fox Dobbs K., Wheatley P. V., Koch P. L., Doak D. F. (2009) – Revisiting old bones: coupled carbon isotope analysis of bioapatite and collagen as an ecological and palaeoecological tool. Geological Journal, 44(5), 605-620.

Collins M.J., Nielsen-Marsh C.M., Hiller J., Smith C.I., Roberts J.P. (2002) – The survival of organic matter in bone: a review. Archaeometry, 44, 383–394.

Coltorti M., Feraud G., Marzoli A., Ton-That T., Voinchet P., Bahain J.-J., Minelli A., Thun Hohenstein U., Peretto C. (2005) – New $^{40}Ar/^{39}Ar$ stratigraphic and palaeoclimatic data on the Isernia la Pineta lower palaeolithic site, Molise, Italy. Quaternary International, 131(1), 11-22.

Cortesi G. (1806) – Sulle ossa fossili dei grandi animali terrestri e marini. 35 p.

Cortesi G. (1819) – Saggi geologici degli strati di Parma e Piacenza. Piacenza, 165 p.

Couthures J. (1979) – La stratigraphie du gisement Plio-Pléistocène de Vialette (Haute-Loire).). Bulletin de l'Association française pour l'étude du Quaternaire, 16(4), 171–173.

Croizet J.B., Jobert A. (1828) – Recherches sur les ossements fossiles du department du Puy-de-Dome. Delahays A. (Ed.), Paris, 224 p.

Crusafont P.M., Aguirre E., Michaux J. (1969) – Un nouveau gisement de mammifères d'age Villafranchien inférieur (Pliocène terminal) décuvert à Layna (Soria, Espagne). C.R. Acad. Sc. Paris, 268, 2174-2176.

Cuvier G. (1822) – Recherches sur les ossements fossiles, nouvelle édition. Dufour et d'Ocagne édit., Paris.

DeNiro M.J., Epstein S. (1978) – Influence of diet on the distribution of carbon isotopes in animals. Geochimica et Cosmochimica Acta, 42(5), 495-506.

DeNiro M.J., Weiner S. (1988) – Organic matter within crystalline aggregates of hydroxyapatite: a new substrate for stable isotopic and possibly other biogeochemical analyses of bone. Geochimica et Cosmochimica Acta, 52(10), 2415-2423.

Depéret C. (1885) – Description géologique du bassin tertiaire du Roussillon. Thèse Fac. Sci. Paris, 67(529).

Depéret C., Mayet L. (1911) – Le gisement de mammifères pliocènes de Senèze (Haute Loire). CR Assoc. fr. Av. Sci., Congrès de Dijon, 14.

Depéret C., Mayet L., Roman F. (1923) – *Les éléphants pliocènes*. Rey A., Lyon, 215 p.

Dinerstein E. (2003) – The return of the unicorns: The natural history and conservation of the greater one horned rhinoceros. Columbia University Press, New York, 384 p.

Dollinger P., Geser S. (2007) – Black Rhinoceros. World Association of Zoos and Aquariums (www.waza.org).

Döppes D., Rabeder G. (1996) – Die pliozänen und pleistozänen Faunen Österreichs. Die Schwerpunkte eines FWF-Projektes. Mitteilungen der Abteilung für Geologie und Paläontologie am Landesmuseum Joanneum, 54, 7-41.

Ehleringer J.R., Cerling T.E., Helliker B.R. (1997) – C4 photosynthesis, atmospheric CO2, and climate. Oecologia, 112(3), 285-299.

Ehleringer J.R., Rundel P.W. (1989) – Stable Isotope: History, Units, and Instrumentation. In: Stable isotopes in ecological research. Springer New York, 1-15.

Eisenmann V., David F. (2002) – Evolution de la taille des chevaux d'Arcy-sur-Cure et de quelques autres chevaux quaternaires. In Schmider B. (Ed.), L'Aurignacien de la Grotte du Renne: les fouilles d'André Leroi-Gourhan à Arcy-sur-Cure (Yonne), Gallia-Préhistoire, 34^{e} supplément, 97-104.

Elhaï H. (1969) – La flore sporo-pollinique du gisement villafranchien de Senèze (Massif-Central, France). Pollen et spores, Paris, vol. XI, n. 1, 127-139.

Elliott J. (2002) – Calcium phosphate biominerals. Reviews in Mineralogy and Geochemistry, 48(1), 427-453.

Emiliani C. (1955) – Pleistocene temperatures. The Journal of Geology, 538-578.

Emslie R., Brooks M. (1999) – African Rhino. Status Survey and Conservation Action Plan. IUCN, the World Conservation Union, 1-105.

Falconer H. (1868) – On the European Pliocene and Postpliocene species of the genus Rhinoceros. In Murchison C., Paleontological Memoires and notes Vol. II, Hardwicke R. (Ed.), London, 309-403.

Fejfar O. (1964) – The lower-Villafranchian vertebrates from Hajnáčka near Filákovo in southern Slovakia. Ústřední ústav geologický, 30, 89-101.

Ferretti M.P. (1999) – *Mammuthus meridionalis* (Mammalia, Proboscidea, Elephantidae) from the "Sabbie Gialle" of Oriolo (Cava La Salita, Faenza, Northern Italy) and other European late populations of southern mammoth. Eclogae Geologicae Helvetiae, 92(3), 503-515.

Foose T.J., Strien N. van (1997) – Asian Rhinos. Status Survey and Conservation Action Plan. IUCN, Gland, Switzerland, and Cambridge, UK.

Fortelius M. (1982) – Ecological aspects of dental functional morphology in the Plio-Pleistocene rhinoceroses of Europe. Teeth: Form, Function and Evolution. Columbia University Press, New York, 163-181.

Fortelius M., Mazza P., Sala B. (1993) – *Stephanorhinus* (Mammalia: Rhinocerotidae) of western European Pleistocene, with a revision of *S. etruscus* (Falconer, 1868). Palaeontographia Italica, 80, 63-155.

Fortelius M., Solounias N. (2000) – Functional characterization of ungulate molars using the abrasion-attrition wear gradient: a new method for reconstructing paleodiets. American Museum Novitates, 1-36.

Fosse P. (1994) – Taphonomie paléolithique: les grands mammifères de Soleihac et de Lunel Viel. Doctoral dissertation, Université de Provence-Aix-Marseille.

Froehlic D.L. (1999) – Phylogenetic systematics of basal Perissodactyls. Journal of Vertebrate Paleontology, 19(1), 140-159.

Gaboardi M., Deng T., Wang Y. (2005) – Middle Pleistocene climate and habitat change at Zhoukoudian, China, from the carbon and oxygen isotopic record from herbivore tooth enamel. Quaternary Research, 63(3), 329-338.

Gadbury C., Todd L., Jahren A.H., Amundson R. (2000) – Spatial and temporal variations in the isotopic composition of bison tooth enamel from the Early Holocene Hudson–Meng Bone Bed, Nebraska. Palaeogeography, Palaeoclimatology, Palaeoecology, 157(1), 79-93.

Gage J.P., Francis M.J., Triffitt J. T. (1989) – Collagen and dental matrices. Butterworth-Heinemann, Boston.

García N.G., Feranec R.S., Arsuaga J.L., de Castro J.B., Carbonell E. (2009) – Isotopic analysis of the ecology of herbivores and carnivores from the Middle Pleistocene deposits of the Sierra De Atapuerca, northern Spain.Journal of Archaeological Science, 36(5), 1142-1151.

Garvie-Lok S.J., Varney T.L., Katzenberg M.A. (2004) – Preparation of bone carbonate for stable isotope analysis: the effects of treatment time and acid concentration. Journal of Archaeological Science, 31(6), 763-776.

Geraads D. (2005) – Pliocene Rhinocerotidae (Mammalia) from Hadar e Dikika (Lower Awash, Ethiopia) and a revision of the origin of modern African rhinos. Journal of Vertebrate Paleontology, 25(2), 451-461.

Gervais P. (1852) – Zoologie et paléontologie françaises ou nouvelles recherches sur les animaux vivants et fossiles de la France. Bertrand A., Paris, v. 1.

Giaourtsakis I., Theodorou G., Roussiakis S., Athanassiou A., Iliopoulos G. (2006) – Late Miocene horned rhinoceroses (Rhinocerotinae, Mammalia) from Kerassia (Euboea, Greece). N. Jb. Paläont. Abh., 239(3), 367-398.

Gliozzi E., Abbazzi L., Argenti P., Azzaroli A., Caloi L., Capasso Barbato L., Di Stefano G., Esu D., Ficcarelli B., Sardella R, Zanalda E., Torre D. (1997) – Biochronology of selected Mammals, Molluscs and Ostracods from the Middle Pliocene to the late Pleistocene in Italy. The state of the art. *Rivista Italiana di Paleontologia e Stratigrafia* 103(3): 369-388.

Gordon K.D. (1988) – A review of methodology and quantification in dental microwear analysis. Scanning Microscopy, 2(2), 1139-1147.

Grimes S.T., Collinson M.E., Hooker J.J., Mattey D.P., Grassineau N.V., Lowry D. (2004) – Distinguishing the diets of coexisting fossil theridomyid and glirid rodents using carbon isotopes. Palaeogeography, Palaeoclimatology, Palaeoecology, 208(1), 103-119.

Grine F.E., Ungar P.S., Teaford M.F. (2002) – Error rates in dental microwear quantification using scanning electron microscopy. Scanning, 24(3), 144-153.

Groves C.P. (1982) – The skulls of Asian rhinoceroses: wild and captive. Zool. Biol., 1, 251-261.

Groves C.P. (1983) – Phylogeny of the living species of rhinoceros. Zeitschr. f. zoo. Systematik u. Evolutionsforsch., 21, 293-313.

Groves C.P., Kurt F. (1972) – *Dicerorhinus sumatrensis*. Mammalian Species, 21, 1-6.

Guérin C. (1972) – Une nouvelle espèce de rhinocéros à Vialette et dans d'autres gisements du Villafranchien inférieur européen: *Dicerorhinus jeanvireti* n. sp. Documents des Laboratoires de Géologie de la Faculte des Sciences de Lyon, 49, 53-150.

Guérin C. (1975) – Les rhinocéros (Mammalia, Perissodactyla) des gisements pliocènes français: intérêt biostratigraphique et paléoécologique. Coll. intern. CNRS, 218, 739-747.

Guérin C. (1980) – Les Rhinocéros (Mammalia, Perissodactyla) du Miocène terminal au Pléistocène supérieur en Europe Occidentale. Comparison avec le espèces actuelles. Documents des Laboratoires de Géologie de Lyon, 79, t. II-III.

Guérin C. (1982) – Première biozonation du Pléistocène Européen,principal résultat biostratigraphique de l'étude des Rhinocerotidae (Mammalia, Perissodactyla) du Miocène terminal au Pléistocène supérieur d'Europe Occidentale. Geobios, 15(4), 593-598.

Guérin C. (1990) – Biozones or mammal units? Methods and limits in biochronology. In: European Neogene mammal chronology, Springer US, 119-130.

Guérin C., Ballesio R., Méon-Vilain H. (1969) – Le *Dicerorhinus megarhinus* (Mammalia, Rhinocerotidae) du Pliocène de Saint-Laurent-des-Arbres (Gard). Docum. Lab. GéoI. Fac. Sei, Lyon, 31, 55-145.

Guérin C., Dewolf Y., Lautridou J.P. (2003) – Révision d'un site paléontologique célèbre: Saint-Prest (Chartres, France). Geobios, 36(1), 55-82.

Guérin C., Santafe-Llopis J.-V. (1978) – *Dicerorhinus miguelcrusafonti* nov. sp., une nouvelle espèce de rhinocéros (Mammalia, Perissodactyla) du gisement Pliocène Supérieur de Layna (Soria, Espagne) et de la formation Pliocène de Perpignan (Pyrénées-orientales, France). Géobios, 11(4), 457-491.

Guérin C., Tsoukala E. (2013) – The Tapiridae, Rhinocerotidae and Suidae (Mammalia) of the Early Villafranchian site of Milia (Grevena, Macedonia, Greece). Geodiversitas, 35(2), 447-489.

Guy R. D., Reid D. M., Krouse H. R. (1986) – Factors affecting $^{13}C/^{12}C$ ratios of inland halophytes. I. Controlled studies on growth and isotopic composition of *Puccinellia nuttalliana*. Canadian journal of botany, 64(11), 2693-2699.

Hassan A.A., Ortner D.J. (1977) – Inclusions in bone material as a source of error in radiocarbon dating. Archaeometry, 19(2), 131-135.

Hatch M.D., Slack C.R. (1970) – Photosynthetic CO_2-fixation pathways. Annual review of plant physiology, 21(1), 141-162.

Heintz E. (1970) – Les Cervidés villafranchiens de France et d'Espagne. Bulletin du Muséum national d'Histoire naturelle, Paris, 22, 1-303.

Heintz E., Guérin C., Martin P., Prat F. (1974) – Principaux gisements villafranchiens de France: listes fauniques et biostratigraphie. Mémoires du Bureau de Recherches géologiques et minières, 78(1), 169-182.

Heissig K. (1999) – The Miocene Land Mammals of Europe. Rössner G.E. and Heissig K. Pfeil-Verlag (Ed), München, 515 p.

Hernesniemi E., Blomstedt K., Fortelius M. (2011) – Multi-view stereo three-dimensional reconstruction of lower molars of Recent and Pleistocene rhinoceroses for mesowear analysis. Palaeontologia Electronica, 14, 1-15.

Hillman-Smith A.K.K., Groves C.P. (1994) – *Diceros bicornis.* Mammalian Species, 455, 1-8.

Hohenstein U.T., Di Nucci A., Moigne A.M. (2009) – Mode de vie à Isernia La Pineta (Molise, Italie). Stratégie d'exploitation du Bison schoetensacki par les groupes humains au Paléolithique inférieur. L'anthropologie, 113(1), 96-110.

Holden J.L., Clement J.G., Phakey P.P. (1995) – Age and temperature related changes to the ultrastructure and composition of human bone material. Journal of Bone and Material Research, 10, 1400-1409.

Hoppe K.A., Amundson R., Vavra M., McClaran M.P., Anderson D.L. (2004) – Isotopic analysis of tooth enamel carbonate from modern North American feral horses: implications for paleoenvironmental reconstructions. Palaeogeography, Palaeoclimatology, Palaeoecology, 203(3), 299-311.

Hoppe K.A., Koch P.L., Furutani T.T. (2003) – Assessing the preservation of biogenic strontium in fossil bones and tooth enamel. International Journal of Osteoarchaeology, 13(1-2), 20-28.

Hurzeler J. (1967) – Nouvelles découvertes de Mammifères dans les sédiments fluviolacustres de Villafranca d'Asti. C.N.R.S. Paris, 163, 633-636.

Iacumin P., Bocherens H., Huertas A.D., Mariotti A., Longinelli A. (1997) – A stable isotope study of fossil mammal remains from the Paglicci cave, Southern Italy. N and C as palaeoenvironmental indicators. Earth and Planetary Science Letters, 148(1), 349-357.

Jäger G.F. (1839) – Über die fossilen Saügetiere welche in Würtemberg in verschiedenen Formationen aufgefunden worden sind, nebst geognotischen Bemerkungen über diese Formationen. C. Erhard Verlag, Stuttgart.

Jones A.M., O'Connell T.C., Young E.D., Scott K., Buckingham C.M., Iacumin P., Brasier M.D. (2001) – Biogeochemical data from well preserved 200 ka collagen and skeletal remains. Earth and Planetary Science Letters, 193(1), 143-149.

Kahler M.-L. (1969) – Fossile Backenzahnfunde aus Süssenborn in Goethes Mineraliensammlung und deren Bedeutung fur Goethe. Paläontologische Abhandlungen A III.

Kahlke H.-D. (1961) – Revision der Säugetierfaunen der klassischen deutschen Pleistozän-Fundstellen von Süßenborn, Mosbach und Taubach. Geologie, 10(4/5), 493-532.

Kahlke H.-D. (1965) – Die Rhinocerotiden-Reste aus den Tonen von Voigtstedt in Thü ringen. Paläontologische Abhandlungen A II, 451–519.

Kahlke H.-D. (1969) – Die Rhinocerotiden-Reste aus den Kiesen von Süssenborn bei Weimar. Paläontologische Abhandlungen A III, 667-709.

Kahlke H.-D. (1973) – The macro-faunas of continental Europe during the middle Pleistocene: stratigraphic sequence and problems of inter-correlation. Stratigraphy and patterns of cultural change in the middle Pleistocene. Burg Wartenstein Symposium, 58, 02.-11.07.1973, Wenner-Gren Foundation for Anthropological Research, 60, S., New York.

Kahlke H.-D. (1990) – On the Evolution, Distribution and Taxonomy of Fossil Elk/Moose. Quartärpaläontologie, 8, 83-106.

Kahlke H.-D. (2001) – Die Rhinocerotiden-Reste aus dem Unterpleistozän von Untermassfeld. In: Kahlke R.-D. (Ed), Das Pleistozän von Untermassfeld bei Meiningen, Thüringen. Teil 2, Monographien des Römisch-Germanischen Zentralmuseums Mainz, Dr R. Habelt Gmbh, Bonn, 40 (2), 501-556.

Kahlke R.-D. (1997) – Bisheriger Gesamtbefund zur Geologie, Paläozoologie, Taphonomie, Ökologie und Stratigraphie der unterpleistozänen Komplex-fundstelle Untermassfeld. In Kahlke R.-D. (Ed.), Das Pleistozän von Untermassfeld bei Meiningen (Thüringen), Part 1, Monographien des Römisch-Germanischen Zentralmuseums Mainz, Bd. 40(1), 385-418.

Kahlke R.-D. (1999) – The history of the origin, evolution and dispersal of the Late Pleistocene Mammuthus-Coelodonta faunal complex in Eurasia (large mammals). Mammoth Site of Hot Springs.

Kahlke R.-D. (2000) – The Early Pleistocene (Epivillafranchian) faunal site of Untermassfeld (Thuringia, Central Germany): Synthesis of new results. ERAUL (Études et Recherches Archéologiques de l'Université de Liège), 92, 123-138.

Kahlke R.-D. (2002) – The Quaternary large mammal faunas of Thuringia (Central Germany). In: Meyrick R.A., Schreve D.C. (Dds.), The Quaternary of Central Germany. Field Guide, Quaternary Research Association London, 59-78.

Kahlke R.-D. (2002) – The Quaternary large mammal faunas of Thuringia (Central Germany). In Meyrick R.A., Schreve D.C. (Ed.), The Quaternary of Central Germany (Thuringia & Surroundings). Field Guide (p. 59-78). London, Quaternary Research Association.

Kahlke R.-D. (2006) – Untermassfeld: a late early Pleistocene (Epivillafranchian) fossil site near Meiningen (Thuringia, Germany) and its position in the development of the European mammal fauna (Vol. 1578). British Archaeological Reports Ltd.

Kahlke R.F., Kaiser T.M. (2011) – Generalism as a subsidence strategy: advantages and limitations of the highly flexible feeding traits of Pleistocene *Stephanorhinus hundsheimensis* (Rhinocerotidae, Mammalia). Quaternary Science Reviews, 30, 2250-2261.

Kaiser T.M., Bernor R.L., Scott R.S., Franzen J.L., Solounias N. (2003) – New Interpretations of the Systematics and Palaeoecology of the Dorn-Dürkheim 1 hipparions (Late Miocene, Turolian Age [MN11]), Rheinhessen, Germany. Senckenbergiana lethaea, 83, 103–133.

Kaiser T.M., Kahlke R.-D. (2005) – The highly flexible feeding strategy of *Stephanorhinus etruscus* (Falconer, 1859)(Rhinocerotidae, Mammalia) during the early Middle Pleistocene in Central Europe. Berichte des Institutes für Erdwissenschaften, Karl-Franzens-Universität Graz, 10, 50-53.

Kingston J.D., Harrison T. (2007) – Isotopic dietary reconstructions of Pliocene herbivores at Laetoli: Implications for early hominin paleoecology. Palaeogeography, Palaeoclimatology, Palaeoecology, 243(3), 272-306.

Klug H.P., Alexander L.E. (1974) – X-ray Diffraction Procedures for Polycrystalline and Amorphous Materials. London, Wiley Interscience, p. 966.

Koch P.L. (1998) – Isotopic reconstruction of past continental environments. Annual Review of Earth and Planetary Sciences, 26, 573-613.

Koch P.L. (2007) – Isotopic study of the biology of modern and fossil vertebrates. Stable isotopes in ecology and environmental science, 2, 99-154.

Koch P.L., Tuross N., Fogel M.L. (1997) – The effects of sample treatment and diagenesis on the isotopic integrity of carbonate in biogenic hydroxylapatite, Journal of Archaeological Science, 24, 417–429.

Koenigswald W. von (1997) – Die fossilen Säugetiere aus den Sanden von Mauer. Homo heidelbergensis von Mauer. Das Auftreten des Menschen in Europa, 215-240.

Koenigswald W. von, Smith B.H., Keller T. (2007) – Supernumerary teeth in a subadult rhino mandible (*Stephanorhinus hundsheimensis*) from the middle Pleistocene of Mosbach in Wiesbaden (Germany). Paläontologische Zeitschrift, 81(4), 416-428.

Koenigswald W. von, Tobien H. (1987) – Bemerkungen zur Altersstellung der pleistozänen Mosbach-Sande bei Wiesbaden. Geologische Jahrbücher Hessen, 115, 227-237.

Kohn M.J., Cerling T.E. (2002) – Stable isotope compositions of biological apatite. Reviews in mineralogy and geochemistry, 48, 455-488.

Kortschak H.P., Hartt C.E., Burr G.O. (1965) – Carbon dioxide fixation in sugarcane leaves. Plant Physiology, 40(2), 209.

Kraatz R. (1985) – *Homo erectus heidelbergensis*. Neue Untersuchungen über die Fundstelle, die Fauna und den Unterkiefer von Mauer. In: Semper Apertus: Sechshundert Jahre Ruprecht-Karls-Unversität Heidelberg 1386-1986, 4, 258-273, 10 Abb., Berlin.

Krauskopf K.B., Bird D.K. (1995) – Introduction to Geochemistry, third ed. McGraw-Hill, New York.

Kretzoï M. (1942) – Bemerkungen zum system der nachmiozänen NashornGattungen. Földtani Közlöny, 72(412), 309-318.

Krueger H.W. (1991) – Exchange of carbon with biological apatite. Journal of Archaeological Science, 18(3), 355-361.

Krueger H.W., Sullivan C.H. (1984) – Models for carbon isotope fractionation between diet and bone. Stable isotopes in nutrition, 258, 205-220.

Kurtén B. (1963) – *Villafranchian faunal evolution*. Elsinki.

Lacombat F. (2005) – Les Rhinocéros fossiles des sites préhistoriques de l'Europe méditerranéenne et du Massif Central, Paléontologie et implications biochronologiques. British Archaeological Research International Series, 1419, 1-175.

Lacombat F. (2006) – Morphological and biometrical differentiation of the teeth from Pleistocene species of *Stephanorhinus* (Mammalia, Perissodactyla, Rhinocerotidae) in Mediterranean Europe and the Massif Central, France. Palaeontographica, Abt. A, 274(3-6), 71-111.

Lacombat F. (2006)b – Pleistocene Rhinoceroses in Mediterranean Europe and in Massif Central (France). In R.-D. Kahlke, L. C. Maul, & P. Mazza (eds.), Late Neogene and Quaternary biodiversity and evolution: Regional developments and interregional correlations. Proceedings of the 18th International Senckenberg Conference (VI International Palaeontological Colloquium in Weimar), Vol. I, Courier Forschungsinstitut Senckenberg, 256, 57-69.

Lacombat F. (2007) – Phylogeny of the genus *Stephanorhinus* in the Plio-Pleistocene of Europe. Hallesches Jahrbuch für Geowissenschaften, 23, 63-64.

Lacombat F. (2009) – Biochronologie et grands mammifères au Pléistocène moyen et supérieur en Europe occidentale: l'apport des Rhinocerotidae (genre *Stephanorhinus*). Quaternaire. Revue de l'Association française pour l'étude du Quaternaire, 20(4), 429-435.

Lacombat F., Abbazzi L., Ferretti M.P., Martínez-Navarro B., Moulle P.E., Palombo M.R., Rook L., Turner A., Valli A.M.F. (2008) – New data on the Early Villafranchian fauna from Vialette (Haute-Loire, France) based on the collection of the Crozatier Museum (Le Puy-en-Velay, Haute-Loire, France). Quaternary International, 179(1), 64-71.

Lacombat F., Mörs T. (2008) – The northernmost occurrence of the rare Late Pliocene rhinoceros *Stephanorhinus jeanvireti* (Mammalia, Perissodactyla). Neues Jahrbuch für Geologie und Paläontologie-Abhandlungen, 249(2), 157-165.

Land L. S., Lundelius E. L., Valastro S. (1980) – Isotopic ecology of deer bones. Palaeogeography, Palaeoclimatology, Palaeoecology, 32, 143-151.

Laurie W.A., Lang E.M., Groves C.P. (1983) – *Rhinoceros unicornis*. Mammalian Species, 211, 1-6.

Le Bail A. (2005) – Whole powder pattern decomposition methods and applications: A retrospection. Powder Diffraction, 20(04), 316-326.

Lee-Thorp J., Sponheimer M. (2003) – Three case studies used to reassess the reliability of fossil bone and enamel isotope signals for paleodietary studies.Journal of Anthropological Archaeology, 22(3), 208-216.

Lee-Thorp J.A. (1989) – Stable carbon isotopes in deep time: Diet of fossil fauna and hominids, PhD Thesis, University of Cape Town, Cape Town.

Lee-Thorp J.A. (2000) – Preservation of biogenic carbon isotopic signals in Plio-Pleistocene bone and tooth mineral. In: Biogeochemical Approaches to Paleodietary Analysis, Kluwer Academic/Plenum Publishers, New York, 89-115.

Lee-Thorp J.A., Manning L., M. Sponheimer M. (1997) – Problems of and prospects for carbon isotope analysis of very small samples of tooth enamel, Bulletin de la Societé géologique de la France, 168, 767–773.

Lee-Thorp J.A., Sealy J. C., van Der Merwe N. J. (1989) – Stable carbon isotope ratio differences between bone collagen and bone apatite, and their relationship to diet. Journal of archaeological science, 16(6), 585-599.

Lee-Thorp J.A., van der Merwe N.J. (1987) – Carbon isotope analysis of fossil bone apatite. South African Journal of Science, 83, 71–74.

Lee-Thorp J.A., van der Merwe N.J. (1991) – Aspects of the chemistry of modern and fossil biological apatites. Journal of Archaeological Science, 18(3), 343-354.

LeGeros R.Z. (1981) – Apatites in biological systems. In Pamplin B. (Ed.), Inorganic Biological Crystal Growth. Progress Crystal Growth and Characterization, 4, 1–45.

LeGeros R.Z. (1991) – Calcium Phosphates in Oral Biology and Medicine, Monographs in Oral Science, 15, Karger, Basel.

LeGeros R.Z., LeGeros J. P., Trautz O. R., Klein E. (1969) – Two types of carbonate substitution in apatite structure. Experienta, 24, 5–7.

LeGeros R.Z., LeGeros J.P. (1983) – Carbonate analyses of synthetic, mineral and biological apatites. In: Journal of Dental Research, 62, 259-259.

LeGeros R.Z., LeGeros J.P. (1984) – Phosphate minerals in human tissues. In: Phosphate minerals, Springer Berlin Heidelberg, 351-385.

Leuenberger M., Siegenthaler U., Langway C. (1992) – Carbon isotope composition of atmospheric CO_2 during the last ice age from an Antarctic ice core. 488-490.

Libby W.F., Berger R., Mead J., Alexander G., Ross J. (1964) – Replacement rates for human tissue from atmospheric radiocarbon. Science, 146, 1170-1172.

Lindars E.S., Grimes S.T., Mattey D.P., Collinson M.E., Hooker J.J., Jones T.P. (2001) – Phosphate $\delta^{18}O$ determination of modern rodent teeth by direct laser fluorination: an appraisal of methodology and potential application to palaeoclimate reconstruction. Geochimica et Cosmochimica Acta, 65, 2535-2548.

Lister A.M. (1993) – Cervidae, including a method for comparing body size in small samples of a fossil species. In: Singer R., Gladfelter B.G., Wymer J.J. (Eds.), The Lower Palaeolitich Site at Hoxone, England. Chicago University Press, 174-190.

Loose H. (1975) – Pleistocene Rhinocerotidae of W. Europe with reference to the recent two-horned species of Africa and S.E. Asia. Scripta Geologica, 33, 59 p.

Lowenstam H.A., Weiner S. (1989) – On biomineralization, New York, Oxford University Press.

Luz B., Kolodny Y. (1985) – Oxygen isotope variations in phosphate of biogenic apatites, IV. Mammal teeth and bones. Earth and Planetary Science Letters, 75(1), 29-36.

MacFadden B.J. (1998) – Tale of two rhinos: isotopic ecology, paleodiet, and niche differentiation of Aphelops and Teloceras from the Florida Neogene. Paleobiology, 274-286.

MacFadden B.J., Solounias N., Cerling T.E. (1999) – Ancient diets, ecology, and extinction of 5-million-year-old horses from Florida. Science, 283(5403), 824-827.

Made J. van der (2010) – The rhinos from the Middle Pleistocene of Neumark-Nord (Saxony-Anhalt). In: Neumark-Nord: Ein interglaziales Ökosystem des mittelpaläolithischen Menschen. Veröffentlichungen des Landesmuseums für Vorgeschichte, 62, 433-527

Made J. van der (2015) – The rhinoceros *Stephanorhinus* aff. *etruscus* from the latest Early Pleistocene of Cueva Victoria (Murcia, Spain). Mastia 11-12-13, 359-383.

Made J. van der, Grube R. (2010) – The rhinoceroses from Neumark-Nord and their nutrition. Elefantenreich–eine Fossilwelt in Europa: Halle (Saale), Landesmuseum für Vorgeschichte, Begleithefte zu Sonderausstellungen, 2, 383-398.

Made J. van der, Stefaniak K., Marciszak A. (2014) – The Polish fossil record of the wolf *Canis* and the deer *Alces*, *Capreolus*, *Megaloceros*, *Dama* and *Cervus* in evolutionary perspective. Quaternary International, 326-327, 406-430.

Maiorino L. (2008) – Geometric morphometrics analysis in 2-dimensions applied to skulls and mandibles of Plio-Pleistocene Rhinoceroses of Europe. Master Thesis.

Marino B.D., McElroy M. B., Salawitch R. J., Spaulding W. G. (1992) – Glacial-to-interglacial variations in the carbon isotopic composition of atmospheric CO_2. Nature, 357(6378), 461-466.

Marino B.D., McElroy M.B. (1991) – Isotopic composition of atmospheric CO_2 inferred from carbon in C4 plant cellulose. Nature, 349(6305), 127-131.

Markey S. (2006) – West African Black Rhino Extinct, Group Says. National Geographic.

Martínez-Navarro B., Espigares M. P., Ros S. (2003) – Estudio preliminar de las asociaciones de grandes mamíferos de Fuente Nueva-3 y Barranco León-5 (Orce, Granada, España)(Informe de las campañas de 1999–2002). El Pleistoceno inferior de Barranco León y Fuente Nueva, 3, 1999-2002.

Masini F., Sala B. (2007) – Large and small mammal distribution patterns and chronostratigraphic boundaries from the Late Pliocene to the Middle Pleistocene of the Italian peninsula. Quaternary International, 160, 43-56.

Maul L.C., Heinrich W.-D., Parfitt S.A., Paunescu A.-C. (2007) – Comment on the correlation between magnetostratigraphy and the evolution of Microtus (Arvicolidae, Rodentia, Mammalia) during the Early and early Middle Pleistocene. In: Kahlke R.-D., Maul L.C., Mazza P. (Eds.), Late Neogene and Quaternary biodiversity and evolution: Regional developments and interregional correlations. Proceedings of the 18th International Senckenberg Conference (VI International Palaeontological Colloquium in Weimar), vol. II. Courier Forschungsinstitut, Senckenberg, 259, 243-263.

Maurette L. (1910) – Etude paléontologique du ‚Rhinoceros leptorhinus du Pliocène inférieur de Millas (Pyrénées-orientales) et des faunes du Pliocène inférieur en général. Anne Soc. Linn. Lyon, t. LVII, p. 1-26.

Mazza P. (1988) – The Tuscan Early Pleistocene rhinoceros Dicerorhinus etruscus. Palaeontographia Italica, Pisa, 75, 1-87.

Mazza P. (1993) – Ethological inferences on Pleistocene rhinoceroses of Europe. Atti dell'Accademia Nazionale dei Lincei - Rendiconti dell'Accademia dei Lincei, Scienze Fisiche e Naturali, Roma, 9(4), 127-137.

Mazza P., Sala B., Fortelius M. (1993) – A small latest Villafranchian (late Early Pleistocene) rhinoceros from Pietrafitta (Perugia, Umbria, Central Italy), with notes on the Pirro and Westerhoven rhinoceroses. Palaeontographia Italica, Pisa 80, 25-50.

McArthur M.L., Coleman M.L., Bremner J.M. (1980) – Carbon and oxygen isotopic composition of structural carbonate in sedimentary francolite. Journal of the Geological Society, 137(6), 669-673.

McCrea J.M. (1950) – On the isotopic chemistry of carbonates and a paleotemperature scale. The Journal of Chemical Physics, 18(6), 849-857.

Meadow R.H. (1986) – Some Equid remains from Cayönü, Southeastern Turquey. In: Meadow R.H., Uerpmann H.-P. (Eds.), Equids in the Ancient World. Beihefte zum übinger Atlas des Vorderen Orients, Reihe A, 19/1, 266-301.

Meadow R.H. (1999) – The use of size index scaling techniques for research on archaezoological collections from the Middle East. In C. Becker, H. Manhart, J. Peters, J. Schibler (Eds.), Historia Animalium ex Ossibus. Beiträge aur Paläoanatomie, Archäologie, Ägyptologie, Ethnologie und Geschichte der Tiermedizin., 8, 285-300.

Méon-Vilain H. (1972) – Analyses palynologiques de la flore du gisement villafranchien de Vialette (Haute-Loire). Docum. Lab. GéaI. Fac. Sei. Lyon, 49, 151-156.

Merceron G., Escarguel G., Angibault J. M., Verheyden-Tixier H. (2010) – Can dental microwear textures record inter-individual dietary variations? PLoS One, 5(3), e9542.

Metcalfe J. Z., Longstaffe F. J., White C. D. (2009) – Method-dependent variations in stable isotope results for structural carbonate in bone bioapatite. Journal of archaeological science, 36(1), 110-121.

Meyer H. von (1842) – Brief an Prof. Bronn (1842). - Neues Jahrbuch für Mineralogie, Geognosie, Geologie und Petrefakten-Kunde, Jg. 1842: 583-589, Stuttgart.

Meyer H. von (1864) – Die diluvialen Rhinoceros-Arten. - Palaeontographica, 11: 233-283, 9. Taf., Cassel.

Michaux J. (1969) – Les gisements de vertébrés de la région montpelliéraine: 3. Gisements pliocènes. Bull. Bur. Rech. géoI. min., Paris, n? 1, p. 31-37.

Michel V., Ildefonse P., Morin G. (1995) – Chemical and structural changes in *Cervus elaphus* tooth enamels during fossilization (Lazaret cave): a combined IR and XRD Rietveld analysis. Applied Geochemistry, 10(2), 145-159.

Mihlbachler M.C., Solounias N. (2006) – Coevolution of tooth crown height and diet in oreodonts (Merycoidodontidae, Artiodactyla) examined with phylogenetically independent contrasts. Journal of Mammalian Evolution, 13, 11-36.

Muggenthaler E. von, Reinhart P., Limpany B., Craft R.B. (2003) – Songlike vocalizations from the Sumatran Rhinoceros (*Dicerorhinus sumatrensis*). Acoustics Research Letters Online, 4(3), 83.

Munteanu T., Dumitraşcu G., Macaleţ R., Călin M. (2008) – Pleistocene Confined Aquifer in the South-Western Part of Braşov Depression, Romania.

Nielsen-Marsh C.M., Hedges R.E.M. (1997) – Dissolution experiments on modern and diagenetically altered bone and the effect on the infrared splitting factor, Bulletin de la Societé géologique de la France, 168, 485–490.

Nomade S., Pastre J. F., Guillou H., Faure M., Guérin C., Delson E., Debard E., Voinchet P., Messager E. (2014) – $^{40}Ar/^{39}Ar$ constraints on some French landmark Late Pliocene to Early Pleistocene large mammalian paleofaunas: Paleoenvironmental and paleoecological implications. Quaternary Geochronology, 21, 2-15.

Nowak R.M. (1991) – Walker's Mammals of World. Johns Hopkins University Press, Baltimore, V Ed., Vol. II, 1629 p.

O'Learly M.H. (1981) – Carbon isotope fractionation in plants. Phytochemistry, 20(4), 553-567.

Owen-Smith N. (1984) – Rhinoceroses. In Macdonald D., The encyclopedia of mammals. Facts on File Publ., New York, XLVIII, 895 p.

Palombo M. R., Filippi M. L., Iacumin P., Longinelli A., Barbieri M., Maras A. (2005) – Coupling tooth microwear and stable isotope analyses for palaeodiet reconstruction: the case study of Late Middle Pleistocene Elephas (*Palaeoloxodon*) antiquus teeth from Central Italy (Rome area). Quaternary International, 126, 153-170.

Palombo M. R., Mussi M., Agostini S., Barbieri M., Di Canzio E., Di Rita F., Fiore I., Iacumin P., Magri D., Speranza F., Tagliacozzo A. (2010) – Human peopling of Italian intramontane basins: The early Middle Pleistocene site of Pagliare di Sassa (L'Aquila, central Italy).Quaternary International, 223, 170-178.

Palombo M.R. (2004) – Biochronology of Plio-Pleistocene mammalian faunas on the Italian peninsula: knowledge, problems and perspectives. Il Quaternario, 17, 565-582.

Palombo M.R., Valli A.M.F. (2004) – Remarks on the biochronology of mammalian faunal complexes from the Pliocene to the Middle Pleistocene in France. Geologica Romana, 37, 145-163.

Pandolfi L. (2013) – New and revised occurrences of *Dihoplus megarhinus* (Mammalia, Rhinocerotidae) in the Pliocene of Italy. Swiss Journal of Palaeontology, 132(2): 239-255.

Pantanelli D. (1886) – Vertebrati fossili delle lignite di Spoleto. Arti. Soc. Tosc. Sci. Nat., 7(1), 93-100.

Parfitt S.A. (1998) – Pleistocene vertebrate faunas of the West Sussex Coastal Plain: their stratigraphic and palaeoenvironmental significance. In: Murton J.B., Whiteman C.A., Bates M.R., Bridgland D.R., Long A.J., Roberts M.B., Walker M.P. (Eds.), The Quaternary of Kent and Sussex: Field Guide. Quaternary Research Association, London, 121-134.

Park R., Epstein S. (1960) – Carbon isotope fractionation during photosynthesis. Geochimica et Cosmochimica Acta, 21(1), 110-126.

Passey B.H., Robinson T. F., Ayliffe L. K., Cerling T. E., Sponheimer M., Dearing M. D., Beverly L.R., Ehleringer J. R. (2005) – Carbon isotope fractionation between diet, breath CO2, and bioapatite in different mammals. Journal of Archaeological Science, 32(10), 1459-1470.

Peretto C. (1994) – Il Giacimento Paleolitico. Le industrie litiche del giacimento Paleolitico di Isernia La Pineta: La tipologia, le tracce di utilizzazione, la sperimentazione. Cosmo Iannone, Isernia, 29-40.

Person A., Bocherens H., Saliège J.-F., Paris F., Zeitoun V., Gérard, M. (1995) – Early diagenetic evolution of bone phosphate: an X-ray diffractometry analysis. Journal of Archaeological Science, 22, 211–221.

Pfeiffer T. (1998) – *Capreolus sussenbornensis* Kahlke 1956 (Cervidae, Mammalia) aus den Mosbach-Sanden (Wiesbaden-Biebrich). Mainzer maturwiss. Archiv, 36, 47-76.

Pictet F.J. (1853) – Traité de paléontologie, Histoire naturelle des animaux fossiles considérés dans leurs rapports zoologiques et géologiques. Baillière J.B., Paris, 584 p.

Piper P.J. (2007) – The Javan Rhinoceros, *Rhinoceros sondaicus*, in Borneo. The Raffles Bulletin of Zoology, 55(1), 217-220.

Pomel A. (1954) – Catalogue méthodique et descriptif des vertébrés fossiles découverts dans le bassin hydrographique supérieur de la Loire, et surtout dans la vallée de son affluent principal l'Allier. Baillière J.B., Paris, 193 p.

Preece R.C., Parfitt S.A. (2000) – The Cromer Forest-bed Formation: new thoughts on an old problem. In: Lewis S.G., Whiteman C.A., Preece R.C. (Eds.), The Quaternary of Norfolk and Suffolk: Field Guide. Quaternary Research Association, London, 1-27.

Preece R.C., Parfitt S.A. (2008) – The Cromer Forest-bed Formation: some recent developments relating to early human occupation and lowland glaciation. In: Candy I., Lee J.R., Harrison A.M. (Eds.), The Quaternary of Northern East Anglia, Field Guide. Quaternary Research Association, London, 60-83.

Prevot M., Dalrymple G.B. (1970) – Un bref épisode de polarité géomagnétique normale au cours de l'époque inverse Matuyama. C.R. Acad. Sci. Paris, 271, 2221-2224.

Prithiviraj F., Polet G., Foead N., Ng L.S., Pastorini J., Melnick D.J. (2006) – Genetic diversity, phylogeny and conservation of the Javan rhinoceros (*Rhinoceros sondaicus*). Conservation Genetics, 7, 439-448.

Prothero D.R., Guérin C., Manning E. (1989) – The history of the Rhinocerotoidea. In Prothero D.R., Schoch R.M. (Eds.), The evolution of Perissodactyls. Oxford University Press. New York, 321-340.

Pushkina D., Bocherens H., Ziegler R. (2015) – Unexpected palaeoecological features of the Middle and Late Pleistocene large herbivores in southern Germany revealed by stable isotopic abundances in tooth enamel. Quaternary International, 339-340, 164-178.

Quade J., Cerling T.E., Barry J., Morgan M.M., Pilbeam D.R., Chivas A.R., Lee-Thorp J.A., van der Merwe N J. (1992) – A 16-Ma record of paleodiet using carbon and oxygen isotopes in fossil teeth from Pakistan. Chemical Geology, 94, 183-192.

Rabinowitz A. (1995) – Helping a Species Go Extinct: The Sumatran Rhino in Borneo. Conservation Biology, 9(3), 482-488.

Radulescu C., Samson P.M., Petculescu A., Stiuca E. (2003) – Pliocene large mammales of Romania. Coloquios de Paleontologia, 1, 549-558.

Ravazzi C. (1993) – Variazioni ambientali e climatiche al margine meridionale delle Alpi nel Pleistocene Inferiore. Stratigrafia e analisi pollinica della serie di Leffe. Unpublished PhD thesis, University of Milan (Italy).

Rensberger J.M., Koenigswald W. von (1980) – Functional and phylogenetic interpretation of enamel microstructure in rhinoceroses. Paleobiology, 477-495.

Rivals F., Solounias N., Mihlbachler M.C. (2007) – Evidence for geographic variation in the diets of late Pleistocene and early Holocene Bison in North America, and differences from the diets of recent Bison. Quaternary research, 68(3), 338-346.

Roberts M., Parfitt S. (1999) – Boxgrove: a Middle Pleistocene Hominid Site at Eartham Quarry, West Sussex. In: English Heritage Archaeological Report, 17, 1-480.

Roger S., Coulon C., Thouveny N., Féraud G., Van Velzen A., Fauquette S., Verosub K.L. (2000) – $^{40}Ar/^{39}Ar$ dating of a tephra layer in the Pliocene Senèze maar lacustrine sequence (French Massif Central): constraint on the age of the Réunion–Matuyama transition and implications on paleoenvironmental archives. Earth and Planetary Science Letters, 183(3), 431-440.

Rook L., Martínez-Navarro B. (2010) – Villafranchian: the long story of a Plio-Pleistocene European large mammal biochronologic unit. Quaternary International, 219, 134-144.

Rookmaaker K. (1997) – Records of the Sundarbans Rhinoceros (*Rhinoceros sondaicus inermis*) in India and Bangladesh. Pachyderm, 24, 37-45.

Rookmaaker L.C. (1984) – The taxonomic history of the recent forms of Sumatran Rhinoceros (*Dicerorhinus sumatrensis*). Journal of the Malayan Branch of the Royal Asiatic Society, 57(1), 12-25.

Rookmaaker L.C. (2002) – Historical records of the Javan rhinoceros in North-East India. Newsletter of the Rhino Foundation of Nature in North-East India, 4, 11-12.

Rookmaaker L.C. (2005) – Review of the European perception of the African rhinoceros. Journal of Zoology, 265(4), 365-376.

Ruske R. (1965) – Zur petrographischen Ausbildung und Genese der "Lehmzone" von Voigtstedt in Thüringen. Paläontologische Abhandlungen, Abt. A, II, 2-3, 251-258.

Sacco F. (1895) – Le Rhinocéros de Dusino. (*Rhinoceros etruscus* Falc., var. *astensis* Sacc.). Archives du Muséum d'Histoire Naturelle de Lyon, 6, 1-31.

Schoeninger M.J., DeNiro M.J. (1984) – Nitrogen and carbon isotopic composition of bone collagen from marine and terrestrial animals. Geochimica et Cosmochimica Acta, 48(4), 625-639.

Schoeninger M.J., Reeser H., Hallin K. (2003) – Paleoenvironment of Australopithecus anamensis at Allia Bay, East Turkana, Kenya: evidence from mammalian herbivore enamel stable isotopes. Journal of Anthropological Archaeology, 22(3), 200-207.

Schreiber H. D. (2005) – Osteological investigations on skeleton material of Rhinoceroses (Rhinocerotidae, Mammalia) from the early Middle Pleistocene locality of Mauer near Heidelberg (SW-Germany). Quaternaire, Hors-série, 2, 103-111.

Schreiber H. D., Löscher M., Maul L.C., Unkel I. (2007) – Die Tierwelt der Mauerer Waldzeit. In G. A. Wagner, H. Rieder, L. Zöller & E. Mick (éds.), *Homo heidelbergensis* – Schlüsselfund der Menschheitsgeschichte, Thesis, 127-159.

Schreiber H.D. (1999) – Untersuchungen zur Variabilität von *Stephanorhinus hundsheimensis* (TOULA, 1902) und der Nachweis von *S. kirchbergensis* (JÄGER, 1839) (Rhinocerotidae, Mammalia) an Skelettmaterial aus dem Mittelpleistozän von Mauer bei Heidelberg (SW-Deutschland). Diplomarbeit Fakultät an der Rheinischen Friedrich-Wihelms-Universität Bonn, 152 p.

Schroeder H. (1898) – Revision der Mosbacher Säugetierfauna. Jahrbuch des Nassauischen Vereins für Naturkunde, 51, 211-230, Wiesbaden.

Scott R.S., Clavel J., DeMiguel D., Kaya T., Kostopoulos D.S., Mayda S., Merceron G. (2013) – Ecology of European hipparionines and the diversity of Late Miocene hominids in Western Eurasia, poster.

Scott R.S., Ungar P.S., Bergstrom T.S., Brown C.A., Childs B.E., Teaford M.F., Walker A. (2006) – Dental microwear texture analysis: technical considerations. Journal of Human Evolution, 51(4), 339-349.

Scott R.S., Ungar P.S., Bergstrom T.S., Brown C.A., Grine F.E., Teaford M.F., Walker A. (2005) – Dental microwear texture analysis shows within-species diet variability in fossil hominins. Nature, 436(7051), 693-695.

Serres M. de (1819) – Observations sur divers fossils de quadrupèds vivipares nouvellement découverts dans le sol des environs de Montpellier. Jour. Phys. Chim. Hist. Nat. et Arts, Paris, 382-417.

Shackleton N.J. (1995) – New data on the evolution of Pliocene climatic variability. In: Vrba E.S., Denton G.H., Parthridge T.C., Buckle L.H. (Eds.), Paleoclimate and Evolution, with Emphasis on Human Origins. Yale University Press, New Haven and London, 242-248.

Sharp Z.D., Atudorei V., Furrer H. (2000) – The effect of diagenesis on oxygen isotope ratios of biogenic phosphates. American Journal of Science, 300(3), 222-237.

Sillen A. (1989) – Diagenesis of the inorganic phase of cortical bone. In: Price T.D. (Ed.), The Chemistry of Prehistoric Human Bone. Cambridge University Press, Cambridge, 211-229.

Simkiss K., Wilbur K.M. (1989) – Biomineralization: Cell Biology and Mineral Deposition. Academic Press, San Diego, CA.

Smith B.N., Epstein S. (1971) – Two categories of 13C/12C ratios for higher plants. Plant physiology, 47(3), 380-384.

Soergel W. (1914) – Die diluvialen Säugetiere Badens. I. Alteres und mittleres Diluvium. Mitteilungs grossherzgl. Badischen Geologischen Landesanstalt, 9, 1-254.

Solounias N., Semprebon G. (2002) – Advances in the reconstruction of ungulate ecomorphology with application to early fossil equids. American Museum Novitates, 1-49.

Strien N.J. van (1974) – *Dicerorhinus sumatrensis* (Fischer), the Sumatran or two-horned rhinoceros: a study of literature. Mededelingen Landbouwhogeschool Wageningen, 74 (16), 1-82.

Strien N.J. van (2001) – Conservation Programs for Sumatran and Javan Rhino in Indonesia and Malaysia. Proceedings of the International Elephant and Rhino Research Symposium, Wien, June 7-11, 2001.

Stuart A.J., Lister A.M. (2010) – The West Runton freshwater bed and the West Runton mammoth: summary and conclusions. Quaternary International, 228(1), 241-248.

Suc J.P., Bertini A., Combourieu-Nebout N., Diniz F., Leroy S., Russo-Ermolli E.,Zheng Z., Bessais E., Ferrier J. (1995) – Structure of West Mediterranean vegetation and climate since 5.3 ma. Acta Zoologica Cracoviensia, 38(1).

Suc J.P., Clauzon G., Bessedik M., Leroy S., Zheng Z., Drivaliari A., Roiron P., Ambert P., Martinell J., Doménech R., Matias I., Juli R., Anglada R. (1992) – Neogene and Lower Pleistocene in southern France and northeastern Spain. Mediterranean environments and climate. Cahiers de Micropaleontologie, 7(1-2), 165-186.

Suc J.P., Cravatte J. (1982) – Etude palynologique du Pliocène de Catalogne (nord-est de l'Espagne). Paléobiol. Cont., 13(1), 1-31.

Suc J.P., Zagwijn W.H. (1983) – Plio-Pleistocene correlations between the northwestern Mediterranean region and northwestern Europe according to recent biostratigraphic and palaeoclimatic data. Boreas, 12(3), 153-166.

Thenius E. (1955) – Die verknöcherung der nasenscheidewand bei Rhinocerotiden und ihr systematischer wert. Schweizerische Palaeontologische Abhandlungen, 71, 1-17.

Thouveny N., Bonifay E. (1984) – New chronological data on European Plio-Pleistocene faunas and hominid occupation sites. Nature, 308(5957), 355-358.

Tieszen L.L. (1991) – Natural variations in the carbon isotope values of plants: implications for archaeology, ecology, and paleoecology. Journal of Archaeological Science, 18(3), 227-248.

Tobien H. (1980) – Taxonomic status of some Cenozoic mammalian local faunas from the Mainz Basin. Mainzer Geowissenschaftliche Mitteilungen, 9, 203-235.

Toula F. (1902) – Das Nashorn von Hundsheim: *Rhinoceros* (*Ceratorhinus* Osborn) *hundsheimensis* nov.form.: mit Ausfuhrungen uber die Verhaltnisse von elf Schadeln von *Rhinoceros* (*Ceratorhinus*) *sumatrensis*. Abhandlungen der Geologischen Reichsanstalt 19(1), 1-92.

Toula F. (1906) – Das gebiss und Reste der Nasenbeine von *Rhinoceros* (*Ceratorhinus* Osborn) *hundsheimensis*. Abhandlungen der Geologischen Reichsanstalt 20(2), 1-38.

Trueman C.N.G., Behrensmeyer A.K., Tuross N., Weiner S. (2004) – Mineralogical and compositional changes in bones exposed on soil surfaces in Amboseli National Park, Kenya: diagenetic mechanisms and the role of sediment pore fluids, Journal of Archaeological Science, 31, 721-39.

Uerpmann H. -P. (1986) – Hakafian equid remains from Shams ed-Din Tannira in Northern Syria. In: Meadow R.H., Uerpmann H.-P. (Eds.), Equids in the Ancient World. Beihefte zum Tübinger Atlas des Vorderen Orients, Reihe A, Nr. 19/1, 246-265.

Ungar P.S., Brown C.A., Bergstrom T.S., Walker A. (2003) – Quantification of Dental Microwear by Tandem Scanning Confocal Microscopy and Scale Sensitive Fractal Analyses. Scanning, 25(4), 185-193.

Urey H.C. (1947) – The thermodynamic properties of isotopic substances. Journal of the Chemical Society (Resumed), 562-581.

Viret J. (1954) – Le loess à bancs durcis de St. Vallier (Drome) et sa faune de mammifères villafranchiens. Nouvelles archives du Muséum d'Histoire naturelle de Lyon, 4, 200 p.

Wang Y., Cerling T.E. (1994) – A model for fossil tooth and bone diagenesis: implications for paleodiet reconstruction from stable isotopes. Palaeogeography, Palaeoclimatology, Palaeoecology, 107, 281-289.

Weiner S., Price P. (1986) – Disaggregation of bone into crystals, Calcified Tissue International, 39, 365–375.

West R.G. (1980) – The Pre-glacial Pleistocene of the Norfolk and Suffolk Coasts. Cambridge University Press, Cambridge, 203 pp.

Wheeler E.J., Lewis D. (1977) – An X-ray study of the paracrystalline nature of bone apatite. Calcified Tissue Research, 24, 243-248.

White W.M. (2013) – Geochemistry, Wiley-Blackwell.

Widga C., Walker J.D., Stockli L.D. (2010) – Middle Holocene Bison diet and mobility in the eastern Great Plains (USA) based on $\delta^{13}C$, $\delta^{18}O$, and $^{87}Sr/^{86}Sr$ analyses of tooth enamel carbonate. Quaternary Research, 73(3), 449-463.

Wiegank F. (1990) – Magnetostratigraphisch-geochronologische Untersuchungen zur Geschichte des Plio-Pleistozäns in Mitteleuropa und ihrer Beziehungen zur globalen geologischen, paläoklimatischen und paläoökologischen Entwicklung. Akademie der Wissenschaften der DDR, Zentralinstitut für Physik der Erde, 113.

Wopenka B., Pasteris J.D. (2005) – A mineralogical perspective on the apatite in bone. Materials Science & Engineering C: Biomimetic and Supramolecular Systems, 25, 131-143.

Wüst E. (1901) – Untersuchungen über das Pliozän und das ältere Pleistozän Thüringens nördlich vom Thüringer Walde und westlich von der Saale. Abhandlungen der Naturforschenden Gesellschaft zu Halle, 23, 1-35.

Attachments

Attachment I - Thermal and acid treatments: table of weight data.

N°	**Thermal treatment**				**Acid treatment**		
	Pre-treat.	Post-treat.	weight loss	%	Pre-treat.	Post-treat.	weight loss
B15	0,0697	0,0644	0,0053	7,604	0,0642	0,0149	0,0493
B16	0,0663	0,0617	0,0046	6,938	0,0623	0,0448	0,0175
B17	0,0642	0,0612	0,0030	4,673	0,0612	0,0421	0,0191
B18	0,0647	0,0628	0,0019	2,937	0,0623	0,0107	0,0516
B19	0,0754	0,0716	0,0038	5,040	0,0719	0,0155	0,0564
B20	0,0706	0,0670	0,0036	5,099	0,0667	0,0167	0,0500
B21	0,0735	0,0692	0,0043	5,850	0,0689	0,0456	0,0233
B22	0,0884	0,0850	0,0034	3,846	0,0845	0,0214	0,0631
B23	0,0634	0,0518	0,0116	18,297	0,0515	0,0045	0,0470
B24	0,0681	0,0638	0,0043	6,314	0,0637	0,0125	0,0512
B26	0,0646	0,0548	0,0098	15,170	0,0535	0,0388	0,0147
B27	0,0633	0,0584	0,0049	7,741	0,0579	0,0395	0,0184
B28	0,0746	0,0705	0,0041	5,496	0,0705	0,0192	0,0513
B29	0,0752	0,0705	0,0047	6,250	0,0702	0,0235	0,0467
D01	0,0620	0,0584	0,0036	5,806	0,0581	0,0374	0,0207
D02	0,0732	0,0699	0,0033	4,508	0,0694	0,0098	0,0596
D04	0,0635	0,0607	0,0028	4,409	0,0600	0,0439	0,0161
D05	0,0728	0,0699	0,0029	3,984	0,0696	0,0506	0,0190
D06	0,0620	0,0546	0,0074	11,935	0,0547	0,0414	0,0133
M01	0,1196	0,0838	0,0358	29,933	0,0839	0,0605	0,0234
M02	0,2646	0,1779	0,0867	32,766	0,0965	0,0125	0,0840
M03	0,2505	0,1701	0,0804	32,096	0,1434	0,0252	0,1182
M04	0,3604	0,2548	0,1056	29,301	0,2060	0,0468	0,1592
M05	0,2537	0,1767	0,0770	30,351	0,1209	0,0218	0,0991
M06	0,2713	0,1761	0,0952	35,090	0,1421	0,0208	0,1213
M07	0,3625	0,2413	0,1212	33,434	0,1499	0,0429	0,1070

Attachment II - List of specimens: dental material of Stephanorhinus megarhinus from Montpellier, S. elatus from Vialette and S. etruscus from Senèze and of the five extant species. (R=right, L=left; P or M=upper teeth; m=lower teeth).

MHNL= Musée des Confluences Lyon
MNHN=Muséum National d'Histoire Naturelle Paris
NHM=Natural History Museum London
NHMW=Naturhistorisches Museum Wien
NMB=Naturhistorisches Museum Basel
UCBL=Laboratoire de Géologie de Lyon, University Claude Bernard Lyon1

Locality	Elem.	Museum	Catalogue	Side	Biometry	Morphology	Mesowear	3D-DMTA
Montpellier	P2	UCBL	FSL 40026	R		x		
Montpellier	P2	UCBL	FSL 40119a	L	x	x		
Montpellier	P2	UCBL	FSL 40119b	L	x	x		
Montpellier	P2	UCBL	FSL 40122	L	x			
Montpellier	P2	UCBL	FSL 40123	L	x			
Montpellier	P2	UCBL	FSL 40126	L	x	x		
Montpellier	P2	UCBL	FSL 40441	L	x	x		
Montpellier	P2	UCBL	FSL 40447	R	x	x		
Montpellier	P2	UCBL	FSL 40447	L	x	x		
Montpellier	P2	UCBL	FSL 40449	L	x			
Montpellier	P2	NMB	M.P. 134	L	x	x		
Montpellier	P2	NMB	M.P. 135	R	x	x		
Montpellier	P2	NMB	M.P. 307	R		x		
Montpellier	P2	NMB	M.P. 446	R		x		
Montpellier	P3	MNHN	1876-17	L	x	x		
Montpellier	P3	UCBL	FSL 40026	R		x		
Montpellier	P3	UCBL	FSL 40118	R	x			
Montpellier	P3	UCBL	FSL 40118	R		x		
Montpellier	P3	UCBL	FSL 40119a	L	x	x		
Montpellier	P3	UCBL	FSL 40119b	L	x			
Montpellier	P3	UCBL	FSL 40122a	L	x			
Montpellier	P3	UCBL	FSL 40122b	L	x			
Montpellier	P3	UCBL	FSL 40122c	R	x			
Montpellier	P3	UCBL	FSL 40122d	R	x	x		
Montpellier	P3	UCBL	FSL 40123	R	x			
Montpellier	P3	UCBL	FSL 40126	R	x	x		
Montpellier	P3	UCBL	FSL 40131	L	x	x		
Montpellier	P3	UCBL	FSL 40134	R	x			
Montpellier	P3	UCBL	FSL 40435	R	x	x		
Montpellier	P3	UCBL	FSL 40435	L	x	x		
Montpellier	P3	UCBL	FSL 40441	R	x	x		
Montpellier	P3	UCBL	FSL 40447	R	x	x		
Montpellier	P3	UCBL	FSL 40447	L	x	x		
Montpellier	P3	UCBL	FSL 40449	L	x			
Montpellier	P3	NMB	M.P. 123	R		x		

					Biometry	Morphology	Mesowear	3D-DMTA
Montpellier	P3	NMB	M.P. 307	R		x		
Montpellier	P3	NMB	M.P. 446	R		x		
Montpellier	P3	NMB	M.P. 521	R	x	x		
Montpellier	P3	NMB	M.P. 55	R		x		
Montpellier	P3	NMB	M.P. 723	L	x	x		
Montpellier	P4	MNHN	1876-17	L	x	x		
Montpellier	P4	UCBL	FSL 40026	R		x		
Montpellier	P4	UCBL	FSL 40117	R	x	x		
Montpellier	P4	UCBL	FSL 40118	L	x	x		
Montpellier	P4	UCBL	FSL 40122	L	x	x		
Montpellier	P4	UCBL	FSL 40123a	L	x	x		
Montpellier	P4	UCBL	FSL 40123b	L	x	x		
Montpellier	P4	UCBL	FSL 40123c	R	x	x		
Montpellier	P4	UCBL	FSL 40123d	R	x	x		
Montpellier	P4	UCBL	FSL 40131	R	x			
Montpellier	P4	UCBL	FSL 40435	R	x	x		
Montpellier	P4	UCBL	FSL 40435	L	x	x		
Montpellier	P4	UCBL	FSL 40441	R	x	x		
Montpellier	P4	UCBL	FSL 40447	R	x	x		
Montpellier	P4	UCBL	FSL 40447	L	x	x		
Montpellier	P4	UCBL	FSL 40449	L	x			
Montpellier	P4	NMB	M.P. 12	L	x	x		
Montpellier	P4	NMB	M.P. 308	R	x	x		
Montpellier	P4	NMB	M.P. 446	R		x		
Montpellier	P4	NMB	M.P. 447	L	x	x		
Montpellier	P4	NMB	M.P. 522	R	x			
Montpellier	P4	NMB	M.P. 724	R	x	x		
Montpellier	P4	NMB	M.P. 908	R	x	x		
Montpellier	P4	NMB	M.P. 980	R	x	x		
Montpellier	M1	UCBL	FSL 40026	R		x		
Montpellier	M1	UCBL	FSL 40113	R	x	x	x	
Montpellier	M1	UCBL	FSL 40116	L	x	x		
Montpellier	M1	UCBL	FSL 40118	L	x			
Montpellier	M1	UCBL	FSL 40119a	L	x			
Montpellier	M1	UCBL	FSL 40119b	R	x			
Montpellier	M1	UCBL	FSL 40123a	R	x	x	x	
Montpellier	M1	UCBL	FSL 40123b	R	x	x	x	
Montpellier	M1	UCBL	FSL 40125a	R	x	x		
Montpellier	M1	UCBL	FSL 40125b	L	x	x		
Montpellier	M1	UCBL	FSL 40435	R	x	x		
Montpellier	M1	UCBL	FSL 40435	L	x	x		
Montpellier	M1	UCBL	FSL 40441	R	x	x		
Montpellier	M1	UCBL	FSL 40447	R	x	x		
Montpellier	M1	UCBL	FSL 40447	L	x	x	x	
Montpellier	M1	UCBL	FSL 40449	L	x			
Montpellier	M1	NMB	M.P. 225	R		x		

					Biometry	Morphology	Mesowear	3D-DMTA
Montpellier	M1	NMB	M.P. 310	R	x	x		
Montpellier	M1	NMB	M.P. 38	L		x		
Montpellier	M1	NMB	M.P. 446	R	x	x		
Montpellier	M1	NMB	M.P. 54	R	x	x	x	
Montpellier	M1	NMB	M.P. 726	R		x		
Montpellier	M1	NMB	M.P. 851	L	x	x	x	
Montpellier	M2	MNHN	1876-17	L	x	x		x
Montpellier	M2	UCBL	FSL 40026	R		x	x	
Montpellier	M2	UCBL	FSL 40123a	R	x	x	x	
Montpellier	M2	UCBL	FSL 40123b	L	x	x	x	x
Montpellier	M2	UCBL	FSL 40123c	L	x			
Montpellier	M2	UCBL	FSL 40124	R	x			
Montpellier	M2	UCBL	FSL 40131a	L	x	x	x	x
Montpellier	M2	UCBL	FSL 40131b	L	x	x		
Montpellier	M2	UCBL	FSL 40435	L	x	x		x
Montpellier	M2	UCBL	FSL 40435	R		x		
Montpellier	M2	UCBL	FSL 40438	R	x	x		
Montpellier	M2	UCBL	FSL 40438	L	x			
Montpellier	M2	UCBL	FSL 40441	R	x	x	x	x
Montpellier	M2	UCBL	FSL 40447	R	x	x		x
Montpellier	M2	UCBL	FSL 40447	L	x	x		
Montpellier	M2	UCBL	FSL 40449	L	x			x
Montpellier	M2	NMB	M.P. 14	R	x	x		
Montpellier	M2	NMB	M.P. 446	R	x	x		
Montpellier	M2	NMB	M.P. 981	R	x	x	x	
Montpellier	m2	MHNL	M 14	R				x
Montpellier	m2	MHNL	M 9	R				x
Montpellier	m2	UCBL	FSL 40078	L				x
Montpellier	m2	UCBL	FSL 40079	L				x
Montpellier	m2	UCBL	FSL 40129	L				x
Montpellier	m2	UCBL	FSL 40410	R				x
Montpellier	m2	UCBL	FSL 40429	L				x
Montpellier	M3	UCBL	FSL 40026	R		x		
Montpellier	M3	UCBL	FSL 40115	R	x	x		
Montpellier	M3	UCBL	FSL 40116	L	x			
Montpellier	M3	UCBL	FSL 40117	L	x	x		
Montpellier	M3	UCBL	FSL 40118a	L	x	x		
Montpellier	M3	UCBL	FSL 40118b	L	x	x		
Montpellier	M3	UCBL	FSL 40118c	L	x	x		
Montpellier	M3	UCBL	FSL 40118d	R	x	x		
Montpellier	M3	UCBL	FSL 40123	L	x			
Montpellier	M3	UCBL	FSL 40435	R	x	x		
Montpellier	M3	UCBL	FSL 40435	L	x	x		
Montpellier	M3	UCBL	FSL 40438	R	x			
Montpellier	M3	UCBL	FSL 40438	L	x			
Montpellier	M3	UCBL	FSL 40447	R	x	x		

					Biometry	Morphology	Mesowear	3D-DMTA
Montpellier	M3	UCBL	FSL 40447	L	x	x		
Montpellier	M3	UCBL	FSL 40449	L	x			
Montpellier	M3	NMB	M.P 1012	R	x	x		
Montpellier	M3	NMB	M.P. 1011	L	x	x		
Montpellier	M3	NMB	M.P. 128	R	x	x		
Vialette	P2	MNHN	VIA 435	L	x	x		
Vialette	P2	MNHN	VIA 473	L	x	x		
Vialette	P2	MNHN	VIA 477	R		x		
Vialette	P2	NMB	Vt.621	R	x	x		
Vialette	P2	NMB	Vt.621	L	x	x		
Vialette	P3	MNHN	VIA 435	L	x	x		
Vialette	P3	MNHN	VIA 474	R	x	x		
Vialette	P3	MNHN	VIA 483	R		x		
Vialette	P3	NMB	Vt.621	R	x	x		
Vialette	P3	NMB	Vt.621	L	x	x		
Vialette	P4	UCBL	FSL 211182	R		x		
Vialette	P4	MNHN	VIA 434	R	x	x		
Vialette	P4	MNHN	VIA 435	L		x		
Vialette	P4	NMB	Vt.621	R	x	x		
Vialette	P4	NMB	Vt.621	L	x	x		
Vialette	M1	MNHN	VIA 434	R	x	x		
Vialette	M1	MNHN	VIA 435	L	x	x		
Vialette	M1	NMB	Vt.621	R	x	x		
Vialette	M1	NMB	Vt.621	L	x	x		
Vialette	m1	MNHN	VIA 475	L				x
Vialette	M2	MNHN	VIA 434	R	x	x	x	
Vialette	M2	MNHN	VIA 435	L	x	x		x
Vialette	M2	MNHN	VIA 472	R	x	x	x	x
Vialette	M2	NMB	Vt. 209	R	x	x	x	
Vialette	M2	NMB	Vt.621	R	x	x	x	
Vialette	M2	NMB	Vt.621	L	x	x		
Vialette	m2	MNHN	VIA 433	R				x
Vialette	m2	MNHN	VIA 482	L				x
Vialette	m2	MHNL	V 377	L				x
Vialette	M3	UCBL	FSL 211183	L		x		
Vialette	M3	MNHN	VIA 434	R	x	x		
Vialette	M3	NMB	Vt. 145	R	x	x		
Vialette	M3	NMB	Vt.621	R	x	x		
Vialette	M3	NMB	Vt.621	L	x	x		
Vialette	m3	MNHN	VIA 484	L				x
Senèze	P2	UCBL	FSL 211118	R	x	x		
Senèze	P2	UCBL	FSL 211118	L	x	x		
Senèze	P2	NMB	Se. 1416	L	x	x		
Senèze	P2	NMB	Se. 187	L	x	x		
Senèze	P2	NMB	Se.1785	L	x	x		
Senèze	P2	NMB	Se.548	L	x	x		

					Biometry	Morphology	Mesowear	3D-DMTA
Senèze	P3	UCBL	FSL 211118	R		x		
Senèze	P3	UCBL	FSL 211118	L		x		
Senèze	P3	NMB	Se. 1416	L	x	x		
Senèze	P3	NMB	Se. 187	L	x	x		
Senèze	P3	NMB	Se.1785	L	x	x		
Senèze	P3	NMB	Se.548	L	x	x		
Senèze	P4	UCBL	FSL 211118	R		x		
Senèze	P4	UCBL	FSL 211118	L		x		
Senèze	P4	NMB	Se. 1416	L	x	x		
Senèze	P4	NMB	Se. 187	L	x	x		
Senèze	P4	NMB	Se.1785	L	x	x		
Senèze	P4	NMB	Se.548	L	x	x		
Senèze	M1	UCBL	FSL 211118	R	x			
Senèze	M1	UCBL	FSL 211118	L	x	x		
Senèze	M1	NMB	Se. 187	L		x		
Senèze	M1	NMB	Se.1785	L	x	x		
Senèze	M1	NMB	Se.548	L	x	x		
Senèze	M2	UCBL	FSL 210958	R				x
Senèze	M2	UCBL	FSL 211118	R	x	x	x	x
Senèze	M2	UCBL	FSL 211118	L	x	x		
Senèze	M2	NMB	Se. 187	L	x	x		
Senèze	M2	NMB	Se. 334	L	x	x		
Senèze	M2	NMB	Se.1785	L	x	x	x	
Senèze	M2	NMB	Se.548	L	x	x	x	
Senèze	m2	MNHN	1923-4	R				x
Senèze	m2	UCBL	FSL 210927	R				x
Senèze	m2	UCBL	FSL 210929	R				x
Senèze	m2	UCBL	FSL 210957	R				x
Senèze	m2	UCBL	FSL 211109	L				x
Senèze	m2	UCBL	FSL 211112	L				x
Senèze	m2	UCBL	FSL 211113	R				x
Senèze	M3	UCBL	FSL 210925	L	x	x		
Senèze	M3	UCBL	FSL 211118	R	x	x		
Senèze	M3	UCBL	FSL 211118	L		x		
Senèze	M3	NMB	Se. 187	L	x	x		
Senèze	M3	NMB	Se.1785	L	x	x		
Senèze	M3	NMB	Se.548	L	x	x		
Extant species								Notes
C. simum	M2	MNHN	1928-310	R			x	-
C. simum	M2	NMB	8029	R			x	Uganda
C. simum	M2	NHMW	3086/ST318	L			x	Sudan
C. simum	M2	NHM	1851.12.23.1	L			x	Sudafrica
C. simum	M2	NHM	30.7.26.1	L			x	Congo
C. simum	M2	NHM	25.5.23.1	L			x	Uganda
D. bicornis	M1	NHMW	4291	R			x	Somalia
D. bicornis	M2	NHM	1907.2.26.1	R			x	Kenya

					Biometry	Morphology	Mesowear	Notes
D. bicornis	M2	NHM	1918.6.17.1	R			x	Kenya
D. bicornis	M2	NHM	1948.1.28.5	R			x	Kenya
D. bicornis	M2	NHM	1962.7.6.3	R			x	Kenya
D. bicornis	M2	NHM	1919.7.15.511	R			x	Zimbawe
D. bicornis	M2	NHM	1949.1.28.7	R			x	Boruma
R. unicornis	M2	MNHN	1967-101	R			x	Captivity-4yrs
R. unicornis	M1	NMB	009	R			x	-
R. unicornis	M2	NHM	1884.1.22.1+2	R			x	India
R. unicornis	M2	NHM	1950.10.18.5	R			x	Nepal
R. unicornis	M2	NHM	1872.12.30.1	R			x	India
R. unicornis	M2	NHM	1901.3.10.1	L			x	India
R. unicornis	M2	NHM	1972.739	R			x	India
R. sondaicus	M2	MNHN	1932-42	R			x	-
R. sondaicus	M2	MNHN	1896-2003	L			x	Vietnam
R. sondaicus	M2	MNHN	2009-400	R			x	-
R. sondaicus	M2	MNHN	1932-48	L			x	-
R. sondaicus	M2	NMB	10885	L			x	Java
R. sondaicus	M2	NHMW	7066	R			x	-
R. sondaicus	M2	NHM	79.11.21.178	L			x	Malay Penins.
R. sondaicus	M2	NHM	20.10.13.1	R			x	Java
R. sondaicus	M2	NHM	1876.3.30.1	L			x	Bengal
R. sondaicus	M2	NHM	1932.10.21.1	R			x	-
D. sumatrensis	M2	NMB	10529	L			x	Zoo
D. sumatrensis	M2	NHMW	7529	R			x	Zoo
D. sumatrensis	M2	NHMW	1500/ST317	L			x	Zoo
D. sumatrensis	M2	NHM	1872.12.31.1	R			x	Malay Penins.
D. sumatrensis	M2	NHM	1921.2.8.2	L			x	Malay Penins.
D. sumatrensis	M2	NHM	1894.9.24.1	L			x	Sumatra

Attachment III - List of specimens: postcranial material of *Stephanorhinus hundsheimensis*.

IPW=Institute for Palaeontology University of Wien
IQW=Institute for Quaternary Palaeontology Weimar
MNHM=Naturhistorisches Museum Mainz
MNHN=Muséum National d'Histoire Naturelle de Paris
MPI=Museo del Paleolitico Isernia
MPLB=Museo Paleontologico Luigi Boldrini Pietrafitta
MPPL=Museo Paleontologico Piero Leonardi Ferrara
NHM=Natural History Museum London
NHMW=Naturhistorisches Museum Wien
SMNK=Staatliches Museum für Naturkunde Karlsruhe

Element	Side	Locality	Catalogue	Age	Association
Humerus	L	Mauer	SMNK MS 0266		
Humerus	L	Mauer	SMNK MS 0261		
Humerus	R	Mauer	SMNK MS 0359		
Humerus	R	Mauer	SMNK MS 0360		
Humerus	L	Mauer	SMNK MS 0366		
Humerus	L	Mauer	SMNK MS 0361		
Humerus	R	Mauer	SMNK MS 0367		
Humerus	L	Mosbach2	MNHM 1975/264		
Humerus	R	Mosbach2	MNHM 1957/206		
Humerus	R	Mosbach2	MNHM 1955/1109		
Humerus	L	Voigtstedt	IQW 1966/7415 (Voi.3280)		Voi.I/74
Humerus	R	Voigtstedt	IQW 1966/5841 (Voi.3279)	young	
Humerus	L	Voigtstedt	IQW 1966/7438 (Voi.738)		
Humerus	R	Voigtstedt	IQW 1966/5615 (Voi.713)	young	
Humerus	R	Süssenborn	IQW 1964/665 (Süß. 194/52)		
Humerus	R	Untermassfeld	IQW 1980/15362 (Mei.14874)		individual I
Humerus	L	Untermassfeld	IQW 1980/16117 (Mei.15628)		individual II
Humerus	L	Untermassfeld	IQW 1980/16170 (Mei.15680)		individual III
Humerus	L	Untermassfeld	IQW 1980/16122 (Mei.15633)		individual IV
Humerus	R	Untermassfeld	IQW 1980/15219 (Mei.14701)	young	individual X
Humerus	R	Untermassfeld	IQW 1985/20386 (Mei.19906)	young	ant.limb I
Humerus	R	Untermassfeld	IQW 1981/17715 (Mei.17237)		
Humerus	L	Untermassfeld	IQW 1982/17795 (Mei.17315)		
Humerus	L	Untermassfeld	IQW 1988/22801 (Mei.22320)		

Element	Side	Locality	Catalogue	Age	Association
Humerus	R	Untermassfeld	IQW 1996/25703 (Mei.25232)		
Humerus	R	Pietrafitta	MPLB #021		
Humerus	L	Saint-Prest	MNHN SPR 130		
Humerus	R	Mundesley	NHM M 17841		
Humerus	R	Trimingham	NHM M 17228		
Humerus	R	Trimingham	NHM M 17843		
Humerus	R	Pakefield	NHM 1147		
Humerus	R	Pakefield	NHM 509		
Humerus	R	Hundsheim	NHMW 2013/0282/0001		
Humerus	L	Hundsheim	NHMW 2013/0282/0001		
Radius	L	Mauer	SMNK MS 0349		
Radius	R	Mauer	SMNK MS 0698		
Radius	R	Mauer	SMNK MS 0347		
Radius	L	Mauer	SMNK MS 1477		
Radius	R	Mauer	SMNK MS 0350		
Radius	R	Mauer	SMNK MS 0370		
Radius	L	Mauer	SMNK MS 0804		
Radius	R	Mauer	SMNK MS 5021		
Radius	R	Mosbach2	MNHM 1963/573		
Radius	R	Mosbach2	MNHM 1958/216		
Radius	L	Mosbach2	MNHM 1958/631		
Radius	R	Voigstedt	IQW 1966/7415 (Voi.3280)		Voi.I/66
Radius	L	Voigstedt	IQW 1966/7415 (Voi.3280)		Voi.I/63
Radius	R	Voigstedt	IQW 1966/7416 (Voi.3279)	young	Voi.II/5
Radius	R	Voigstedt	IQW 1966/5861 (Voi.1116)	young	
Radius	R	Voigstedt	IQW 1966/5693 (Voi.63)		
Radius	L	Voigstedt	IQW 1966/5692 (Voi.64)		
Radius	R	Süssenborn	IQW 1964/333 (Süß.9138)		
Radius	L	Untermassfeld	IQW 1980/15866 (Mei.15377)		individual I
Radius	R	Untermassfeld	IQW 1980/15803 (Mei.15314)		individual II
Radius	L	Untermassfeld	IQW 1980/17475 (Mei.16997)		individual III
Radius	L	Untermassfeld	IQW 1985/20616 (Mei.20135)		individual V
Radius	L	Untermassfeld	IQW 1990/23580 (Mei.23109)		ant.limb II
Radius	L	Untermassfeld	IQW 1989/23388 (Mei.22907)	young	ant.limb VI
Radius	R	Untermassfeld	IQW 1983/19230 (Mei.18750)		ant.limb VII
Radius	R	Untermassfeld	IQW 1948/20293 (Mei.19813)	young	ant.limb I
Radius	L	Untermassfeld	IQW 1980/17397 (Mei.16919)		

Element	Side	Locality	Catalogue	Age	Association
Radius	L	Untermassfeld	IQW 1989/23390 (Mei.22909)		
Radius	L	Untermassfeld	IQW 1986/21748 (Mei.21267)		
Radius	L	Untermassfeld	IQW 1989/23350 (Mei.22869)	young	
Radius	L	Pietrafitta	MPLB #022		
Radius	L	St Prest	MNHN SPR 129		
Radius	R	Mundesley	NHM M 7054		
Radius	R	Overstrand	NHM M 17840		
Radius	R	Overstrand	NHM M 12830		
Radius	L	Trimingham	NHM M 19236		
Radius	R	Trimingham	NHM M 17844		
Radius	R	Trimingham	NHM M 17845		
Radius	R	Hundsheim	NHMW 2013/0282/0001		
Radius	L	Hundsheim	NHMW 2013/0282/0001		
Radius	L	Hundsheim	NHMW 1909II.540		
Radius	R	Hundsheim	NHMW 1909II.541		
Radius	R	Hundsheim	IPW C38		
Radius	L	Hundsheim	IPW no num		
Radius	R	Hundsheim	IPW "R"		
Ulna	R	Mauer	SMNK MS 0610		
Ulna	L	Voigstedt	IQW 1966/7415 (Voi.3280)		Voi.I/64
Ulna	R	Voigstedt	IQW 1966/7416 (Voi.3279)	young	Voi.II/6
Ulna	R	Voigstedt	IQW 1966/5613 (Voi.195)		
Ulna	R	Voigstedt	IQW 1966/5855 (Voi.460)	young	
Ulna	R	Voigstedt	IQW 1966/5605 (Voi.560)		
Ulna	L	Voigstedt	IQW 1966/3476 (Voi.66)		
Ulna	R	Süssenborn	IQW 1964/334 (Süß.9139)		
Ulna	L	Untermassfeld	IQW 1980/16105 (Mei.15616)		individual I
Ulna	R	Untermassfeld	IQW 1980/15802 (Mei.15313)		individual II
Ulna	L	Untermassfeld	IQW 1980/15776 (Mei.15288)		individual II
Ulna	L	Untermassfeld	IQW 1980/17479 (Mei.17001)		individual III
Ulna	L	Untermassfeld	IQW 1985/20617 (Mei.20136)		individual V
Ulna	L	Untermassfeld	IQW 1989/23253 (Mei.22772)		individual IX
Ulna	R	Untermassfeld	IQW 1984/20294 (Mei.19814)	young	ant.limb I
Ulna	L	Untermassfeld	IQW 1990/23609 (Mei.23138)		ant.limb II
Ulna	L	Pietrafitta	MPLB #023		
Ulna	R	Boxgrove	NHM F 412		

Element	Side	Locality	Catalogue	Age	Association
Ulna	R	Hundsheim	NHMW 2013/0282/0001		
Ulna	L	Hundsheim	NHMW 2013/0282/0001		
Scaphoid	L	Mauer	SMNK MS 0249		
Scaphoid	R	Mauer	SMNK MS 1201		
Scaphoid	L	Mauer	SMNK MS 1336		
Scaphoid	R	Mauer	SMNK MS 1338		
Scaphoid	R	Mauer	SMNK MS 1337		
Scaphoid	L	Mosbach	MNHM 1953/269		
Scaphoid	L	Mosbach	MNHM 1955/1366		
Scaphoid	R	Mosbach	MNHM 1955/154		
Scaphoid	R	Mosbach	MNHM 1956/285		
Scaphoid	R	Voigstedt	IQW 1966/7415 (Voi.3280)		Voi.I/34
Scaphoid	L	Voigstedt	IQW 1966/7415 (Voi.3280)		Voi.I/33
Scaphoid	R	Voigstedt	IQW 1966/7416 (Voi.3279)	young	Voi.II/44
Scaphoid	L	Voigstedt	IQW 1966/7248 (Voi.3351)		
Scaphoid	R	Voigstedt	IQW 1965/3908 (Voi.240)		
Scaphoid	L	Süssenborn	IQW 1964/344 (Süß.9149)		
Scaphoid	L	Untermassfeld	IQW 1986/21139 (Mei.20658)		individual V
Scaphoid	R	Untermassfeld	IQW 1990/23521 (Mei.23050)	young	individual VII
Scaphoid	R	Untermassfeld	IQW 1989/23220 (Mei.22739)		individual IX
Scaphoid	R	Untermassfeld	IQW 1984/20291 (Mei.19811)	young	ant.limb I
Scaphoid	L	Untermassfeld	IQW 1990/23560 (Mei.23089)		ant.limb II
Scaphoid	R	Untermassfeld	IQW 1988/22591 (Mei.22110)		ant.limb V
Scaphoid	L	Untermassfeld	IQW 1987/22080 (Mei.21599)		
Scaphoid	R	Untermassfeld	IQW 1997/26380 (Mei.25909)		
Scaphoid	L	Soleilhac	MNHN Sol 118		
Scaphoid	R	Soleilhac	MNHN Sol 117		
Scaphoid	R	West Runton	NHM M 19519		
Scaphoid	R	Hundsheim	NHMW 2013/0282/0001		
Scaphoid	L	Hundsheim	NHMW 2013/0282/0001		
Scaphoid	L	Hundsheim	NHMW 1909II.543		
Scaphoid	R	Hundsheim	IPW no num.		
Scaphoid	R	Hundsheim	IPW A104		
Scaphoid	L	Hundsheim	IPW C165		
Scaphoid	L	Hundsheim	IPW no num.		
Scaphoid	L	Hundsheim	IPW C104		
Scaphoid	L	Hundsheim	IPW C8		
Semilunar	L	Mauer	SMNK MS 1331		
Semilunar	R	Mauer	SMNK MS 1330		

Element	Side	Locality	Catalogue	Age	Association
Semilunar	R	Mosbach	MNHM 1961/593		
Semilunar	R	Mosbach	MNHM 1967/76		
Semilunar	R	Mosbach	MNHM 1955/518		
Semilunar	R	Mosbach	MNHM 1966/173		
Semilunar	L	Isernia	MPPL 53.4		
Semilunar	R	Voigstedt	IQW 1966/7415 (Voi.3280)		Voi.I/38
Semilunar	R	Voigstedt	IQW 1966/7416 (Voi.3279)	young	Voi.II/102
Semilunar	R	Süssenborn	IQW 1965/2175 (Süß.9503)		
Semilunar	R	Untermassfeld	IQW 1980/15497 (Mei.15009)		individual I
Semilunar	L	Untermassfeld	IQW 1985/20744 (Mei.20263)		individual V
Semilunar	R	Untermassfeld	IQW 1990/23575 (Mei.23104)	young	individual VII
Semilunar	L	Untermassfeld	IQW 1989/23183 (Mei.22702)		ant.limb II
Semilunar	R	Untermassfeld	IQW 1988/22592 (Mei.22111)		ant.limb V
Semilunar	R	Untermassfeld	IQW 1983/19249 (Mei.18769)		ant.limb VII
Semilunar	R	Untermassfeld	IQW 1990/24880 (Mei.24419)		
Semilunar	L	Soleilhac	MNHN Sol 95		
Semilunar	R	Sidestrand	NHM M 18158		
Semilunar	R	Hundsheim	NHMW 2013/0282/0001		
Semilunar	L	Hundsheim	NHMW 2013/0282/0001		
Semilunar	R	Hundsheim	IPW C167		
Semilunar	R	Hundsheim	IPW no num.		
Semilunar	L	Hundsheim	IPW A3		
Semilunar	L	Hundsheim	IPW C122		
Semilunar	L	Hundsheim	IPW C107		
Pyramidal	R	Mauer	SMNK MS 1187		
Pyramidal	R	Mauer	SMNK MS 0791		
Pyramidal	L	Mosbach	MNHM 1957/651		
Pyramidal	L	Mosbach	MNHM 1955/789		
Pyramidal	R	Voigstedt	IQW 1966/7415 (Voi.3280)		Voi.I/37
Pyramidal	R	Voigstedt	IQW 1966/7416 (Voi.3279)	young	Voi.II/32
Pyramidal	L	Voigstedt	IQW 1965/3830 (Voi.977)		
Pyramidal	L	Isernia	MPPL 326		
Pyramidal	L	Untermassfeld	IQW 1980/16736 (Mei.16257)		individual I
Pyramidal	L	Untermassfeld	IQW 1980/16737 (Mei.16737)		individual II
Pyramidal	L	Untermassfeld	IQW 1980/16971 (Mei.16492)		individual III
Pyramidal	L	Untermassfeld	IQW 1985/20742 (Mei.20261)		individual V

Element	Side	Locality	Catalogue	Age	Association
Pyramidal	L	Untermassfeld	IQW 1990/23495 (Mei.23014)	young	individual VII
Pyramidal	R	Untermassfeld	IQW 1984/20287 (Mei.19807)	young	ant.limb I
Pyramidal	L	Soleilhac	MNHN Sol 114		
Pyramidal	L	Soleilhac	MNHN Sol 116		
Pyramidal	L	Boxgrove	NHM F 30087		
Pyramidal	R	Hundsheim	NHMW 2013/0282/0001		
Pyramidal	L	Hundsheim	NHMW 2013/0282/0001		
Pyramidal	R	Hundsheim	NHMW 1909II.544		
Pyramidal	R	Hundsheim	NHMW 1909II.544		
Pyramidal	L	Hundsheim	NHMW 1909II.545		
Pyramidal	L	Hundsheim	NHMW 1909II.553		
Pyramidal	R	Hundsheim	IPW A107		
Pyramidal	R	Hundsheim	IPW no num.		
Pyramidal	L	Hundsheim	IPW B1		
Pyramidal	L	Hundsheim	IPW C24		
Unciform	R	Mauer	SMNK MS 1335		
Unciform	L	Mauer	SMNK MS 0738		
Unciform	R	Mauer	SMNK MS 1327		
Unciform	R	Mauer	SMNK MS 1325		
Unciform	L	Mauer	SMNK MS 1324		
Unciform	L	Mauer	SMNK MS 1326		
Unciform	L	Mosbach	MNHM 1958/277		
Unciform	L	Mosbach	MNHM 1956/314		
Unciform	L	Mosbach	MNHM 1954/80		
Unciform	R	Mosbach	MNHM 1962/216		
Unciform	R	Mosbach	MNHM 1955/316		
Unciform	R	Isernia	MPI 787		
Unciform	R	Voigstedt	IQW 1966/7415 (Voi.3280)		Voi.I/56
Unciform	R	Voigstedt	IQW 1966/7416 (Voi.3279)	young	Voi.II/101
Unciform	L	Voigstedt	IQW 1965/3911 (Voi.1565)		
Unciform	L	Voigstedt	IQW 1965/3918 (Voi.3288)		
Unciform	L	Süssenborn	IQW 1964/343 (Süß.9148)		
Unciform	L	Untermassfeld	IQW 1980/15683 (Mei.15195)		individual I
Unciform	L	Untermassfeld	IQW 1980/16593 (Mei.16114)		individual II
Unciform	L	Untermassfeld	IQW 1985/20745 (Mei.20264)		individual V
Unciform	R	Untermassfeld	IQW 1992/23998 (Mei.23527)	young	individual VII
Unciform	L	Untermassfeld	IQW 1990/23620 (Mei.23149)	young	individual XII
Unciform	R	Untermassfeld	IQW 1984/20289 (Mei.19809)	young	ant.limb I

Element	Side	Locality	Catalogue	Age	Association
Unciform	L	Untermassfeld	IQW 1990/23421 (Mei.22940)		ant.limb II
Unciform	R	Untermassfeld	IQW 1988/22578 (Mei.22097)		ant.limb V
Unciform	R	Untermassfeld	IQW 1982/18245 (Mei.17766)		ant.limb VII
Unciform	L	Untermassfeld	IQW 1997/26006 (Mei.25535)		
Unciform	L	Soleilhac	MNHN Sol 111		
Unciform	R	Trimingham	NHM M 18155		
Unciform	R	West Runton	NHM M 17832		
Unciform	L	Boxgrove	NHM F 30930		
Unciform	R	Hundsheim	NHMW 2013/0282/0001		
Unciform	L	Hundsheim	NHMW 2013/0282/0001		
Unciform	R	Hundsheim	NHMW 1909II.548		
Unciform	L	Hundsheim	NHMW 1909II.548		
Unciform	R	Hundsheim	IPW C167		
Unciform	R	Hundsheim	IPW no num.		
Unciform	L	Hundsheim	IPW C157		
Magnum	R	Mauer	SMNK MS 1194		
Magnum	R	Mauer	SMNK MS 1332		
Magnum	R	Mauer	SMNK MS 1176		
Magnum	R	Mauer	SMNK MS 1196		
Magnum	R	Mauer	SMNK MS 1192		
Magnum	L	Mauer	SMNK MS 1197		
Magnum	L	Mauer	SMNK MS 1195		
Magnum	L	Mosbach	MNHM 1954/466		
Magnum	L	Mosbach	MNHM 1959/742		
Magnum	R	Isernia	MPI 66.50		
Magnum	R	Isernia	MPPL 50.366		
Magnum	R	Isernia	MPPL 365		
Magnum	R	Voigstedt	IQW 1966/7415 (Voi.3280)		Voi.I/31
Magnum	R	Voigstedt	IQW 1966/7416 (Voi.3279)	young	Voi.II/37 + Voi.II/24
Magnum	R	Voigstedt	IQW 1965/3915 (Voi.569)		
Magnum	R	Süssenborn	IQW 1964/662 (Süß.7762)		
Magnum	L	Süssenborn	IQW 1964/661 (Süß.7702)		
Magnum	L	Untermassfeld	IQW 1980/15403 (Mei.14915)		individual IV
Magnum	L	Untermassfeld	IQW 1990/23509 (Mei.23028)	young	individual VII
Magnum	L	Untermassfeld	IQW 1989/23204 (Mei.22723)		individual IX
Magnum	L	Untermassfeld	IQW 1990/23616 (Mei.23145)		ant.limb II
Magnum	R	Untermassfeld	IQW 1980/15632 (Mei.15144)		

Element	Side	Locality	Catalogue	Age	Association
Magnum	L	Soleilhac	MNHN Sol 110		
Magnum	L	Overstrand	NHM M 19521		
Magnum	R	Trimingham	NHM M 19520		
Magnum	L	Pakefield	NHM 429		
Magnum	L	Boxgrove	NHM F 7283		
Magnum	L	Boxgrove	NHM F 5268		
Magnum	R	Hundsheim	NHMW 2013/0282/0001		
Magnum	L	Hundsheim	NHMW 2013/0282/0001		
Magnum	L	Hundsheim	NHMW 1909II.547		
Magnum	R	Hundsheim	IPW C16		
Magnum	R	Hundsheim	IPW A103		
Magnum	L	Hundsheim	IPW C154		
McII	L	Mauer	SMNK MS 1173		
McII	R	Mauer	SMNK MS 1167		
McII	L	Mosbach	MNHM 1961/119		
McII	R	Voigstedt	IQW 1966/7415 (Voi.3280)		Voi.I/15
McII	L	Voigstedt	IQW 1966/7415 (Voi.3280)		Voi.I/26
McII	R	Voigstedt	IQW 1966/7416 (Voi.3279)	young	Voi.II/99
McII	L	Voigstedt	IQW 1965/3921 (Voi.220)		
McII	L	Voigstedt	IQW 1965/3831 (Voi.745)		
McII	R	Süssenborn	IQW 1964/655 (Süß.R1)		
McII	L	Süssenborn	IQW 1964/350 (Süß.9155)		
McII	R	Untermassfeld	IQW 1980/15882 (Mei.15393)		individual I
McII	L	Untermassfeld	IQW 1980/17440 (Mei.16962)		individual IV
McII	L	Untermassfeld	IQW 1985/20740 (Mei.20259)		individual V
McII	L	Untermassfeld	IQW 1990/23491 (Mei.23010)	young	individual VII
McII	R	Untermassfeld	IQW 1980/16003 (Mei.15514)	young	individual X
McII	R	Untermassfeld	IQW 1984/20285 (Mei.19805)	young	ant.limb I
McII	L	Untermassfeld	IQW 1992/23918 (Mei.23447)		ant.limb II
McII	R	Untermassfeld	IQW 1980/15469 (Mei.14981)		
McII	L	Untermassfeld	IQW 1989/23389 (Mei.22908)		
McII	L	Pietrafitta	MPLB #020		
McII	L	Soleilhac	MNHN Sol 123		
McII	R	Sidestrand	NHM M 19517		
McII	R	Sidestrand	NHM M 19515		
McII	R	Sidestrand	NHM M 6675		
McII	R	West Runton	NHM M 19516		
McII	R	Hundsheim	NHMW 2013/0282/0001		

Element	Side	Locality	Catalogue	Age	Association
McII	L	Hundsheim	NHMW 2013/0282/0001		
McII	L	Hundsheim	IPW A109		
McII	L	Hundsheim	IPW C57		
McII	L	Hundsheim	IPW C157		
McII	R	Hundsheim	IPW C159		
McII	R	Hundsheim	IPW no num.		
McIII	L	Mauer	SMNK MS 1475		
McIII	R	Mauer	SMNK MS 0236		
McIII	R	Mauer	SMNK MS 1544		
McIII	L	Mauer	SMNK MS 1543		
McIII	L	Mosbach	MNHM 1956/28		
McIII	L	Mosbach	MNHM 1963/518		
McIII	L	Mosbach	MNHM 1959/791		
McIII	L	Mosbach	MNHM 1962/931		
McIII	R	Voigstedt	IQW 1966/7415 (Voi.3280)		Voi.I/24
McIII	L	Voigstedt	IQW 1966/7415 (Voi.3280)		Voi.I/69
McIII	R	Voigstedt	IQW 1966/7416 (Voi.3279)	young	Voi.II/10
McIII	R	Voigstedt	IQW 1966/7244 (Voi.3377)		
McIII	R	Voigstedt	IQW 1965/3823 (Voi.765)		
McIII	R	Voigstedt	IQW 1965/3777 (Voi.1173)		
McIII	L	Süssenborn	IQW 1964/656 (Süß.7716)		
McIII	R	Untermassfeld	IQW 1980/15581 (Mei.15093)		individual I
McIII	R	Untermassfeld	IQW 1980/16503 (Mei.16024)		individual III
McIII	L	Untermassfeld	IQW 1980/15412 (Mei.14924)		individual IV
McIII	L	Untermassfeld	IQW 1985/20738 (Mei.20257)		individual V
McIII	L	Untermassfeld	IQW 1980/17452 (Mei.16974)		individual VI
McIII	R	Untermassfeld	IQW 1990/23655 (Mei.23184)	young	individual VII
McIII	L	Untermassfeld	IQW 1989/23313 (Mei.22832)		individual IX
McIII	R	Untermassfeld	IQW 1980/15850 (Mei.15361)	young	individual X
McIII	R	Untermassfeld	IQW 1984/20283 (Mei.19803)	young	ant.limb I
McIII	L	Untermassfeld	IQW 1990/23514 (Mei.23043)		ant.limb II
McIII	L	Untermassfeld	IQW 1990/23496 (Mei.23015)	young	ant.limb VI
McIII	R	Untermassfeld	IQW 1982/18202 (Mei.17722)		ant.limb VII
McIII	R	Untermassfeld	IQW 1980/15801 (Mei.15312)		

Element	Side	Locality	Catalogue	Age	Association
McIII	R	Untermassfeld	IQW 1980/16389 (Mei.15900)		
McIII	R	Untermassfeld	IQW 1987/21976 (Mei.21496)		
McIII	R	Pietrafitta	MPLB #018		
McIII	L	Soleilhac	MNHN Sol 122		
McIII	R	East Runton	NHM M 6682		
McIII	R	Sidestrand	NHM M 17829		
McIII	L	Sidestrand	NHM M 17826		
McIII	R	Hundsheim	NHMW 2013/0282/0001		
McIII	L	Hundsheim	NHMW 2013/0282/0001		
McIII	R	Hundsheim	NHMW 1909II.549		
McIII	L	Hundsheim	NHMW 1909II.550		
McIII	L	Hundsheim	IPW no num.		
McIII	R	Hundsheim	IPW C77		
McIII	L	Hundsheim	IPW C57		
McIV	L	Mauer	SMNK MS 0247		
McIV	L	Mauer	SMNK MS 5046		
McIV	L	Mauer	SMNK MS 1545		
McIV	L	Mauer	SMNK MS 0238		
McIV	L	Mosbach	MNHM 1959/555		
McIV	L	Mosbach	MNHM 1957/121		
McIV	L	Mosbach	MNHM 1959/195		
McIV	R	Voigstedt	IQW 1966/7415 (Voi.3280)		Voi.I/25
McIV	L	Voigstedt	IQW 1966/7415 (Voi.3280)		Voi.I/28
McIV	R	Voigstedt	IQW 1966/7416 (Voi.3279)	young	Voi.II/13
McIV	R	Voigstedt	IQW 1965/3774 (Voi.202)		
McIV	L	Süssenborn	IQW 1964/654 (Süß.7707)		
McIV	L	Untermassfeld	IQW 1980/15687 (Mei.15199)		individual I
McIV	L	Untermassfeld	IQW 1980/15733 (Mei.15245)		individual II
McIV	R	Untermassfeld	IQW 1980/16186 (Mei.15697)		individual III
McIV	L	Untermassfeld	IQW 1980/17118 (Mei.16639)		individual III
McIV	L	Untermassfeld	IQW 1980/15413 (Mei.14925)		individual IV
McIV	L	Untermassfeld	IQW 1985/20739 (Mei.20258)		individual V
McIV	L	Untermassfeld	IQW 1982/17954 (Mei.17474)		individual VI
McIV	R	Untermassfeld	IQW 1990/23702 (Mei.23231)	young	individual VII
McIV	R	Untermassfeld	IQW 1983/19030 (Mei.18550)		individual VIII

Element	Side	Locality	Catalogue	Age	Association
McIV	R	Untermassfeld	IQW 1980/12849 (Mei.15360)	young	individual X
McIV	R	Untermassfeld	IQW 1984/20284 (Mei.19804)	young	ant.limb I
McIV	L	Untermassfeld	IQW 1990/23612 (Mei.23141)		ant.limb II
McIV	L	Untermassfeld	IQW 1990/23497 (Mei.23016)	young	ant.limb VI
McIV	R	Untermassfeld	IQW 1982/18079 (Mei.17599)		ant.limb VII
McIV	R	Pietrafitta	MPLB #019		
McIV	L	Soleilhac	MNHN Sol 124		
McIV	R	Trimingham	NHM M 19511		
McIV	R	Hundsheim	NHMW 2013/0282/0001		
McIV	L	Hundsheim	NHMW 2013/0282/0001		
McIV	R	Hundsheim	IPW C153		
McIV	L	Hundsheim	IPW no num.		
McIV	R	Hundsheim	IPW C169		
Femur	L	Mauer	SMNK MS 0265		
Femur	R	Mauer	SMNK MS 1457		
Femur	L	Mauer	SMNK MS 1469		
Femur	R	Mauer	SMNK MS 0375		
Femur	L	Mauer	SMNK MS 0377		
Femur	R	Voigstedt	IQW 1966/7415 (Voi.3280)		Voi.I/72
Femur	L	Voigstedt	IQW 1966/7415 (Voi.3280)		Voi.I/71
Femur	R	Voigstedt	IQW 1966/7416 (Voi.3279)	young	Voi.II/93
Femur	L	Voigstedt	IQW 1966/7416 (Voi.3279)	young	Voi.II/3
Femur	L	Süssenborn	IQW 1964/911 (Süß.9229)		
Femur	R	Untermassfeld	IQW 1980/16430 (Mei.15941)		individual II
Femur	R	Untermassfeld	IQW 1980/16047 (Mei.15558)		individual III
Femur	L	Untermassfeld	IQW 1980/16049 (Mei.15560)		individual III
Femur	L	Untermassfeld	IQW 1981/17748 (Mei.17269)		individual IV
Femur	L	Untermassfeld	IQW 1989/23860 (Mei.22771)	young	individual VII
Femur	R	Untermassfeld	IQW 1990/23680 (Mei.23209)		
Femur	L	Untermassfeld	IQW 1995/25326 (Mei.24855)		
Femur	R	Pietrafitta	MPLB #001		
Femur	L	Pietrafitta	MPLB #002		
Femur	L	Pietrafitta	MPLB #003		
Femur	L	Pietrafitta	MPLB #004		
Femur	R	Pietrafitta	MPLB #005		

Element	Side	Locality	Catalogue	Age	Association
Femur	R	Hundsheim	NHMW 2013/0282/0001		
Femur	L	Hundsheim	NHMW 2013/0282/0001		
Femur	R	Hundsheim	NHMW no num.		
Femur	L	Hundsheim	NHMW no num.		
Femur	R	Hundsheim	IPW no num.	young	
Femur	L	Hundsheim	IPW no num.	young	
Tibia	R	Mauer	SMNK MS 0381		
Tibia	L	Mauer	SMNK MS 0391		
Tibia	L	Mauer	SMNK MS 1470		
Tibia	L	Mauer	SMNK MS 0262		
Tibia	L	Mauer	SMNK MS 0263		
Tibia	R	Mauer	SMNK MS 0834		
Tibia	R	Mauer	SMNK MS 0382		
Tibia	R	Mauer	SMNK MS 0392		
Tibia	R	Mauer	SMNK MS 0389		
Tibia	L	Mauer	SMNK MS 0398		
Tibia	L	Mosbach	MNHM 1956/648		
Tibia	R	Mosbach	MNHM 1956/601		
Tibia	R	Mosbach	MNHM 1970/171		
Tibia	R	Voigstedt	IQW 1966/7415 (Voi.3280)		Voi.I/9
Tibia	L	Voigstedt	IQW 1966/7415 (Voi.3280)		Voi.I/70
Tibia	R	Voigstedt	IQW 1966/7416 (Voi.3279)	young	Voi.II/4
Tibia	L	Voigstedt	IQW 1966/7416 (Voi.3279)	young	Voi.II/7
Tibia	L	Voigstedt	IQW - - (Voi.701)		
Tibia	R	Voigstedt	IQW 1966/7442 (Voi.1683)		
Tibia	R	Süssenborn	IQW 1965/2172 (sus.7039)		
Tibia	L	Untermassfeld	IQW 1980/15364 (Mei.14876)		individual I
Tibia	R	Untermassfeld	IQW 1980/16118 (Mei.15629)		individual II
Tibia	L	Untermassfeld	IQW 1980/16429 (Mei.15940)		individual II
Tibia	R	Untermassfeld	IQW 1981/17716 (Mei.17238)		individual III
Tibia	L	Untermassfeld	IQW 1980/17156 (Mei.16677)		individual III
Tibia	R	Untermassfeld	IQW 1980/16433 (Mei.15944)		individual IV
Tibia	L	Untermassfeld	IQW 1980/16673 (Mei.16194)		individual IV
Tibia	L	Untermassfeld	IQW 1986/21300 (Mei.20819)		
Tibia	L	Untermassfeld	IQW 1998/26418 (Mei.25947)		
Tibia	L	Untermassfeld	IQW 1996/25690 (Mei.25219)		

Element	Side	Locality	Catalogue	Age	Association
Tibia	R	Untermassfeld	IQW 1995/25042 (Mei.24571)		
Tibia	L	Sidestrand	NHM M 6674		
Tibia	L	Sidestrand	NHM M 17849		
Tibia	R	Trimingham	NHM M 18486		
Tibia	R	Hundsheim	NHMW 2013/0282/0001		
Tibia	L	Hundsheim	NHMW 2013/0282/0001		
Astragalus	L	Mauer	SMNK MS 1472		
Astragalus	R	Mauer	SMNK MS 1700		
Astragalus	L	Mauer	SMNK MS 1200		
Astragalus	L	Mauer	SMNK MS 1184		
Astragalus	L	Mauer	SMNK MS 1183		
Astragalus	L	Mauer	SMNK MS 1202		
Astragalus	R	Mauer	SMNK MS 1203		
Astragalus	R	Mauer	SMNK MS 1334		
Astragalus	R	Mauer	SMNK MS 1175		
Astragalus	R	Mauer	SMNK MS 1199		
Astragalus	R	Mauer	SMNK MS 0246		
Astragalus	R	Mauer	SMNK MS 0243		
Astragalus	R	Mauer	SMNK MS 1186		
Astragalus	L	Mauer	SMNK MS 0733		
Astragalus	R	Mauer	SMNK MS 0823		
Astragalus	R	Mosbach	MNHM 1962/1281		
Astragalus	R	Mosbach	MNHM 1947/16		
Astragalus	R	Mosbach	MNHM 1955/692	young	
Astragalus	R	Mosbach	MNHM 1962/1282		
Astragalus	L	Mosbach	MNHM 1959/197		
Astragalus	L	Mosbach	MNHM 1955/693		
Astragalus	L	Mosbach	MNHM 1955/167		
Astragalus	L	Mosbach	MNHM 1952/376		
Astragalus	L	Mosbach	MNHM 1957/980		
Astragalus	R	Voigstedt	IQW 1966/7415 (Voi.3280)		Voi.I/32
Astragalus	R	Voigstedt	IQW 1966/7416 (Voi.3279)	young	Voi.II/20
Astragalus	L	Voigstedt	IQW 1966/7416 (Voi.3279)	young	Voi.II/31
Astragalus	R	Voigstedt	IQW 1965/3716 (Voi.669)		
Astragalus	L	Voigstedt	IQW 1966/5595 (Voi.1150)		
Astragalus	R	Süssenborn	IQW 1964/650 (Süß.7948)		
Astragalus	L	Süssenborn	IQW 1964/336 (Süß.9141)		
Astragalus	L	Süssenborn	IQW 1964/663 (Süß.7624)		
Astragalus	L	Untermassfeld	IQW 1980/15659 (Mei.15171)		individual I
Astragalus	R	Untermassfeld	IQW 1980/16671 (Mei.16192)		individual II
Astragalus	L	Untermassfeld	IQW 1980/16839 (Mei.16360)		individual III

Element	Side	Locality	Catalogue	Age	Association
Astragalus	R	Untermassfeld	IQW 1980/17052 (Mei.16573)		individual III
Astragalus	L	Untermassfeld	IQW 1980/16690 (Mei.16211)		individual IV
Astragalus	R	Untermassfeld	IQW 1986/21643 (Mei.21162)		individual V
Astragalus	R	Untermassfeld	IQW 1982/18527 (Mei.18047)		individual VI
Astragalus	L	Untermassfeld	IQW 1990/23585 (Mei.23114)	young	individual VII
Astragalus	L	Untermassfeld	IQW 1983/19186 (Mei.18706)		individual VIII
Astragalus	L	Untermassfeld	IQW 1989/23219 (Mei.22738)		individual IX
Astragalus	L	Untermassfeld	IQW 1980/16071 (Mei.15582)	young	individual XI
Astragalus	R	Untermassfeld	IQW 1995/25396 (Mei.24925)		
Astragalus	L	Untermassfeld	IQW 1995/24988 (Mei.24517)		
Astragalus	R	Pietrafitta	MPLB #006		
Astragalus	L	Pietrafitta	MPLB #007		
Astragalus	L	Pietrafitta	MPLB #008		
Astragalus	R	Pietrafitta	MPLB #009		
Astragalus	L	Overstrand	NHM M 19525		
Astragalus	L	Sidestrand	NHM M 6780		
Astragalus	L	Sidestrand	NHM M 19526		
Astragalus	L	Sidestrand	NHM M 19527		
Astragalus	L	Trimingham	NHM M 19524		
Astragalus	R	West Runton	NHM M 19523		
Astragalus	L	Boxgrove	NHM F 30402		
Astragalus	L	Isernia	MPPL 368		
Astragalus	R	Hundsheim	NHMW 2013/0282/0001		
Astragalus	L	Hundsheim	NHMW 2013/0282/0001		
Astragalus	R	Hundsheim	NHMW 1909II.569		
Astragalus	L	Hundsheim	IPW C155		
Astragalus	L	Hundsheim	IPW C71		
Astragalus	R	Hundsheim	IPW C69		
Astragalus	R	Hundsheim	IPW F3		
Calcaneus	R	Mauer	SMNK MS 1701		
Calcaneus	L	Mauer	SMNK MS 0253		
Calcaneus	R	Mauer	SMNK MS 1185		
Calcaneus	L	Mauer	SMNK MS 1188		
Calcaneus	L	Mauer	SMNK MS 1189		
Calcaneus	R	Mosbach	MNHM 1961/544		
Calcaneus	R	Mosbach	MNHM 1960/199		
Calcaneus	R	Mosbach	MNHM 1967/79		

Element	Side	Locality	Catalogue	Age	Association
Calcaneus	R	Mosbach	MNHM 1956/996		
Calcaneus	R	Mosbach	MNHM 1965/270		
Calcaneus	R	Mosbach	MNHM 1959/792		
Calcaneus	L	Mosbach	MNHM 1961/616		
Calcaneus	L	Mosbach	MNHM 1959/197		
Calcaneus	R	Voigstedt	IQW 1966/7416 (Voi.3279)	young	Voi.II/52
Calcaneus	L	Voigstedt	IQW 1966/7416 (Voi.3279)	young	Voi.II/8
Calcaneus	L	Voigstedt	IQW 1965/3702 (Voi.766)		
Calcaneus	L	Voigstedt	IQW 1965/3715 (Voi.824)		
Calcaneus	R	Voigstedt	IQW 1965/3721 (Voi.1210)		
Calcaneus	L	Süssenborn	IQW 1964/337 (Süß.9142)	young	
Calcaneus	L	Süssenborn	IQW 1964/649 (Süß.7870)	young	
Calcaneus	R	Untermassfeld	IQW 1980/16719 (Mei.16240)		individual I
Calcaneus	L	Untermassfeld	IQW 1980/15658 (Mei.15170)		individual I
Calcaneus	R	Untermassfeld	IQW 1980/16401 (Mei.15912)		individual II
Calcaneus	L	Untermassfeld	IQW 1980/16840 (Mei.16361)		individual III
Calcaneus	L	Untermassfeld	IQW 1980/16687 (Mei.16208)		individual IV
Calcaneus	R	Untermassfeld	IQW 1986/21639 (Mei.21158)		individual V
Calcaneus	R	Untermassfeld	IQW 1982/18528 (Mei.18048)		individual VI
Calcaneus	L	Untermassfeld	IQW 1990/23586 (Mei.23115)		individual VII
Calcaneus	L	Untermassfeld	IQW 1983/19140 (Mei.18660)		individual VIII
Calcaneus	R	Untermassfeld	IQW 1986/21736 (Mei.21255)		
Calcaneus	R	Untermassfeld	IQW 1987/22076 (Mei.21595)		
Calcaneus	L	Untermassfeld	IQW 1988/22577 (Mei.22096)		
Calcaneus	R	Untermassfeld	IQW 1992/24103 (Mei.23632)		
Calcaneus	R	Untermassfeld	IQW 1995/24987 (Mei.24516)		
Calcaneus	L	Pietrafitta	MPLB #010		
Calcaneus	R	Soleilhac	MNHN Sol 109		
Calcaneus	R	Sidestrand	NHM M 19528		
Calcaneus	R	Trimingham	NHM M 6687		
Calcaneus	L	Trimingham	NHM M 19536		
Calcaneus	L	Trimingham	NHM M 17833		
Calcaneus	L	Boxgrove	NHM F 30400		

Element	Side	Locality	Catalogue	Age	Association
Calcaneus	R	Isernia	MPI 57.41		
Calcaneus	R	Hundsheim	NHMW 2013/0282/0001		
Calcaneus	L	Hundsheim	NHMW 2013/0282/0001		
Calcaneus	R	Hundsheim	IPW C71		
Calcaneus	R	Hundsheim	IPW no num.		
Calcaneus	L	Hundsheim	IPW A144		
Calcaneus	L	Hundsheim	IPW no num.		
Cuboid	R	Mauer	SMNK MS 1593		
Cuboid	R	Mauer	SMNK MS 2879		
Cuboid	R	Voigstedt	IQW 1966/7415 (Voi.3280)		Voi.I/35
Cuboid	R	Voigstedt	IQW 1966/7416 (Voi.3279)	young	Voi.II/32
Cuboid	L	Voigstedt	IQW 1966/7416 (Voi.3279)	young	Voi.II/103
Cuboid	R	Voigstedt	IQW 1965/3722 (Voi.346)		
Cuboid	L	Süssenborn	IQW 1964/338 (Süß.9143)		
Cuboid	L	Untermassfeld	IQW 1980/15971 (Mei.15482)		individual I
Cuboid	R	Untermassfeld	IQW 1980/16700 (Mei.16221)		individual II
Cuboid	R	Untermassfeld	IQW 1980/16720 (Mei.16241)		individual III
Cuboid	L	Untermassfeld	IQW 1980/16688 (Mei.16209)		individual IV
Cuboid	R	Untermassfeld	IQW 1986/21638 (Mei.21157)		individual V
Cuboid	R	Untermassfeld	IQW 1982/17932 (Mei.17452)		individual VI
Cuboid	L	Untermassfeld	IQW 1980/16811 (Mei.16332)	young	individual XI
Cuboid	R	Untermassfeld	IQW 1985/20811 (Mei.20330)		
Cuboid	R	Untermassfeld	IQW 1980/15584 (Mei.15096)		
Cuboid	R	Untermassfeld	IQW 1992/24080 (Mei.23609)		
Cuboid	R	Untermassfeld	IQW 1985/20432 (Mei.19952)		
Cuboid	L	Untermassfeld	IQW 1989/23175 (Mei.22694)		
Cuboid	L	Untermassfeld	IQW 1984/19947 (Mei.19467)		
Cuboid	L	Sidestrand	NHM M 17608		
Cuboid	L	Boxgrove	NHM F 30057		
Cuboid	L	Isernia	MPI 26		
Cuboid	R	Isernia	MPI 68.34		
Cuboid	R	Isernia	MPPL 375		
Cuboid	R	Isernia	MPPL 376		
Cuboid	L	Isernia	MPPL 374		

Element	Side	Locality	Catalogue	Age	Association
Cuboid	R	Hundsheim	NHMW 2013/0282/0001		
Cuboid	L	Hundsheim	NHMW 2013/0282/0001		
Cuboid	R	Hundsheim	NHMW 1909II.575		
Cuboid	L	Hundsheim	NHMW 1909II.575		
Cuboid	L	Hundsheim	IPW C14		
Cuboid	L	Hundsheim	IPW C102		
Cuboid	R	Hundsheim	IPW C162		
Navicular	R	Voigstedt	IQW 1966/7415 (Voi.3280)		Voi.I/36
Navicular	R	Voigstedt	IQW 1966/7416 (Voi.3279)	young	Voi.II/53
Navicular	L	Voigstedt	IQW 1966/7416 (Voi.3279)	young	Voi.II/14
Navicular	L	Voigstedt	IQW 1965/3708 (Voi.1622)		
Navicular	L	Voigstedt	IQW 1965/3707 (Voi.665)		
Navicular	L	Untermassfeld	IQW 1980/15662 (Mei.15174)		individual I
Navicular	R	Untermassfeld	IQW 1980/16699 (Mei.16220)		individual II
Navicular	L	Untermassfeld	IQW 1980/16689 (Mei.16210)		individual IV
Navicular	R	Untermassfeld	IQW 1986/21654 (Mei.21173)		individual V
Navicular	R	Untermassfeld	IQW 1982/18445 (Mei.17965)		individual VI
Navicular	R	Untermassfeld	IQW 1985/20430 (Mei.19950)		
Navicular	R	Untermassfeld	IQW 1992/24066 (Mei.23595)		
Navicular	L	Untermassfeld	IQW 1988/22702 (Mei.22221)		
Navicular	R	Untermassfeld	IQW 1993/24339 (Mei.23869)		
Navicular	L	Pietrafitta	MPLB #017		
Navicular	R	Hundsheim	NHMW 2013/0282/0001		
Navicular	L	Hundsheim	NHMW 2013/0282/0001		
Navicular	R	Hundsheim	NHMW 1909II.574		
Navicular	L	Hundsheim	NHMW 1909II.574		
Navicular	R	Hundsheim	IPW C71		
Navicular	L	Hundsheim	IPW A144		
MtII	L	Mauer	SMNK MS 0237		
MtII	R	Mauer	SMNK MS 1547		
MtII	L	Mauer	SMNK MS 1548		
MtII	R	Voigstedt	IQW 1966/7416 (Voi.3279)	young	Voi.II/17
MtII	L	Voigstedt	IQW 1966/7416 (Voi.3279)	young	Voi.II/12
MtII	L	Untermassfeld	IQW 1980/15666 (Mei.15178)		individual I
MtII	R	Untermassfeld	IQW 1980/16701 (Mei.16222)		individual III

Element	Side	Locality	Catalogue	Age	Association
MtII	R	Untermassfeld	IQW 1986/21641 (Mei.21160)		individual V
MtII	R	Untermassfeld	IQW 1982/18442 (Mei.17962)		individual VI
MtII	L	Untermassfeld	IQW 1980/15457 (Mei.14969)	young	individual X
MtII	L	Untermassfeld	IQW 1993/24365 (Mei.23894)		
MtII	L	Pietrafitta	MPLB #015		
MtII	R	Soleilhac	MNHN Sol 121		
MtII	R	Sidestrand	NHM M 18156		
MtII	R	Isernia	MPPL 175.379		
MtII	R	Hundsheim	NHMW 2013/0282/0001		
MtII	R	Hundsheim	IPW A97		
MtII	L	Hundsheim	IPW no num.		
MtII	L	Hundsheim	IPW A144		
MtIII	L	Mauer	SMNK MS 5047		
MtIII	R	Mosbach	MNHM 1957/394		
MtIII	L	Mosbach	MNHM 1955/1225		
MtIII	R	Mosbach	MNHM 1964/503		
MtIII	R	Mosbach	MNHM 1955/832		
MtIII	R	Voigstedt	IQW 1966/7415 (Voi.3280)		Voi.I/27
MtIII	R	Voigstedt	IQW 1966/7416 (Voi.3279)	young	Voi.II/100
MtIII	L	Voigstedt	IQW 1966/7416 (Voi.3279)	young	Voi.II/18
MtIII	L	Süssenborn	IQW 1964/652 (Süß.5203)		
MtIII	R	Süssenborn	IQW 1964/339 (Süß.9144)		
MtIII	R	Untermassfeld	IQW 1980/15844 (Mei.15355)		individual I
MtIII	L	Untermassfeld	IQW 1980/15663 (Mei.15175)		individual I
MtIII	R	Untermassfeld	IQW 1980/16703 (Mei.16224)		individual III
MtIII	R	Untermassfeld	IQW 1986/21642 (Mei.21161)		individual V
MtIII	R	Untermassfeld	IQW 1982/18443 (Mei.17963)		individual VI
MtIII	R	Untermassfeld	IQW 1993/24314 (Mei.23843)	young	individual XII
MtIII	L	Untermassfeld	IQW 1987/22098 (Mei.21617)		post.limb I
MtIII	R	Untermassfeld	IQW 1980/16920 (Mei.16441)		
MtIII	R	Untermassfeld	IQW 1984/20181 (Mei.19701)		
MtIII	L	Untermassfeld	IQW 1993/24368 (Mei.23897)		
MtIII	L	Pietrafitta	MPLB #013		

Element	Side	Locality	Catalogue	Age	Association
MtIII	nd	Sidestrand	NHM M 6783		
MtIII	L	Sidestrand	NHM M 17827		
MtIII	L	Trimingham	NHM M 6676		
MtIII	R	Isernia	MPPL 80.378		
MtIII	R	Hundsheim	NHMW 2013/0282/0001		
MtIII	L	Hundsheim	NHMW 2013/0282/0001		
MtIII	R	Hundsheim	NHMW 1909II.571		
MtIII	R	Hundsheim	IPW D16		
MtIII	R	Hundsheim	IPW A32		
MtIII	L	Hundsheim	IPW C129		
MtIII	L	Hundsheim	IPW C99		
MtIV	R	Mauer	SMNK MS 1552		
MtIV	L	Mauer	SMNK MS 1553		
MtIV	L	Mauer	SMNK MS 1190		
MtIV	R	Mauer	SMNK MS 1555		
MtIV	L	Mosbach	MNHM 1953/488		
MtIV	L	Mosbach	MNHM 1954/564		
MtIV	R	Mosbach	MNHM 1959/790		
MtIV	R	Mosbach	MNHM 1958/84		
MtIV	R	Voigstedt	IQW 1966/7415 (Voi.3280)		Voi.I/67
MtIV	R	Voigstedt	IQW 1966/7416 (Voi.3279)	young	Voi.II/11
MtIV	L	Voigstedt	IQW 1966/7416 (Voi.3279)	young	Voi.II/19
MtIV	L	Untermassfeld	IQW 1980/15660 (Mei.15172)		individual I
MtIV	L	Untermassfeld	IQW 1980/16311 (Mei.15822)		individual IV
MtIV	R	Untermassfeld	IQW 1986/21640 (Mei.21159)		individual V
MtIV	R	Untermassfeld	IQW 1982/18055 (Mei.17575)		individual VI
MtIV	L	Untermassfeld	IQW 1982/17907 (Mei.17427)		individual VI
MtIV	R	Untermassfeld	IQW 1983/19581 (Mei.19101)		individual VIII
MtIV	L	Untermassfeld	IQW 1980/15455 (Mei.14967)	young	individual X
MtIV	L	Untermassfeld	IQW 1993/24364 (Mei.23893)		
MtIV	L	Untermassfeld	IQW 1997/26241 (Mei.25770)		
MtIV	L	Pietrafitta	MPLB #014		
MtIV	R	Isernia	MPPL 380		
MtIV	L	Isernia	MPI 89.160		
MtIV	R	Hundsheim	NHMW 2013/0282/0001		
MtIV	L	Hundsheim	NHMW 2013/0282/0001		

Attachment IV - Biometric method. Drawings by M. Ballatore.

Humerus (left bone – A, caudal; B, proximal; C, medial; D, cranial; E, lateral)

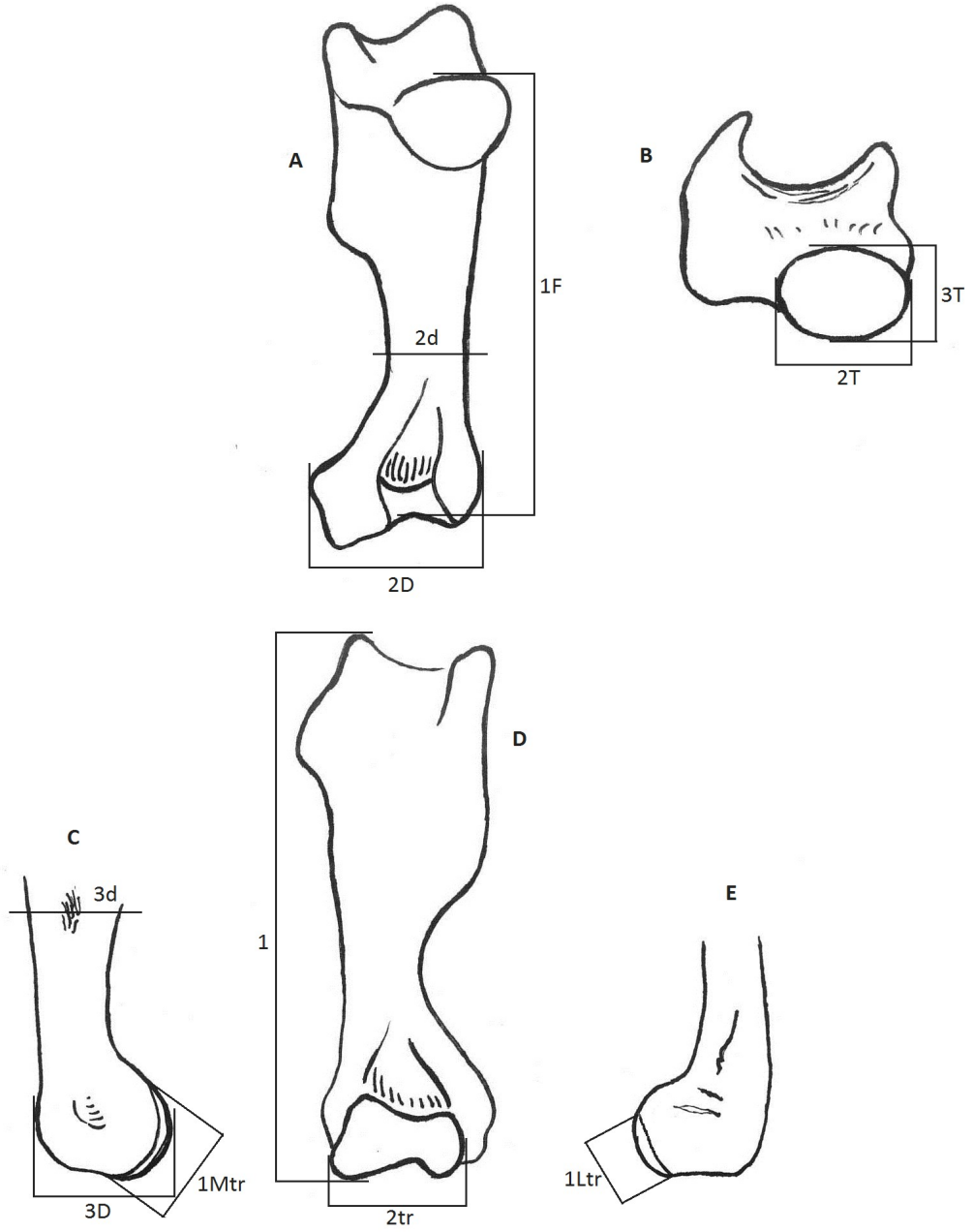

Num.	View	Description
1	cranial	Maximum length
1F	caudal	Physiological length, from the top of the articular head to the bottom of the trochlea valley; parallel to the axis of the bone
2d	caudal	Breadth of the diaphysis, at the level of minimum
3d	medial	Depth of the diaphysis, at the level of the coracobrachialis insertion (it is not the same level of 2d!)
2D	caudal	Distal breadth, from the more medial edge of the medial epicondyle ramus to the most lateral prominence of the lateral epicondyle ramus (transversal crest)
3D	medial	Distal depth, from the cranial edge of the trochlea to the caudal prominence of the medial epicondyle ramus
1Mtr	medial	Trochlear medial height, from the proximal to the distal edge of the trochlea; transversally
1Ltr	lateral	Trochlear lateral height, from the proximal to the distal edge of the trochlea; transversally
2tr	cranial	Trochlear breadth, parallel to the axis of the trochlea
2T	proximal	Medio-lateral diameter of the head
3T	proximal	Cranio-caudal diameter of the head

Radius (left bone – A, proximal; B, distal; C, dorsal; D, section)

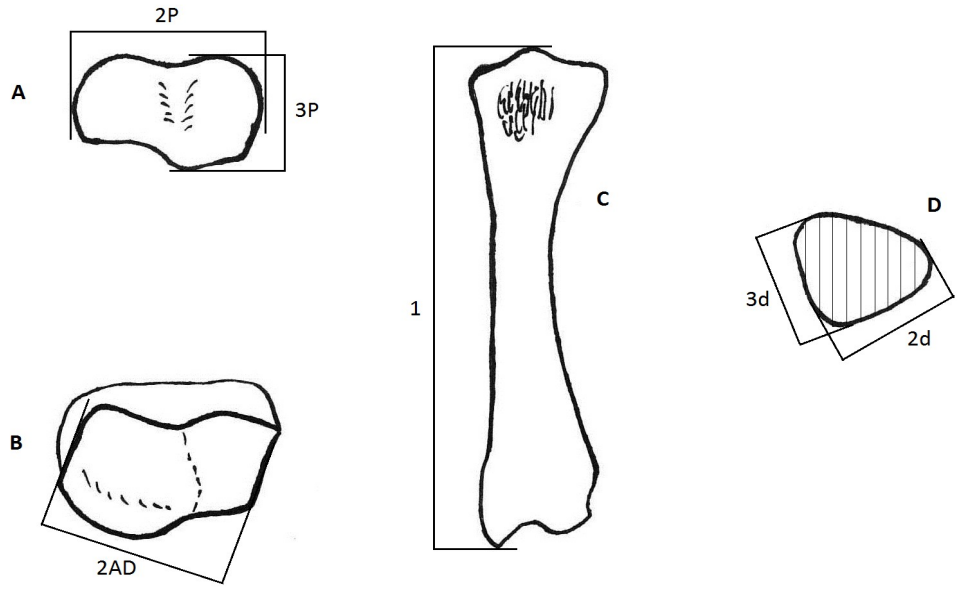

Num.	View	Description
1	dorsal	Length, from the apex of the dorsal prominence (the palmar prominence is higher, but rarely preserved!) to the medial prominence of the distal epiphysis; parallel to the axis of the bone
2P	proximal	Proximal breadth, in the middle of the art. surf. (max axis); considering the dorsal outline as horizontal reference
3P	proximal	Proximal depth, perpendicular to 2D, along the medial side
2d	dorsal-lateral	Breadth of the diaphysis, just above the lateral muscular insertion
3d	medial-dorsal	Depth of the diaphysis, at the same level of 2d
2AD	distal	Distal articular breadth, the distal art. surf. has a shape of parallelogram, we consider the measure perpendicular to the short sides

Ulna (left bone – A, medial; B, dorsal; C, distal)

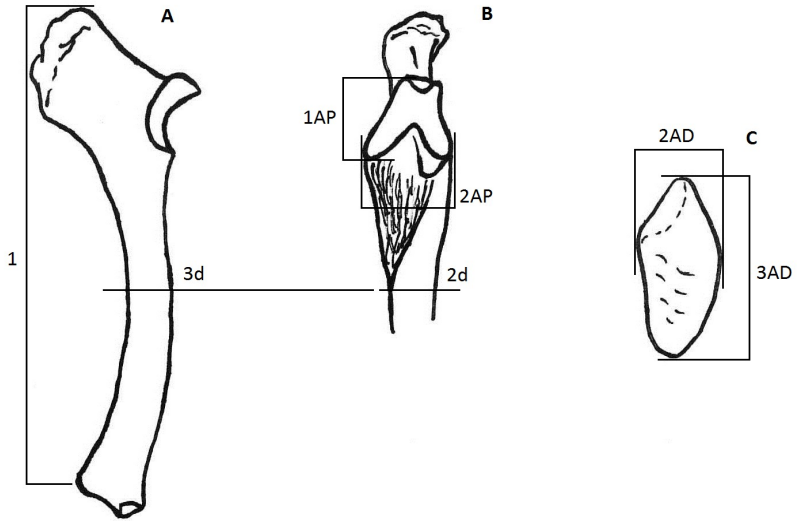

Num.	View	Description
1	medial	The maximum length from the top of the olecranon to the plantar edge of the distal epiphysis; it is not parallel to the axis of the bone
1AP	dorsal	Height of the proximal articular surface, at the medial side of the trochlear notch, parallel to the axis of the bone
2AP	dorsal	Breadth of the proximal articular surface, at the distal side of the trochlear notch, perpendicular to the axis of the bone
2d	dorsal	Breadth of the diaphysis, just beyond the rough surface for the radius contact
3d	medial	Depth of the diaphysis, at the same level of 2d
2AD	distal	The smallest articular diameter
3AD	distal	The biggest articular diameter

Scaphoid

Right bone
A, proximal
B, dorsal
C, distal

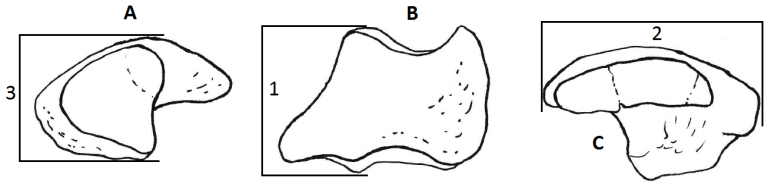

Num.	View	Description
1	dorsal	The biggest height, at the lateral side
2	distal	The biggest breadth
3	proximal	The biggest depth, perpendicular to the medial-lateral axis of the bone

Semilunar

Right bone
A, lateral
B, dorsal

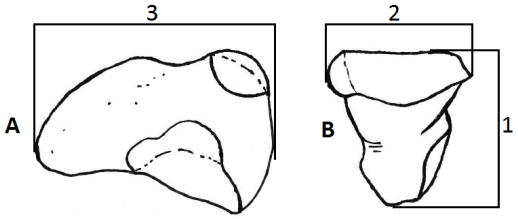

Num.	View	Description
1	dorsal	The biggest height
2	dorsal	The biggest breadth
3	lateral	The biggest depth, parallel to the dorsal-palmar axis of the bone

Pyramidal

Right bone
A, dorsal
B, medial
C, distal

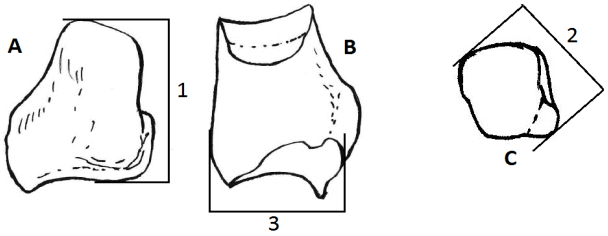

Num.	View	Description
1	very dorsal	Height, at the medial side, not including the distal prominence of the lateral-palmar angle
2	distal	Transversal diameter from the dorsal-lateral bulging to the medial-palmar tubercle
3	medial	Depth, at the distal side, not including the lateral-palmar tubercle

Unciform

Right bone
A, proximal
B, dorsal

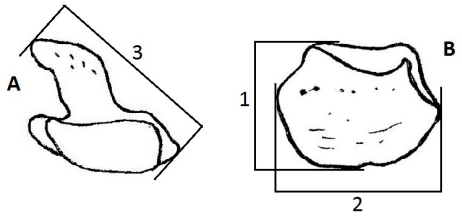

Num.	View	Description
1	dorsal	The biggest height, perpendicular to the medial-lateral axis of the dorsal wall
2	dorsal	The biggest breadth, parallel to the medial-lateral axis of the dorsal wall
3	proximal	Transversal diameter from the medial-dorsal angle to the lateral-palmar prominence

Magnum

Right bone
A, lateral
B, dorsal

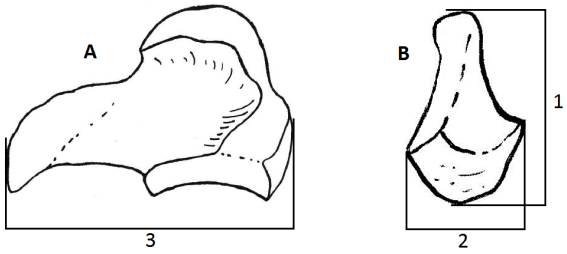

Num.	View	Description
1	lateral	The biggest height, perpendicular to the dorsal-palmar axis of the bone
2	dorsal	The biggest breadth, erpendicular to the proximal-distal axis of the bone
3	lateral	The biggest depth, parallel to the dorsal-palmar axis of the bone

Metacarpal II

Right bone

A, lateral; B, dorsal; C, proximal; D, palmar

Num.	View	Description
1	dorsal	At the lateral side, the biggest length; parallel to the axis of the bone
2P	proximal	The biggest breadth, from the medial tubercle and the baseline connecting the dorsal and palmar prominence at the lateral side
3P	lateral	Proximal depth, perpendicular to the axis of the bone
2AP	proximal	The biggest breadth of the art. surf. for the trapezoid
2D	palmar	Distal maximum breadth
3D	lateral	Distal depth at the middle of the articular head (median crest)
2AD	palmar	The breadth of the articular head

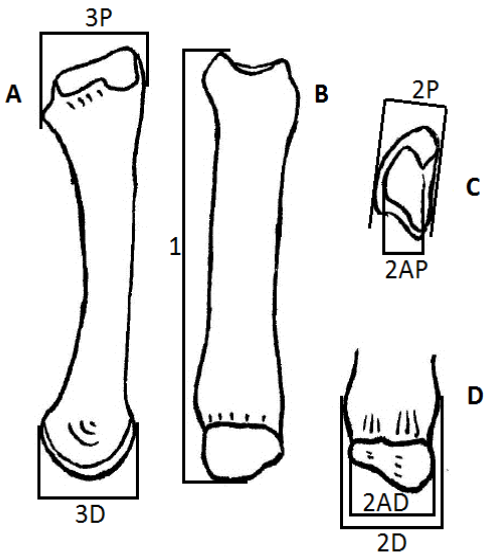

Metacarpal III

Right bone

A, lateral; B, dorsal; C, proximal

Num.	View	Description
1	dorsal	The biggest length at the lateral side, parallel to the axis of the bone
2P	proximal	Proximal breadth, parallel to the dorsal outline as horizontal reference
3P	lateral	Proximal depth, perpendicular to the axis of the bone (it is not perpendicular to 2P!)
2d	dorsal	Breadth of the diaphysis, at the middle of the bone
3d	lateral	Depth of the diaphysis, at the same level of 2d
2D	dorsal	Distal breadth, perpendicular to the axis of the bone
2AD	dorsal	Distal articular breadth at the distal side in the middle of the articular head (it is not always perpendicular to the axis of the bone since the head can be not aligned with the axis)
3D	lateral	Distal depth at the middle of the articular head

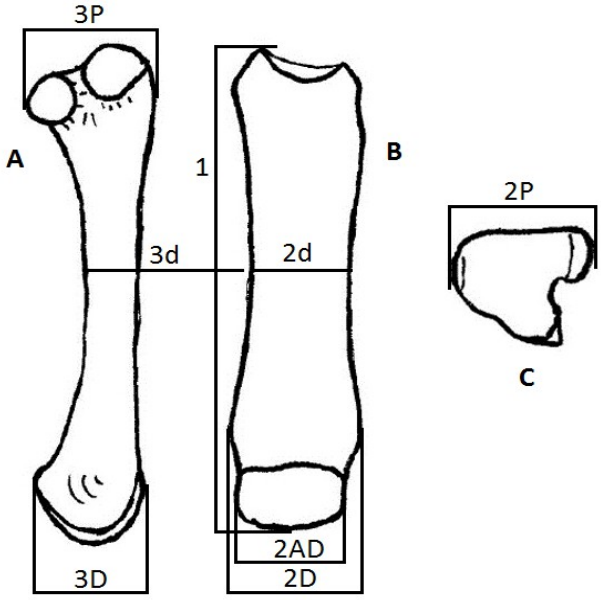

Metacarpal IV

Right bone

A, palmar; B, medial; C, proximal

Num.	View	Description
1	medial	The biggest length at the palmar side, parallel to the axis of the bone
2P	proximal	Proximal breadth at the palmar-lateral side
3P	medial	Proximal depth perpendicular to the axis of the bone (it is not perpendicular to 2P!)
2AD	palmar	Distal articular breadth, the breadth of the articular head
2D	palmar	Distal maximum breadth
3D	medial	Distal depth, at the middle of the articular head (median crest)

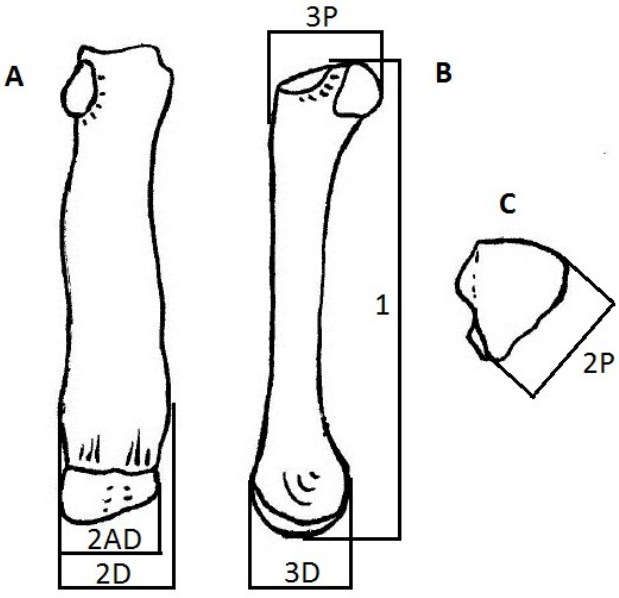

Femur
left bone
A, medial;
B, cranial;
C, lateral

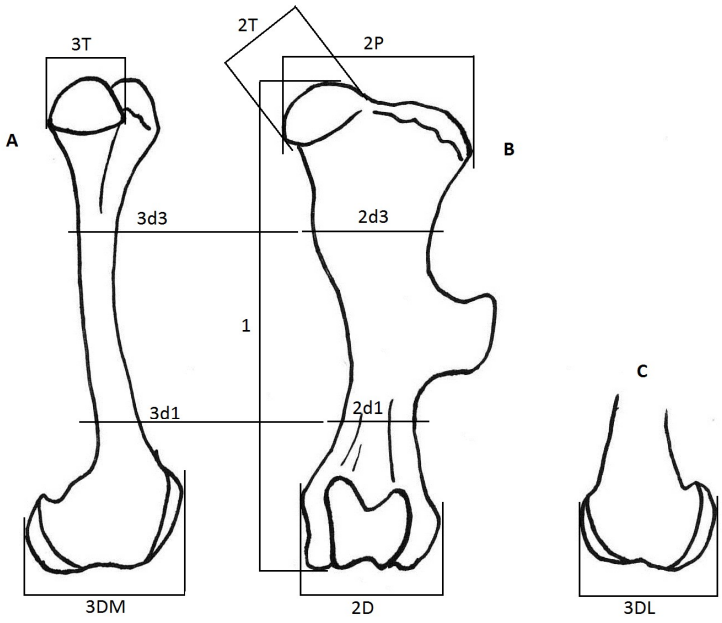

Num.	View	Description
1	cranial	From the top of the articular head to the top of the medial condyle; parallel to the axis of the bone
2P	cranial	The biggest breadth (proximal) perpendicular to the axis of the bone
2d1	cranial	Breadth of the diaphysis, beyond the third trochanter (at the middle, not minimum), perpendicular to the axis of the bone
3d1	medial	Depth of the diaphysis, at the same level of 2d1
2d3	cranial	Breadth of the diaphysis, at the level of the small trochanter, perpendicular to the axis of the bone
3d3	medial	Depth of the diaphysis, at the same level of 2d2
2D	cranial	Distal maximum breadth, perpendicular to the axis of the bone
3DM	medial	The biggest depth (distal), perpendicular to the axis of the bone
3DL	lateral	The biggest depth (distal), perpendicular to the axis of the bone
2T	cranial	Medio-lateral diameter of the head, perpendicular to the axis of the articular head (not that of the bone!)
3T	medial	Cranio-caudal diameter of the head, perpendicular to 2T

Tibia
left bone
A, lateral
B, dorsal
C, plantar
D, section
E, distal

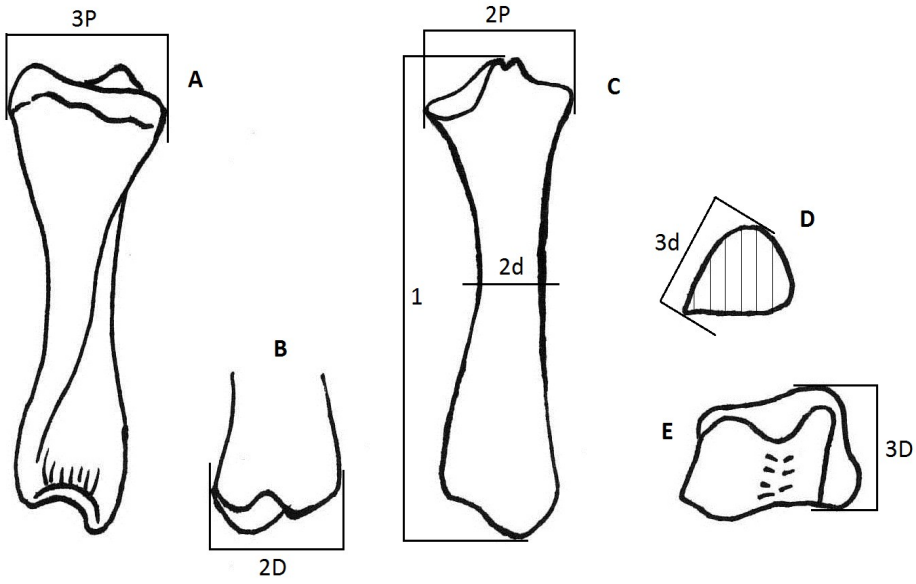

Num.	View	Description
1	plantar	Length, from the top of the top of the lateral intercondyloid prominence to the medial-distal elongation; parallel to the axis of the bone
2P	plantar	The biggest breadth (proximal), perpendicular to the axis of the bone
3P	lateral	The biggest depth (proximal), perpendicular to the axis of the bone (it is not perpendicular to 2P in proximal view)
2d	plantar	Breadth of the diaphysis, at the middle of the diaphysis
3d	lateral-dorsal	Depth of the diaphysis, at the same level of 2d
2D	dorsal	Distal maximum breadth, perpendicular to the axis of the bone
3D	distal	Distal maximum depth, at the medial side, perpendicular to 2D

Astragalus (right bone – A, lateral; B, dorsal; C, medial; D, distal)

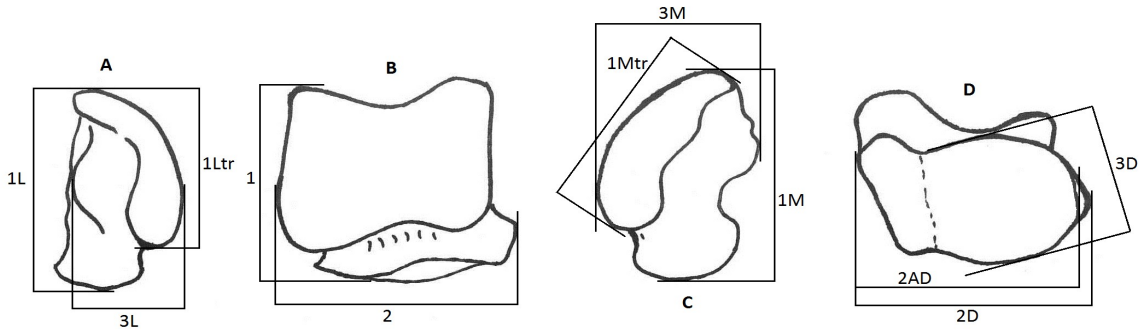

Num.	View	Description
1	dorsal	Height, at the lateral side, from the top of the lateral trochlear lip to the angle between the two distal art. surf.
1M	medial	Medial height, parallel to the proximal-distal axis of the bone
1L	lateral	Lateral height, parallel to the proximal-distal axis of the bone
1Mtr	medial	Trochlear medial height, from the extremities of the trochlear lip (not parallel to the axis of the bone!)
1Ltr	lateral	Trochlear lateral height, Parallel to the proximal-distal axis of the bone
2	dorsal	Breadth at the distal side, parallel to the medial-lateral axis of the bone
3M	medial	Medial depth, at the proximal side, perpendicular to the proximal-distal axis of the bone
3L	lateral	Lateral depth, from the dorsal edge of the lip to the plantar angle of the proximal art. surf. for the calcaneus, perpendicular to the proximal-distal axis of the bone
2D	distal	Distal breadth, from the median tubercle to the dorsal-lateral angle of the art. surf. for the cuboid
2AD	distal	Distal articular breadth, the same of 2D but just articular
3D	distal	Distal depth, at the middle of the art. surf. for the navicular, parallel to its dorsal and plantar edges

Calcaneus (right bone – A, dorsal; B, lateral)

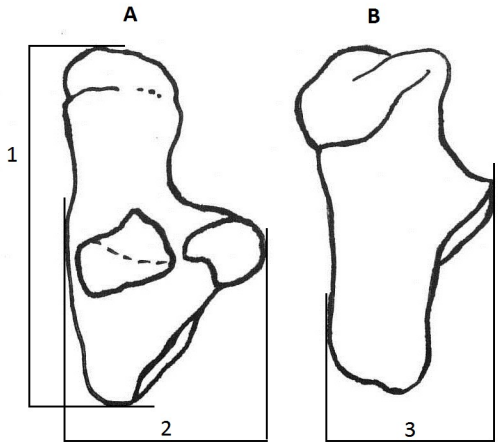

Num.	View	Description
1	dorsal	Height, at the lateral side, parallel to the axis of the bone
2	dorsal	Breadth, at the level of the sustentaculum tali, perpendicular to the axis of the bone
3	lateral	Depth, from the anterior process to the plantar-distal bulging (it is not the biggest depth!), perpendicular to the axis of the bone

Cuboid (right bone – A, dorsal; B, medial)

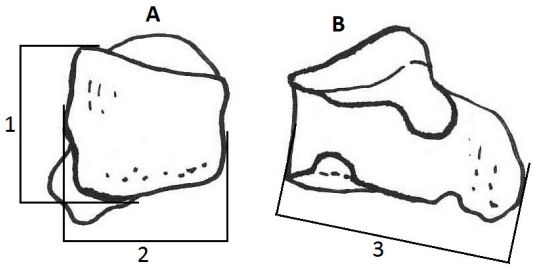

Num.	View	Description
1	dorsal	The biggest height of the dorsal wall, parallel to the proximal-distal axis
2	dorsal	The biggest breadth of the dorsal wall, perpendicular to the proximal-distal axis
3	medial	The biggest depth, parallel to the dorsal-plantar axis

Navicular (right bone – A, proximal; B, medial)

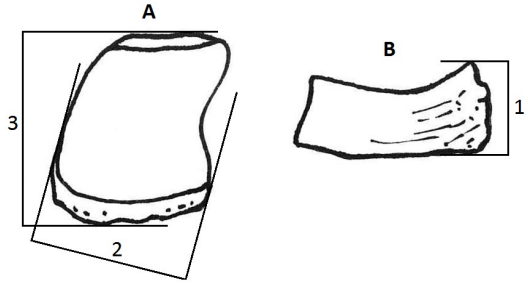

Num.	View	Description
1	medial	Height at the plantar side, perpendicular to the dorsal-plantar axis
2	proximal	Breadth at the plantar side, considering the medial edge as horizontal reference
3	proximal	Depth at the medial side, considering the dorsal edge as horizontal reference

Metatarsal II

Right bone

A, lateral; B, dorsal; C, proximal; D, plantar

Num.	View	Description
1	lateral	At the dorsal side, the biggest length; parallel to the axis of the bone
2P	proximal	Proximal maximum breadth, considering the baseline connecting the dorsal and palmar prominence at the lateral side
3P	lateral	Proximal depth, at the proximal side, perpendicular to the axis of the bone
2D	palmar	Distal maximum breadth
2AD	dorsal	Distal articular breadth, at the middle of the articular head
3D	lateral	Distal depth, at the middle of the articular head (median crest)

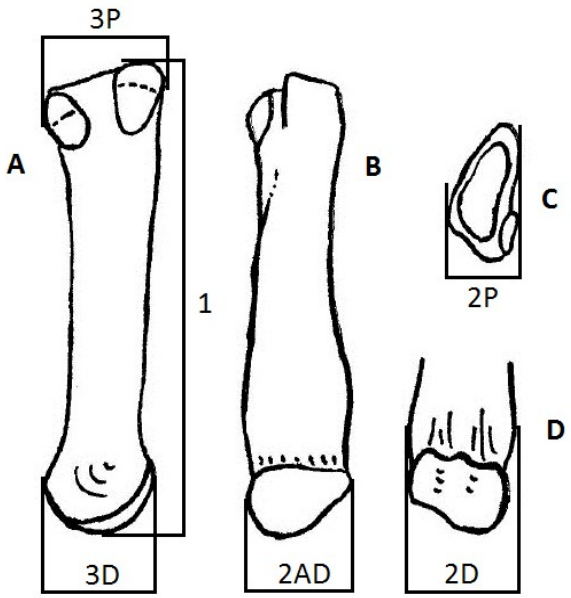

Metatarsal III

Right bone

A, lateral; B, dorsal; C, proximal

Num.	View	Description
1	dorsal	The biggest length at the lateral side, parallel to the axis of the bone
2P	proximal	Proximal breadth, parallel to the dorsal outline as horizontal reference
3P	proximal	Proximal depth, At the lateral side, perpendicular to 2P
2d	dorsal	Breadth of the diaphysis, at the middle of the bone
3d	lateral	Depth of the diaphysis, at the same level of 2d
2D	dorsal	Distal breadth, perpendicular to the axis of the bone
2AD	distal	Distal articular breadth, at the middle of the articular head
3D	lateral	Distal depth, at the middle of the articular head

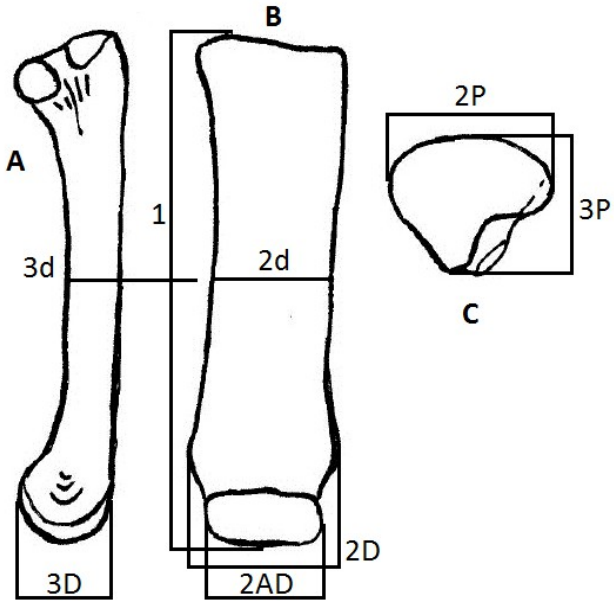

Metatarsal IV

Right bone

A, medial; B, plantar; C, proximal

Num.	View	Description
1	medial	The biggest length at the palmar side, parallel to the axis of the bone
2P	proximal	Proximal breadth, at the plantar side, perpendicular to medial plan (often given by the plantar facet for the MtIII)
3P	proximal	Proximal depth, at the middle of the art. surf., perpendicular to 2P
2AD	palmar	Distal articular breadth, the breadth of the articular head
3D	medial	Distal depth, at the middle of the articular head (median crest)

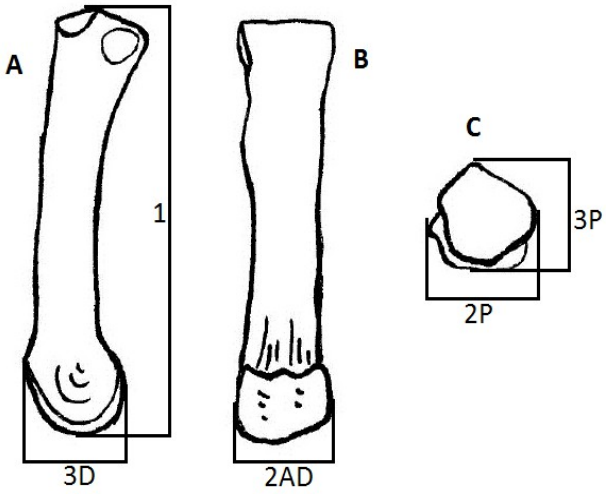

Attachment V - Metric raw data of *Stephanorhinus hundsheimensis*. Measure with a dot are not precise (e.g. missing or deteriorated periostium).

IPW=Institute for Palaeontology University of Wien
IQW=Institute for Quaternary Palaeontology Weimar
MNHM=Naturhistorisches Museum Mainz
MNHN=Muséum National d'Histoire Naturelle de Paris
MPI=Museo del Paleolitico Isernia
MPLB=Museo Paleontologico Luigi Boldrini Pietrafitta
MPPL=Museo Paleontologico Piero Leonardi Ferrara
NHM=Natural History Museum London
NHMW=Naturhistorisches Museum Wien
SMNK=Staatliches Museum für Naturkunde Karlsruhe

Humerus			**1**	**1F**	**2D**	**2d**	**3D**	**3d**	**2H**	**3H**	**1Mtr**	**1Ltr**	**2tr**
SMNK MS 0266	L		409	365	131	62	114	61	95	85	89	65	98
SMNK MS 0261	L		434	385	137	67	121	70	99	85	93	70	102
SMNK MS 0359	R		-	-	152	74	125	66	-	-	93	73	98
SMNK MS 0360	R		-	-	-	66	111	63	-	-	-	-	-
SMNK MS 0366	L		-	-	137	65	113	65	-	-	88	67	96
SMNK MS 0361	L		-	-	-	68	115	67	-	-	91	-	-
SMNK MS 0367	R		-	-	138	65	118	-	-	-	90	67	95
MNHM 1975/264	L		-	-	-	-	-	-	92	81	-	-	-
MNHM 1957/206	R		-	-	129	70	116	64	-	-	95	74	103
MNHM 1955/1109	R		-	-	-	-	-	-	90	85	-	-	-
IQW 1966/7415 (Voi.3280)	L		390	370	138	66	114	61	100	83	92	70	103
IQW 1966/5841 (Voi.3279)	R	young	365	350	130	58	111	58	>90	85	92	61	96
IQW 1966/7438 (Voi.738)	L		-	-	.132	66	.117	59	-	-	93	65	.90
IQW 1966/5615 (Voi.713)	R	young	-	-	134	63	.116	64	-	-	95	70	.98
IQW 1964/665 (Süß. 194/52)	R		-	-	146	66	125	65	-	-	92	73	95
IQW 1980/15362 (Mei.14874)	R		>375	360	125	60	108	59	90	81	83	58	>83
IQW 1980/16117 (Mei.15628)	L		-	-	128	62	115	60	-	-	88	63	92
IQW 1980/16170 (Mei.15680)	L		-	-	134	61	116	59	-	-	91	68	.92
IQW 1980/16122 (Mei.15633)	L		-	-	128	-	116	-	-	-	90	66	97
IQW 1980/15219 (Mei.14701)	R	young	>355	340	130	56	108	56	87	77	85	63	92
IQW 1985/20386 (Mei.19906)	R	young	-	-	126	61	110	60	-	-	88	68	91
IQW 1981/17715 (Mei.17237)	R		-	-	137	63	117	65	-	-	91	71	98
IQW 1982/17795 (Mei.17315)	L		-	-	128	60	115	60	-	-	91	68	96
IQW 1988/22801 (Mei.22320)	L		-	-	137	63	118	65	-	-	93	70	94
IQW 1996/25703 (Mei.25232)	R		-	-	136	67	116	63	-	-	87	64	97
MPLB #021	R		390	335	113	56	102	52	76	75	75	55	85
MNHN SPR 130	L		>360	335	121	60	98	57	76	73	81	60	82
NHM M 17841	R		-	-	.135	-	>96	-	-	-	96	71	104
NHM M 17228	R		>280	-	>120	62	>100	52	-	-	92	-	-
NHM M 17843	R		>320	-	>122	60	107	55	-	-	92	.70	>85
NHM 1147	R		-	-	132	62	109	56	-	-	85	67	93
NHM 509	R		-	-	-	62	114	60	-	-	93	-	95
NHMW 2013/0282/0001	R		420	355	130	68	115	59	96	85	93	71	102

NHMW 2013/0282/0001	L		-	350	-	68	116	60	93	82	93	72	104
Radius			**1**	**2P**	**2AD**	**2d**	**3P**	**3d**		**2P/3P**	**2d/2P**		
SMNK MS 0349	L		375	95	.69	41	61	46		1,56	0,43		
SMNK MS 0698	R		383	100	76	42	59	46		1,69	0,42		
SMNK MS 0347	R		-	-	76	-	-	-					
SMNK MS 1477	L		-	-	77	-	-	-					
SMNK MS 0350	R		-	94	-	42	59	42		1,59	0,45		
SMNK MS 0370	R		-	96	-	-	62	-		1,55			
SMNK MS 0804	L		-	100	-	-	59	-		1,69			
SMNK MS 5021	R		-	100	-	-	66	-		1,52			
MNHM 1963/573	R		400	97	73	43	61	45		1,59	0,44		
MNHM 1958/216	R		365	91	69	39	59	42		1,54	0,43		
MNHM 1958/631	L		-	-	72	-	-	-					
IQW 1966/7415 (Voi.3280)	R		398	102	78	45	67	44		1,52	0,44		
IQW 1966/7415 (Voi.3280)	L		395	101	79	44	65	45		1,55	0,44		
IQW 1966/7416 (Voi.3279)	R	young	390	98	78	41	63	40		1,56	0,42		
IQW 1966/5861 (Voi.1116)	R	young	>350	95	-	45	65	41		1,46	0,47		
IQW 1966/5693 (Voi.63)	R		425	108	84	55	66	48		1,64	0,51		
IQW 1966/5692 (Voi.64)	L		420	108	82	-	70	50		1,54			
IQW 1964/333 (Süß.9138)	R		422	100	79	45	67	47		1,49	0,45		
IQW 1980/15866 (Mei.15377)	L		400	107	89	48	72	44		1,49	0,45		
IQW 1980/15803 (Mei.15314)	R		-	98	-	38	66	41		1,48	0,39		
IQW 1980/17475 (Mei.16997)	L		375	90	71	38	62	40		1,45	0,42		
IQW 1985/20616 (Mei.20135)	L		375	92	72	37	60	39		1,53	0,40		
IQW 1990/23580 (Mei.23109)	L		371	98	79	44	68	44		1,44	0,45		
IQW 1989/23388 (Mei.22907)	L	young	375	.92	79	40	>60	43					
IQW 1983/19230 (Mei.18750)	R		400	-	76	43	73	45					
IQW 1948/20293 (Mei.19813)	R	young	420	94	76	40	62	44		1,52	0,43		
IQW 1980/17397 (Mei.16919)	L		412	103	84	43	70	47		1,47	0,42		
IQW 1989/23390 (Mei.22909)	L		.388	96	.79	46	60	42		1,60	0,48		
IQW 1986/21748 (Mei.21267)	L		-	93	-	41	65	44		1,43	0,44		
IQW 1989/23350 (Mei.22869)	L	young	-	100	-	41	63	37		1,59	0,41		
MPLB #022	L		350	87	69	43	55	40		1,58	0,49		
MNHN SPR 129	L		362	80	68	42	55	38		1,45	0,53		
NHM M 7054	R		>320	110	-	47	68	48		1,62	0,43		
NHM M 17840	R		>190	100	-	.48	68	.50		1,47			
NHM M 12830	R		>210	88	-	45	62	40		1,42	0,51		
NHM M 19236	L		>250	.90	-	40	.58	48					
NHM M 17844	R		>250	95	-	42	62	49		1,53	0,44		
NHM M 17845	R		.395	.92	-	41	.57	47					
NHMW 2013/0282/0001	R		390	104	78	47	66	47		1,58	0,45		
NHMW 2013/0282/0001	L		390	105	77	47	67	47		1,57	0,45		
NHMW 1909II.540	L			>93	74		62						
NHMW 1909II.541	R				76								
IPW C38	R		373	95	73	45	66	42		1,44	0,47		
IPW no num	L		390	-	77	51	-	46					

IPW "R"	R		>290	-	75	-	-	-					
Ulna			**1**	**1AP**	**2AP**	**2AD**	**2d**	**3AD**	**3d**				
SMNK MS 0610	R		-	63	76	-	34	-	35				
IQW 1966/7415 (Voi.3280)	L		500	72	84	35	41	63	43				
IQW 1966/7416 (Voi.3279)	R	young	>485			35	45	63	39				
IQW 1966/5613 (Voi.195)	R		535	74	85	39	53	70	41				
IQW 1966/5855 (Voi.460)	R	young	-	68	86	-	45	-	42				
IQW 1966/5605 (Voi.560)	R		-	-	-	36	-	68	-				
IQW 1966/3476 (Voi.66)	L		-	-	-	39	-	72	-				
IQW 1964/334 (Süß.9139)	R		>48	68	85	38	51	70	44				
IQW 1980/16105 (Mei.15616)	L		>460	70	89	39	51	61	41				
IQW 1980/15802 (Mei.15313)	R		-	73	83	-	45	-	41				
IQW 1980/15776 (Mei.15288)	L		-		82	-	46	-	41				
IQW 1980/17479 (Mei.17001)	L		472	62	76	30	37	54	35				
IQW 1985/20617 (Mei.20136)	L		>450	62	79	32	40	59	44				
IQW 1989/23253 (Mei.22772)	L		510	65	91	35	41	62	39				
IQW 1984/20294 (Mei.19814)	R	young	>500	67	82	35	42	.62	41				
IQW 1990/23609 (Mei.23138)	L		470	69	84	38	37	62	38				
MPLB #023	L		460	61	69	32	38	58	40				
NHM F 412	R		-	71	78	-	40	-	46				
NHMW 2013/0282/0001	R		490	71	82	37	-	71	46				
NHMW 2013/0282/0001	L		480	73	82	.36	46	71	46				
Scaphoid			**1**	**2**	**3**								
SMNK MS 0249	L		62	-	52								
SMNK MS 1201	R		66	82	50								
SMNK MS 1336	L		67	82	52								
SMNK MS 1338	R		-	78	49								
SMNK MS 1337	R		66	79	53								
MNHM 1953/269	L		61	81	46								
MNHM 1955/1366	L		62	75	47								
MNHM 1955/154	R		61	78	51								
MNHM 1956/285	R		63	79	54								
IQW 1966/7415 (Voi.3280)	R		69	86	57								
IQW 1966/7415 (Voi.3280)	L		69	88	59								
IQW 1966/7416 (Voi.3279)	R	young	66	81	55								
IQW 1966/7248 (Voi.3351)	L		66	88	58								
IQW 1965/3908 (Voi.240)	R		71	89	59								
IQW 1964/344 (Süß.9149)	L		67	86	51								
IQW 1986/21139 (Mei.20658)	L		55	74	50								
IQW 1990/23521 (Mei.23050)	R	young	60	73	42								
IQW 1989/23220 (Mei.22739)	R		69	78	59								
IQW 1984/20291 (Mei.19811)	R	young	>61	83	56								
IQW 1990/23560 (Mei.23089)	L		69	87	59								
IQW 1988/22591 (Mei.22110)	R		73	85	60								
IQW 1987/22080 (Mei.21599)	L		69	79	56								
IQW 1997/26380 (Mei.25909)	R		66	82	56								
MNHN Sol 118	L		57	73	49								

MNHN Sol 117	R		57	78	44								
NHM M 19519	R		57	83	55								
NHMW 2013/0282/0001	R		66	-	51								
NHMW 2013/0282/0001	L		65	85	53								
NHMW 1909II.543	L		63	81	49								
IPW no num.	R		63	80	49								
IPW A104	R		65	-	47								
IPW C165	L		60	82	45								
IPW no num.	L		58	79	49								
IPW C104	L		63	84	49								
IPW C8	L		62	80	42								
Semilunar			**1**	**2**	**3**								
SMNK MS 1331	L		58	50	71								
SMNK MS 1330	R		.54	.50	72								
MNHM 1961/593	R		49	49	69								
MNHM 1967/76	R		50	52	72								
MNHM 1955/518	R		50	53	69								
MNHM 1966/173	R		51	-	69								
MPPL 53.4	L		53	>50	72								
IQW 1966/7415 (Voi.3280)	R		52	55	72								
IQW 1966/7416 (Voi.3279)	R	young	51	52	72								
IQW 1965/2175 (Süß.9503)	R		.46	.41	.68								
IQW 1980/15497 (Mei.15009)	R		57	56	68								
IQW 1985/20744 (Mei.20263)	L		48	48	63								
IQW 1990/23575 (Mei.23104)	R	young	49	-	62								
IQW 1989/23183 (Mei.22702)	L		56	54	70								
IQW 1988/22592 (Mei.22111)	R		56	52	70								
IQW 1983/19249 (Mei.18769)	R		51	54	69								
IQW 1990/24880 (Mei.24419)	R		55	55	69								
MNHN Sol 95	L		46	47	61								
NHM M 18158	R		48	51	66								
NHMW 2013/0282/0001	R		55	55	73								
NHMW 2013/0282/0001	L		54	55	73								
IPW C167	R		53	.48	71								
IPW no num.	R		53	50	67								
IPW A3	L		50	48	67								
IPW C122	L		50	53	65								
IPW C107	L		52	.51	72								
Pyramidal			**1**	**2**	**3**								
SMNK MS 1187	R		50	54	36								
SMNK MS 0791	R		58	56	38								
MNHM 1957/651	L		51	53	36								
MNHM 1955/789	L		48	51	34								
IQW 1966/7415 (Voi.3280)	R		60	57	36								
IQW 1966/7416 (Voi.3279)	R	young	58	56	43								
IQW 1965/3830 (Voi.977)	L		59	57	40								
MPPL 326	L		52	57	40								

IQW 1980/16736 (Mei.16257)	L		52	58	40								
IQW 1980/16737 (Mei.16737)	L		57	60	42								
IQW 1980/16971 (Mei.16492)	L		50	53	38								
IQW 1985/20742 (Mei.20261)	L		47	50	35								
IQW 1990/23495 (Mei.23014)	L	young	48	49	35								
IQW 1984/20287 (Mei.19807)	R	young	50	55	42								
MNHN Sol 114	L		42	46	39								
MNHN Sol 116	L		48	51	39								
NHM F 30087	L		49	55	37								
NHMW 2013/0282/0001	R		54	60	38								
NHMW 2013/0282/0001	L		53	57	40								
NHMW 1909II.544	R		55	58	39								
NHMW 1909II.544	R		51	55	37								
NHMW 1909II.545	L		45	56	40								
NHMW 1909II.553	L		45	.49	-								
IPW A107	R		53	52	42								
IPW no num.	R		51	54	40								
IPW B1	L		54	55	39								
IPW C24	L		51	53	39								
Unciform			**1**	**2**	**3**								
SMNK MS 1335	R		51	71	-								
SMNK MS 0738	L		52	66	-								
SMNK MS 1327	R		55	67	89								
SMNK MS 1325	R		52	63	94								
SMNK MS 1324	L		53	66	89								
SMNK MS 1326	L		47	61	-								
MNHM 1958/277	L		53	71	-								
MNHM 1956/314	L		44	61	77								
MNHM 1954/80	L		53	71	83								
MNHM 1962/216	R		51	69	89								
MNHM 1955/316	R		53	63	80								
MPI 787	R		53	66	90								
IQW 1966/7415 (Voi.3280)	R		59	71	94								
IQW 1966/7416 (Voi.3279)	R	young	60	72	87								
IQW 1965/3911 (Voi.1565)	L		61	70	90								
IQW 1965/3918 (Voi.3288)	L		57	75	95								
IQW 1964/343 (Süß.9148)	L		58	73	93								
IQW 1980/15683 (Mei.15195)	L		57	74	95								
IQW 1980/16593 (Mei.16114)	L		55	68	94								
IQW 1985/20745 (Mei.20264)	L		50	62	-								
IQW 1992/23998 (Mei.23527)	R	young	52	61	74								
IQW 1990/23620 (Mei.23149)	L	young	52	61	72								
IQW 1984/20289 (Mei.19809)	R	young	54	66	86								
IQW 1990/23421 (Mei.22940)	L		54	69	93								
IQW 1988/22578 (Mei.22097)	R		59	75	91								
IQW 1982/18245 (Mei.17766)	R		59	70	-								
IQW 1997/26006 (Mei.25535)	L		55	68	-								

MNHN Sol 111	L		47	62	75								
NHM M 18155	R		55	69	90								
NHM M 17832	R		53	68	-								
NHM F 30930	L		54	73	97								
NHMW 2013/0282/0001	R		56	76	93								
NHMW 2013/0282/0001	L		55	75	-								
NHMW 1909II.548	R		50	72	-								
NHMW 1909II.548	L		51	68	-								
IPW C167	R		55	72	91								
IPW no num.	R		54	69	87								
IPW C157	L		57	72	-								
Magnum			**1**	**2**	**3**								
SMNK MS 1194	R		69	50	-								
SMNK MS 1332	R		67	47	-								
SMNK MS 1176	R		-	-	-								
SMNK MS 1196	R		69	51	94								
SMNK MS 1192	R		65	43	-								
SMNK MS 1197	L		.62	.44	-								
SMNK MS 1195	L		-	46	93								
MNHM 1954/466	L		66	46	91								
MNHM 1959/742	L		67	49	95								
MPI 66.50	R		72	47	-								
MPPL 50.366	R		.58	>41	>90								
MPPL 365	R		65	45	-								
IQW 1966/7415 (Voi.3280)	R		68	47	99								
IQW 1966/7416 (Voi.3279)	R	young	67	50	98								
IQW 1965/3915 (Voi.569)	R		68	46	110								
IQW 1964/662 (Süß.7762)	R		67	50	95								
IQW 1964/661 (Süß.7702)	L		66	47	-								
IQW 1980/15403 (Mei.14915)	L		70	52	93								
IQW 1990/23509 (Mei.23028)	L	young	60	42	79								
IQW 1989/23204 (Mei.22723)	L		62	47	99								
IQW 1990/23616 (Mei.23145)	L		69	49	109								
IQW 1980/15632 (Mei.15144)	R		72	50	103								
MNHN Sol 110	L		60	45	85								
NHM M 19521	L		64	45	94								
NHM M 19520	R		>62	>38	>80								
NHM 429	L		66	53	92								
NHM F 7283	L		67	50	100								
NHM F 5268	L		64	49	99								
NHMW 2013/0282/0001	R		74	54	-								
NHMW 2013/0282/0001	L		73	54	>88								
NHMW 1909II.547	L		67	50	92								
IPW C16	R		67	48	98								
IPW A103	R		66	47	-								
IPW C154	L		67	52	-								
McII			**1**	**2P**	**2AP**	**2D**	**2AD**	**3P**	**3D**		**1/2P**		

SMNK MS 1173	L		-	36	26	-	-	47	-				
SMNK MS 1167	R		-	31	25	-	-	45	-				
MNHM 1961/119	L		173	42	26	43	32	47	41		4,12		
IQW 1966/7415 (Voi.3280)	R		196	44	28	49	41	52	43		4,45		
IQW 1966/7415 (Voi.3280)	L		197	45	29	48	39	52	43		4,38		
IQW 1966/7416 (Voi.3279)	R	young	196	37	26	43	35	50	41		5,30		
IQW 1965/3921 (Voi.220)	L		220	41	31	47	38	51	45		5,37		
IQW 1965/3831 (Voi.745)	L		-	.40	31	-	-	48	-				
IQW 1964/655 (Süß.R1)	R		188	.35	26	44	.35	.43	38				
IQW 1964/350 (Süß.9155)	L		-	43	29	-	-	50	-				
IQW 1980/15882 (Mei.15393)	R		175	46	25	41	34	46	38		3,80		
IQW 1980/17440 (Mei.16962)	L		193	47	27	47	39	47	41		4,11		
IQW 1985/20740 (Mei.20259)	L		-	47	27	-	-	43	-				
IQW 1990/23491 (Mei.23010)	L	young	-	39	26	-	-	40	-				
IQW 1980/16003 (Mei.15514)	R	young	-	43	28	-	-	42	-				
IQW 1984/20285 (Mei.19805)	R	young	-	49	30	-	-	45	-				
IQW 1992/23918 (Mei.23447)	L		184	54	30	51	38	50	43		3,41		
IQW 1980/15469 (Mei.14981)	R		189	54	29	50	38	50	44		3,50		
IQW 1989/23389 (Mei.22908)	L		189	56	30	-	-	-	-		3,38		
MPLB #020	L		>130	29	23	-	-	40	-				
MNHN Sol 123	L		172	34	-	46	36	46	39		5,06		
NHM M 19517	R		194	40	30	47	35	50	41		4,85		
NHM M 19515	R		-	38	26	-	-	44	-				
NHM M 6675	R		>175	-	-	46	35	-	44				
NHM M 19516	R		-	39	29	-	-	44	-				
NHMW 2013/0282/0001	R		190	43	31	47	39	50	44		4,42		
NHMW 2013/0282/0001	L		190	42	31	48	40	49	44		4,52		
IPW A109	L		188	37	27	43	35	50	42		5,08		
IPW C57	L		177	.34	27	43	33	.45	42				
IPW C157	L		-	40	28	-	-	48	-				
IPW C159	R		-	37	28	-	-	51	-				
IPW no num.	R		190	37	27	43	35	47	42		5,14		
McIII			**1**	**2P**	**2d**	**2D**	**2AD**	**3P**	**3d**	**3D**			
SMNK MS 1475	L		209	54	47	.56	49	47	20	47			
SMNK MS 0236	R		220	59	57	70	56	57	26	51			
SMNK MS 1544	R		203	.53	53	59	50	.44	20	47			
SMNK MS 1543	L		-	.57	56	64	52	55	22	48			
MNHM 1956/28	L		198	.52	51	.62	49	47	25	44			
MNHM 1963/518	L		211	.51	47	.53	43	49	23	42			
MNHM 1959/791	L		-	.54	49	-	-	.45	23	-			
MNHM 1962/931	L		-	56	-	-	-	46	-	-			
IQW 1966/7415 (Voi.3280)	R		220	57	56	65	52	51	22	45			
IQW 1966/7415 (Voi.3280)	L		217	58	58	64	51	53	23	48			
IQW 1966/7416 (Voi.3279)	R	young	221	62	57	69	51	52	22	47			
IQW 1966/7244 (Voi.3377)	R		-	62	-	-	-	50	-	-			
IQW 1965/3823 (Voi.765)	R		-	64	50	-	-	54	22	-			
IQW 1965/3777 (Voi.1173)	R		-	61	-	-	-	53	-	-			

IQW 1964/656 (Süß.7716)	L		-	59	-	-	-	52	-	-			
IQW 1980/15581 (Mei.15093)	R		-	57	-	-	-	52	-	-			
IQW 1980/16503 (Mei.16024)	R		215	60	55	65	55	54	23	50			
IQW 1980/15412 (Mei.14924)	L		216	66	51	.61	52	52	24	46			
IQW 1985/20738 (Mei.20257)	L		200	55	49	54	49	49	23	44			
IQW 1980/17452 (Mei.16974)	L		213	55	47	53	46	49	20	41			
IQW 1990/23655 (Mei.23184)	R	young	-	52	39	-	-	44	19	-			
IQW 1989/23313 (Mei.22832)	L		221	60	52	60	54	53	23	47			
IQW 1980/15850 (Mei.15361)	R	young	-	56	45	-	-	48	22	-			
IQW 1984/20283 (Mei.19803)	R	young	-	56	55	-	-	48	25	-			
IQW 1990/23514 (Mei.23043)	L		204	58	54	58	52	53	23	47			
IQW 1990/23496 (Mei.23015)	L	young	-	60	52	-	-	51	23	-			
IQW 1982/18202 (Mei.17722)	R		-	59	50	-	-	54	24	-			
IQW 1980/15801 (Mei.15312)	R		-	70	58	-	-	57	28	-			
IQW 1980/16389 (Mei.15900)	R		-	56	56	-	-	50	21	-			
IQW 1987/21976 (Mei.21496)	R		-	61	56	-	-	57	22	-			
MPLB #018	R		192	50	47	.60	46	45	.17	42			
MNHN Sol 122	L		195	53	46	54	43	48	20	43			
NHM M 6682	R		>185	>53	53	-	-	>43	22	-			
NHM M 17829	R		-	-	-	55	48	-	-	43			
NHM M 17826	L		>155	51	53	-	-	44	21	-			
NHMW 2013/0282/0001	R		215	62	62	50	54	24	51	51			
NHMW 2013/0282/0001	L		213	62	-	51	54	23	51	51			
NHMW 1909II.549	R		-	.59	-	-	.48	-	-	-			
NHMW 1909II.550	L		-	60	-	-	51	-	-	-			
IPW no num.	L		202	61	56	46	50	23	45	45			
IPW C77	R		209	60	57	-	.44	23	.46	.46			
IPW C57	L		-	.55	-	-	.49	-	-	-			
McIV			**1**	**2P**	**2D**	**2AD**	**3P**	**3D**					
SMNK MS 0247	L		175	50	45	39	45	47					
SMNK MS 5046	L		179	49	49	38	44	.39					
SMNK MS 1545	L		184	-	54	43	.41	45					
SMNK MS 0238	L		178	.47	50	35	.39	40					
MNHM 1959/555	L		165	-	-	36	.40	40					
MNHM 1957/121	L		172	-	44	38	42	38					
MNHM 1959/195	L		177	43	47	37	42	41					
IQW 1966/7415 (Voi.3280)	R		180	51	46	40	45	43					
IQW 1966/7415 (Voi.3280)	L		182	53	48	40	45	44					
IQW 1966/7416 (Voi.3279)	R	young	186	49	45	39	47	45					
IQW 1965/3774 (Voi.202)	R		187	50	46	41	48	47					
IQW 1964/654 (Süß.7707)	L		-	50	-	-	46	-					
IQW 1980/15687 (Mei.15199)	L		-	51	-	-	46	-					
IQW 1980/15733 (Mei.15245)	L		-	52	-	-	48	-					
IQW 1980/16186 (Mei.15697)	R		-	48	-	-	42	-					
IQW 1980/17118 (Mei.16639)	L		177	47	-	36	41	41					
IQW 1980/15413 (Mei.14925)	L		177	47	43	42	44	43					
IQW 1985/20739 (Mei.20258)	L		164	44	41	39	43	41					

IQW 1982/17954 (Mei.17474)	L		187	48	46	41	42	42					
IQW 1990/23702 (Mei.23231)	R	young		40		-	39	-					
IQW 1983/19030 (Mei.18550)	R		177	45	42	38	43	40					
IQW 1980/12849 (Mei.15360)	R	young		44		-	43	-					
IQW 1984/20284 (Mei.19804)	R	young		47		-	42	-					
IQW 1990/23612 (Mei.23141)	L		166	51	47	41	45	44					
IQW 1990/23497 (Mei.23016)	L	young	-	50	-	-	>43	-					
IQW 1982/18079 (Mei.17599)	R		-	46	-	-	45	-					
MPLB #019	R		153	41	40	36	>33	35					
MNHN Sol 124	L		160	42	43	36	>35	38					
NHM M 19511	R		168	49	42	36	44	42					
NHMW 2013/0282/0001	R		182	-	49	-	49	45					
NHMW 2013/0282/0001	L		182	51	48	40	50	45					
IPW C153	R		168	49	44	39	.42	.38					
IPW no num.	L		-	48	-	-	45	-					
IPW C169	R		-	50	-	-	48	-					
Femur			**1**	**2P**	**2D**	**2d1**	**2d3**	**2T**	**3DM**	**3DL**	**3d1**	**3d3**	**3T**
SMNK MS 0265	L		490	-	148	73	122	85	160	130	58	48	83
SMNK MS 1457	R		460	165	137	65	106	90	159	130	57	50	88
SMNK MS 1469	L		.485	165	-	-	101	84	.153	125	-	46	83
SMNK MS 0375	R		.400	-	-	75	119	88	-	-	59	39	87
SMNK MS 0377	L		.360	-	-	69	115	-	-	-	59	47	-
IQW 1966/7415 (Voi.3280)	R		-	-	140	-	-	-	158	.127	-	-	-
IQW 1966/7415 (Voi.3280)	L		-	-	141	-	-	-	162	130	-	-	-
IQW 1966/7416 (Voi.3279)	R	young	465	>165	130	68	98	85	-	130	50	46	83
IQW 1966/7416 (Voi.3279)	L	young	460	>156	132	65	100	85	-	135	51	49	81
IQW 1964/911 (Süß.9229)	L		470	-	>118	65	93	82	-	-	53	49	81
IQW 1980/16430 (Mei.15941)	R		498	-	.133	68	107	93	-	131	54	47	86
IQW 1980/16047 (Mei.15558)	R		500	185	140	69	102	89	162	130	61	44	88
IQW 1980/16049 (Mei.15560)	L		500	.180	143	69	105	-	162	131	54	43	-
IQW 1981/17748 (Mei.17269)	L		495	-	141	65	-	92	162	-	57	43	86
IQW 1989/23860 (Mei.22771)	L	young	-	-	139	-	-	-	159	124	-	-	-
IQW 1990/23680 (Mei.23209)	R		510	193	145	74	118	91	164	130	55	43	86
IQW 1995/25326 (Mei.24855)	L		513	.190	146	64	105	94	170	141	58	45	93
MPLB #001	R		435	.162	.125	62	102	75	.130	-	44	32	68
MPLB #002	L		435	.165	124	64	-	75	.133	-	47	42	70
MPLB #003	L		-	-	-	68	103	-	-	-	46	35	-
MPLB #004	L		-	.150	115	54	87	-	-	-	45	32	-
MPLB #005	R		-	-	-	-	-	72	-	-	-	-	69
NHMW 2013/0282/0001	R		490	185	140	67	103	88	170	137	55	43	88
NHMW 2013/0282/0001	L		490	185	139	67	103	88	170	138	55	44	86
NHMW no num.	R		-	-	-	61	-	85	-	-	-	38	78
NHMW no num.	L		-	180	-	61	110	83	-	-	-	38	78
IPW no num.	R	young	475	175	-	65	103	85	-	-	50	42	84
IPW no num.	L	young	478	180	130	63	103	85	-	-	50	43	84
Tibia			**1**	**2P**	**2D**	**2d**	**3P**	**3D**	**3d**				
SMNK MS 0381	R		383	.118	.92	55	.98	71	52				

SMNK MS 0391	L		385	122	94	54	-	72	54				
SMNK MS 1470	L				-	55	112	-	57				
SMNK MS 0262	L		405	125	.100	60	130	71	60				
SMNK MS 0263	L		-	121	103	-	116	71	-				
SMNK MS 0834	R		-	-	-	55	-	-	61				
SMNK MS 0382	R		-	-	.95	55	-	69	61				
SMNK MS 0392	R		-	-	.95	54	-	70	60				
SMNK MS 0389	R		-	-	.100	52	-	-	61				
SMNK MS 0398	L		-	-	94	-	-	65	-				
MNHM 1956/648	L		360	111	89	51	-	69	48				
MNHM 1956/601	R		357	117	95	53	113	70	55				
MNHM 1970/171	R		-	117	-	-	.122	-	-				
IQW 1966/7415 (Voi.3280)	R		388	130	104	60	128	73	58				
IQW 1966/7415 (Voi.3280)	L		389	130	105	60	127	73	56				
IQW 1966/7416 (Voi.3279)	R	young	390	122	103	55	126	73	57				
IQW 1966/7416 (Voi.3279)	L	young	390	120	101	56	125	73	56				
IQW - - (Voi.701)	L		400	135	102	64	136	76	63				
IQW 1966/7442 (Voi.1683)	R		-	-	102	54	-	73	51				
IQW 1965/2172 (sus.7039)	R		-	-	.93	51	-	71	52				
IQW 1980/15364 (Mei.14876)	L		390	129	110	57	135	72	52				
IQW 1980/16118 (Mei.15629)	R		392	123	107	58	130	73	56				
IQW 1980/16429 (Mei.15940)	L		391	119	101	60	134	72	51				
IQW 1981/17716 (Mei.17238)	R		396	134	113	63	129	74	56				
IQW 1980/17156 (Mei.16677)	L		398	130	109	62	.118	79	55				
IQW 1980/16433 (Mei.15944)	R		396	121	106	61	137	71	57				
IQW 1980/16673 (Mei.16194)	L		400	122	108	56	120	73	51				
IQW 1986/21300 (Mei.20819)	L		420		105	55	>115	73	56				
IQW 1998/26418 (Mei.25947)	L		393	128	.102	56	137	>62	53				
IQW 1996/25690 (Mei.25219)	L		420	126	105	62	134	77	59				
IQW 1995/25042 (Mei.24571)	R		391	122	104	61	129	68	54				
NHM M 6674	L		-	-	102	-	-	70	-				
NHM M 17849	L		-	-	>90	-	-	>68	-				
NHM M 18486	R		390	107	100	57	115	68	62				
NHMW 2013/0282/0001	R		390	125	105	58	130	77	61				
NHMW 2013/0282/0001	L		390	124	108	58	132	77	61				
Astragalus			**1**	**1M**	**1Mtr**	**1L**	**1Ltr**	**2**	**2D**	**2AD**	**3D**		
SMNK MS 1472	L		80	72	61	74	61	89	75	74	44		
SMNK MS 1700	R		83	80	65	.80	65	94	76	.71	50		
SMNK MS 1200	L		90	82	-	80	-	-	81	-	50		
SMNK MS 1184	L		90	81	-	82	63	95	81	-	-		
SMNK MS 1183	L		-	76	-	-	-	94		-	46		
SMNK MS 1202	L		77	73	58	70	52	87	75	72	44		
SMNK MS 1203	R		-	73	-	-	-	91	76	-	-		
SMNK MS 1334	R		86	75	65	-	-	92		-	46		
SMNK MS 1175	R		89	80	-	85	62	93	77	-	41		
SMNK MS 1199	R		82	73	-	78	53	90	72	-	47		
SMNK MS 0246	R		90	79	70	83	64	94	83	83	53		

SMNK MS 0243	R		86	77	67	78	60	94	76	76	50		
SMNK MS 1186	R		78	69	63	70	55	88	73	73	45		
SMNK MS 0733	L		81	75	-	-	-	92	78	-	-		
SMNK MS 0823	R		84	74	-	-	-	97	82	80	50		
MNHM 1962/1281	R		87	78	64	83	59	97	81	77	49		
MNHM 1947/16	R		86	79	63	75	58	94	82	78	49		
MNHM 1955/692	R	young	79	79	63	74	59	86	74	72	47		
MNHM 1962/1282	R		81	75	62	74	58	88	73	73	47		
MNHM 1959/197	L		78	74	60	74	59	86	71	70	44		
MNHM 1955/693	L		79	79	64	72	55	87	70	70	46		
MNHM 1955/167	L		76	76	65	71	58	92	77	71	47		
MNHM 1952/376	L		77	72	60	72	55	82	72	70	44		
MNHM 1957/980	L		84	81	66	79	61	92	73	69	47		
IQW 1966/7415 (Voi.3280)	R		90	76	68	82	66	98	78	78	46		
IQW 1966/7416 (Voi.3279)	R	young	84	76	65	76	59	99	74	74	46		
IQW 1966/7416 (Voi.3279)	L	young	85	77	64	76	58	96	74	74	45		
IQW 1965/3716 (Voi.669)	R		89	81	67	80	65	98	71	71	48		
IQW 1966/5595 (Voi.1150)	L		90	82	70	85	62	95	77	77	48		
IQW 1964/650 (Süß.7948)	R		97	80	68	83	65	99	72	71	45		
IQW 1964/336 (Süß.9141)	L		82	78	-	75	60	86	73	72	-		
IQW 1964/663 (Süß.7624)	L		-	78	66	-	-	91	73	73	45		
IQW 1980/15659 (Mei.15171)	L		83	78	65	75	57	89	75	73	47		
IQW 1980/16671 (Mei.16192)	R		85	79	66	78	60	92	78	74	47		
IQW 1980/16839 (Mei.16360)	L		86	81	71	79	63	93	78	74	51		
IQW 1980/17052 (Mei.16573)	R		87	78	71	82	62	98	82	77	49		
IQW 1980/16690 (Mei.16211)	L		85	80	78	78	60	91	75	73	45		
IQW 1986/21643 (Mei.21162)	R		81	74	62	73	58	92	76	74	48		
IQW 1982/18527 (Mei.18047)	R		80	-	66	76	59	95	81	77	50		
IQW 1990/23585 (Mei.23114)	L	young	81	76	.65	73	57	91	73	70	46		
IQW 1983/19186 (Mei.18706)	L		87	81	69	76	60	92	80	75	51		
IQW 1989/23219 (Mei.22738)	L		80	78	64	74	61	89	78	75	48		
IQW 1980/16071 (Mei.15582)	L	young	75	72	.60	66	55	80	66	65	42		
IQW 1995/25396 (Mei.24925)	R		80	72	63	75	60	93	79	76	48		
IQW 1995/24988 (Mei.24517)	L		84	82	70	77	60	91	78	73	49		
MPLB #006	R		77	68	60	71	58	78	62	60	39		
MPLB #007	L		74	65	60	66	55	77	63	63	38		
MPLB #008	L		-	-	-	-	-	-	-	-	-		
MPLB #009	R		-	-	-	-	-	-	-	-	-		
NHM M 19525	L		73	68	61	.67	49	85	.74	.71	.41		
NHM M 6780	L		.73	70	55	.68	50	80	65	65	40		
NHM M 19526	L		78	72	59	68	51	86	71	69	42		
NHM M 19527	L		85	80	66	77	64	>84	>70	-	-		
NHM M 19524	L		>75	75	60	>70	>53	92	78	75	.40		
NHM M 19523	R		87	78	70	.80	.63	98	75	75	47		
NHM F 30402	L		85	78	67	76	60	97	-	-	-		
MPPL 368	L		81	78	56	76	56	89	73	70	52		
NHMW 2013/0282/0001	R		84	79	69	76	58	96	85	85	-		

NHMW 2013/0282/0001	L		84	79	-	75	59	96	82	-	-		
NHMW 1909II.569	R		84	75	65	75	57	92	78	-	-		
IPW C155	L		77	70	60	72	54	90	73	-	-		
IPW C71	L		81	.74	57	72	58	88	-	-	-		
IPW C69	R		83	74	59	73	56	91	76	-	-		
IPW F3	R		75	70	56	68	56	89	70	-	-		
Calcaneum			**1**	**2**	**3**								
SMNK MS 1701	R		125	.72	59								
SMNK MS 0253	L		127	74	59								
SMNK MS 1185	R			80	63								
SMNK MS 1188	L		124	79	60								
SMNK MS 1189	L		135	-	58								
MNHM 1961/544	R		117	69	59								
MNHM 1960/199	R		130	78	.64								
MNHM 1967/79	R		121	68	64								
MNHM 1956/996	R		117	75	65								
MNHM 1965/270	R		128	77	63								
MNHM 1959/792	R		119	74	61								
MNHM 1961/616	L		-	76	66								
MNHM 1959/197	L		.113	80	66								
IQW 1966/7416 (Voi.3279)	R	young	127	-	64								
IQW 1966/7416 (Voi.3279)	L	young	127	79	61								
IQW 1965/3702 (Voi.766)	L		.135	83	64								
IQW 1965/3715 (Voi.824)	L		137	84	60								
IQW 1965/3721 (Voi.1210)	R		138	84	67								
IQW 1964/337 (Süß.9142)	L	young	117	74	62								
IQW 1964/649 (Süß.7870)	L	young	129	-	62								
IQW 1980/16719 (Mei.16240)	R		128	82	73								
IQW 1980/15658 (Mei.15170)	L		125	83	62								
IQW 1980/16401 (Mei.15912)	R		129	80	66								
IQW 1980/16840 (Mei.16361)	L		-	80	66								
IQW 1980/16687 (Mei.16208)	L		124	79	62								
IQW 1986/21639 (Mei.21158)	R		123	79	64								
IQW 1982/18528 (Mei.18048)	R		-	80	70								
IQW 1990/23586 (Mei.23115)	L		120	73	65								
IQW 1983/19140 (Mei.18660)	L		108	84	67								
IQW 1986/21736 (Mei.21255)	R		124	79	66								
IQW 1987/22076 (Mei.21595)	R		125	86	69								
IQW 1988/22577 (Mei.22096)	L		120	80	.62								
IQW 1992/24103 (Mei.23632)	R		145	86	67								
IQW 1995/24987 (Mei.24516)	R		126	81	66								
MPLB #010	L		115	70	60								
MNHN Sol 109	R		115	70	52								
NHM M 19528	R		>107	.78	.66								
NHM M 6687	R		>118	.77	>64								
NHM M 19536	L		132	79	65								
NHM M 17833	L		115	64	52								

NHM F 30400	L		.132	79	69								
MPI 57.41	R		132	83	68								
NHMW 2013/0282/0001	R		137	85	64								
NHMW 2013/0282/0001	L		137	84	65								
IPW C71	R		122	75	65								
IPW no num.	R		-	77	65								
IPW A144	L		124	75	61								
IPW no num.	L		126	>58	62								
Cuboid			**1**	**2**	**3**		**1/2**						
SMNK MS 1593	R		45	.39	64								
SMNK MS 2879	R		43	46	-		0,93						
IQW 1966/7415 (Voi.3280)	R		52	46	67		1,13						
IQW 1966/7416 (Voi.3279)	R	young	45	47	68		0,96						
IQW 1966/7416 (Voi.3279)	L	young	45	48	68		0,94						
IQW 1965/3722 (Voi.346)	R		47	45	69		1,04						
IQW 1964/338 (Süß.9143)	L		42	39	-		1,08						
IQW 1980/15971 (Mei.15482)	L		46	47	70		0,98						
IQW 1980/16700 (Mei.16221)	R		44	45	66		0,98						
IQW 1980/16720 (Mei.16241)	R		44	45	71		0,98						
IQW 1980/16688 (Mei.16209)	L		41	44	67		0,93						
IQW 1986/21638 (Mei.21157)	R		42	43	68		0,98						
IQW 1982/17932 (Mei.17452)	R		46	42	65		1,10						
IQW 1980/16811 (Mei.16332)	L	young	36	41	59		0,88						
IQW 1985/20811 (Mei.20330)	R		49	45	73		1,09						
IQW 1980/15584 (Mei.15096)	R		46	42	68		1,10						
IQW 1992/24080 (Mei.23609)	R		46	47	69		0,98						
IQW 1985/20432 (Mei.19952)	R		47	44	64		1,07						
IQW 1989/23175 (Mei.22694)	L		42	42	60		1,00						
IQW 1984/19947 (Mei.19467)	L		40	40	68		1,00						
NHM M 17608	L		47	45	65		1,04						
NHM F 30057	L		45	48	68		0,94						
MPI 26	L		38	43	65		0,88						
MPI 68.34	R		43	35	64		1,23						
MPPL 375	R		48	40	67		1,20						
MPPL 376	R		45	38			1,18						
MPPL 374	L		44	43	65		1,02						
NHMW 2013/0282/0001	R		45	-	76								
NHMW 2013/0282/0001	L		47	53	77		0,89						
NHMW 1909II.575	R		46	45	67		1,02						
NHMW 1909II.575	L		45	50	71		0,90						
IPW C14	L		41	48	63		0,85						
IPW C102	L		.44	-	62								
IPW C162	R		40	43	61		0,93						
Navicular			**1**	**2**	**3**								
IQW 1966/7415 (Voi.3280)	R		33	51	63								
IQW 1966/7416 (Voi.3279)	R	young	31	52	58								
IQW 1966/7416 (Voi.3279)	L	young	30	51	58								

IQW 1965/3708 (Voi.1622)	L		28	52	63								
IQW 1965/3707 (Voi.665)	L		32	52	64								
IQW 1980/15662 (Mei.15174)	L		29	53	61								
IQW 1980/16699 (Mei.16220)	R		32	50	58								
IQW 1980/16689 (Mei.16210)	L		30	51	61								
IQW 1986/21654 (Mei.21173)	R		29	50	61								
IQW 1982/18445 (Mei.17965)	R		30	52	63								
IQW 1985/20430 (Mei.19950)	R		31	53	62								
IQW 1992/24066 (Mei.23595)	R		34	-	64								
IQW 1988/22702 (Mei.22221)	L		30	49	59								
IQW 1993/24339 (Mei.23869)	R		29	.50	60								
MPLB #017	L		27	.40	55								
NHMW 2013/0282/0001	R		33	49	62								
NHMW 2013/0282/0001	L		32	49	61								
NHMW 1909II.574	R		34	51	63								
NHMW 1909II.574	L		35	50	62								
IPW C71	R		26	46	55								
IPW A144	L		31	44	57								
MtII			**1**	**2P**	**2D**	**2AD**	**3P**	**3D**					
SMNK MS 0237	L		149	31	40	31	41	39					
SMNK MS 1547	R		165	29	35	30	45	39					
SMNK MS 1548	L		165	30	42	32	42	41					
IQW 1966/7416 (Voi.3279)	R	young	172	30	37	30	44	41					
IQW 1966/7416 (Voi.3279)	L	young	174	33	38	30	46	40					
IQW 1980/15666 (Mei.15178)	L		173	32	36	31	43	39					
IQW 1980/16701 (Mei.16222)	R		-	29	-	-	42	-					
IQW 1986/21641 (Mei.21160)	R		160	32	38	33	.45	41					
IQW 1982/18442 (Mei.17962)	R		-	31	-	-	44	-					
IQW 1980/15457 (Mei.14969)	L	young	143	26	-	.28	38	37					
IQW 1993/24365 (Mei.23894)	L		166	32	37	34	45	41					
MPLB #015	L		146	>25	35	31	35	34					
MNHN Sol 121	R		162	27	-	28	40	37					
NHM M 18156	R		>107	26	-	-	42	-					
MPPL 175.379	R		159	25	36	30	40	40					
NHMW 2013/0282/0001	R		170	30	40	33	45	40					
IPW A97	R		164	28	38	31	45	35					
IPW no num.	L		170	30	39	35	47	41					
IPW A144	L		-	.27	35	31	42	36					
MtIII			**1**	**2P**	**2d**	**2D**	**2AD**	**3P**	**3d**	**3D**			
SMNK MS 5047	L		185	53	42	57	45	45	23	42			
MNHM 1957/394	R		191	49	44	-	47	40	25	40			
MNHM 1955/1225	L		196	49	44	55	43	42	25	29			
MNHM 1964/503	R		-	55	44	-	-	48	24	-			
MNHM 1955/832	R		-	50	-	-	-	45	-	-			
IQW 1966/7415 (Voi.3280)	R		198	58	50	61	47	49	25	42			
IQW 1966/7416 (Voi.3279)	R	young		57		-	-	48	-	-			
IQW 1966/7416 (Voi.3279)	L	young	200	57	46	60	44	50	22	42			

IQW 1964/652 (Süß.5203)	L		-	52	43	-	-	46	-	-			
IQW 1964/339 (Süß.9144)	R		-	55	-	-	-	44	-	-			
IQW 1980/15844 (Mei.15355)	R		230	56	47	56	47	50	28	42			
IQW 1980/15663 (Mei.15175)	L		210	55	43	55	48	47	24	42			
IQW 1980/16703 (Mei.16224)	R			54	42	-	-	45	24	-			
IQW 1986/21642 (Mei.21161)	R		179	55	43	55	47	46	23	42			
IQW 1982/18443 (Mei.17963)	R			52	43	-	-	-	24	-			
IQW 1993/24314 (Mei.23843)	R	young		48	33	-	-	42	19	-			
IQW 1987/22098 (Mei.21617)	L			53		-	-	44	-	-			
IQW 1980/16920 (Mei.16441)	R		198	56	45	60	48	51	28	41			
IQW 1984/20181 (Mei.19701)	R		189	51	40	56	45	43	25	38			
IQW 1993/24368 (Mei.23897)	L		196	50	42	54	44	42	24	43			
MPLB #013	L		165	48	42	54	43	43	20	33			
NHM M 6783	nd		-	-	-	57	45	-	-	42			
NHM M 17827	L		>140	51	40	-	-	42	27	-			
NHM M 6676	L		194	53	40	56	43	48	23	40			
MPPL 80.378	R		181	53	47	56	44	42	22	41			
NHMW 2013/0282/0001	R		197	59	45	59	48	-	26	45			
NHMW 2013/0282/0001	L		198	60	45	62	47	-	26	-			
NHMW 1909II.571	R		188	53	44	57	44	41	25	42			
IPW D16	R		185	56	43	.52	43	47	24	41			
IPW A32	R		190	-	41	54	41	41	23	42			
IPW C129	L			-	42	51	43	-	23	40			
IPW C99	L		188	56	43	-	41	46	24	40			
MtIV			**1**	**2P**	**2D**	**2AD**	**3P**	**3D**					
SMNK MS 1552	R		167	44	36	31	38	42					
SMNK MS 1553	L		166	39	34	28	36	38					
SMNK MS 1190	L		160	41	34	29	35	39					
SMNK MS 1555	R		165	40	34	30	37	43					
MNHM 1953/488	L		-	41	-	-	42	-					
MNHM 1954/564	L		-	37	-	-	36	-					
MNHM 1959/790	R		-	41	-	-	41	-					
MNHM 1958/84	R		155	39	31	28	38	37					
IQW 1966/7415 (Voi.3280)	R		174	47	39	35	44	42					
IQW 1966/7416 (Voi.3279)	R	young	172	45	35	31	40	40					
IQW 1966/7416 (Voi.3279)	L	young	175	42	38	30	40	40					
IQW 1980/15660 (Mei.15172)	L		174	44	37	34	43	43					
IQW 1980/16311 (Mei.15822)	L		168	43	37	33	40	42					
IQW 1986/21640 (Mei.21159)	R		158	46	37	33	43	42					
IQW 1982/18055 (Mei.17575)	R			46		-	43	-					
IQW 1982/17907 (Mei.17427)	L		166	44	38	36	41	40					
IQW 1983/19581 (Mei.19101)	R			43		-	40	-					
IQW 1980/15455 (Mei.14967)	L	young		.38		-	.35	-					
IQW 1993/24364 (Mei.23893)	L			40	34	34	39	40					
IQW 1997/26241 (Mei.25770)	L		162	40	37	35	40	37					
MPLB #014	L		143	38	35	32	37	35					

MPPL 380	R		162	44	35	31	42	42					
MPI 89.160	L		162	-	-	36	36	38					
NHMW 2013/0282/0001	R		170	46	.37	34	46	40					
NHMW 2013/0282/0001	L		170	46	38	35	46	41					